



EMBL

EUROPEAN MOLECULAR BIOLOGY LABORATORY

RESEARCH REPORTS 1981

TABLE OF CONTENTS

	PAGE
<u>DIVISION OF CELL BIOLOGY</u>	6
Developmental, structural and functional studies on the insect nervous system	7
Enveloped viruses as experimental tools to study membrane biogenesis and traffic in the animal cell	18
Early events in protein secretion and membrane biogenesis	24
Balbiani rings and giant secretory proteins in <u>Chironomus</u>	30
Gene expression and its control	36
Molecular genetics of prokaryotes	42
<u>Drosophila</u> gene organization and expression	46
Dosage compensation in <u>Drosophila melanogaster</u> . Hybrids between different species of <u>Drosophila</u> .	50
Organization of middle repetitive DNA in the human genome: functional and structural aspects	53
Genetic studies of restriction and modification enzymes	59
Cloning and sequence analysis in eukaryotic molecular biology	70
Gene expression	74

	PAGE
<u>DIVISION OF BIOLOGICAL STRUCTURES</u>	86
Organization and dynamics of cytoskeletal elements	87
Transport of plasma membrane proteins through the Golgi complex	94
Mitochondrial electron transfer enzymes	99
Biogenesis of cell surface domains as displayed by epithelial cells	105
Electron microscopy of nucleic acids	114
Electron microscopy and computer image analysis	123
Electron microscopy applications group	132
Structure and assembly of filamentous bacterial viruses	138
Structural studies on clathrin coats and on proteins interacting with nucleic acids	147
Cloning of the clathrin gene	153
Structure of bacterial polypeptide elongation factors	159
X-ray analysis of DNAase I and the actin:DNAase I complex	164
Structural basis of control in aspartate transcarbamylase (ATCase)	169
X-ray crystallography of insecticyanin	176
Protein sequencing	179
Nucleotide sequence data base group	187

	PAGE
<u>DIVISION OF INSTRUMENTATION</u>	190
Electron microscope development group	191
Data analysis Group	198
Computer Group	207
Position-sensitive detectors	212
Applications of lasers	214
Development of microanalytical techniques	219
Operating principle of a self-pumping continuous-flow centrifuge	223
Cell separations using magnetically manipulated adsorption media	225
Isolation of organelles with antibodies	232
 <u>THE OUTSTATIONS</u>	 237
The Outstation of the DESY, Hamburg	238
The Outstation at the ILL, Grenoble	275

DIVISION OF CELL BIOLOGY

Developmental, structural and functional studies of the insect nervous system

Members: N.J. Strausfeld, H. Anderson, U. Bassemir, G. Geiger, D.R. Nässel

Fellows: D. Byers*, B. Mulloney*, R.N. Singh*

Visiting workers: J. Altman*, J. Bacon*, H. Duve*, K.-G. Fischbach*, J.T. Leutscher-Hazelhoff*, P. Sivasubrahmanian*, R. Stocker*, A. Thorpe

Technical assistant: H. Seyan

Studies of nervous system development

H. Anderson is investigating the interactions among developing neurons and between growing axons and their substrates. The study of the mechanisms underlying sensory axon guidance and navigation (see Annual Report 1980 and Anderson, H.J., 1980 a and b) has been extended to the Drosophila nervous system for which many mutants are available as experimental tools for manipulating development. In the wing, sensory neurons form a characteristic pattern of nerves. Analysis of axon trajectories in the Hairy wing mutant has shown that supernumerary neurons in abnormal locations tend to run through the wing in the vein 3 nerve and not to form supernumerary nerves in other closer veins. It has been suggested that earlier differentiating "pioneer" axons are present within this vein and act as "guiding factors" (Palka, 1982), as proposed for the establishment of peripheral pathways in other insects. Electron microscopy of developing wings, 6-30 hours after puparium formation, was used to establish the time of axon outgrowth and the nature of the axonal substrates in the wing at this time. There is no evidence for "pioneer" neurons within the wing. Rather it seems that in the wildtype, veins which are formed prior to neuron differentiation provide the substrate for axon outgrowth. Axon outgrowth occurs at 21-24 hours after puparium formation, providing a time point for a parallel investigation of the mutants.

A locust embryo culture has now been established. This preparation is favourable for research at the level of identified neurons since individual neurons may be observed in the living animal, impaled with microelectrodes for electrophysiological recording, filled with dyes for morphological investigation, and treated with an increasing

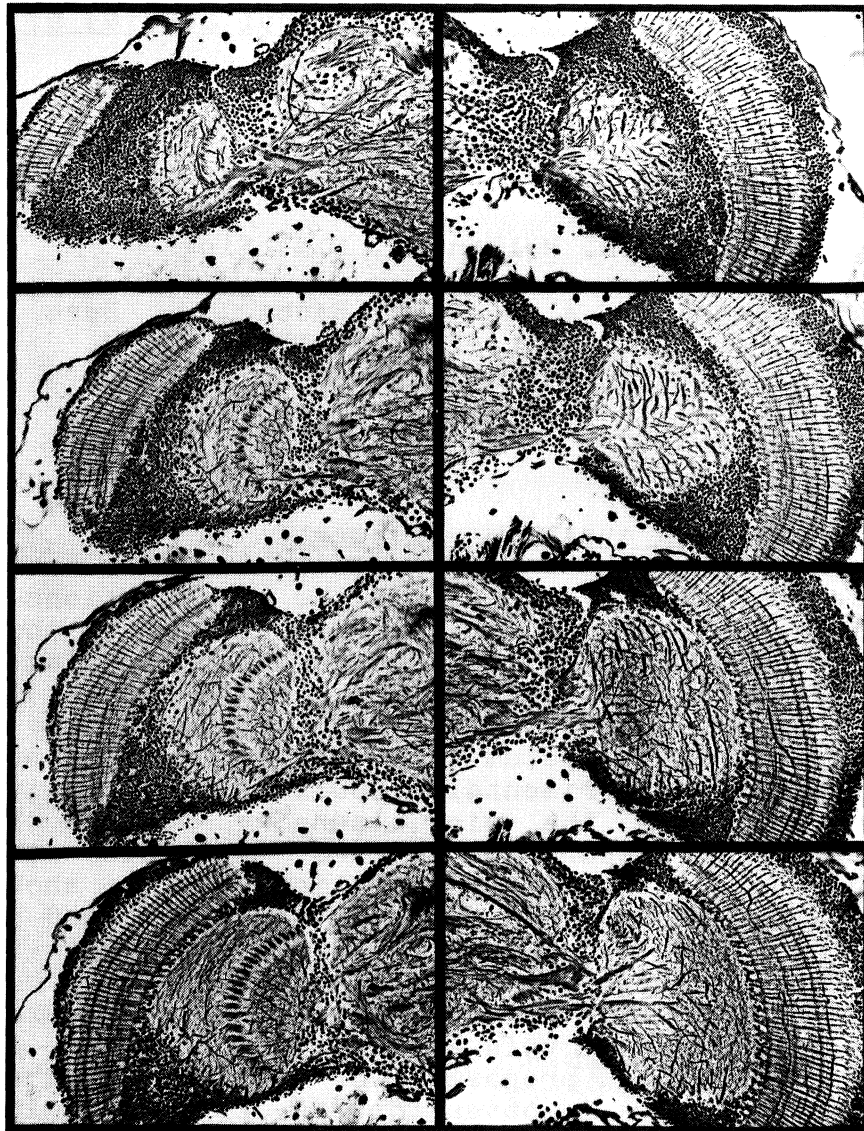


PLATE 1

A photomicrographic series through the brain of the housefly (Musca) illustrating the effects of laser microsurgery on the first instar larva deleting precursor cells of the H and V cell system. To the right is shown the normal appearance of the optic lobes in which vertical cells (top three photographs) and horizontal cells (bottom photograph) are clearly visible as large diameter argyrophilic elements. The lobula plate in the operated optic lobe is typically thinner, lacks these neurons but contains some small diameter elements.

number of antibodies now available for use as cell markers. A preliminary description of developing stages and the modification of histological methods have now been undertaken for a major investigation of the developmental interactions between primary sensory neurons and presumptive interneurons that play an important role in the development of the visual system.

Functional correlates to structure and development

G. Geiger and D.R. Nässel have used the laser micro-surgery unit to investigate two major subsystems - the horizontal (H) and vertical (V) motion-sensitive system of the optic lobes (Hausen, 1981). Unilateral ablation of these cells' precursors leads to their absence in one adult optic lobe but not in the other, so that a control was present in the operated animal (Plate 1). Before histological examination by H. Seyan the experimental flies' eyes were subjected to quantitative visual behaviour tests. Lack of H and V cells does not adversely affect some behaviours, such as the ability to fixate and track a single narrow object, but does quantitatively diminish optomotor response to moving gratings (Geiger & Nässel, 1981). However, this ability is not entirely lost. It is concluded that response to small-field objects in the visual field does not depend on the presence of the H and V system. Responses to wide-field moving gratings are affected by loss of H and V cells. This suggests that at least two pathways exist for movement information processing, one for small-field objects ("Figure"), another for wide-field objects ("Ground"). Experiments are currently being performed on other identifiable cell systems. Microbeam surgery is also being used to examine certain aspects of brain development such as the role of precursor cells and their interactions in areas of the larval brain in regulating the organization of the adult brain.

Structural analysis of synaptic connections

Migration of cobalt ions between certain "cobaltomissive" neurons has been correlated with cobalt-silver deposits at special regions of the synaptic apparatus. "Trans-synaptic" cobalt resolves a major behavioural pathway involving the tergotrochantal (TTM) muscle of the midleg, the TTM's motor neuron and the giant descending neuron (GDN, resembling a Mauthner cell of fish). Together, these are thought to elicit sudden extension of the midleg (Levine & Tracy, 1973; King & Wyman, 1980; Tanouye & Wyman, 1980). U. Bassemir, N.J. Strausfeld, & J. Bacon (MPI,

PLATE 2

Top left. Cobalt coupling of descending neurons (DNVS) to the vertical cell system (V) showing at least two DNVS cells that project in parallel from the brain. Top right. A DNVS cell that has been recorded and filled with the fluorescent dye Lucifer yellow. Bottom left. Double marking: DNVS neuron filled with cytochrome C (see 1980 Annual Report) and an ocellar interneuron filled with silver chromate. Bottom right. Double marking: silver chromate in a T4 small field neuron from the medulla onto a vertical cell that was transsynaptically filled with cobalt and intensified. Scale for top left and right: 25 μm , scale for bottom left: 0.2 μm , bottom right: 0.5 μm .

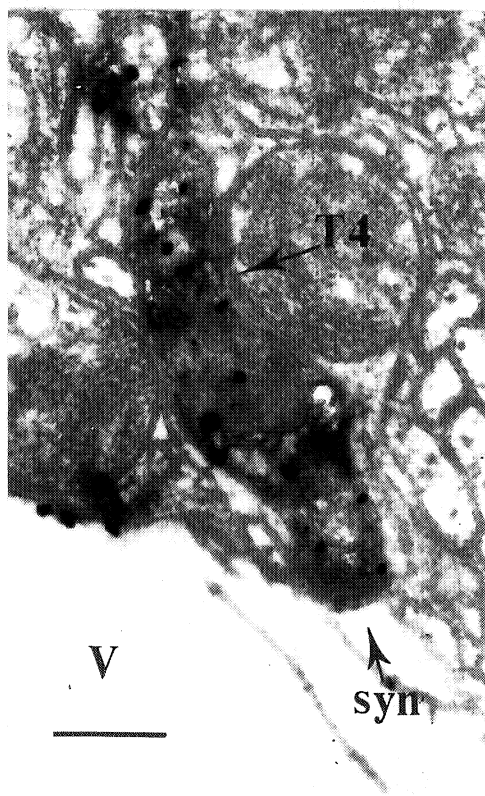
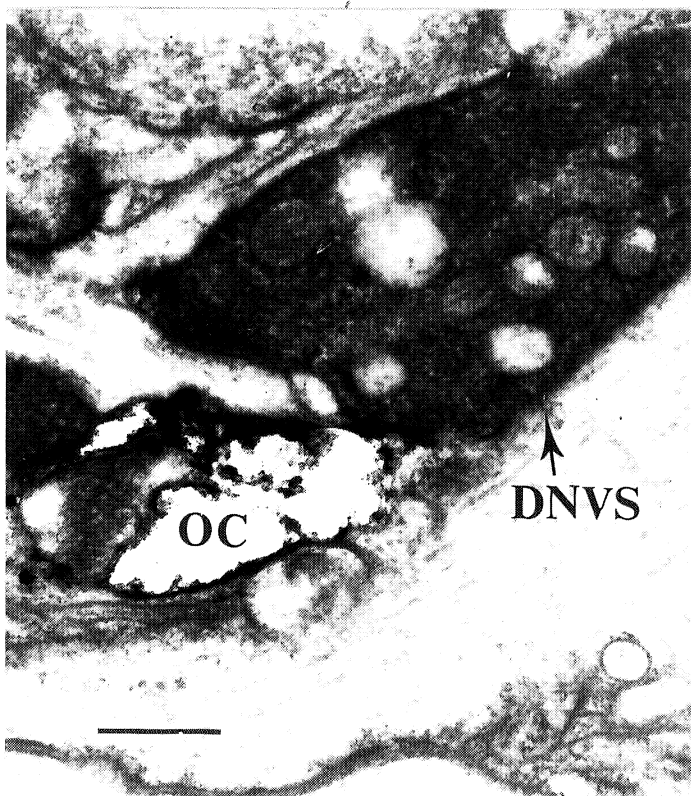
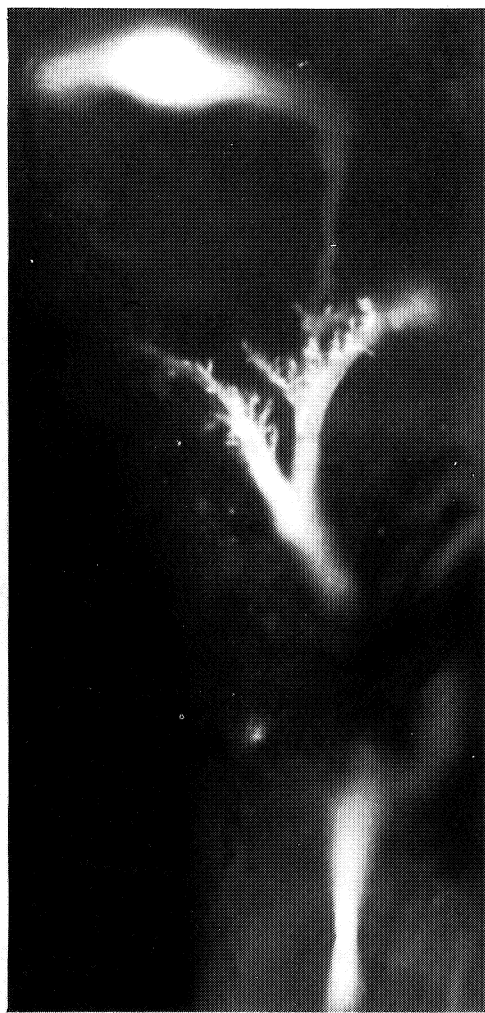
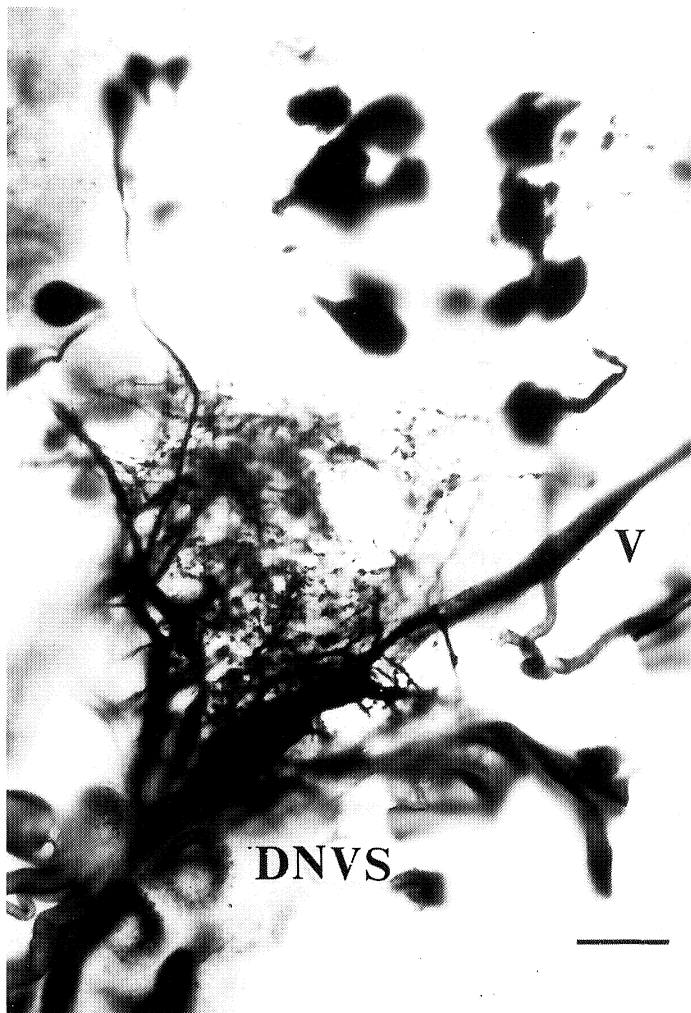
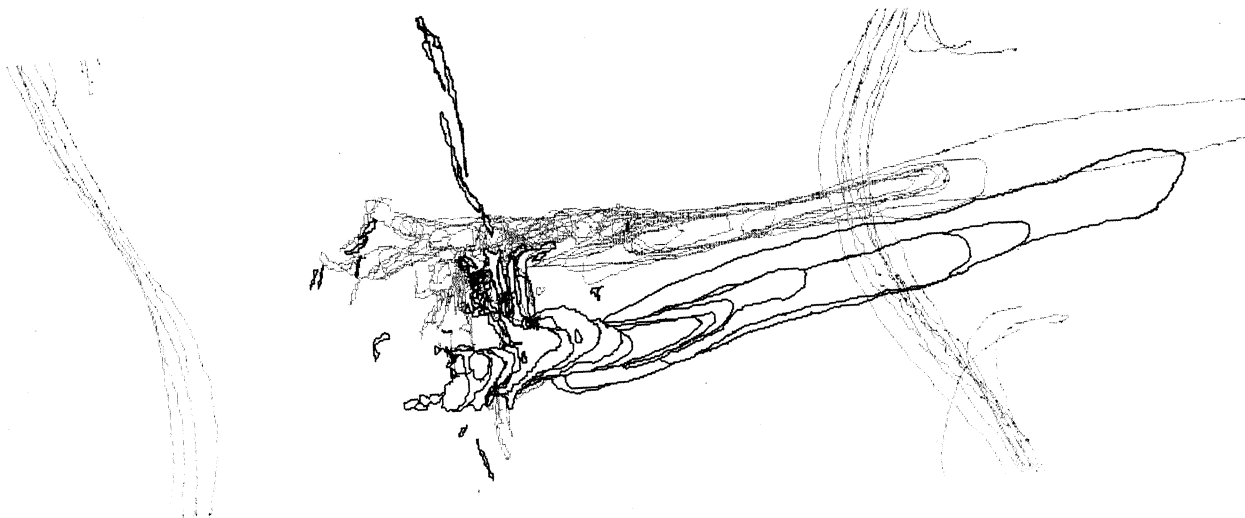
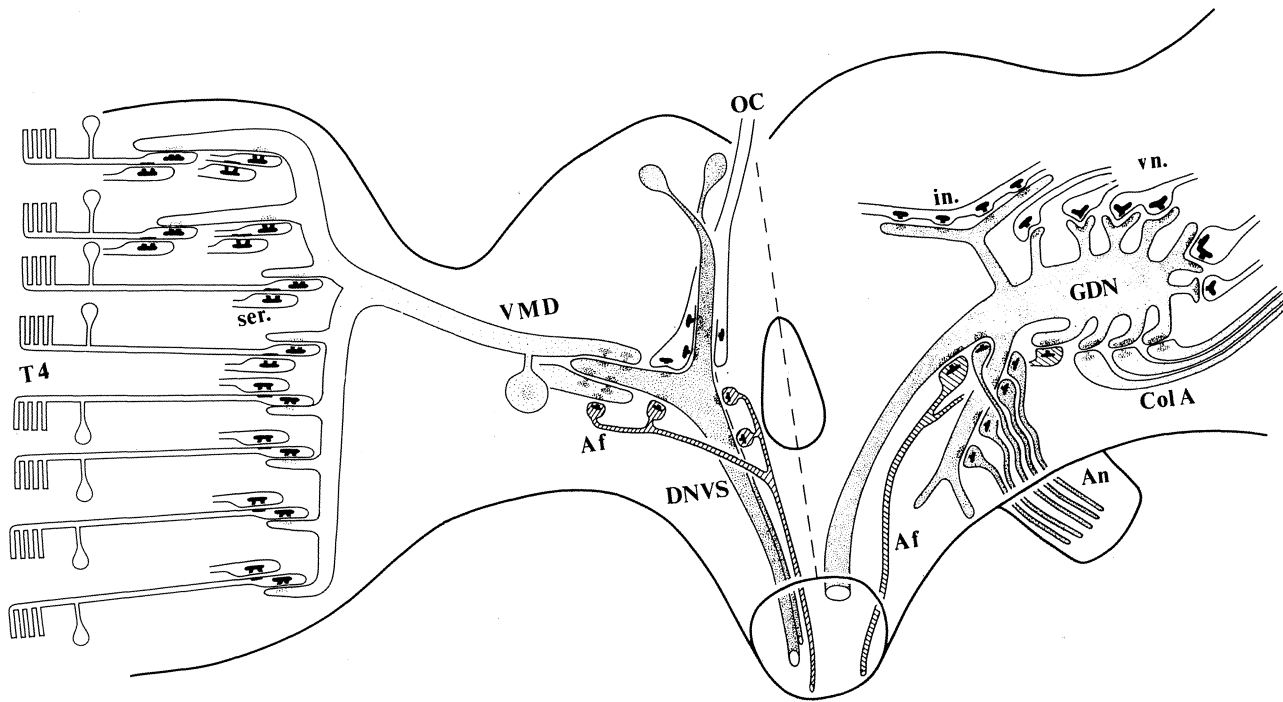


PLATE 3

Summary of two synaptic pathways resolved in the highly complex neuropil of the visual system and dorso-posterior brain. T4 cells are pre-synaptic to the vertical cell system (Vertical motion "detector" VDM) and are also serially (ser) postsynaptic to other elements entering the lobula plate. Descending neurons (DNVS and GDN) have common attributes, being postsynaptic to converging sensory systems and postsynaptic to terminals from the thoracic ganglia. Ocellar interneurons (OC) and VDM are presynaptic to DNVS; retinotopic Col A cells (see 1979 Report) and antennal fibres are presynaptic to GDN. In addition, other visual neurons (vn) and interneurons (in) have inputs onto GDN at specific dendrites but these do not take up cobalt transsynaptically. Synapses involved in transsynaptic cobalt pathways are shown stippled.

PLATE 4

A computer graphic reconstruction of part of the pair of GDN endings in the thoracic ganglia illustrating connexions between them. One cell is labelled with thin open profiles, the other with thick hidden-line profiles. Stereopairs from two viewing angles of the GDN dendrites in the brain are shown in Plate 1 of the Annual Report.



Seewiesen and S.U.N.Y., Albany, New York) have investigated functional and structural properties of this pathway (Strausfeld et al., 1981) and have correlated trans-synaptic cobalt migration with functional connections between neurons. Properties of neurons leading to and conveying information from the vertical motion-sensitive neurons in the brain have also been investigated.

Double marking techniques for electron microscopy (Plate 2) enable cell profiles of identified neurons to be recognized according to certain features, such as electron-opacity of the marking substances (silver chromate, cobalt-silver, cytochrome c; see also Annual Report for 1980). Retinotopic inputs to giant descending neurons (GDN; Col A cells) are accompanied by sensory endings from antenna. Fluorescent dye coupling with Lucifer yellow is also seen between the GDN and the male unique neuron (Hausen & Strausfeld, 1980). Electrophysiological recording and fluorescent marking reveal that GDN neurons respond to mechanical displacement of the antenna and "light-off", corroborating structural studies. J. Bacon has also shown that the TTM motor neuron is trans-synaptically cobalt-coupled to GDN. Double recording from the TTM motor neuron and GDN shows these to be functionally connected.

Double marking resolves V-cells postsynaptic to retinotopically organized "T4" small field neurons. Terminals of the latter are postsynaptic to another unidentified cell type. This arrangement meets the requirements of some hypothetical models of motion detection derived from behavioural studies (Hassenstein & Reichardt, 1956; Reichardt, 1970). Recording and marking descending neurons (DNVS) leading from the vertical motion-sensitive system substantiate cobalt tracing that shows at least two pairs of DNVS in the brain. Thus, there can be several identical nerve cells in the brain that subsequently diverge to different targets in thoracic ganglia.

DNVS also receive inputs from the ocellar system. Electrophysiological recording shows them to respond to darkening and movement. Synaptic organizations summarized in Plate 3 show that both investigated systems (DNVS and GDN) share principles of connections, including feedback from thoracic ganglia. The existence of identical descending neurons and feedback pathways is reminiscent of wiring in the peripheral optic cartridges of the lamina (Strausfeld & Campos-Ortega, 1977). We are now investigating if, as it seems, neuronal connections in the brain are basically conservative, involving a small repertory of synaptic configurations. Structural

relationships between descending neurons and motor neuron are also being investigated in normal and mutant (bithorax) Drosophila (R.N. Singh, N.J. Strausfeld).

Computer graphics for visualizing neurons in three dimensions

P. Speck of the Data Analysis Group has further refined the computer graphics unit. Cells can be viewed in eight orthogonal views, and each can be obtained with its stereopair. Highly complex cells can be reconstructed, and both hidden and open lines combined in one picture. This allows a better understanding of spatial relationships in connectivity studies (Plate 4).

Publications during the year

Anderson, H.J. (1981a). Projections from sensory neurons developing at ectopic sites in insects. J. Embryol. exp. Morph., 65 (Supplement), 209-224.

Anderson, H.J. (1981b). Building a nervous system. Nature, 293, 510-511.

Anderson, H.J. (1982). Early responses to neuronal injury. In Repair and Regeneration of the Nervous System, Dahlem Konferenzen ed.; J.G. Nicholls Berlin, Heidelberg, New York, Springer, (in press).

Bassemir, U. & Strausfeld, N.J. (1982). Block intensification of cobalt filled neurons for electron microscopy. In Experimental Entomology (Series Ed. T.A. Miller). Experimental neuroanatomy, (Vol. Ed. N.J. Strausfeld), (in press).

Geiger, G., Boulin, C. & Bücher, R. (1981). How the two eyes add together: monocular properties of the visually guided orientation behaviour of flies. Biol. Cybern., 41, 71-78.

Geiger, G. & Nässel, D.R. (1981). Visual orientation of flies after laser-beam elimination of specific interneurons. Neurosci, abstr. 11, 117.3.

Geiger, G. & Nässel, D.R. (1981). Visual orientation behaviour of flies after selective laser beam ablation of interneurons. Nature, 293, 398-399.

Geiger, G., Nässel, D.R. & Seyan, H. (1982). On the use of laser microsurgery in the study of neural development and behaviour of flies. In Experimental Entomology (Series Ed. T.A. Miller). Experimental neuroanatomy, (Vol. Ed. N.J. Strausfeld), (in press).

Geiger, G. & Poggio, T. (1981). Asymptotic oscillations in the tracking behaviour of the fly Musca domestica. Biol. Cybern., 41, 197-201.

Nässel, D.R. (1981). Pathways resolved by transneuronal uptake of horseradish peroxidase in C.N.S. of flies. Neurosci., abstr. 11, 88.5.

Nässel, D.R. (1982). Horseradish peroxidase and other hemeproteins as neuronal markers. In Experimental Entomology (Series Ed. T.A. Miller). Experimental neuroanatomy (Vol. Ed. N.J. Strausfeld), (in press).

Spindler-Barth, M., Bassemir, U., Kuppert, P. & Spindler, K.-D. (1981). Isolation of nuclei from crayfish tissues and demonstration of nuclear ecdysteroid receptors. Z. Naturforsch., 36c, 326-332.

Strausfeld, N.J., Bacon, J., Bassemir, U. & Nässel, D.R. (1981). Structure, input, coupling and physiology of the giant descending neurons (GDNs) of the fly (Musca) Neurosci., abstr. 11, 437.

Other references

Hassenstein, B. & Reichardt, W. (1956). Systemtheoretische Analyse der Zeit-, Reihenfolge- und Vorzeichenauswertung bei der Bewegungspitze des Rüsselkäfers Chlorophanus. Z. Naturforsch., 11b, 513-524.

Hausen, K. (1981). Monocular and binocular computation of motion in the lobula plate of the fly. Verh. Dtsch. Zool. Ges., 49-70.

Hausen, K. & Strausfeld, N.J. (1980). Sexually dimorphic interneuron arrangements in the fly visual system. Proc. Roy. Soc. Lond., B 208, 57-71.

King, D.G. & Wyman, R.J. (1980). Anatomy of the giant fibre pathway in Drosophila. I. Three thoracic components of the pathway. J. Neurocytol., 9, 753-770.

Levine, J. & Tracey, D. (1973). Structure and function of the giant motoneuron of Drosophila melanogaster. J. Comp. Physiol., 87, 213-235.

Palka, J. (1982). Genetic manipulation of sensory pathways in Drosophila. In Neuronal Development, N.C. Spitzer ed.; New York, Plenum Press, (in press).

Reichardt, W. (1970). The insect eye as a model for analysis of uptake, transduction and processing of optical data in the nervous system. In The Neurosciences, Second Study Program, F.O. Schmitt ed.; New York: Rockefeller University Press, 494-511.

Strausfeld, N.J. & Campos-Ortega, J.A. (1977). Vision in insects: pathways possibly underlying neural adaptation and lateral inhibition. Science, 195, 894-897.

Tanouye, M.A. & Wyman, R.J. (1980). Motor outputs of giant nerve fibre in Drosophila. J. Neurophysiol., 44, 405-421.

Enveloped viruses as experimental tools to study membrane biogenesis and traffic in the animal cell

Members: K. Simons, H. Garoff, A. Helenius*, K. Matlin*

Fellows: S. Fuller*, C. Kondor-Koch, M. Marsh*, G. van Meer*, M. Pesonen, J. White

Student: H. Riedel

Visiting workers: D. Bainton*, N. Genty*, M. Kielian*

Technical assistants: E. Bolzau*, A. Ohlsen, B. Skene*, B. Timm, H. Virta

Until recently the efforts of the group have been concentrated on the study of Semliki Forest virus. The mechanism by which the virus enters its host cell has been elucidated, as has the biogenesis of the particle, especially its membrane. These findings have recently been summarized in a Scientific American article ("How an animal virus gets in and out of its host cell", Simons, Garoff & Helenius, February 1982). Not only have these studies unravelled the life cycle of Semliki Forest virus in its host cell at the molecular level, but the work has also shed light on the general principles governing membrane assembly and membrane traffic in the animal cell. The emphasis of the work is now being shifted to another experimental system. The cell line that has been chosen for study is the MDCK cell, derived from the kidney tubular epithelium. These cells grow as monolayers with their plasma membranes polarized into two domains, the apical surface membrane facing the extracellular medium, separated from the basolateral plasma membrane by a junctional complex encircling the apex of the cell. D. Louvard and his coworkers have shown that these surface domains have different protein compositions. Somehow the cell manages to sort its plasma membrane proteins into the two separate domains. For the study of the sorting process use is being made of the finding of Rodriguez-Boulan and Sabatini that influenza virus (FPV) inserts its surface glycoproteins only into the apical domain of MDCK cells during infection, whereas vesicular stomatitis virus (VSV) directs its membrane glycoproteins to the basolateral membrane. Using these viruses as tools it is hoped to find out where and how the sorting of the apical and basolateral proteins occurs. The first objective has been to map the routes that the virus surface glycoproteins use during their transport through the cell. One approach is to follow the

newly synthesized proteins on their way from their sites of synthesis to their final destinations. Using biochemical and morphological methods it is hoped to find out where in the cell the FPV glycoproteins part from the VSV glycoproteins. Does this occur intracellularly, e.g. in the Golgi apparatus, or at the cell surface? Another approach to the characterization of the sorting process is to follow the endocytotic routes from the two surface domains. Are these separate recycling circuits from the apical and the basolateral cell surfaces, or are they connected? Can proteins inserted into the "wrong" membrane be routed to the right membrane again? To study this problem use is made of the mechanism by which VSV and FPV enter MDCK cells. It has been shown, in collaboration with H. Reggio, that both these viruses make use of a receptor-mediated adsorptive pathway involving coated pits, coated vesicles, endosomes and lysosomes as stations along the route of entry. In the lysosomal compartment a fusion reaction is triggered by the low intra-lysosomal pH between the virus membrane and the lysosomal membrane, which leads to release of the nucleocapsid into the cytoplasm. However, a fusion reaction can also be induced at the cell surface if the extracellular pH is temporarily lowered. In this way the virus membrane can be implanted by fusion either into the apical membrane or, alternatively, into the basolateral membrane. In the latter case the MDCK cells have to be grown on Millipore filters. The basolateral membrane can be reached through the filter, and implantation experiments can be attempted from this side. Thus far the studies made are in too preliminary a stage to give definite answers. It can, however, be said that endocytosis and recycling of the virus proteins take place after implantation. The tools are thus now at hand for the accurate tracing of the membrane traffic to the cell surface.

The apical and the basolateral proteins must carry signals which direct them to their respective destinations. Studies are in progress to identify these signals. This work is being carried out by H. Garoff, C. Kondor-Koch, H. Riedel and B. Timm. The aim is to express cDNA molecules coding for the SFV, VSV and FPV surface glycoproteins in MDCK cells and then to construct genes coding for hybrid molecules, for instance having the external surface domain from an apical protein (FPV) and the internal "cytoplasmic" domain from a basolateral protein (VSV). The virus glycoproteins span the lipid bilayer with one external domain comprising most of the protein, and a small internal C-terminus on the inside of the bilayer connected by a hydrophobic peptide segment 20-30 amino-acids long. It is hoped to identify the portions of the protein molecule

which are recognized by the cellular sorting machinery as apical or basolateral "address tags".

1. Studies using biochemical, immunological and morphological methods have shown that the FPV surface glycoproteins can be detected in the "wrong" membrane (basolateral) during infection. Preliminary studies suggest that the newly synthesized FPV surface glycoproteins might first reach the basolateral membrane before transport to the apical membrane. It is possible that the FPV haemagglutinins are inserted into the basolateral and then sorted to the apical membrane. Some VSV surface glycoprotein can also be detected in the "wrong" membrane (apical) during infection. In this case the explanation might simply be "leaky" sorting. Further studies are being carried out to answer these questions.
2. If VSV or FPV is bound to the apical side of the MDCK cells at 0°C and then subjected to a pH of 5.3 for 20 seconds, virus membranes fuse with the apical plasma membrane. In this way the virus surface proteins and the lipids are implanted into the lipid bilayer of the apical cell surface. The virus proteins do not remain in the surface membrane but are rapidly endocytosed. After 2 minutes they are found inside the cell in membrane vesicles. Ten minutes after implantation the VSV glycoproteins begin to appear on the basolateral side, and some also return to the apical surface. The recycling both to the basolateral and the apical membranes is inhibited by monensin and NH_4Cl . The FPV haemagglutinin also recycles after implantation. The process is also inhibited by monensin and NH_4Cl . We are at present trying to map the routes used by the different virus proteins during recycling.
3. Attempts to implant virus membrane into the basolateral side are only beginning. The MDCK cells grow in a strictly polarized fashion on Millipore filters with different pore sizes and do not require collagen coating. Both VSV and FPV can infect MDCK cells from the basolateral side through the filter.
4. A cDNA expression system has been constructed which is convenient for our purposes. The cDNA is engineered with the aid of oligonucleotide linker molecules into a unique site of an SV40 vector (gift from P. Berg) so that it will be downstream from the early promoter and upstream from RNA processing signals. After replication of the recombinant DNA molecule in E. coli with the aid of plasmid DNA sequences present in the vector part of

the molecule, the DNA is introduced with the aid of a micro-capillary directly into the nucleus of the cell. During the following few hours an efficient transcription and translation takes place in the injected cells, and the proteins expressed from the cDNA can conveniently be analysed by indirect immunofluorescence. The major advantage of this expression system, e.g. in comparison to the lytic SV-40 CV1 cell system, is that it can probably be used in all cells that can be microinjected. There are no size limitations on the cDNA insert and the technique is very rapid, allowing the screening of several cDNA constructions in a single day.

Our expression system has been successfully tested with the cDNA encoding the structural proteins of SFV in baby hamster kidney cells. All structural proteins of SFV were made after injecting the approximately 4 kb coding sequence engineered into the expression vector into the nucleus of the cell. The viral nucleocapsid protein appeared to be released into the cytoplasm of the cell, whereas the viral membrane proteins were inserted into the endoplasmic reticulum and transported to the cell surface.

We are now in the process of making the appropriate DNA constructions to be expressed in the polarized MDCK cell. As basolateral marker protein genes we are using the cDNA encoding the SFV proteins and that containing the VSV G-protein sequences (the latter is a gift from J. Rose). Our apical probes are various cDNA clones coding for influenza haemagglutinins (gifts from W. Fiers, S. Emtage and M.-J. Gething).

Publications during the year

Ansorge, W. & Garoff, H. (1981). DNA sequencing on very thin (0.2 mm) gels. In Electrophoresis '81: ed. Allen, R. C. & Arnaud, P.; Walter de Gruyter, Berlin, p.635-646.

Balcarova, J., Helenius, A. & Simons, K. (1980). Antibody response to spike protein vaccines prepared from Semliki Forest virus. J. Gen. Virol., **53**, 85-92.

Breggeregere, F., Abastado, J.P., Kvist, S., Rask, L., Lallanne, J.L., Garoff, H., Cami, B., Wiman, K., Larhammar, D., Peterson, P.A., Gachelin, G., Kourilsky, P. & Dobberstein, B. (1981). Structure of the C-terminal half of two H-2 antigens deduced from their cloned mRNA sequences. Nature (London), **292**, 78-81.

Garoff, H. (1981). Semliki Forest virus: a model system to study membrane structure and assembly. In Proceedings of the Sigrid Juselius Symposium on Expression of Eukaryotic, Viral or Cellular Genes; Academic, London, p.205-215.

Garoff, H. & Ansorge, W. (1981). Improvements of DNA sequencing gels. Analyt. Biochem., 115, 450-457.

Garoff, H., Kondor-Koch, C. & Riedel, H. (1982). Structure and assembly of alpha viruses: a review. Current topics in microbiology and immunology, (in press).

Garoff, H., Riedel, H. & Lehrach, H. (1982). A procedure to verify an amino acid sequence which has been derived from a nucleotide sequence: Application to the 26s RNA of Semliki Forest virus. Nucl. Acids Res. (in press).

Helenius, A., Marsh, M. & White, J. (1982). Inhibition of Semliki Forest virus penetration by lysosomotropic weak bases. J. Gen. Virol., (in press).

Helenius, A., Sarvas, M. & Simons, K. (1980). Asymmetric and symmetric membrane reconstitution by detergent elimination: studies with Semliki Forest virus spike glycoprotein and penicillinase from the membrane of *B. licheniformis*. Eur. J. Biochem., 116, 27-35.

Kondor-Koch, C. & Garoff, H. (1982). Construction of a hybrid plasmid molecule containing the total coding region of Semliki Forest virus 26S mRNA. J. Gen. Virol., (in press).

Kvist, S., Bregegere, F., Rask, L., Cami, B., Garoff, H., Daniel, F., Wiman, K., Larhammar, D., Abastado, J. P., Gachelin, G., Peterson, P. A., Dobberstein, B. & Kourilsky, P. (1981). A cDNA clone coding for part of a mouse H-2^d major histocompatibility antigen. Proc. Nat. Acad. Sci., USA, 78, 2772-2776.

Kvist, S., Wiman, K., Claessman, L., Peterson, P.A. & Dobberstein, B. (1982). Membrane insertion and oligomeric assembly of HLA-DR histocompatibility antigens. Cell, (in press).

Marsh, M., Matlin, K., Simons, K., Reggio, H., White, J., Kartenbeck, J. & Helenius, A. (1981). Are lysosomes a site of enveloped virus penetration? Cold Spring Harbour Symp. Quant. Biol., 46, "Organisation of the Cytoplasm", (in press).

Matlin, K., Reggio, H., Helenius, A. & Simons, K. (1981). The entry of enveloped viruses into an epithelial cell line. In Membranes in Growth and Development: ed. Giebisch, G.; Alan Liss, New York, (in press).

Matlin, K., Reggio, H., Helenius, A. & Simons, K. (1981). Infectious entry pathway of influenza virus in a canine kidney cell line. J. Cell. Biol., 91, 601-613.

Matlin, K., Reggio, H., Helenius, A. & Simons, K. (1982). The pathway of vesicular stomatitis virus entry leading to infection. J. Mol. Biol., (in press).

Morein, B., Sundquist, S., Höglund, S. Helenius, A. & Simons, K. (1982). Preparation of protein micelles and virosomes from parainfluenza III virus. Protides of Biological Fluids, (in press).

Riedel, H., Lehrach, H. & Garoff, H. (1982). The nucleotide sequence at the junction between the nonstructural and the structural genes of the Semliki Forest virus genome. J. Virol. (in press).

Simons, K., Garoff, H. & Helenius, A. (1982). How an animal virus gets into and out from the host cell. Scientific American, 246, 46-54.

Van Meer, G., Simons, K., Op den Kamp, J. A. F., van Deenen, L. L. M. (1981). Phospholipid asymmetry in Semliki Forest virus grown on baby hamster kidney (BHK-21) cells. Biochemistry, 20, 1974-1981.

White, J. & Helenius, A. (1982). Membrane fusion activity of influenza virus. EMBO Journal, (in press).

White, J., Matlin, K. & Helenius, A. (1981). Cell fusion by Semliki Forest, influenza and vesicular stomatitis virus. J. Cell Biol., 89, 674-679.

Early events in protein secretion and membrane biogenesis

Members: B. Dobberstein, S. Kvist, D. Meyer*

Fellows: D. Meyer*, L. Roberts, J.-H. Xin*

Technical assistants: U. Hellert*, E. Krause

Translocation of proteins across the membrane of the endoplasmic reticulum

D. Meyer, E. Krause, B. Dobberstein (in collaboration with D. Louvard)

Secretory and membrane-spanning proteins are translocated - only partially in the case of membrane proteins - across the membrane of the endoplasmic reticulum. We are studying this mechanism by characterizing membrane components involved in the translocation. Two components have so far been identified and their function and relationship have been studied during the last year.

One component is a large protein complex of about 250,000 daltons composed of six non-identical subunits. It interacts with the membrane via a salt linkage. Walter et al. (1981) have proposed that this complex arrests translation of secretory protein after about 70 amino acids have been polymerized. The block in translation can be relieved when the ribosomal complex consisting of nascent polypeptide chain and complex interacts with the microsomal membranes.

The second component is a membrane-integrated protein of 72 kD from which a soluble 60 kD cytoplasmic-disposed domain can be released by limited treatment with elastase and 0.5M KCl (Meyer & Dobberstein, 1980 a and b). This analysis has been made possible by the use of antibodies raised against the 60 kD fragment (Meyer et al., 1982a).

Both complexes and 60 kD fragment are required for protein translocation to occur and their functions are distinct. The complex is unable to bind to membrane depleted of the 60 kD fragment, but binds, however, in its presence. The fragment can interact with the membrane regardless of the presence of complex. This would suggest that the fragment functions as the membrane receptor for the complex. Also a functional relationship between complex and fragment could

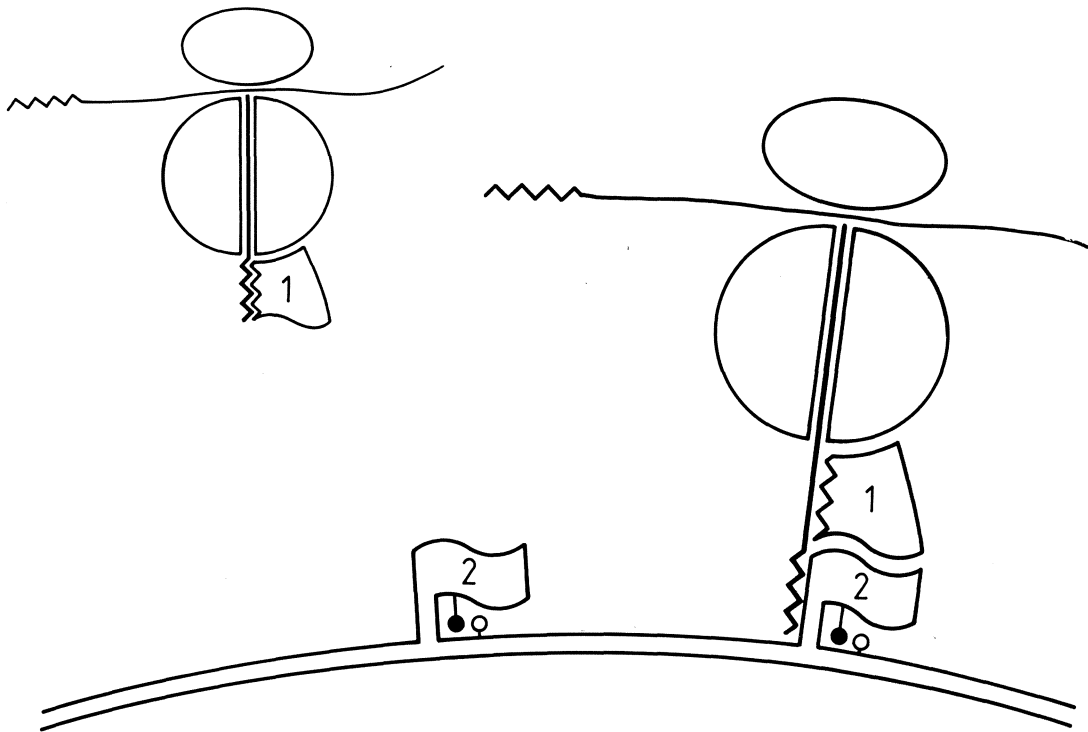


PLATE 5

Early events in the translocation of a secretory protein across the membrane of the endoplasmic reticulum (ER).

Translation of an mRNA coding for a secretory protein starts on a free ribosome. After about 70-80 amino acids have been polymerized and the signal sequence emerges from the large ribosomal subunit, further translation is blocked by the "signal recognition protein" (component 1). This arrest in translation persists until contact is made with the "docking protein" (component 2) which is a 72 kD, ER-specific membrane protein. Translation then resumes and translocation of the nascent polypeptide chain proceeds.

be demonstrated. The arrest of translation as induced by complex can be overcome by the fragment irrespective of the presence of the membrane.

The 60 kD fragment was found to be required for translocation regardless of the source of the cell-free system used, wheat germ or rabbit reticulocyte. The complex was, however, only required when translocation was tested in the wheat germ cell-free system. When the rabbit reticulocyte system was used the complex was not required, and translocation with high efficiency occurred across membranes which were completely depleted of complex. It was found that rabbit reticulocyte lysate contains a protein which performs the function of the complex; it has the same biochemical properties (e.g. it is 250,000 kD in size) and hydrophobic properties, and it arrests translation of secretory proteins.

From our observations, the first steps in the translocation of secretory proteins can be outlined as follows (Plate 5): when synthesis of a secretory protein is initiated on a free ribosome, the 250 kD complex interacts with it and arrests translation after the signal sequence has emerged from the large ribosomal subunit. When complex and initiated ribosome then interact with the 60 kD domain of the 72 kD membrane, protein translation, now coupled to membrane translocation, resumes. Such a mechanism would (1) easily account for the site-specific translocation observed in eukaryotic cells (exclusively across the endoplasmic reticulum) and (2), guarantee that proteins destined for secretion do not accumulate in the cytoplasm. That the 72 kD membrane protein is indeed restricted to the endoplasmic reticulum has been demonstrated by immunofluorescence labelling of epithelial cells. Progress made in the last year on the characterization of membrane proteins involved in translocation will make possible further studies of their molecular structures, and also a characterization of proteins involved in later events of the translocation process.

Characterization of genes coding for major histocompatibility antigens (H-2)

S. Kvist, L. Roberts, J.-H. Xin, U. Hellert, B. Dobberstein (in collaboration with A. Frischauf and H. Lehrach).

Genes located in the major histocompatibility complex (MHC) play a fundamental role in several aspects of the cellular immune response. They code for at least two classes of proteins, class I antigens or transplantation antigens, and H-2K,D,L and class II or immune-associated antigens, Ia in the mouse and HLA-DR in man. A molecular analysis of these antigens and their genes has been approached (1), by studying the biosynthesis and cell surface expression of H-2K, D,L and HLA-DR antigens (Kvist et al., 1982), (2), by isolating and characterizing cDNA clones coding for H-2 antigens (Kvist et al., 1981, Bregegere et al., 1981) and supporting the isolation of a cDNA clone coding for an HLA-DR antigen in P.A. Peterson's laboratory (Wiman et al., 1982) and (3), by characterizing a gene located in the Qa region and one at the K locus of the MHC. Genes located at the H-2K,D,L loci and those at the Qa and Tla regions code for structurally similar antigens: they span the membrane close to their C termini and are non-covalently bound to β_2 -microglobulin.

1. Characterization of cDNAs coding for H-2 antigens

In collaboration with A. Frischauf, three more H-2 specific cDNA clones have been selected and characterized by sequence analysis. They reveal that the number of transplantation antigens is larger than had been previously anticipated. By now cDNA clones coding for five different transplantation antigens have been characterized. Extensive homology is generally found in the coding region and in part of the 3' non-coding region. A non-homologous region in the 3' non-coding region has been identified and one of the cDNAs identified to code for an H-2K^d locus antigen.

2. A gene located in the Qa region of the MHC

In collaboration with the laboratory of H. Lehrach, a gene in the Qa region of the MHC was isolated from a genomic DNA library (DBA 2 mice, d haplotype) and partially characterized by sequence analysis. It shows large homology with that previously characterized by Steinmetz et al. (1981). It contains a charged amino-acid residue in the membrane-spanning portion, and the stop codon TGA following the two basic amino-acid residues thought to flank the membrane-spanning segment on the cytoplasmic side of the membrane.

3. Identification of gene(s) located at the K locus of the MHC

Southern blot analysis of mouse DNA using the coding region of an H-2 cDNA clone as a probe had revealed that genes coding for H-2 like genes constitute a large multigene family. Therefore to characterize a gene from a particular region or locus it was necessary to obtain probes specific for a subgroup of H-2 genes. Such a probe was found to be contained in the 3' non-coding region of one of the cDNA clones (pH-2^d-5). It comprises the 120 nucleotide residues upstream of the stretch of poly A. Using congenic and recombinant congenic mice and Southern blot, at least one gene containing this fragment was mapped to the K locus. It was isolated from a genomic DNA library and is now further characterized by sequence analysis and expression in L cells via transfection.

Publications during the year

Breggeregere, F., Abastado, J.P., Kvist, S., Rask, L., Lallanne, J.L., Garoff, H., Cami, B., Wiman, K., Larhammar, D., Peterson, P.A., Gachelin, G., Kourilsky, P. & Dobberstein, B. (1981). Structure of C-terminal half of two H-2 antigens from cloned mRNA. Nature, 292, 78-81.

Dobberstein, B. & Meyer, D.I. (1982). Protein translocation across the membrane of the endoplasmic reticulum. In Membranes and Transport: A Critical Review, ed. A. Martonosi, Plenum, New York.

Kvist, S., Breggeregere, F., Rask, L., Cami, B., Garoff, H., Daniel, F., Wiman, K., Larhammar, D., Abastado, J.P., Gachelin, G., Peterson, P.A., Dobberstein, B. & Kourilski, P. (1981). cDNA clone coding for part of a mouse H-2^d major histocompatibility antigen. PNAS, 78, 2772-2776.

Kvist, S., Wiman, K., Claessman, L., Peterson, P.A. & Dobberstein, B. (1982). Membrane insertion and oligomeric assembly of HLA-DR histocompatibility antigens. Cell, (in press).

Meyer, D.I., & Dobberstein, B. (1980a). A membrane component essential for vectorial translocation of nascent proteins across the endoplasmic reticulum: requirements for its extraction and reassociation with the membrane. J. Cell Biol., 87, 497-502.

Meyer, D.I., & Dobberstein, B. (1980b). Identification and characterization of a membrane component essential for the translocation of nascent protein across the membrane of the endoplasmic reticulum. J. Cell Biol., 87, 503-508.

Meyer, D.I., Louvard, D. & Dobberstein, B. (1982). Characterization of molecules involved in protein translocation using a specific antibody. J. Cell Biol., (in press).

Meyer, D.I., Kvist, S. & Dobberstein, B. (1982). Assembly of membrane proteins. In Membranes in Growth and Development G. Giebisch, ed. (in press).

Steinmetz, M., Moore, K.W., Frelinger, J.G., Sher, B.T., Shen F.W., Boyse, E.A. & Hood, L. (1981). A pseudo gene homologous to mouse transplantation antigens: transplantation antigens are encoded by eight discrete exons that correlate with protein domains. Cell, 25, 683-692.

Walter, P. & Blobel, G. (1981). Translocation of proteins across the endoplasmic reticulum. III. Signal recognition protein (SRP) causes signal sequence-dependent and site-specific arrest of chain elongation that is released by microsomal membranes. J. Cell Biol., 91, 557-561.

Wiman, K., Larhammar, D., Claesson, L., Gustafsson, K., Schenning, L., Bill, P., Boehme, J., Denaro, M., Dobberstein, B., Hammerling, U., Kvist, S., Serenius, B., Sundelin, J., Peterson, P.A. & Rask, L. (1982). Isolation and identification of a cDNA clone corresponding to an HLA-DR antigen α -chain. PNAS, (in press).

Balbiani rings and giant secretory proteins in Chironomus

Members: J-E. Edström, H. Jäckle

Fellows: J. Cury de Almeida, D. Röhme*

Student: M. Heck*

Visiting workers: J. Girard*, M.M. Green*, C. Grond*, W. Hennig, T. Hertner, H. Kress, T. Moeritz, R. Tanguay

Technicians: M. Andersson*, K. Burvall*, H. Kluding, N. Riedel

The work of the group is devoted to the following areas:

Balbiani rings and giant secretory proteins

Balbiani rings (BR), giant puffs in polytene chromosomes, and their products, the giant secretory proteins of salivary glands of Chironomus, provide an attractive system for studies of gene expression and its control. This is because of (a) the giant size of transcription and translation units which permits correlative chemical and morphological studies (see (1)), (b) the possibilities of controlling the genetic activity in a number of ways (see (2) and (3)), and (c) the giant size of cells and nuclei which facilitates microinjection and following chemical and morphological analysis of coded products of injected macromolecules (see (4)). So far, it has been difficult to obtain genomic clones from the BR. However, the technical problems are now being solved (see (5)). The group is in particular interested in understanding the functional significance of the quantitatively prominent switches between different giant secretory proteins during certain types of defined metabolic stress. Work is proceeding along the following lines:

1. A discrete class of giant polysomes has been studied by Miller spreads, characterized by about 75 actively translating ribosomes followed at the 3' end by a small group of terminal ribosomes after completed translation (Plate 6) (Francke et al., in press). On the basis of previous biochemical work it can be concluded that the polysomes are likely to represent the translation units for giant mRNA from the large Balbiani rings BR1 and BR2 and produce a polypeptide with a molecular weight about 10^6 .

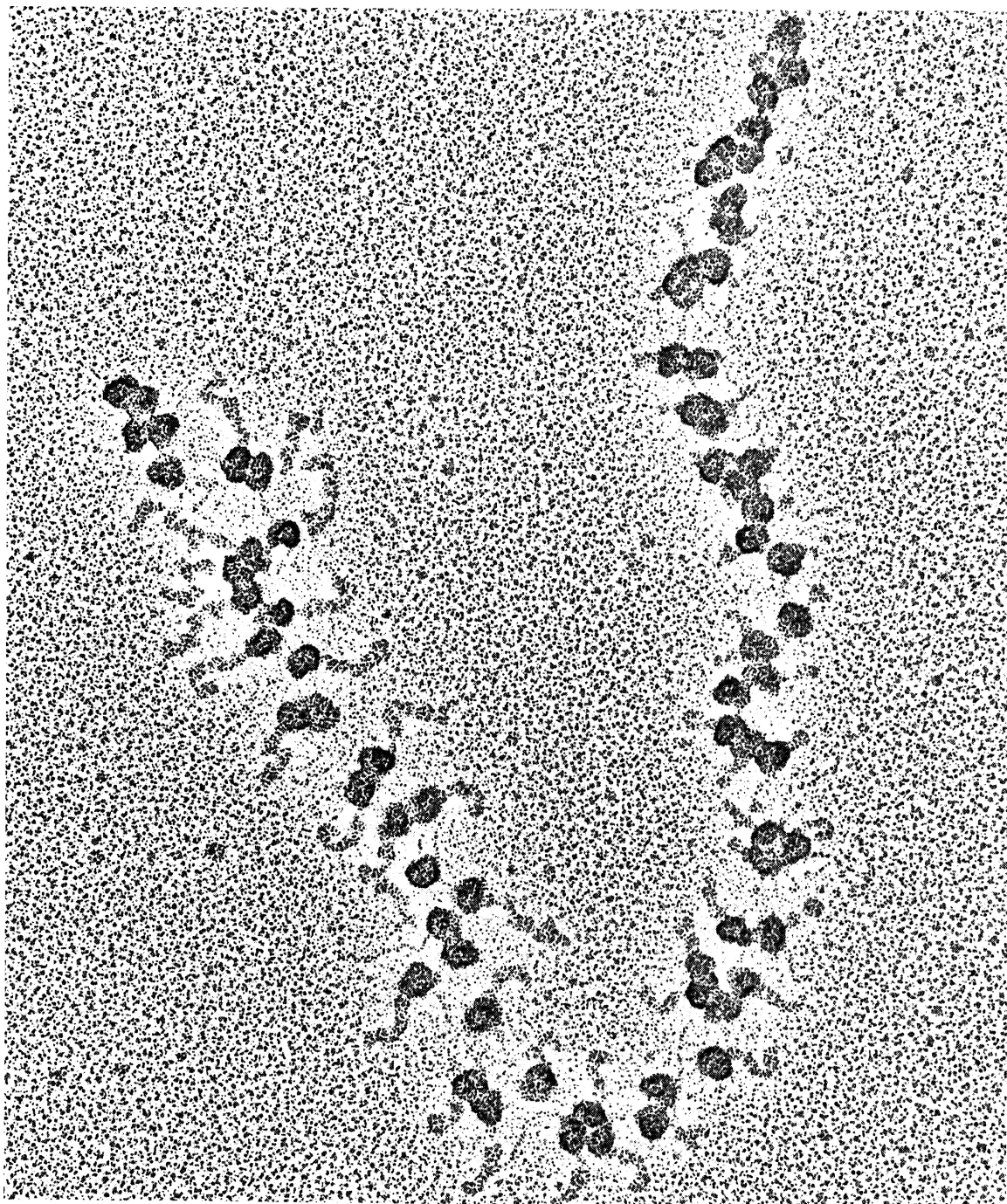


PLATE 6

Miller-spread polysome from lysed Chironomus salivary glands containing 74 ribosomes of which 4 have finished translation but remain attached to the mRNA. This polysome provides a direct morphological demonstration of the putative translation unit for mRNA from Balbiani ring 1 and 2. Magnification 139,000 times. From Francke et al. (in press).

Further work aims towards complete in vitro translation of the giant mRNAs.

2. The unique size of the translation units for the main class of differentiated products permits their differential inhibition with very low doses of cycloheximide. Such treatment leads to a doubling of cellular ATP levels and ATP/ADP ratios, and the migration of the mitochondria from the cell periphery towards the interior of the cell, corresponding to a cytoplasmic organization typical for early developmental stages (Thyberg et al., in press). Recent work has established that this treatment also leads to a differential inhibition of the transcription in BR1 and BR2 and tests are carried out with intracytoplasmic and intranuclear injections to learn whether this effect is mediated by the increased ATP levels.
3. A number of compounds like galactose, glycerol and ethanol dramatically shift the production of giant secretory protein from the normally dominant component towards a new giant species. This switch may encompass a quarter of the total cellular protein synthesis. This reaction is accompanied by changes in BR development and transcription of giant RNAs, and correlated with a decrease in inorganic phosphate. These changes can be reversed or prevented by administration of phosphate (Edström et al., in press). The reaction is likely to be an adaptation to changed metabolic conditions. Work on the amino acid composition carried out elsewhere and ongoing nucleotide sequencing of the relevant genes is required as a guide for further investigations on the functional significance of this genetic switch.
4. A system for testing transcriptional activity of circularized BR genes is currently being worked out. The approach is based on a technique (Scaleghe et al., 1981) for isolating the DNA from microdissected chromosome segments. Such DNA is restricted and ligated and used directly for injection into salivary gland nuclei. Several restriction enzymes leave the BR genes intact owing to their repetitive sequences. Miller spreads are carried out on the contents of the isolated nuclear sap after in vitro culture of the glands. This test system should permit analysis of control levels in BR gene switches and studies of the build-up of active and inactive chromatin from physiologically relevant DNA. A possible extension of this study is the mapping

of transcriptional units in microdissected chromosome segments. Parallel work is planned with intracytoplasmic injections of BR-mRNAs. Advantage will be taken of the fact that different related species produce giant proteins that can be distinguished electrophoretically.

5. Genomic clones from different BR's will be produced and one 1.3 kb large BR2 clone is now being characterized. It will be desirable to extend clones towards flanking sequences, possibly with the aid of mini-libraries obtained with the microcloning technique.

The mammalian Y-chromosome

There is increasing support for the idea that the spread of new genes during evolution may be dependent on (asymmetric) gene conversion. If so the Y-chromosome DNA occupies a unique position since the Y-chromosome largely or entirely lacks a homologous segment. It is possible, therefore, that Y-specific evolving DNA only exists in small amounts if at all. This proposition is being tested in two species with DNA clones from manually isolated chromosomes. Our results so far show that clones several kb in size from the Y-chromosome are present not only in male DNA, but also, at lower multiplicities, in female DNA. Further work aims towards establishing the origin of these sequences (X chromosome vs autosomes) and locating them to Y-chromosome regions (euchromatin vs heterochromatin).

Microtechniques

The group has been interested in extending the use of the microcloning technique (Scalenghe et al., 1981), which was originally worked out for polytene chromosomes, to other material like lampbrush loops and mammalian chromosomes. Both applications function well and the technique will now also be tried in collaboration with H. Lehrach for a selected part of a mammalian chromosome, i.e. the region of the mouse chromosome 17 encompassing the H2 antigen and T loci. Another extension of the technique which is realistic and has been tried in collaboration with S. Gerbi and U. Scheer is to use the micro-extracted DNA directly for electron microscopy. Polytene chromosomes offer many structures of interest for such applications. Collaboration has been carried out with a number of groups to obtain cloned DNA from a variety of sources as listed below:

<u>Material</u>	<u>Principal Investigator</u>
<u>Drosophila</u> Y-chromosome loops	W. Hennig, Nijmegen
<u>Drosophila</u> tip of 2L (giant,-lethal)	O. Schmidt, Freiburg
<u>Drosophila</u> tip of X (yellow)	M.M. Green, Davis, California
<u>Drosophila</u> 74EF-75B (ecdysen loci)	O. Pongs, Bochum
<u>Drosophila</u> (polycomb region)	J. Lauer, Edinburgh
<u>Sciara</u> DNA puffs	S. Gerbi, Brown Un., R.I.
<u>Chironomus</u> globin loci	M. Tichy, MPI Tübingen
<u>Chironomus</u> I-18C (ecdysen puff)	M. Lezzi, Zürich
<u>Drosophila</u> 5S RNA locus	K. Kress, München

Publications during the year

Edström, J.E., Sierakowska, H. & Burvall, H. (1982). Dependence of Balbiani ring induction in Chironomus salivary glands on inorganic phosphate. Develop. Biol., (in press).

Francke, C., Edström, J.-E., McDowall, A.W. & Miller, O.L. (1982). Electron microscopic visualization of a discrete class of giant translation units in salivary gland cells of Chironomus tentans, EMBO Journal, (in press).

Scalenghe, F., Turco, E., Edström, J.-E., Pirrotta, V. & Melli, M. (1981). Microdissection and cloning of DNA from a specific region of Drosophila melanogaster polytene chromosomes. Chromosoma, **82**, 205-216.

Tanguay, R. & Vincent, M. (1982). Intracellular translocation of cellular and heat shock induced proteins upon heat shock in Drosophila Kc cells. Can. J. Biochem., (in press).

Thyberg, J., Sierakowska, H., Edström, J.-E., Burvall, K. & Pigon, A. (1982). Mitochondrial distribution and ATP levels in Chironomus salivary glands as related to growth,

metabolic activity, and atmospheric oxygen tension.
Develop. Biol., (in press).

Other reference

Scalenghe, F., Turco, E., Edström, J.E., Pirrotta, V. and Melli, M. (1981) Microdissection and cloning of DNA from a specific region of Drosophila melanogaster chromosomes, Chromosoma 82, 205-216.

Gene expression and its control

Members: K. Murray, A.R. Dunn

Fellows: N.M. Gough, R. Perez-Mellado, U. Reif*

Visitors: R. Koshy*, M. Viola*

Technical assistants: D. Hubsch, H. Krischke

Studies of gene expression have continued on both histone and viral antigen genes. Histone genes are of interest both for their product and for control of expression. The viral antigen genes are also of interest in relation to the regulation of their expression, particularly in connection with their involvement in host cell transformation.

Histone genes from sea urchins and yeast have been cloned in both plasmid and bacteriophage λ vectors and propagated in E.coli. The principal objective behind these experiments is the production of histones in E.coli so that specific mutant genes can be engineered to give a range of derivatives that will enable the approaches of biochemical genetics to be directed to the analysis of histone function. Histone genes were therefore placed in bacteriophage λ vectors so that their expression could be controlled by λ promoters. Sites for the binding of E.coli RNA polymerase and the initiation of transcription in vitro were located in the DNA by electron microscopy and these experiments showed that promoter-like sites occurred within the cloned DNA. Analysis of the transcription products after infection of E.coli with the recombinant phages confirmed that these sites would function in vivo and showed that the histone genes were also transcribed from the λ P_L promoter. The results permitted the construction of a transcription map of the sea urchin gene cluster, but translation of the transcripts in vivo could not be demonstrated (Mellado et al. 1981). The yeast H3 gene (of which the parent organism has only two copies; M.M. Smith & K. Murray, submitted for publication) has been transferred from the phage λ vector in which it was isolated to a plasmid, pR1-8 carrying part of the gene for β -galactosidase fused to the gene for the core antigen of hepatitis B virus (Stahl et al., 1982). In these constructions the intention was to utilize the sequences controlling transcription and initiation of translation of the β -galactosidase gene which function efficiently in E.coli by fusing the initial part of this gene to the

histone H3 gene. The new DNA molecules were engineered so that their expression products would comprise a short region from the amino-terminus of β -galactosidase linked to the H3 sequence from which either the first two or first sixteen amino acid residues had been eliminated. These hybrid genes were transcribed in E.coli cultures harbouring the relevant plasmids, but, as with the original recombinants carrying histone genes, translation products could not be detected in the transformed cells. However, in an in vitro system for coupled transcription and translation derived from E.coli the hybrid genes gave rise to polypeptides of the anticipated molecular weight. When these polypeptides were analysed by the Edman degradation method, radioactively labelled methionine and lysine residues were found in the predicted positions within the first 24 amino acid residues in each case (R.P. Mellado & K. Murray, submitted for publication). These results indicate that a major difficulty in the expression of histone genes in E.coli could be instability of the polypeptides in vivo, a problem that is being encountered increasingly frequently with the expression of eukaryotic genes in bacteria.

Transformation of mammalian cells. Evidence from a number of viral systems suggests that only a few viral gene functions are involved in the changes accompanying neoplastic transformation of mammalian cells by DNA tumour viruses. In an attempt to identify some of these genes and to study the changes that they induce in the host cell, cloned segments of SV40 antigen genes have been introduced into mutant lines of rat cells by co-transformation with the selectable thymidine kinase gene of herpes simplex virus. Examination of independently derived lines of transformants by indirect immunofluorescence with antisera against SV40 T antigen showed extreme heterogeneity in the levels of intranuclear T antigen. The same cells were analysed, again by immunofluorescence, for the expression of a host cell gene product, the 53k protein, which has been reported to exist as a complex with T antigen. A double-label antibody method was used to show that the cells expressing T antigen exhibited a virtually precise correspondence, both qualitatively and quantitatively, in 53k protein synthesis. When these cells were seeded at low density and allowed to develop there was a marked heterogeneity in the morphology of individual islands of cells; some colonies appeared typical of morphologically transformed cells, while others appeared normal or, occasionally, mosaic. The same heterogeneity in viral antigen expression and cell morphology was observed when the cells were passaged under soft agar which is known to

depend upon T antigen expression. Analysis of the cell lines for integrated viral genes revealed that each cell line contained between ten and twenty intact copies of the early region of the SV40 genome. Investigation of the regulation of these genes and the relationship of this expression to the transformed phenotype will be continued by A.R. Dunn at the Ludwig Institute in Melbourne.

Hepatitis B virus (HBV) poses a major threat to public health throughout the world. Some claim that it is the world's largest single cause of viraemia and there is a strong correlation between histories of HBV infection and chronic liver disease, including primary hepatocellular carcinoma. Normally, the virus infects only humans and some higher apes and there is no satisfactory tissue culture system for propagation of the virus. Recently a similar virus has been found in some rodent species and in the Peking duck, but all the viruses have an absolute host specificity. Little is known at present of the life cycle of HBV or of its interaction with its host, although viral genomic sequences have been shown to be integrated into the DNA of some hepatoma cell lines (Brechot et al., 1980; Chakraborty et al., 1980).

HBV has a small DNA genome which has been cloned in E.coli and some of the viral genes can be expressed in E.coli (Burrell et al., 1979; MacKay et al., 1981a). The surface antigen of the virus, HBsAg, carries group and sub-type determinants and is found not only as part of the virus, but also as a particulate aggregate in plasma of infected individuals. Removal of the surface antigen from the virus leaves a core particle, 27 nm in diameter, which consists of the core antigen, HBcAg, and the genome of the virus. The virus also has a DNA-dependent DNA polymerase and a third antigen, the e antigen, HBeAg, which is found not only in preparations of the virus, but also free or associated with other proteins in plasma and liver. Recently, it has been established that HBeAg is derived from HBcAg (MacKay et al., 1981b). Determination of the nucleotide sequence of the cloned DNA revealed the organization of the viral genome (Pasek et al., 1979), but this information alone is insufficient to establish all of the HBV gene products, the regions from which the genes are transcribed, and the sequences that control their expression. In addition to the genes for HBcAg, HBsAg and (tentatively) the viral DNA polymerase, the nucleotide sequence contains an open translational reading frame giving a polypeptide of 156 residues which is not at present known; this sequence is designated gene X. Some of

the recombinant plasmids of HBV and pBR322 have been used as substrates for transcription with various cell free extracts, including HeLa cell extracts, but these experiments have not established a clear transcription map and have not yet enabled sequences controlling expression to be located.

Some of the cloned HBV recombinants isolated previously (Burrell *et al.*, 1979) contained segments of HBV DNA greater than unit genome length. One of these, containing some 15% more than the normal HBV genome, has been used for the construction of further recombinants containing two or four copies of the HBV genome in a tandem head-to-tail arrangement. The recombinant containing the tetrameric HBV genome has been introduced into thymidine kinase (TK) mutant rat fibroblast cells by co-transformation with the herpes simplex virus TK gene as a selectable marker. Several transformants were analysed for the presence of HBV DNA and the expression of the viral antigens, and one which contained multiple copies of the HBV genome was examined in detail. This cell line synthesized both HBsAg and HBeAg but HBcAg could not be detected. However, since HBeAg can be derived from HBcAg by mild proteolysis (MacKay *et al.*, 1981b), the production of HBeAg indicates expression of the gene for HBcAg. Analysis of the RNA produced in these cells showed the presence of at least three abundant species of polyadenylated mRNA which hybridized with HBV DNA, and one of them was a transcript of gene X. Since it has been reported that mouse L cells containing dimers of the HBV genome synthesize HBsAg, but neither HBcAg nor HBeAg (Dubois *et al.*, 1980), the recombinant carrying the tetrameric HBV genome was introduced into TK mutant L cells by co-transformation and one transformant was isolated that produced both HBsAg and HBeAg (but no detectable HBcAg). This suggests that a multimeric HBV genome may be necessary for HBeAg biosynthesis. While the mechanism for HBeAg production from the HBcAg gene is unknown, one reason for the requirement of a multimeric HBV genome could be that a mature mRNA for HBeAg (or HBcAg) is processed from a precursor that contains repeated transcripts of the entire genome, such as that described for the late mRNAs of polyoma virus (Treisman, 1980). It is of particular interest, therefore, that one of the abundant mRNA species from the transformed rat cell is some 1000 nucleotides longer than the HBV genome.

A study of the integration of HBV DNA sequences into the host genome in hepatoma cell lines is being continued in collaboration with P.-H. Hofschneider and his colleagues R.

Koshy and A. von Loringhoven von Freytag (M.P.I. Martinsried). Digests of DNA from the cells have been cloned in phage λ vectors and one of the clones containing HBV DNA sequences is being used for nucleotide sequence determination. The points of immediate interest are the sequences at the sites of integration and the extent of the HBV sequence included.

HBcAg synthesized in E.coli is found in aggregated form in cell extracts and it cross-reacts efficiently with antibodies to HBcAg; it is also a good immunogen (Stahl et al., 1982). Precipitates of crude extracts with antibodies to HBcAg were examined in the electron microscope by J. Richmond and B.J. Cohen (Public Health Service Laboratory, London) who observed well-defined particles, diameter 27 nm, which closely resembled HBV core particles extracted from human liver (unpublished observations communicated by J.R. and B.J.C.). These particles contain nucleic acid and are being examined further as part of a study (with H. Delius) of the interaction between HBcAg and DNA in relation to HBV morphogenesis.

Publications during the year

Gough, N.M. (1981). The rearrangements of immunoglobulin genes. Trends in Biochemical Sciences, 6, 203-205.

Gough, N.M. (1981). Gene rearrangements can extinguish as well as activate and Diversify immunoglobulin genes. Trends in Biochemical Sciences, 6, 300-302.

Mellado, R.P., Delius, H., Klein, B. & Murray, K. (1981). Transcription of sea urchin histone genes in Escherichia coli. Nucleic Acids Research, 9, 3889-3906.

Murray (1981). The expression of hepatitis B virus genes in Escherichia coli. In Biological Products for Viral Diseases. Proc. Sixth Munich Symposium on Microbiology, Ed. P.A. Bachmann, London; Taylor and Francis, p. 45-69.

Other references

Brechot, C., Pourcel, C., Louise, A., Rain, B. & Tiollais, P. (1980). Nature (London), 286, 533-535.

Burrell, C.J., MacKay, P., Greenaway, P.J., Hofschneider, P.-H. & Murray, K. (1979). Nature (London), 279, 43-47.

Chakraborty, P.R., Ruiz-Opazo, N., Shouval, D. & Shafritz, D.A. (1980). Nature (London), 286, 531-533.

Dubois, M.-F., Pourcel, C., Rousset, S., Chany, C. & Tiollais, P. (1980). Proc. Natl. Acad. Sci. USA, 77, 4549-4553.

MacKay, P., Pasek, M., Magazin, M., Kovacic, R.T., Allet, B., Stahl, S., Gilbert, W., Schaller, H., Bruce, S.A., & Murray, K. (1981a). Proc. Natl. Acad. Sci. USA, 78, 4510-4514.

MacKay, P., Lees, J. & Murray, K. (1981b). J. Med. Virol., 8, 237-243.

Mellado, R.P., Delius, H., Klein, B. & Murray, K. (1981). Nucleic Acids Research, 9, 3889-3906.

Pasek, M., Goto, T., Gilbert, W., Zink, B., Schaller, H., MacKay, P., Leadbetter, G. & Murray, K. (1979). Nature (London), 282, 575-579.

Stahl, S., MacKay, P., Magazin, M., Bruce, S.A. & Murray, K. (1982). Proc. Natl. Acad. Sci. USA, 79, in press.

Treisman, R. (1980). Nucleic Acids Research, 8, 4867-4888.

Molecular genetics of prokaryotes

Member: N.E. Murray, G. Cesareni

Fellow: R.M. Lacatena*

Student: F. Pace*

Visitors: *L. Bullas*, G. Churchward*, J.S. Parkinson*, A. van Putten

Technical assistants: J. Gough, H. Senior

This group is studying DNA replication and the specificity of bacterial restriction and modification systems via a combination of genetic and molecular approaches. We also continue to improve cloning systems.

Genetic analysis of replication

One of our interests concerns the control of initiation of DNA replication in bacteria. Our model system is a family of small multicopy plasmids related to the colicinogenic plasmid ColE1.

We have characterized two molecular mechanisms that regulate plasmid copy number by modulating the amount of primer available for initiation of DNA synthesis by DNA polymerase I.

The first mechanism is mediated by a small RNA molecule (RNA 1) which in vitro inhibits the processing of the primer by the enzyme RNAase H (Tomizawa et al., 1981). We have shown that a series of mutations that affect the sensitivity of the target to the wild type RNA 1 map in the region that codes for RNA 1. Thus the target of RNA 1 coincides with part of its coding sequence (Cesareni, 1981). From the analysis of the phenotype of these mutants we conclude that a mutation in the target of this repression system causes a complementary alteration of the inhibitor itself so that the control mechanism remains functional despite a change in specificity. These properties are consistent with a repression mechanism dependent on base pairing between complementary nucleic acids. Sequence analysis of these mutants suggested that RNA 1 controls initiation of plasmid replication via base

pairing of the central loop of its clover-leaf structure with the complementary sequence in the primer precursor. (Lacatena & Cesareni, 1981).

We have recently characterized a second independent regulatory circuit that participates in the control of plasmid copy-number (Twigg & Sherratt, 1980). By the construction of fusions in which the β -galactosidase enzyme is synthesized under the control of the promoter of the primer precursor we were able to prove that transcription starting from this promoter is under the negative control of a trans-acting gene. This gene, which we called rop for repressor of primer, maps in a region that codes for a polypeptide of 63 aminoacids whose sequence is exactly conserved in the two plasmids ColE1 and pMB1. Our results suggest that the rop gene product participates in the regulation of ColE1 replication by limiting the amount of primer precursor available for RNase H processing.

Host specificity (hsd) systems

Restriction and modification enzymes exemplify an important class of proteins that recognize specific DNA sequences. The restriction endonucleases encoded by chromosomal genes of E.coli are particularly complex and, in contrast to many other restriction enzymes, do not break DNA at specific targets. Nevertheless, these systems retain sequence specificity in that modification is the methylation of a specific DNA sequence. Information relevant to DNA sequence-specificity resides within the subunit determined by the hsdS gene (Boyer & Roulland-Dussoix, 1969; Arber & Linn, 1969; Hubacek & Glover, 1970). Thus a hybrid protein having polypeptides determined by the hsdM and R genes of E.coli K and the hsdS gene of E.coli B has B-specificity. The nucleotide sequence recognized by E.coli K and B are now known to be closely related.

We have cloned the hsd genes of E.coli K12 (Sain & Murray, 1980) and deduced the order of the three closely linked genes and their positions relative to restriction targets. Defined parts of the hsd genes have been subcloned in plasmids and used as probes to detect homologous DNA sequences in bacterial DNAs. Natural isolates of E.coli, and related enteric bacteria, have provided a reservoir of host specificity systems. At least three allelic systems have been detected in E.coli strains and two in Salmonella spp. Each recognizes a different nucleotide sequence and yet each retains homology with the hsdS gene of E.coli K12.

We have determined the DNA sequence of the hsdS gene of E.coli K12 and are now obtaining sequences for the hsdS genes conferring alternative specificities. In the case of the two Salmonella spp, genetic evidence (Bullas et al., 1976) suggests a new substrate specificity as the result of genetic recombination. Comparative DNA sequences of the various hsdS genes should aid the understanding of both protein-DNA interactions and evolutionary diversification.

Only a minority of the natural isolates of E.coli analysed have hsd genes sharing homology with those of E.coli K12, but preliminary evidence suggests that an alternative family of specificities, related to that of E.coli A, is frequently present.

Lambda cloning vectors

In collaboration with H. Lehrach and A.-M. Frischauf we have made improved vectors suitable for the selective cloning of large (20kb) fragments of DNA. They are derivatives of the BamHI vector of Karn et al. (1980) in which the plasmid sequence has been replaced by DNA from E.coli, the EcoRI targets removed, and polylinkers substituted for the BamHI targets flanking the central, replaceable, fragment. Each polylinker carries the recognition sequences for the enzymes SalI, BamHI and EcoRI. In vector EMBL 3 the polylinkers are oriented with the SalI sites outermost while in EMBL 4 the linkers are in the alternative orientation (see Plate 10, H. Lehrach and A.-M. Frischauf).

Publications during the year

Cesareni, G., Castagnoli, L. & Lacatena, R.M. (1981). Genetic analysis of pMB1 replication. In: Structure and DNA-protein interaction of replication origins. ICN-UCLA Symp. Mol. Cell. Biol. eds. Dan S. Ray and C.F. Fox. Academic Press. New York. Vol XXI, 143-155.

Cesareni, G. (1981). The target of the negative regulator of pMB1 replication overlaps with part of the repressor coding sequence. Mol.Gen. Genet. 184, 40-45.

Lacatena, R. & Cesareni, G. (1981). Base pairing of RNA1 with its complementary sequence in the primer precursor inhibits ColE1 replication. Nature 292, 623-626.

Murray, N.E. Phage and molecular cloning. In: "The Bacteriophage Lambda". Vol. II. Cold Spring Harbor. (in press).

Other references

Arber, W. & Linn, S. (1969). Ann. Rev. Biochem., 38, 467-500.

Boyer, H.W. & Roulland-Dussoix, D. (1969). J. Mol. Biol., 41, 459-472.

Bullas, L.R., Colson, C. & van Pel, A.V. (1976). J. Gen. Microb., 95, 166-172.

Hubacek, J. & Glover, S.W. (1970). J. Mol. Biol., 50, 111-127.

Karn, K., Brenner, S., Barnett, L. & Cesareni, G. (1980). Proc. Natl. Acad. Sci. USA, 77, 5172-5176.

Tomizawa, J., Itoh, T., Selzer, G. & Som, T. (1981). Proc. Natl. Acad. Sci. USA, 78, 1421-1425.

Twigg, A.J. & Sherratt, D. (1980). Nature, 283, 216-218.

Drosophila gene organization and expression

Members: V. Pirrotta, J. Burckhardt*

Fellows: C. Hadfield, K. Kaiser*, M.C. Mariol*, J. Perera*,
G. Pretorius*, A. Spena

Students: C. Mariani*, H. Steller*, C. Tschudi*

Visiting workers: M. Fontés*, J.F. Julien*, E. Mohier*, A.
Viotti

Technical Assisants: Ch. Bröckl*, J. Telford

Developmental gene regulation

Our study of the expression of genes specific for certain developmental stages of Drosophila has produced a number of molecular clones. Some of these correspond to genes specifically expressed in early embryonic development, others were selected for expression in the dorsal hypoderm of late embryonic or larval stages. We are now studying some of these clones in more detail.

One of the early embryonic clones is localized at 17E in the X chromosome, in the vicinity of the fused locus which affects segmental polarity. We have examined the expression of this clone during development and have cloned its surrounding genomic context. X-ray mutagenesis produced new fused alleles. In one of these mutants, one of the genomic restriction fragments corresponding to our clone is altered, suggesting that this fragment is related to the fused gene.

Another clone whose sequence is expressed in the dorsal hypoderm of late embryos is localized at 23C in the second chromosome. We are now attempting to identify the region responsible for the development control of its expression. The clone contains at least two other independently regulated transcription units. One of these is a copia element. The ability of this element to insert or excise from a genomic site has given rise to polymorphisms in the DNA of this region within our Oregon R population. We can isolate at least four different variants: with copia, without copia, and with different deletions in the region immediately adjacent to one side of the copia element.

The 5S RNA gene cluster

Another region containing extensive polymorphisms is the 5S RNA gene cluster. One Oregon R population called OreR Yale shows a variety of different arrangements of this region. We have studied cloned fragments from a particular variant and have shown that the alteration is due to the insertion of a copia-like element belonging to the B104 gene family. The host of other rearrangements found in the same region in the population suggests that, as in the 23C locus, the insertion or excision of a copia-like element can generate a variety of deletions of flanking sequences and lead to polymorphisms.

The B104 gene family

We have studied in some detail the B104 element itself, which we originally discovered because it is specifically expressed during embryogenesis. It constitutes a highly repeated gene family, present in about 80 copies in the Oregon R genome. The sequence of cDNA clones corresponding to this element shows that transcription initiates and terminates within the terminal repeats which flank the element. The transcript produced is terminally redundant and analogous to the RNA of vertebrate retroviruses with which it shares other sequence features.

The B104 sequence, like that of copia, 412 and other Drosophila repetitive elements, is found in the population of minicircles present in Drosophila nuclei. We find that minicircles extracted from embryos are on the average much smaller than those reported to be in tissue culture cells. Only partial B104 or copia sequences are found in embryonic minicircles. The terminal repeats are frequently missing and the sequence is scrambled with itself and with other sequences. Whether or not these minicircles are the products of excision, in embryos they undergo extensive rearrangements and are unlikely to be able to become reinserted into the genome.

Microdissection and cloning of chromosome fragments

The microtechnique we developed with F. Scalenghe, E. Turco and J.E. Edström has been improved. The resolution has been increased, as well as the overall efficiency and the average size of the DNA inserted in each clone. Cloned fragments now range up to 10 kb in length, averaging more than 3 kb. Using suitable vectors, both EcoRI and HindIII

clones can be obtained, allowing us in principle to obtain overlaps between cloned fragments without recourse to a total genomic clone library. We have used the technique to isolate clones from a variety of chromosomal loci, in collaboration with other laboratories. In particular, we have constructed a minilibrary of microdissection clones which nearly saturates the population of clonable fragments from the 3C region of the X chromosome. We have used this to screen phage and cosmid libraries to obtain overlapping clones which now allow us to map a large part of the 3C region.

Zein genes from maize

In collaboration with A. Viotti of the Istituto Biosintesi Vegetali, Milano, we have isolated a collection of zein cDNA clones and identified among them four major classes of zein sequences. We have then isolated corresponding genomic clones and have begun to characterize them. Electron microscopy (with H. Delius) and DNA sequencing of full-length cDNA clones showed that the two ends of the cDNA contain extensive inverted repeats. The inverted repeated region at the 5' end includes several dozen T residues as well as 30-70 nucleotides complementary to the 3' sequence immediately preceding the 3' poly-A tail. Is this an artefact of the cDNA cloning procedure? The first results from the sequence of a corresponding genomic clone indicates that an imperfect inverted repeat exists at the corresponding positions. The poly-T tail at the 5' end of the cDNA, on the other hand, is absent from the genomic sequence and is probably an artefact resulting from the presence of the inverted repeat.

Publications during the year

F. Scalenghe, E. Turco, J.E. Edström, V. Pirrotta & M. Melli (1981). Microdissection and cloning of DNA from a specific region of Drosophila melanogaster polytene chromosomes. Chromosoma, **82** 205-216.

G. Scherer, J. Telford, C. Baldari & V. Pirrotta (1981). Isolation of cloned genes differentially expressed at early and late stages of Drosophila embryonic development. Develop. Biol., **86**, 438-447.

C. Tschudi & V. Pirrotta (1982). The 5S RNA genes of Drosophila melanogaster. The Cell Nucleus vol. X, H. Busch ed., (in press).

A. Viotti, D. Abildsten, N. Pogna, E. Sala & V. Pirrotta (1982). Multiplicity and diversity of cloned zein cDNA sequences and their chromosomal localization. EMBO J., (in press).

Dosage compensation in Drosophila melanogaster. Hybrids between different species of Drosophila

Member: L. Sanchez *

Technical assistant: W. Hilscher *

Dosage compensation in Drosophila melanogaster

In Drosophila melanogaster the ratio of the X chromosomes to sets of autosomes (X:A) determines sex determination and dosage compensation. Dosage compensation is a process whereby the amounts of many X-linked gene products are equalized in male and female flies, in spite of the fact that only a single copy of each X-linked gene is present in males (X:2A) whereas two copies are present in females (2X:2A). By means of this process, a balance is achieved between the autosomal gene products and the X-linked gene products. Dosage compensation in Drosophila melanogaster does not operate by the mammalian mechanism of inactivating one of the two X chromosomes in females; on the contrary, in Drosophila melanogaster both X chromosomes remain active in female flies.

The achievement of dosage compensation takes place at the transcriptional level: the transcription rate per gene in X:2A flies is twice the transcription rate per gene in 2X:2A flies. All this means that dosage compensation constitutes a good model for studying the regulation of gene activity in eukaryotic organisms.

It is worth stressing that dosage compensation (the rate of transcription of X-linked genes) depends on the X:A ratio, and is independent of sex per se. This is found, for example, in 2X:2A flies that are homozygous for transformer (tra), an autosomal mutation that in homozygous flies transforms 2X:2A flies into phenotypically normal (although sterile) males and has no effect on X:2A flies. In 2X: 2A (tra/tra) "pseudonormals", the transcription rate of the X-linked genes is the same as in 2X:2A females, but not the same as in X:2A male flies. It is believed that the X: A ratio signal is passed on to certain genes by setting up their state of activity in an alternative way: those genes that are active in X:2A flies are inactive in 2X:2A flies, and vice versa. These genes can be divided into two classes: sex-determining genes and genes involved in dosage compensation. These being different genes, the result is

that mutations in the sex-determining genes do not affect dosage compensation, and mutations affecting dosage compensation do not transform sex.

The group is interested in the genetic basis of the mechanism that brings about dosage compensation in Drosophila melanogaster. For this, it is necessary to search for mutations that modify the process. Mutagenesis is being used to isolate sex-specific lethal mutants that express the lethal phenotype according to the X:A ratio, independently of sex. At the same time, a study is being made of the genetic basis of the X:A ratio.

Hybrids between different species of Drosophila

Those biological properties of organisms which prevent gene exchange are called reproductive isolating mechanisms (RIMs), and they can be classified into two categories, prezygotic and postzygotic. Prezygotic RIMs prevent the formation of hybrid zygotes between different species, and postzygotic RIMs reduce the viability or the fertility of the hybrid zygotes. The establishment of RIMs between organisms that constitute a single gene pool (one species) gives rise to the formation of new gene pools (new species) that will evolve independently. Speciation, the process by which one species splits into two or more species, is brought about by the formation of barriers against gene exchange, i.e. by the establishment of RIMs. Little is known about the genetic and molecular bases of RIMs. We are doing experiments to analyse some of these.

1. Hybrid sterility

- a) The cross of D.simulans females with D.mauritiana males produces fertile hybrid females but sterile males. Since crossing-over takes place in the hybrid females, it is possible to characterize the gene(s) responsible for the hybrid sterility of the males. D.simulans females, with markers in the three major chromosomes (X, 2 and 3) will be crossed to wild type D.mauritiana males. The hybrid females will be heterozygous for all genetic markers. These females will be back-crossed to D.simulans males that carry the same genetic markers as the parental females, and the F_2 males will be checked for their phenotype as well as tested for their fertility.

- b) The gonad of Drosophila consists of two components, the soma and the germ line. Gametogenesis requires the interaction of the both tissues. By transplantation of pole cells in Drosophila, it became possible to study problems of sterility and to determine whether it is due to the soma or to the germ cells, or to an interaction of the two. Transplantation of pole cells between species might answer the following questions: (1) what are the causes of sterility in the hybrids between different species?, (2) can the soma of one species support normal development of the germ cells of another species? Furthermore, transplantation of pole cells between different species may constitute a way of producing hybrids between species that do not interbreed. (These experiments are being carried out in collaboration with H. Schmidt in the laboratory of Prof. R. Noethinger, University of Zürich.)

2. Hybrid lethality

The cross between D.melanogaster females and D.simulans males produces only hybrid females, the rare males that appear being patroclinous. The cross of D. simulans females to D.melanogaster males produces hybrid males and sometimes a few hybrid females. We are analysing this hybrid lethal phenotype. At present we are studying the possible existence of a lethal focus by using gynandromorphs. In addition, in view of the central role that the D.melanogaster X-chromosome plays in hybrid lethality, we are carrying out experiments to study the contribution of defined regions of the X-chromosome to hybrid lethality by means of clonal analysis.

Organization of middle repetitive sequences in the human genome: functional and structural aspects

Member: M. Melli

Fellow: E. Ullu

Students: L. Dente*, V. Esposito

Visiting workers: A. Fantoni*, E. Ginelli*, G. Spinelli*

Technical assistant: S. Murphy

Approximately 20% of the human genome is made of interspersed repetitive DNA sequences, with a reiteration frequency varying from 100- to 1×10^6 -fold. The known repeated genes account for a minor proportion of the sequences while the majority of them have still not been assigned a biological function. Although RNA complementary to repeated DNA is found in the cells, it is not clear whether this RNA has a function and what this function might be. The proportion of the total repetitive fraction of the genome coding for RNA is also unknown. Historically it is possible to distinguish two different schools of thought concerning the evolution and significance of eukaryotic repeated DNA. One, put forward by Davidson & Britten (1969), proposes an important regulatory role for such sequences, and the second, proposed thematically by Doolittle & Sapienza (1980) and Orgel & Crick (1980), suggests that repeated DNA has no function and that its conservation in evolution might be accidental, owing to the fact that this DNA, although not useful, is not harmful and therefore not selected against. The recent development of cloning and sequencing techniques has made possible a detailed description of the structure of some repetitive sequences and a precise definition of their relationship to cellular RNA. We have been analysing two species of small RNAs called 7SL and 7SK found respectively in the cytoplasm and nucleus of most organisms so far examined. The main observations are relevant to the problem of the organization and function of middle repetitive sequences in eukaryotes and can be summarized as follows. (1) Both RNA species are derived from families of middle repetitive sequences in closely and distantly related species. The sequences of the cytoplasmic and nuclear components are completely different although both are characterized by unusually high GC content. The sequence of the 7SL RNA has a composite structure and consists of a 140-nucleotide middle repetitive sequence inserted in an Alu sequence.

(2) The sequence of the 7SL RNA is highly conserved in evolution in distantly related species, such as amphibians and echinoderms. The 7SK sequence seems to be somewhat less conserved. (3) The evolutionary conservation of 7S RNA as well as its cellular location strongly suggests a structural role for both RNAs. The general picture emerging from these and other data (van Arsdel et al., 1981; Haynes & Jelinek, 1981), which also shows that several discrete cytoplasmic and nuclear RNA species are derived from middle repetitive DNA, permits a better definition of the role of several families of interspersed repeated sequences. It appears that for each repeated family examined, one or more members are coding for distinct RNA species, often found as ribonucleoproteins, which do not code for proteins, and the function of which is not yet understood. On this view the non-coding members of the families could be considered as pseudogenes. Formally this situation does not seem different from that of other structural genes, for example the globin genes which are unique in their coding properties but are found as small families of repeated genes when the pseudogenes are taken into account. Furthermore the pseudogenes can be interspersed or found within the major globin clusters. Ultimately the major difference between these two classes of genes could simply be the genomic frequency, which is always higher for the so-called repeated genes. As to the conservation of these sequences, it is at least as high or higher than that of the globin genes, suggesting that the high frequency distribution does not hinder whatever correction mechanism might be responsible for sequence conservation.

Cloning and characterization of cDNA copies of 7S RNAs of HeLa cells

We have cloned cDNA copies of in vitro adenylated 7S RNA of HeLa cells (Ullu & Melli, submitted for publication). The most representative clones in the library contain DNA fragments copied from 7SL and 7SK small RNAs. The two classes of recombinants show no homology. The cloned fragments are respectively 303 (7L) and 315 (7K) base pairs long, and closely correspond to the length of the 7SL and 7SK RNAs. Sequence analysis shows that the 7L DNA has a composite structure. A central block of 140 bp is homologous to a new set of human middle repetitive sequences, called the S family (from Sau3a, the restriction endonuclease which can excise the fragment). The 5'- and 3'- end flanking blocks are homologous to the Alu family of repeated DNA. Deininger et al., (1981) have recently

defined an Alu consensus sequence by cloning and sequencing the rapidly renaturing fractions of human DNA. The consensus is present twice in a dimeric structure approximately 300 bp long. The alignment of the 7L DNA sequence with the homologous portions of the Alu consensus sequence (Deininger et al., 1981) shows that 100 bp at the 5'-end and 40 bp at the 3'-end of the 7S molecule are strongly homologous to the left and right Alu monomers. Two 6 bp direct repeats are found at the junctions between the Alu flanking sequences and the central element. The striking similarity between the right half of the Alu consensus sequence and the 7L DNA which disappears abruptly and resumes in coincidence with the presence of short direct repeats, suggests that the sequence might be the result of insertion of the 140 bp fragment in a member of the Alu family. Since the frequency distribution in the haploid genome of the Alu and S family DNAs differs by 2-3 orders of magnitude, this type of structure is an example of the interspersion of middle with highly repetitive DNA. Restriction mapping and sequencing of a number of 7L DNA clones shows the presence of microheterogeneity in the 5'-end Alu block (Ullu et al., submitted for publication). This finding is consistent with the existence of more than one gene coding for 7SL RNA.

The sequence of 7 K DNA shows no homology with Alu DNA but a similar GC content. Southern blot analysis of human placenta DNA also indicates that the 7 K DNA derives from a family of repeated sequences (the K family) with rather low frequency distribution, comparable to that of the S family.

We have now isolated a number of genomic clones containing 7K and L DNA from a human recombinant DNA library and the analysis of the recombinants is in progress.

Cellular location of the 7SL and K RNA sequences

The existing data on the cellular location and possible function of the 7S RNAs are contradictory. The two RNAs have been variously reported to be cytoplasmic, nuclear, polysome- microsome- or membrane-bound in considerable disagreement between different laboratories (Walker et al., 1974; Zieve & Penman, 1976; Gunning et al., 1981a and b; Reddy et al., 1981). We have now carried out a precise study on the location of the two RNAs, using the cDNA clones as hybridization probes. By using a number of techniques which allow the fractionation of different cellular components we have made the following

observations. The 7S K RNA is found exclusively bound to the nuclear matrix and not to nuclear ribonucleoproteins. The use of non-ionic detergents for cell lysis or nuclear purification produces a leakage of the RNA from the nucleus into the cytoplasm, which might explain the different reports mentioned above.

The 7SL RNA is essentially cytoplasmic and is bound to polysomes in the absence of detergent treatment. When protein synthesis is inhibited in vivo by agents (e.g. Na fluoride) which promote the run-off of ribosomes, the 7SL RNA remains attached to the cytoskeleton together with mRNA. Since the binding to cytoskeleton and polysomes is easily disrupted by detergent treatment, it is probably mediated by a protein. This is in agreement with the finding of 7S RNA in ribonucleoprotein particles. The seemingly precise organization of the two RNA species within the cell suggests a defined function that, in the case of 7SL RNA, might be related to the attachment of the polysomes to the cytoskeleton. In a similar approach we are now examining the location of the two RNAs in the mouse erythroid system at early developmental stages and during the cell cycle in synchronized tissue culture cells. In both situations the cell undergoes considerable structural changes which might give an indication of the function of these RNAs.

Evolutionary conservation of the 7SL and K RNAs

The cross-hybridization of 7L DNA to the cytoplasmic RNA and genomic DNA of rodents, birds, amphibians, echinoderms and slime moulds suggests high conservation of both sequence components.

The 7K sequence is somewhat less conserved, since it is not found in the genome of sea urchins or Dictyostelium discoideum. The evolutionary conservation of these RNAs, as well as their presence in all the species examined, suggests a universal role which might be structural. These data show that, in these families of repeated sequences, the members which have a gene function must be under evolutionary constraint and this might explain the evolutionary stability of at least some of the middle repetitive DNA.

Publications during the year

Scalenghe, F., Turco, E., Edström, J.-E., Pirrotta, V. & Melli, M. (1981). Microdissection and cloning of DNA from a specific region of Drosophila melanogaster polytene chromosomes. Chromosoma, 82, 205-216.

Ullu, E. & Melli, M. (1982). Cloning and characterization of cDNA copies of the 7S RNAs of HeLa cells. Nucl. Acid Res., (in press).

Ullu, E., Murphy, S. & Melli, M. (1982). Human 7SL RNA consists of a 140 nucleotide middle repetitive sequence inserted in an Alu sequence. Cell, (in press).

Other references

Davidson, E.H. & Britten, R.J. (1969). Science, 204, 1052-1056.

Deininger, P.S., Jolly, D.J., Rubin, C.M., Friedmann, T. & Schmid, C.W. (1981). J. Mol. Biol., 151, 17-33.

Doolittle, W.F. & Safienza, C. (1980). Nature, 284, 601-603.

Gunning, P.W., Shooter, E.M., Austin, L. & Jeffrey, P.L. (1981a). J. Biol. Chem., 256, 6663-6669.

Gunning, P.W., Béquin, P., Shooter, E.M., Austin, L. & Jeffrey, P.L. (1981b). J. Biol. Chem., 256, 6670-6675.

Haynes, S.R. & Jelinek, W.R. (1981). Proc. Natl. Acad. Sci. USA, 78, 6130-6134.

Orgel, L.E. & Crick, F.H.C. (1980). Nature, 284, 604-606.

Reddy, R., Li, W.-Y., Henning, D., Choi, Y.C., Nohga, K. & Busch, H. (1981). J. Biol. Chem., 256, 8452-8457.

Van Arsdell, S.W., Deinson, R.A., Bernstein, C.B., Weiner, A.M., Mansert, T. & Gesteland, R.F. (1981). Cell, 26, 11-17.

Walker, T.A., Pace, N.R., Erikson, R.L., Erikson, E. & Behr, F. (1974). Proc. Natl. Acad. Sci. USA, 71, 3390-3394.

Zieve, G. & Penman, S. (1976). Cell, 8, 19-31.

Genetic studies of restriction and modification enzymes

Member: M. Zabeau

Student: L. Bougueleret

Technical assistant: C. Kurz*

The main interest of this group is directed towards the problem of how proteins recognize specific sequences in DNA. Sequence specific protein-DNA interactions lie at the heart of important biological processes such as the regulation of gene expression, DNA replication and DNA rearrangements. Recent advances (Anderson et al., 1981; McKay & Steitz, 1981) in structural studies of specific protein-DNA complexes have yielded considerable insight into their overall structure but have so far failed to elucidate the nature of the molecular interactions involved in site-specific recognition. It is precisely this question that we would like to address in our study of bacterial restriction endonucleases and modification methylases, which are known to recognize short well-defined nucleotide sequences. Our molecular genetic approach takes advantage of the recent progress in in vitro gene manipulation technology to develop genetic selection systems for isolating mutations which alter the sequence recognition properties of these enzymes. Correlation of the alterations in protein structure and the changes in sequence specificity should then allow one to identify the amino acid residues responsible for the recognition of the different bases within the target sequence. The fact that companion restriction and modification enzymes recognize exactly the same sequence provides a unique opportunity to study how two different enzymes interact with a given sequence. Further conclusions on the generality - or diversity - of these interactions can be reached by examining other restriction and modification systems. For these studies, we have chosen the well-characterized Escherichia coli enzymes EcoRI. Recently we have initiated a parallel investigation of the newly discovered EcoRV restriction and modification system (Kholmina et al., 1980), which recognizes the target sequence GATATC, closely resembling that of EcoRI, GAATTC.

In our previous report we have described in detail the rationale of our genetic approach. In summary, our strategy for isolating mutant restriction enzymes with altered sequence specificity takes advantage of the fact that such

mutations are expected to be deleterious to the cell: indeed, the companion methylase, which recognizes the same target sequence as the endonuclease, plays an essential role in protecting the cell's own chromosome against restriction enzyme cleavage. Restriction enzyme specificity mutants should thus degrade the cellular chromosome and kill the cell. Such a strategy requires that one must be able to control adequately the expression of the endonuclease enzyme in the cell, so that the mutants can be propagated safely by repressing gene expression. The mutant phenotype can be detected by scoring mutants which are lethal upon induction of enzyme synthesis. To develop such a genetic system, we first manipulated the EcoRI restriction and modification system by cloning the endonuclease and methylase genes separately into plasmid and phage vectors. Subsequently we have used plasmid expression vectors carrying the P_R promoter of phage λ to bring the expression of the endonuclease gene under the control of this easily regulatable promoter. The detailed genetic and biochemical studies of these promoter-endonuclease fusion plasmids, reported below, has provided us considerable insight into the behaviour of this genetic system, and has paved the way for a successful search for specificity mutations. We have also examined in more detail the pleiotrophic properties of mutant EcoRI endonucleases in which the amino-terminus of the cro protein is fused to the EcoRI endonuclease. These mutants not only display a subtle specificity alteration, but exhibit quite different in vivo properties.

As a result of our contacts with the membrane groups of G. Warren, D. Louvard and F. Winkler on the cloning of the clathrin gene, we decided to develop a novel strategy to clone genes coding for proteins for which antibodies are available. This approach, outlined in detail in the report of K. Stanley on page 153, necessitated the construction of a novel β -galactosidase expression vector in which DNA fragments are inserted within a functional lacZ gene. The polypeptide segments specified by the inserted fragments can then be expressed and detected immunologically as part of a β -galactosidase fusion protein. As will be described in detail below, the construction of these expression vectors enabled us to improve considerably the existing β -galactosidase vectors. These plasmids in addition provide an elegant system for improving the structure of expression vectors in general, and should be most useful for the large-scale synthesis of proteins for structural studies.

Studies on the EcoRI system

As we pointed out in last year's Report, the fusion of the EcoRI endonuclease gene to the P_R promoter yielded two types of recombinant plasmids. The first produces a wild-type RI endonuclease, while the second directs the synthesis of a fusion protein in which the first 22 amino acids of the phage λ cro gene are fused to the intact, or slightly shortened, endonuclease gene. In both plasmids the expression of the endonuclease is entirely controlled by the λ P_R promoter, and is repressed in strains which produce the λ cI repressor. By using temperature-sensitive cI repressor mutants, the expression can be experimentally controlled by growing the cells at either low (repressed) or high (induced) temperatures. The initial studies revealed that the two types of plasmids exhibited clearly distinct genetic properties. As a prelude to the isolation of endonuclease mutants, we have further analysed these properties so as to get a better insight into the genetic behaviour of the system.

The most surprising property of the first type of plasmid is that, despite the fact that they overproduce RI endonuclease some 10 to 30 fold, they fail to kill the cell when endonuclease synthesis is induced in RI methylase-deficient strains (see Plate 7). Measurement of the levels of endonuclease synthesized upon induction revealed that methylase-deficient strains produce much lower levels (2-10%) than methylase-proficient strains. Manipulation of the P_R -endonuclease plasmids showed that the mutant cI gene carried by the same plasmid was responsible for the inefficient induction of endonuclease synthesis. Plasmids in which this cI gene is deleted now efficiently kill methylase-deficient strains upon induction. Biochemical analysis of the structure of the chromosomal DNA confirmed that cell killing indeed results from an extensive degradation of the chromosomal DNA.

These studies demonstrate that endonuclease-mediated cell killing is not an all-or-nothing phenomenon but is dependent upon the level of endonuclease activity in the cell. In the presence of low, but appreciable, levels of endonuclease, the cells can remain perfectly viable, while a 10-fold increase will prevent cell growth. Introduction of the P_R -endonuclease plasmids in repressor-producing, methylase-deficient recA strains revealed that the recA mutation markedly reduces the viability. Since the recA function plays a key role in DNA repair processes, we conclude that wild-type E.coli strains are capable of

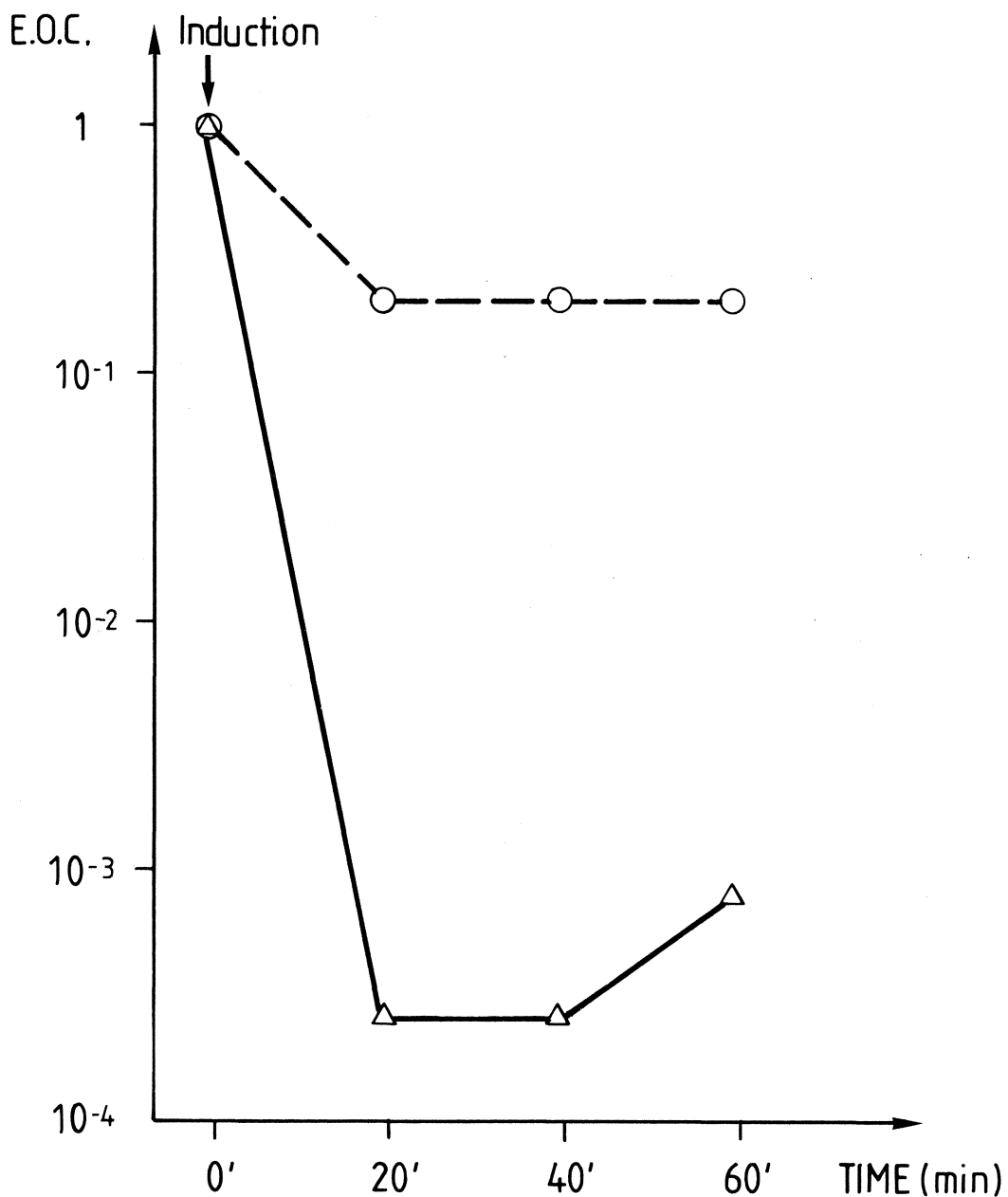


PLATE 7

Quantitative analysis of cell killing upon induction of EcoRI endonuclease in a strain which does not carry the EcoRI methylase. The slow killing (broken line) results from induction of wild-type RI endonuclease, while the fast killing (solid line) was produced by induction of the cro-endonuclease fusion enzyme. e.o.c.: efficiency of colony formation.

repairing endonuclease-induced lesions (single or double stranded breaks). RecA⁻ strains should thus be more sensitive host strains for isolating specificity mutations which would be overlooked in wild-type E.coli strains. Finally, the study of recA⁻ strains carrying the P_R endonuclease plasmids illustrated the importance of efficient repression of endonuclease synthesis: low repressor-producing strains clearly grow more slowly than high level producing strains. Incomplete repression of endonuclease synthesis could thus constitute a strong counterselection against highly deleterious mutants. In summary, these studies have enabled us to evaluate the importance of the different parameters, endonuclease synthesis level, repression efficiency and genetic background of the host strain, for future mutant selection experiments. It is clear that in order to find the mutants of interest different selection conditions will have to be used.

The mutant EcoRI endonuclease enzymes produced by fusing the amino-terminal part of the cro protein to an intact or slightly shortened RI endonuclease display quite remarkable genetic and biochemical properties. First, we have detected a subtle modification in the sequence specificity: in vitro studies show that although these enzymes still produce the same complete digest patterns as the wild-type enzyme, the appearance of partial-digest fragments is quite different. These findings indicate that while the main sequence specificity remains unaffected, the preferential recognition of one target site over another is entirely different from the wild-type enzyme. This alteration, however, cannot account for the observed genetic phenotypes: 1) an enhanced cell-killing activity and 2) a reduced capacity to restrict phages. While strains which do not possess the RI methylase can grow in the presence of low levels of wild-type RI endonuclease, derivatives carrying the cro-endonuclease fusions consistently grow more slowly or do not grow at all (see Plate 7). Since the levels of endonuclease produced by the two types of P_R endonuclease plasmids are similar, the enhanced cell-killing activity must be a property of the fusion protein itself. Analysis of the phage restriction properties of strains producing different cro-endonuclease fusions of the endonuclease protein is essential for in vivo restriction of unmodified DNA: fusion proteins which have lost the first 10 amino acids no longer restrict phage λ , while fusions retaining this segment still restrict, albeit with reduced efficiency. We interpret these results to mean that the activity of the RI endonuclease in the cell is not freely distributed in the cytoplasm, but is somehow

topographically confined through interactions involving that the altered topographical distribution of the enzyme is also responsible for the enhanced cell killing property of these mutants. If true, this would raise the exciting prospect that restriction endonucleases are subject to a dual mode of control: 1) the companion methylase protects the target sites for the enzyme on the chromosome, and 2) topographical confinement further prevents the endonuclease from accidentally attacking non-methylated sites on the chromosome, and at the same time enables the enzyme to degrade incoming foreign DNA efficiently. To confirm this exciting hypothesis, we are at present isolating point mutants which specifically affect the topographical distribution of the enzyme.

In the course of manipulating the original plasmids carrying the P_R -endonuclease gene fusion, we observed that deletion of redundant promoter distal sequences influenced negatively the stability of the plasmids. Similar observations were made in the construction of the β -galactosidase expression vectors (see below). In this case, we have found that this disturbing effect can be overcome by inserting transcription termination signals downstream of the gene. Consequently, we are now using these terminator-carrying plasmids to construct new P_R endonuclease plasmids. In addition, we have re-engineered the restriction sites flanking the gene so that these plasmids are now well suited for a regional in vitro mutagenesis of the endonuclease gene: specific segments of the gene can be isolated by restriction enzyme cleavage, mutagenized in vitro, and reintroduced into the plasmids. In this way, specific portions of the gene can be mutagenized and readily characterized by nucleotide sequence analysis.

Characterization of the EcoRV system

As pointed out earlier, the newly discovered E.coli EcoRV restriction and modification system (Kholmina et al., 1980) provides a most interesting alternative to address the problem of sequence specific recognition. In this project we intend to follow an approach similar to that used in the study of EcoRI so that we can take maximal advantage of our previous experience. The original E.coli strain carrying the EcoRV restriction and modification system harbours at least 4 different plasmids, one of which carries the EcoRV genes. We have cloned the EcoRV plasmid by transforming the mixture of plasmid DNAs into strain K514 and using a phage selection procedure to isolate restricting transformants.

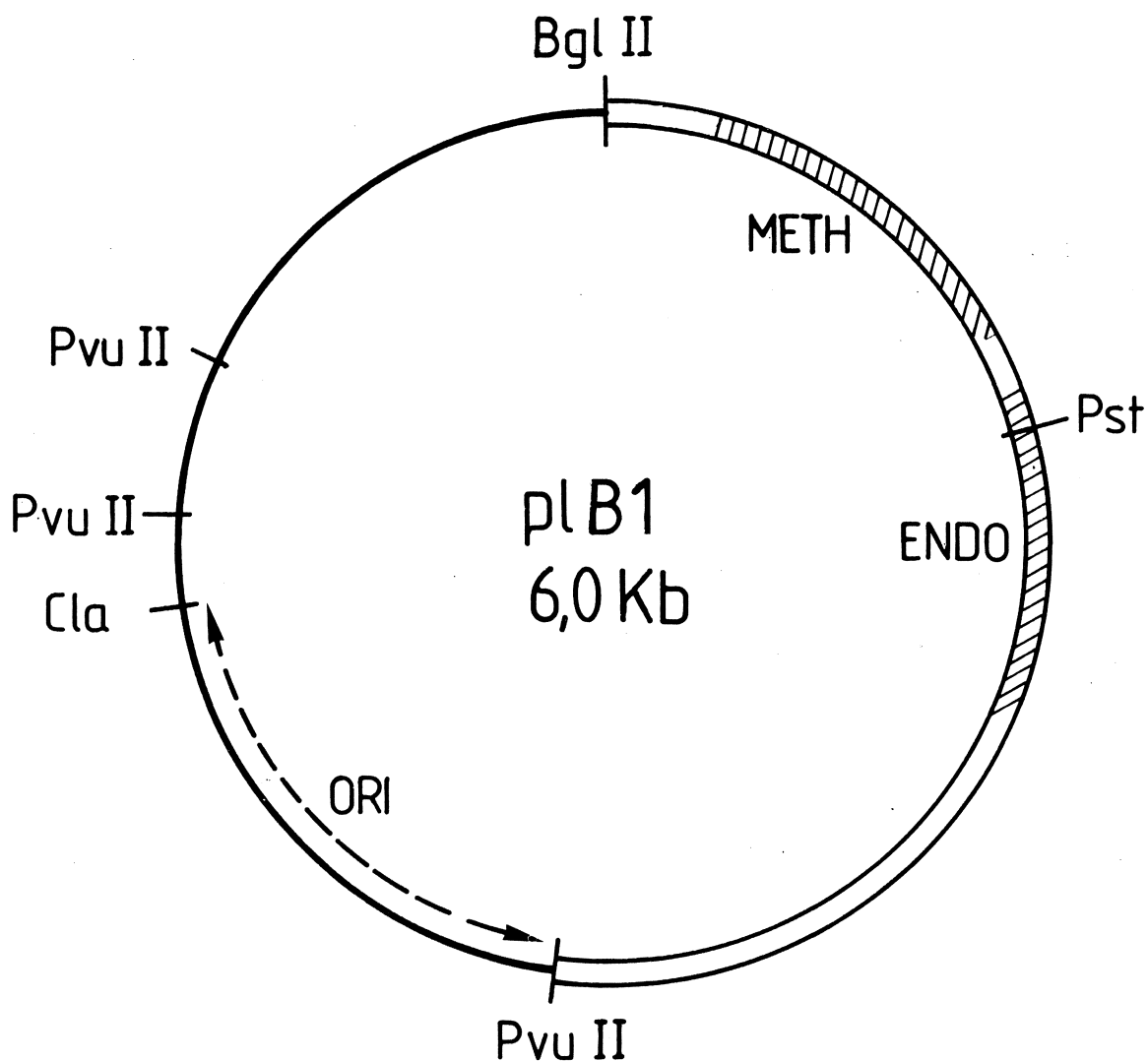


PLATE 8

Genetic and physical map of the EcoRV plasmid pLB1. The boxed segment represents the PvuII-BglIII fragment which was cloned in pBR322 and which carries the EcoRV gene. The shaded areas indicate the approximate positions of the endonuclease (endo) and methylase (meth) genes. The broken line denoted ORI represents the segment which is homologous to the origin of replication region of pBR322.

Transformants expressing EcoRV restriction were found to carry a 6 kb plasmid (pLB1), which apart from the EcoRV restriction and modification system carried no other identifiable gene. A primary restriction map of this plasmid is presented in Plate 8. The unique sites for Pst, ClaI and BglII were used to cointegrate this plasmid into pBR322. The ClaI and BglII cointegrates expressed the EcoRV restriction and modification while the Pst cointegrate had lost the restriction but not the modification function, indicating that the Pst site was located within the endonuclease gene. Subsequent cloning of a 3.1 kb Pvu II-BglII fragment (see Plate 8) in pBR322 revealed that it contained all the genetic information for EcoRV restriction and modification. Finally, we have mapped the relative positions of the two genes and their approximate boundaries by isolating deletion mutants produced by resecting DNA sequences from the PvuII site with the nuclease Bal31. Experiments are in progress to overproduce the EcoRV endonuclease and methylase enzymes by cloning the genes into appropriate expression vectors. In this way large quantities of the enzymes can be obtained for structural studies which will be pursued by the group of F. Winkler.

The mere fact that the two E.coli type II restriction and modification systems recognize related target sequences (RI:GAATTC; RV:GATATC) suggested that the two systems might be genetically related. To test this possibility the group of H. Delius has analysed heteroduplexes made between different RI- and RV- carrying plasmid DNAs. While experiments have thus far failed to uncover sequence homology between the EcoRI and EcoRV genes, two other regions of homology were discovered. One region of homology, 1.3 kb long, covers the origin of replication, indicating that both restriction systems are carried by a similar type of plasmid. The second homologous region lies immediately adjacent to the EcoRI and EcoRV genes. The significance of this homology is at present unclear since this region apparently has no function in the EcoRI restriction and modification system.

The development of improved expression vectors.

The design of the novel cloning strategy, outlined in the introduction, and described in more detail in the report of K. Stanley on page 153, necessitated the construction of a β -galactosidase expression vector in which cloned DNA segments can be transcribed and translated so as to yield fusion proteins consisting of foreign polypeptides joined to an active β -galactosidase enzyme. In this construction

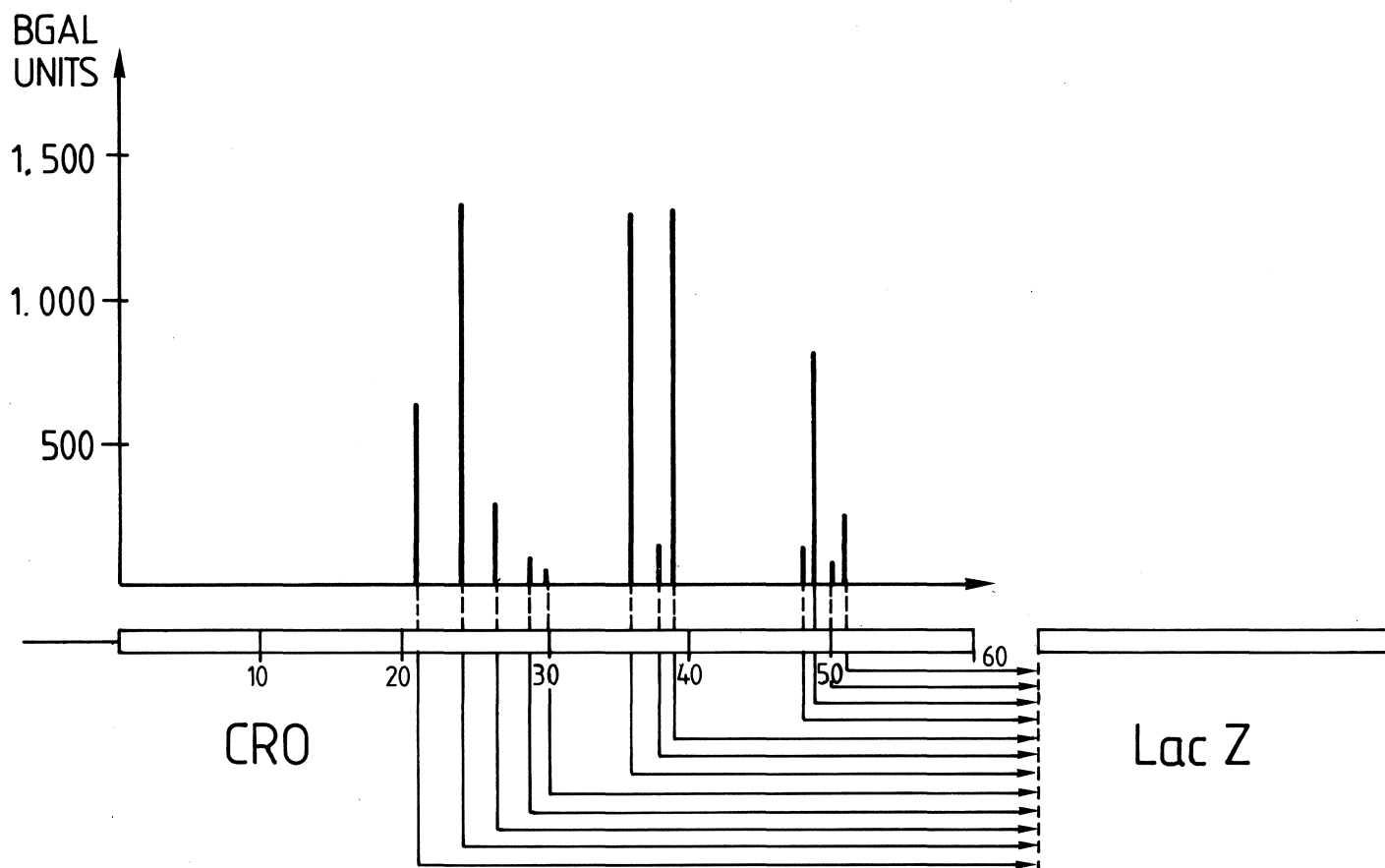


PLATE 9

Physical map of the *cro-lacZ* fusions, and the corresponding β -galactosidase levels. The dotted line represents the position of fusion within the *cro* gene. The distances indicate the number of base pairs from the start of the *cro* gene. The vertical bars represent the units of β -galactosidase synthesized after 1 h of induction.

we have modified the β -galactosidase expression vectors which are currently used to fuse amino-terminal segments of proteins to an active β -galactosidase enzyme (Guarente et al., 1980). The newly developed vector was obtained by fusing the P_R promoter and the amino-terminus of the cro gene to the lacZ gene fragment. The plasmids carrying the cro-lacZ gene fusion retain a unique restriction enzyme cleavage site between the two gene segments in which DNA segments can be inserted. In this construction we took advantage of the fact that by using cl repressor-producing strains, gene fusions could be isolated under conditions where the gene is not expressed. Furthermore a collection of different cro-lacZ fusions was obtained by fusing a randomly resected cro gene segment to the lacZ fragment. The analysis of the levels of β -galactosidase produced by different fusions, presented in Plate 9, clearly shows that there is no apparent correlation between the level of β -galactosidase synthesis and the position of the fusion point within the cro gene. Subsequent nucleotide sequence analysis of the fusion points revealed that high level producer plasmids carry an in-phase fusion of the cro and lacZ genes, while out-of-phase gene fusions only produce low levels of β -galactosidase. The study of frame shift mutations obtained by inserting oligonucleotide linkers between the cro and lacZ genes demonstrated that this low level of β -galactosidase synthesis results from an artefactual translation initiation within the lacZ gene segment.

Much to our surprise, we found that all strains carrying high producer plasmids (but not those carrying low producers) failed to grow under conditions of constitutive β -galactosidase expression. Further manipulation of the plasmids revealed that the lacY gene segment located downstream of the lacZ gene was responsible for this growth inhibition. Deletion of this region allows normal growth of the strains. Under these conditions, however, the plasmids are rapidly lost in the absence of antibiotic selection. Since we had previously observed similar phenomena with certain P_R endonuclease plasmids, we concluded that plasmid curing might be due to an inhibitory effect of the strong P_R promoter on plasmid replication. To test this possibility, we have inserted transcription termination signals downstream of the lacZ gene in order to block the strong transcription wave originating from the P_R promoter. Using a small 100 bp terminator fragment of phage fd, we were able to solve the curing problem to a considerable extent, though not completely. We are at present testing the effects of other terminator fragments.

In conclusion, the newly developed β -galactosidase expression vectors provide a most convenient system for optimizing the structure of plasmid expression vectors in general. New expression vectors derived from the lacZ plasmids in which other genes can be inserted and hyperexpressed are at present being constructed. These improved vectors should prove most useful for the overproduction of proteins such as restriction and modification enzymes for structural studies in the laboratory. Finally, as outlined in the report by K. Stanley on page 153, the newly developed lacZ expression vectors, in which antigenic determinants of foreign proteins can be fused to β -galactosidase, open new exciting perspectives for the study of protein structure and function.

References

Anderson, W.F., Ohlendorf, D.H., Takeda, Y. & Matthews, B.M. (1981). Nature, 290, 754-758.

Guarente, L., Lauer, G., Roberts, T.M. & Ptashne, M. (1980). Cell, 20, 543-553.

Kholmina, G.V., Rebentish, B.A., Skoblov, Yu.S., Mironov, A.A., Yankovskii, N.K., Kozlov, Yu. I., Glatman, L.I., Moroz, A.F. & Debabov, V.G. (1980). Dokl. Akad. Nauk. SSSR, 253, 495-497.

McKay, D.B. & Steitz, T.A. (1981). Nature, 290, 744-749.

Cloning and sequence analysis in eukaryotic molecular biology

Members: H. Lehrach, A. Frischauf

Fellows: D. Leader^{*}, R. Vlasak^{*}

Student: E. Ehrich^{*}

Visitors: R. Crkvenjakov^{*}, W. Hoffmann^{*}, I. Mallitz^{*}, J.C. Perriard^{*}, U. Rosenberg

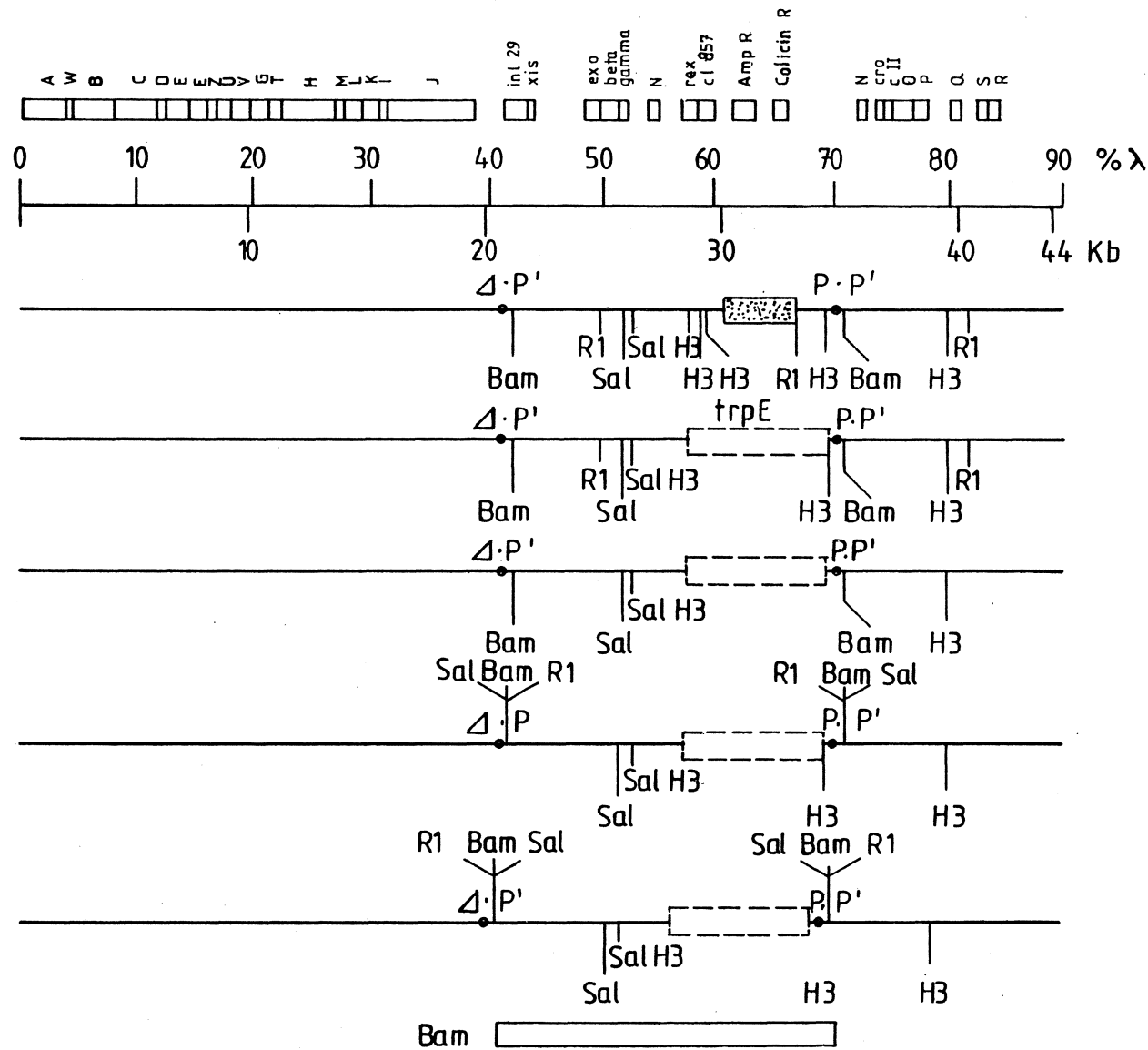
Technical assistants: R. Buckland, A. Poustka

The main effort of the group has been the isolation and characterization of genes from the major histocompatibility complex H2 in mouse, carried out to a large extent in collaboration with the group of B. Dobberstein. This began with the construction of cDNA clones from SL2 cell RNA, and the identification of the cDNA clones coding for histocompatibility antigens by hybridization to previously characterized clones (Kvist *et al.*, 1981). The clones identified have been further characterized by restriction mapping and sequence analysis (with S. Kvist and L. Roberts). In parallel we have constructed genomic libraries of mouse DNA, initially in the replacement vector 1059 (Karn *et al.*, 1980) and most recently in our replacement vector EMBL 3. These libraries were screened by hybridization to histocompatibility antigen probes, and phages carrying histocompatibility antigen genes were identified and characterized. Like other groups we have found about 40 genes hybridizing to an H2 coding probe per genome equivalent screened. A subset of these clones has been screened by hybridization to specific probes (third domain, large intron, 3' noncoding) demonstrating a remarkable degree of homology between these genes; thus in a sample of 10 clones about 50% hybridize to a probe excised from the middle of the large intron of clone VIII-3, a presumptive Qa antigen gene or pseudogene. More detailed information has been gained by electron microscopy, carried out by H. Delius. The analysis of heteroduplexes between different genes has in many cases revealed long stretches of homology extending through intron sequences and non-coding regions, interrupted by short regions of non-homology. On the other hand other clones show interspersed and permuted regions of homology, probably characterizing these clones as containing pseudogenes. E/M analysis of RNA/DNA heteroduplexes also gave initial information on exon-intron patterns of these

genes. The pattern found in the clone best studied by this technique, R11, shows a gene structure interrupted by 9 potential intron loops, in contrast to the 7-intron structure found more generally (M.Steinmetz, personal communication) and also verified by sequence analysis in clone VIII-3 (mentioned above). The sequence analysis of a region of about 2.6 kb of clone VIII-3, which extends from the middle of the large intron between the exons coding for the second and the third domain to a region beyond the 3' end of the molecule, has demonstrated strong sequence similarity to a gene described by Steinmetz et al., (1981) mapped genetically to the Qa region. Like the clone described in that paper it contains a charged amino acid in the transmembrane segment and a stop codon immediately after the potential transmembrane portion, raising questions about the synthesis, localization and function of the protein product potentially encoded by these genes. Further experiments to answer some of these questions are in progress.

To avoid some disadvantages of the λ vector 1059, with which our early experiments were carried out, we constructed a new series of λ replacement vectors (EMBL 1, EMBL 2, EMBL 3, EMBL 4) in collaboration with N. Murray. Especially EMBL 3 and EMBL 4, the most recent additions to this series, have been designed to offer the advantages already present in λ 1059 (large capacity, the possibility to clone DNA partially digested with Sau3A, spi selection) and the possibility to use additional enzymes (Sal and EcoRI) with some new features made possible by the replacement of the BamH1 sites of 1059 by polylinker sequences and the reconstruction of the middle fragment to remove plasmid sequences carried by 1059. These phages do therefore allow the excision of fragments cloned by the ligation of Sau3A partial digests into Bam sites by flanking restriction sites (EcoRI or Sal). In addition this phage can also be used as an EcoRI cloning vector with a cloning capacity approximately 1.5 kb larger than e.g. Charon 4. The structure of the vectors completed up to now is shown in Plate 10.

Another new procedure of general applicability developed and used by us during the course of our work is a rapid restriction mapping protocol applicable to λ and in vivo or in vitro packaged cosmid clones, which makes it possible to read off restriction maps of large molecules unambiguously.



λ 1059

EMBL 1

EMBL 2

EMBL 3

EMBL 4

A significant effort has also been directed towards applying in vivo recombination techniques, both in phage and in cosmid systems, for the selective cloning and manipulation of eukaryotic genes, and we expect these techniques to become a major tool in our work in the future.

Our earlier work on muscle genes has been carried further by D. Leader and has led to the isolation of clones coding for actin genes from a mouse library.

Publications during the year

Garoff, H., Riedel, H. & Lehrach, H. (1982). A procedure to verify an amino-acid sequence which has been derived from a nucleotide sequence: application to the 26s RNA of Semliki Forest virus. Nucleic Acids Research, January.

Riedel, H., Lehrach, H. & Garoff, H. (1982). The nucleotide sequence at the junction between the nonstructural and the structural genes of the Semliki Forest virus genome. J. Virology, May.

Shani, M., Nudel, U., Zevin-Sonkin, D., Zakut, R., Givol, D., Katcoff, D., Carmon, Y., Reiter, J., Frischauf, A.-M. & Yaffe, D. (1981). Skeletal muscle actin mRNA. Characterisation of the 3' untranslated region. NAR, 9, 579-589.

Other references

Karn, J., Brenner, S., Barnett, L. & Cesareni, G. (1980). Proc. Natl. Acad. Sci., 77, 5172-5176.

Kvist, S., Bregegere, F., Rask, L., Cami, B., Garoff, H., Daniel, F., Wiman, K., Larhammer, D., Abastado, J.P., Gachelin, G., Peterson, P.A., Dobberstein, B. & Kourilsky, P. (1981). Proc. Natl. Acad. Sci., 78, 2772-2776.

Steinmetz, M., Moore, K.W., Frelinger, J.G., Sher, B.T., Shen, F.-W., Boyse, E.A. & Hood, L. (1981). Cell, 25, 683-692.

Gene expression

Member: R. Cortese

Fellows: * C. Alvino*, L. Cesarepi, G. Ciliberto*, F. Costanzo*, L. Dente*, L. Mayol*, C. Pietropaolo*, C. Traboni

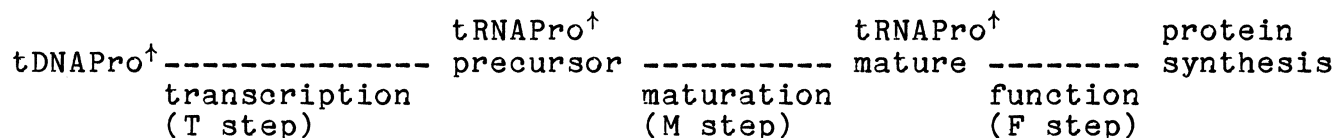
Technical assistant: M. Smith*

The work of the group is concentrated in two areas.

1) Correlation of the structure and function of tRNA genes

Purified segments of DNA can be used to study gene expression and the correlation between the DNA sequence of the gene and the function of the gene product. tRNA genes are particularly suitable for studies aimed at correlating structure with function because they can be expressed in simple experimental systems both in vivo (by oocyte micro-injection) and in vitro (in cell-free extracts), and also because tRNA functions are well characterized.

In previous studies we have established in detail the various steps in the pathway of tRNA gene expression (Cortese et al., 1978; Cortese et al., 1980a; Cortese et al., 1980b; Melton & Cortese, 1979; Melton et al., 1980). The following scheme summarizes the steps through which a functional tRNA^{Pro} is synthesized from a tRNA^{Pro} gene.



During the year we have constructed a series of tDNA mutants with the aim of identifying regions of the gene which are essential for transcription (T mutants), for the normal structure of tRNA precursors (M mutants), and finally for normal functioning of mature tRNA molecules (F mutants).

For an assay of T, M and F steps, tDNA was injected into the nucleus of Xenopus laevis oocytes and the various transcriptional products were detected on polyacrylamide gel: T mutants yielded nondetectable or insignificantly little RNA; M mutants yielded accumulating RNA precursors. Mutants normal for T and M steps yielded a mature tRNA, detected as a radioactive band on a gel. Conventional aminoacylation assays cannot be used because the absolute amounts of tRNA are too small; we have therefore developed a sensitive assay based on the radiochemical purity of the tRNA synthesized by the oocyte. Aminoacylated tRNA binds to purified elongation factor EF-Tu.GTP forming a ternary complex, which can be separated from unbound tRNA by Sephadex G-100 column chromatography. Aminoacylated P^{32} -tRNA will form a ternary complex with EF-Tu and elute at a specific position different from P^{32} -tRNA which could not be aminoacylated.

Construction of mutants

In the year we have invested a large part of our effort into the development of a new, general and powerful method of mutagenesis.

A general protocol for mutagenesis of purified genes must provide: i) an efficient method to induce mutations, ii) a way of confining the mutagenesis event to preselected regions of DNA, iii) a rapid method for the identification of clones carrying the desired mutants. This last point is seldom a problem for prokaryotic genes or, in general, for genes which are expressed in bacteria; in this case it is usually possible to devise a screening or a selection procedure for the desired mutants. This, however, becomes a problem when the gene to be mutagenized is not expressed in bacteria, as is often the case for DNA derived from eukaryotic organisms.

We have developed a method of associating to any DNA segment cloned in E.coli a phenotype directly detectable at the level of plaque or colony.

Convenient properties of M13 derived vectors

In recent years a series of vectors derived from M13 phage (the mp family) has been constructed (Gronenborn & Messing, 1978) and widely used. All the vectors of this family contain a portion of the lac gene of E.coli including

operator, promoter and the region coding for 145 amino acids at the amino-terminus of β -galactosidase (the so-called α -peptide); this part of β -galactosidase is not a functional enzyme. The host E.coli strain 71-18 has its own β -galactosidase gene removed from the chromosome, but carries an episome coding for a defective β -galactosidase lacking amino-acid residues 11-41. When mp phages invade the host the two defective β -galactosidase polypeptides associate and complement each other thus producing a functional enzyme. Plaques of infected cells producing β -galactosidase are readily identified by including a lactose analogue BCIG on the plate: this colourless compound is hydrolysed by β -galactosidase to a blue dye. This confers a blue perimeter on the plaques of mp phages. By contrast, recombinant phages in which foreign DNA has been inserted in a restriction site within the α -peptide of β -galactosidase usually yield white plaques; the inserted DNA interrupts the α -peptide and destroys its ability to complement the defective episomal β -galactosidase.

This last statement needs qualification. The NH_2 -terminal part of the β -galactosidase gene (where all the unique restriction sites used for cloning are located) is known to be non-essential for its enzymatic activity. An active enzyme can be obtained from genes which contain considerable alterations in this part of the sequence. The insertion of foreign DNA will inactivate the β -galactosidase gene and yield a white plaque only when it causes a frameshift or if it contains nonsense codons in frame with β -galactosidase. On the contrary, insertion of a segment of DNA the length of which in nucleotides is a multiple of three, thus not affecting the β -galactosidase correct reading frame, and which does not contain in-frame nonsense codons, will not destroy the β -galactosidase gene and will therefore yield a blue plaque. We have so far found no exception to this rule.

This property can be exploited for site-directed or localized mutagenesis.

Direct identification of mutants by frame-dependent phenotype

In Plate 11 is a diagram which schematically describes the principle of the method. A DNA segment inserted into mp phage vectors will yield blue plaques if its length in nucleotides is a multiple of three. The insertion of a segment of DNA of $(3N + a)$ nucleotides in length (with a

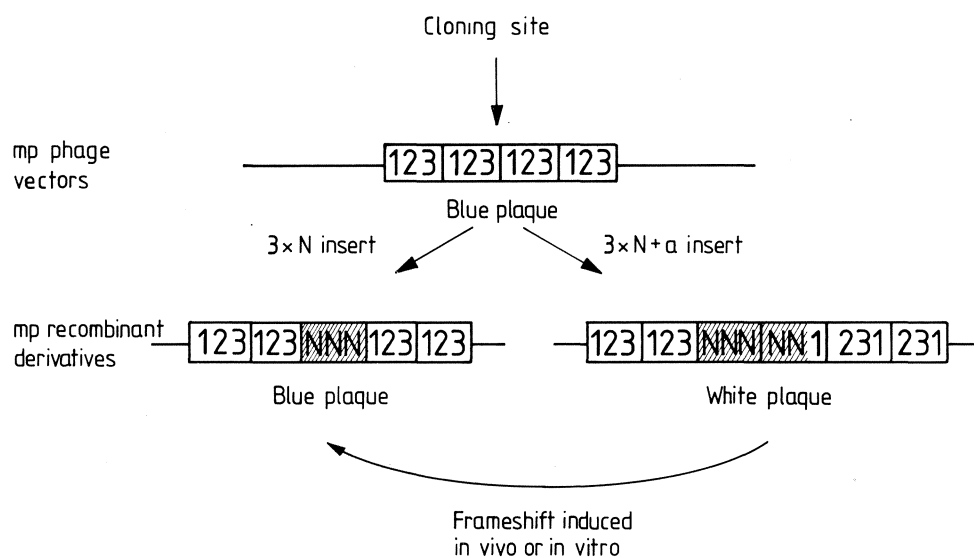


PLATE 11

tDNA ^{Pro}	8 NUCLEOTIDES - GGTCTAGTGG --- 31 NUCLEOTIDES --- GGGTTCAATCC -- 12 NUCLEOTIDES
tDNA ^{Leu}	8 NUCLEOTIDES - GGCCGAGCGG --- 41 NUCLEOTIDES --- GGGTTCAATC -- 12 NUCLEOTIDES
tDNA ^{Met}	8 NUCLEOTIDES - GGCGCAGCGG --- 31 NUCLEOTIDES --- TGGATCGAAAC -- 12 NUCLEOTIDES
GENERALIZED SEQUENCE	8 NUCLEOTIDES - RGYNNARYGG-31- 41 NUCLEOTIDES --- NNG _A ^T TCRANNC -- 12 NUCLEOTIDES

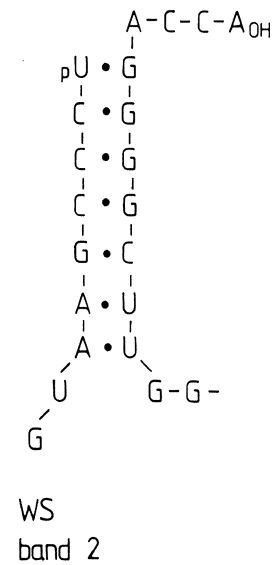
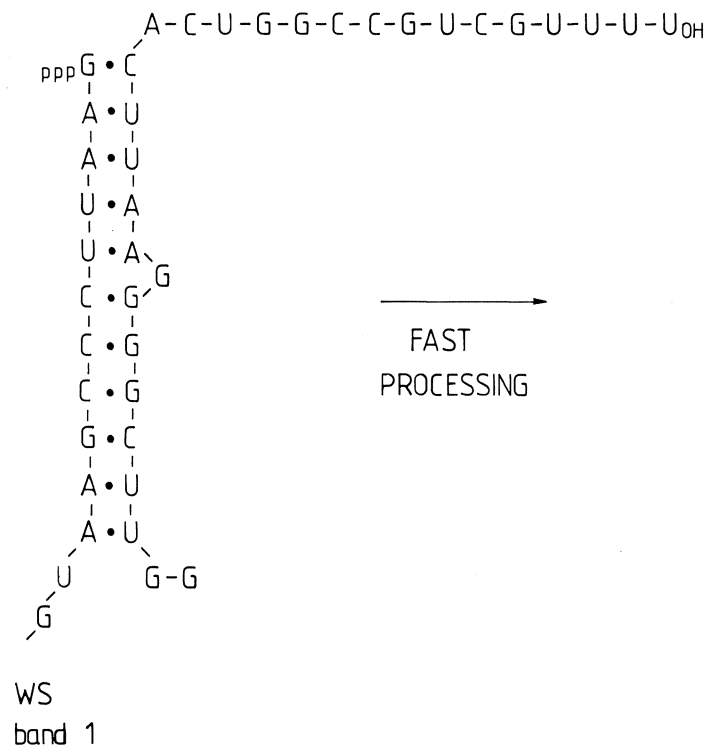
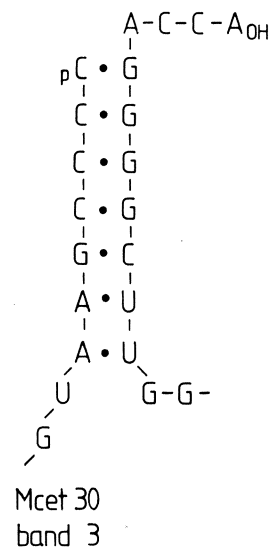
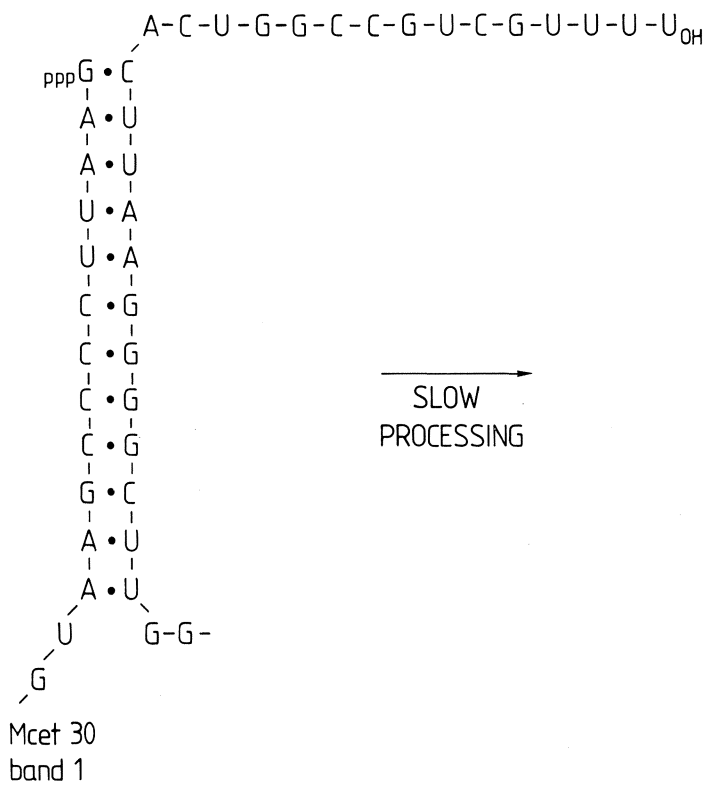
PLATE 12

equal to 1 or 2; for the sake of simplicity we assume that it does not contain nonsense codons) will give rise to a white plaque. From this, a blue plaque can be obtained as a consequence of a deletion of $(3N + a)$ nucleotides or an insertion of $(3N - a)$ nucleotides (where N can obviously be zero). It is useful to indicate the correct reading frame, coding for an active β -galactosidase, as F_{123} , where the subscripts stand for the first, the second and the third base of any codon. Insertion of $(3N + 1)$ or deletion of $(3N + 2)$ nucleotides will shift to a different reading frame (F_{312}), where the first bases of all the original codons now appear as the second bases. Insertion of $(3N + 2)$ or deletions of $(3N + 1)$ will give rise to a frame F_{231} . Even though deletions or insertions causing restoration of the frame can occur also outside the inserted segment, this constitutes the largest part of the potential target region.

A nonsense codon within a $3N$ segment of DNA will cause the formation of a white plaque; such a codon can itself be the target of site-directed mutagenesis, because mutations converting the nonsense into a sense triplet will cause the formation of blue plaques. In addition more mutants can be obtained by exploiting the influence of the sequence surrounding the nonsense triplet on the efficiency of suppression: suppressors are sensitive to this "context effect" whereby some nonsense triplet are weakly or not at all suppressed. Mutagenesis can therefore generate blue plaques by changes in the sequence surrounding the nonsense triplet, resulting in a new context compatible with efficient suppression.

It must be stressed that we are now in a position to exploit for site directed mutagenesis all the methods and knowledge accumulated in the last twenty years' research in E.coli. We have obtained mutants by classical methods such as UV light or mutagen treatment, etc. Of course we also exploited procedures made available by the development of recombinant DNA technology, such as in vitro DNAase treatment.

The essential and non-essential regions of the tRNA^{Pro} gene are identified on the basis of the various assays on a variety of mutants. This identification becomes more and more precise the richer is the mutant collection.



Transcriptional signals

Transcriptional analysis of several mutants leads to the conclusion that the tRNA^{Pro} gene promoter is located within the coding sequence and is composed of two sequences, Box A and Box B, separated by 30-40 nucleotides. Transcription starts at a nucleotide located at about 15 bases upstream of from Box A, and terminates at the first stretch of 40 more T residues. Insertions between Box A and Box B do not change the initiation site and yield transcripts longer than normal, and proportional to the length of the insertion. In contrast, insertions upstream Box A change the initiation site and yield transcripts of length similar to wild-type. The two promoter regions are independent transcriptional signals: transcriptionally active hybrid genes which have Box A and Box B deriving from different tRNA genes can be constructed in vitro. A comparison of all eukaryotic tRNA sequences reveals that Box A and Box B sequences are rather well conserved. From these a generalized sequence can be abstracted for the two Boxes and is shown in Plate 12. We propose that this sequence is the promoter of all eukaryotic tRNA genes.

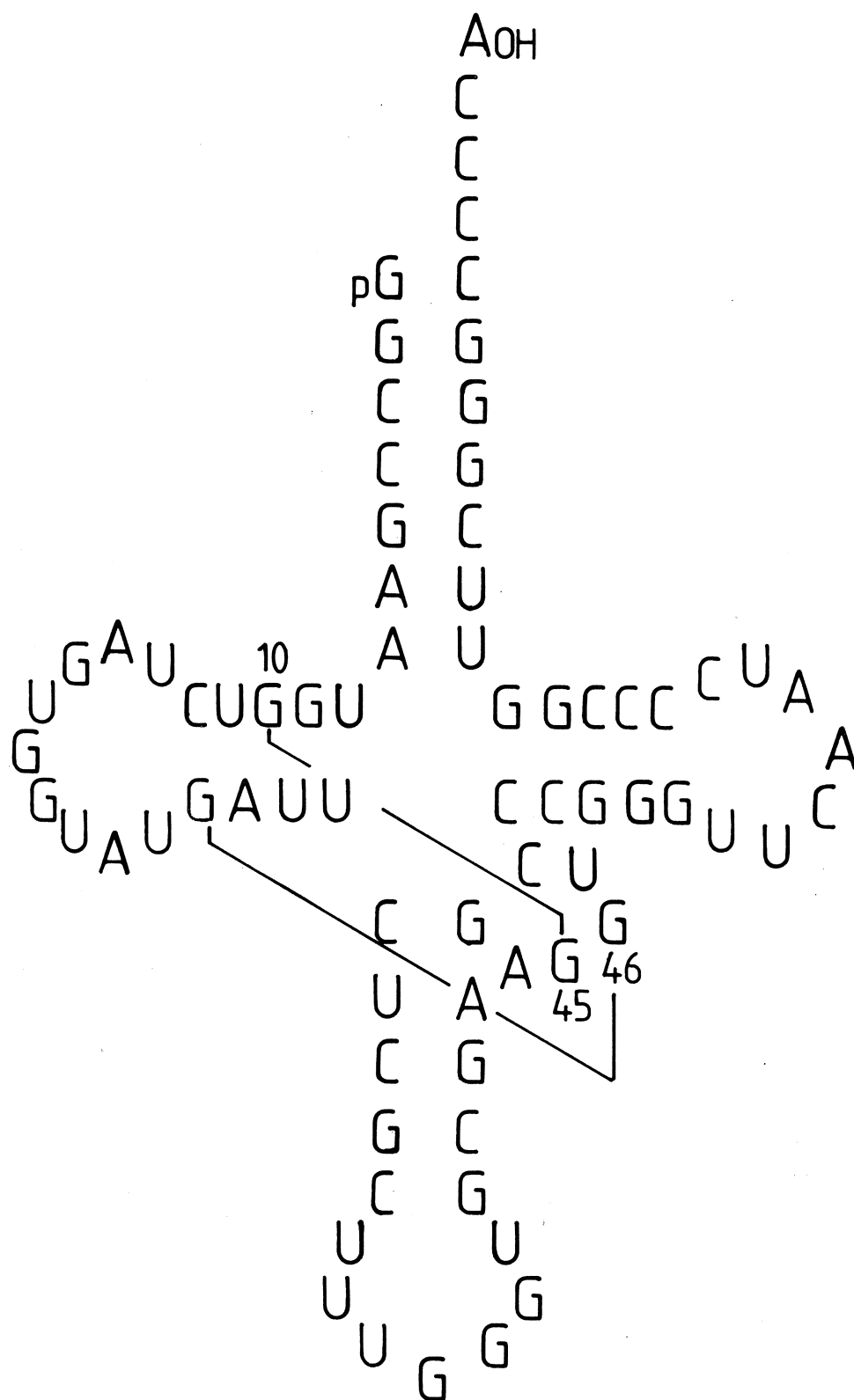
Processing signals

The relationship between the structure of a tRNA precursor and its capacity to function as substrate for processing nucleases is certainly very complex. One important feature appears to be the RNA secondary structure at the cleavage site of 3' and 5' processing enzymes. We can influence the rate of processing by extending the length of the amino-acid acceptor stem (Plate 13). Processing is greatly impaired in substrates like B (Plate 13), whereas it returns to normal in structures like C. We interpret these results by assuming that the single base-pair deletion in C destabilizes the secondary structure: we therefore deduce that the preferred cleavage point should be at a transition between a double helix and a single-stranded region.

An example of the complexity of this system is the fact that a single base-pair change at nucleotide 9 of the coding sequence (a Gg - Ag transition) suppresses the inhibitory affect on processing due to an extended amino-acid acceptor stem.

Functional analysis

Several single base-pair mutants were analysed for their



capacity to be aminoacylated by the cognate aminoacyl tRNA synthetase.

Our mutant collection is not large enough to provide definitive information but we can draw some preliminary conclusions:

- 1) the last base of the coding region, immediately preceding the CCA terminus, can be changed into any other base without affecting the specificity of aminoacylation. This result is interesting and was not expected because there were some indications, in other systems, that this base played a role in the aminoacylation reaction.
- 2) the anticodon loop of tRNA^{Pro} plays an essential role in the aminoacylation reaction: a single base-pair insertion, giving rise to an 8 nucleotide anticodon loop, prevents aminoacylation. Single base-pair insertions in some other regions do not interfere with charging.
- 3) the single base-pair transition mutants G45 - A45 and G46 - A46 are normally aminoacylated. In contrast the double mutant G45G46 - A45A46 is not charged. As shown in Plate 14, these two nucleotides are involved in tertiary non-Watson-Crick base pairing with nucleotides G10 and G22. One interpretation of our results is that either one of these tertiary bonds is sufficient for a correct conformation of tRNA^{Pro}, but if both are absent the resulting alteration of the tRNA structure is incompatible with aminoacylation.

All these observations contribute to a definition of the genetics of the T, P, and F steps in the biosynthesis of tRNA. We hope that the analysis of a larger collection of mutants will allow a more general and coherent understanding of the correlation between the structure of the gene and its function or the function of the gene product.

2) Purification of human genes

The aim of this project is to purify many genes sharing the property of being selectively or preferentially expressed in the human liver. This choice is based on the consideration that many of the gene products, especially plasma proteins, are thoroughly studied molecules, from both a biochemical and a genetic point of view. For several plasma protein genes there is the additional consideration that they have potential applications in medicine and pharmacology.

Our source of material is mRNA from human foetal liver or from an hepatocarcinoma cell line (obtained from B. Knowles) which has retained the capacity to synthesize several plasma proteins. More recently we have used human adult liver.

We have subdivided the genes of interest into two classes: those for which the protein sequence is known and those for which it is unknown. For the first class we have adopted a direct approach: double-stranded cDNA is cleaved with restriction enzymes yielding ends compatible with ligation into MS13 phage vectors: a library of relatively short segments of cDNA is generated and the clones are clarified according to several criteria, such as whether they are liver-specific, whether they hybridize to mRNA or to cDNA, etc. Single-stranded DNA from each clone is sequenced and the sequence is compared with a collection of known protein sequences.

This approach has given encouraging results: starting from a human foetal liver cDNA shot-gun we have sequenced 70 clones and identified 8 serum albumin segments spanning the entire length of the full length cDNA, 5 γ -haemoglobin genes (our source was foetal liver), and two cDNA sequences related to serum albumin in a peculiar way - they contain a stretch of 60 bases identical to a region of serum albumin cDNA, flanked by completely different sequences. Several considerations suggest that these two clones do not derive from α -foetoprotein mRNA; we believe that they come from a duplicated albumin gene from which it has considerably diverged, but with which it underwent a gene-conversion event. A calculation of the relative abundance of mRNA for several other plasma proteins suggests that several of them could be identified by increasing our collection of sequences to include 300-400 clones.

In parallel with the shot-gun approach as a specific strategy, we have set up in our laboratory a solid-phase method for the synthesis of oligodeoxynucleotides. Our purpose is to use these as specific primers for cDNA synthesis or as probes to screen cDNA libraries. Up to now we have synthesized three different oligodeoxynucleotides, a 16mer, a 12mer and an 11mer, the sequences of which were deduced from the amino-acid sequences of human anti-thrombin III, apoAI lipid-binding protein, and prothrombin. Our preliminary results have convinced us that specific priming only occurs with the 16mer. Cloning of specifically primed cDNA is under way.

For genes the gene product sequence of which is unknown we are purifying specific mRNA by classical polysomal immunoprecipitation: it was not difficult to purify (or better to enrich for) albumin mRNA; our problem now is to scale up the procedure to purify rarer messages.

Publications during the year

Ciampi, M. S., Melton, D. A. & Cortese, R. (1982). Site-directed mutagenesis of a tRNA gene: base alterations which affect transcription. Proc. Nat. Acad. Sci., USA, 79, (in press).

Ciliberto, G., Castagnoli, L. & Cortese, R. (1982). Transcription by RNA polymerase III. Current Topics in Developmental Biology, 18, (in press).

Ciliberto, G., Castagnoli, L., Melton, D. A. & Cortese, R. (1982). Promoter of a eukaryotic tRNA^{Pro} gene is composed of three noncontiguous regions. Proc. Nat. Acad. Sci., USA, 79, 1195-1199.

Ciliberto, G., Traboni, C. & Cortese, R. (1982). Relationship between the two components of the split promoter of eukaryotic tRNA genes. Proc. Nat. Acad. Sci., USA, 79, (in press).

Other references

Cortese, R. et al., (1978). Nucl. Acid. Res., 5, 4593-4611.

Cortese, R., et al., (1980a). Proc. Natl. Acad. Sci., U.S.A., 77, 4147-4151.

Cortese, R. et al., (1980b). tRNA: Biological aspects, Cold Spring Harbor Laboratory, 287-293.

Gronenborn, B. & Messing, J. (1978). Nature, 272, 375-377.

Melton, D.A. & Cortese, R. (1979). Cell, 18, 1165-1172.

Melton, D.A. et al., (1980). Nature, 284, 143-148.

DIVISION OF BIOLOGICAL STRUCTURES

Organization and dynamics of cytoskeletal elements

Members: B.M. Jockusch*, G. Griffiths

Fellow: I. Stuhlfauth*

Visiting workers: G. Isenberg*, H. Osinska*, J.W. Sanger*

Technical assistant: K.H. Kelley*

Our work has been mainly concerned with the biochemical and structural characterization of actin-binding proteins, with their interaction with actin in vitro and in vivo, and with the role of clathrin-coated vesicles during transport of membrane material.

Structure and function of vinculin

Vinculin is a protein found in many muscle and non-muscle cells localized at the terminal regions of microfilament bundles (Geiger, 1979; Burridge & Feramisco, 1980; Jockusch & Isenberg, 1981 b). In collaboration with G. Isenberg (MPI München) and K. Leonard (EMBL) a detailed structural analysis of vinculin itself and of vinculin:actin complexes was performed. Vinculin is composed of one polypeptide chain of 130,000 molecular weight which appears in negatively stained or rotary shadowed preparations as a roughly globular particle with a mean diameter of 85 Å and a central depression (Plate 15). With filamentous actin paracrystals are formed (Plate 16), with a packing density reminiscent of Mg-induced paracrystals. Vinculin seems to bind irregularly, since no reflections indicating a periodicity in binding were found (optical diffraction and computer analysis). Vinculin-induced paracrystals are formed with relatively low amounts of vinculin (starting at a molar ratio of vinculin:actin 1:200), but much more can be bound to the surface of the paracrystal (up to a molar ratio of 1:3, see Isenberg, Leonard & Jockusch, 1982).

Structure of α -actinin

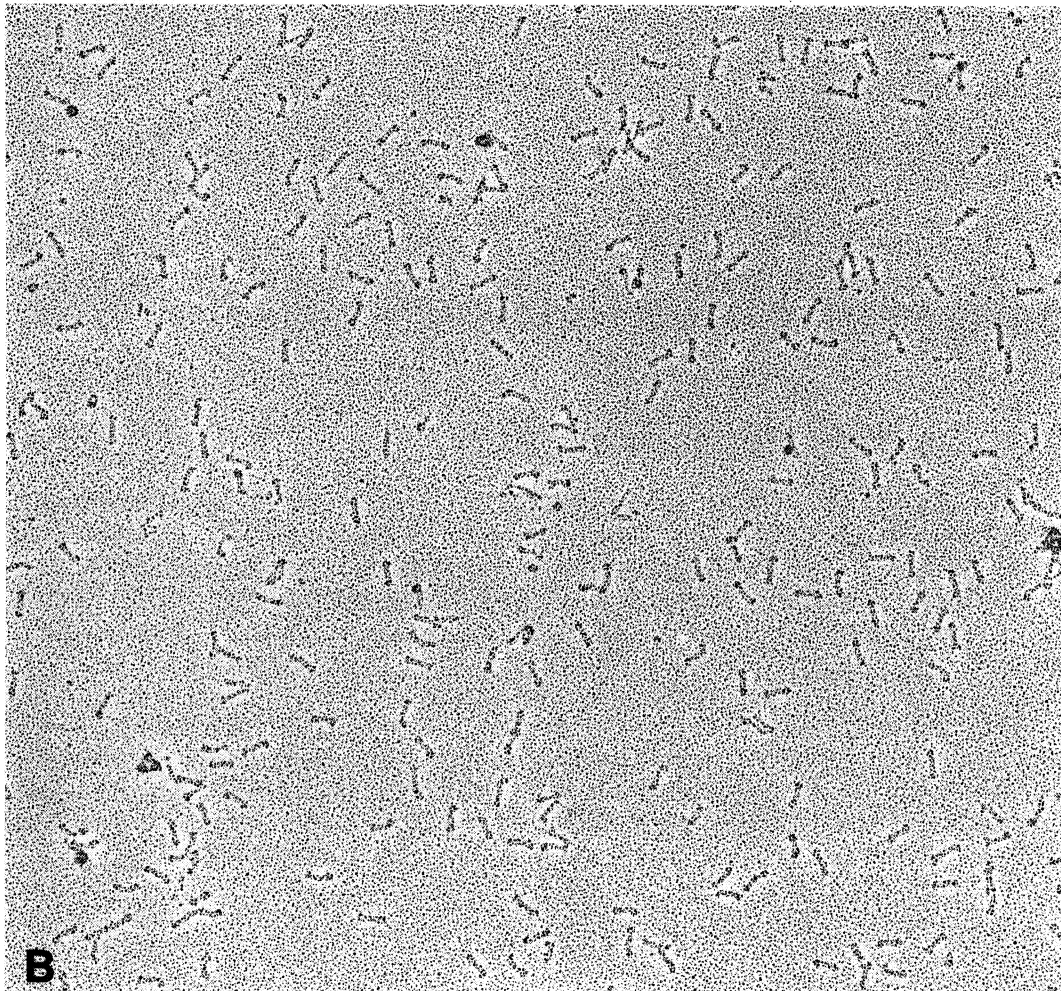
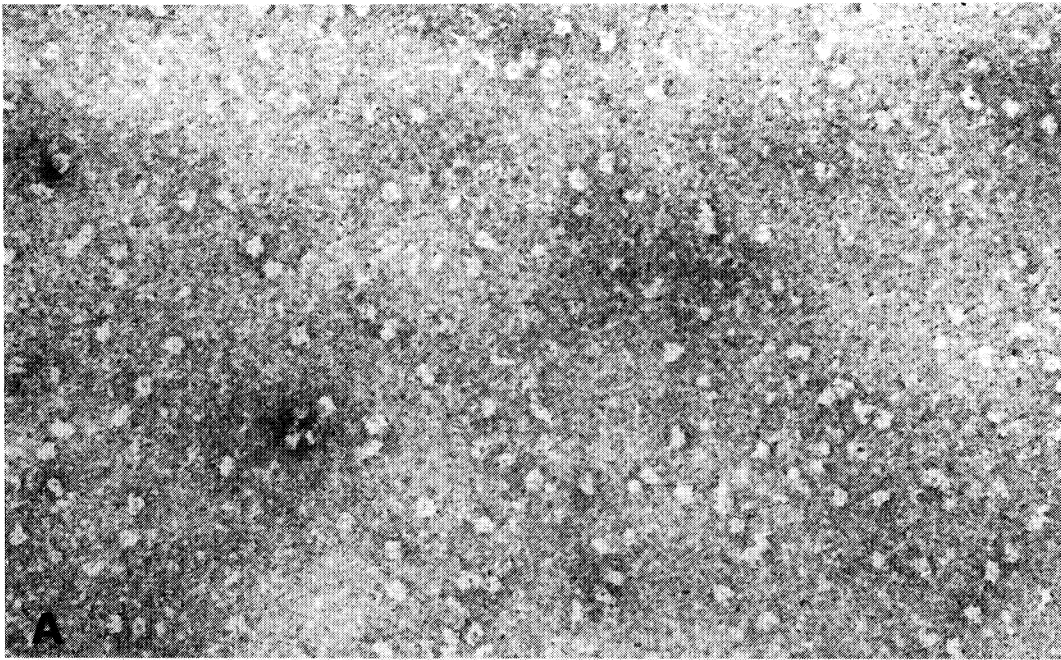
α -actinin, like vinculin, is a widespread actin-binding protein. In vitro, it induces cross-linking of actin filaments into rather rigid networks (Jockusch & Isenberg, 1981, a and b). The interaction with actin is highly temperature-dependent, the cross-linking being much more effective at low (4°C) than at high (30°C) temperature.

PLATE 15

Morphology of two different actin-binding proteins.

(A) Negatively stained preparation of chicken gizzard vinculin. Individual molecules are seen as globular particles, consisting of several lobes. Their average diameter is 85 Å. Magnification: 250,000 x (K. Leonard and B.M. Jockusch).

(B) Rotary shadowed images of chicken gizzard α -actinin. Individual molecules consist of two strands forming rod-like structures of 40 x 400 Å, with distinct knobs at each end. Magnification: 135,000 x (B. Burke and B.M. Jockusch).



Preliminary studies had indicated that this may be due to an allosteric change in the α -actinin molecule itself. To examine this possibility, we isolated α -actinin from skeletal and smooth muscle as well as from brain. All three α -actinins showed the same temperature-dependence in interacting with actin, and were indistinguishable from each other in rotary shadowed preparations (in collaboration with B. Burke, EMBL). Although considerable biochemical differences between different α -actinins have been described (Bretscher *et al.*, 1979), the shape of the molecule seems highly conserved: it is an elongated rod of roughly 40 x 400 Å, composed of two polypeptide chains, with a globular knob at each end (Plate 15). Experiments are in progress to study the conformation and shape of those molecules at different temperatures.

α -actinin in blood platelets

Preliminary evidence had indicated that blood platelets may contain, possibly in addition to "normal" α -actinin, an intrinsic membrane protein immunologically related to α -actinin but with a larger molecular weight. A more detailed analysis of the platelet plasma membrane proteins revealed that platelets contain an α -actinin of the usual type. A considerable proportion of this protein is membrane-associated, but not glycosylated, nor exposed at the surface. On the other hand, the intrinsic glycoprotein had a higher molecular weight and did not show any immunological cross reactivity with anti- α -actinin in blots of 2-dimensional gels (in collaboration with J.J. Sixma, Univ. Utrecht; Sixma *et al.*, 1982).

α -actinin in Nemaline Myopathy

Previous studies had demonstrated that a congenital, hereditary condition in the human (congenital nemaline myopathy, CNM) is characterized by abnormal inclusions in the skeletal muscle (nemaline rods) which are derived from the Z-line and contain α -actinin as a major component (Jockusch *et al.*, 1980). Since α -actinin occurs also in non-muscle cells, we examined various cell types derived from blood, nervous tissue and skin from CNM patients. We found that the defect was confined to the skeletal muscle, and that it is probably not the result of an increased synthesis of skeletal muscle α -actinin but of a faulty distribution within the sarcomeric units (Jennekens *et al.*, 1982).

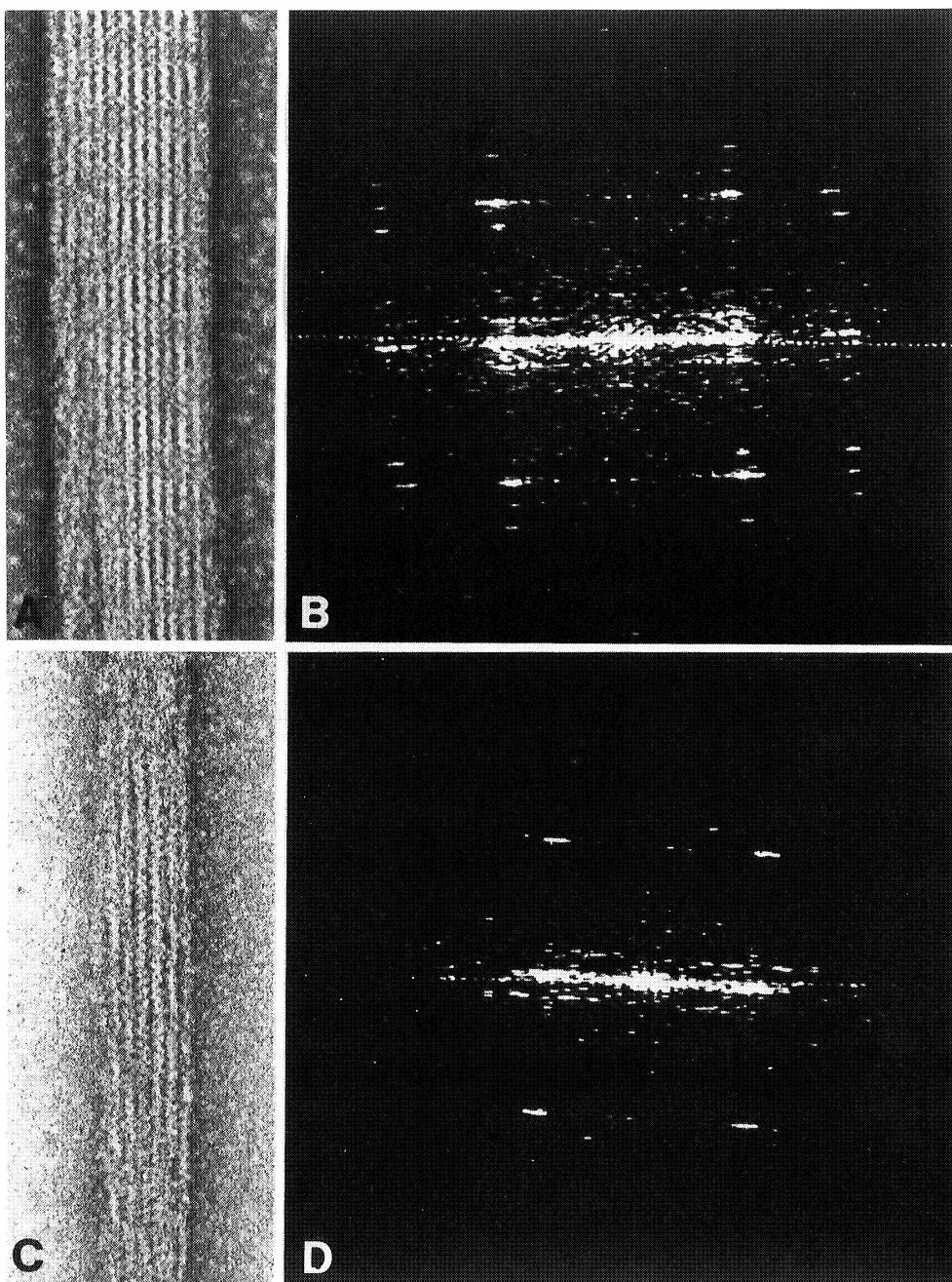


PLATE 16

Optical diffraction patterns (B, C) of actin paracrystals induced by magnesium (A, B) or vinculin (C, D). Packing density and arrangement of actin filaments are very similar in both cases, but vinculin-induced paracrystals are less regular (K. Leonard, G. Isenberg and B.M. Jockusch).

Organization of microfilaments in normal and carcinoma cells

Affinity column-purified antibodies against actin and several actin-binding proteins were used to study the organization of microfilaments with immuno-fluorescence and immuno-electron microscopy. In stationary fibroblasts and epithelial cells, the sarcomeric concept of microfilament organization was confirmed at the electron microscopic level, with α -actinin, myosin and tropomyosin alternating within the microfilament bundle (stress fibre, in collaboration with J.W. Sanger, Sanger et al., 1981a).

The analysis of a human (LICR-HN₁) and a rabbit (V2) carcinoma cell demonstrated a correlation between locomotory activity (which is a parameter of tumour formation and invasion) and the pattern of microfilament organization (with G. Haemmerli, Univ. Zürich; see Haemmerli et al., 1981; Jockusch et al., in preparation).

The role of clathrin-coated vesicles in acrosomal transport

G. Griffiths used an affinity-purified antibody against clathrin to follow the pathway of coated vesicles from the Golgi towards the acrosomal membrane in spermatids, with immuno-fluorescence and immuno-electron microscopy (with G. Warren; see G. Griffiths et al., 1981).

Publications during the year

Boschek, C.B., Jockusch, B.M., Friis, R.R. Back, R., Grundmann, E. & Bauer, H. (1981). Early changes in the distribution and organization of microfilament proteins during cell transformation. Cell, 24, 175-184.

Griffiths, G., Warren, G., Stulfauth, I. & Jockusch, B.M. (1981). The role of clathrin-coated vesicles in acrosome formation. Eur. J. Cell Biol., 26, 52-60.

Haemmerli, G., Strub, A.M., Jockusch, B.M. & Sträuli, P. (1982). Filament patterns associated with in vitro motility of human carcinoma cells. Cell Biol., Int. Rep., in press.

Isenberg, G., Leonard, K. & Jockusch, B.M. (1982). Structural aspects of vinculin-actin interactions. J. Mol. Biol., in press.

Jennekens, F.G.I., Van Oost, B.A., Roord, J.J., Veldman, H., Willemse, J., Stulfauth, I. & Jockusch, B.M. (1982). Congenital nemaline myopathy: defective organization of α -actinin is restricted to muscle. Muscle and Nerve, in press.

Jockusch, B.M. & Isenberg, G. (1981a). Interaction of α -actinin and vinculin with actin: opposite effects on filament network formation. Proc. Nat. Acad. Sci., U.S.A., 78, 3005-3009.

Jockusch, B.M. & Isenberg, G. (1981b). Vinculin and α -actinin: interaction with actin and effect on microfilament network formation. Cold Spring Harbor Symp. Quant. Biol., 46, in press.

Jockusch, H. & Jockusch, B.M. (1981). Structural proteins in the growth cone of cultured spinal cord neurons. Exp. Cell Res., 131, 345-352.

Sanger, J.W., Sanger, J.M. & Jockusch, B.M. (1981a). Cell type differences in sarcomeric periodicities in stress fibers. J. Cell Biol., 91, 296a.

Sanger, J.W., Sanger, J.M. & Jockusch, B.M. (1981b). Differential response of two types of actin filament bundles to depletion of cellular ATP levels. J. Cell Biol., 91, 296a.

Sixma, J.J., Schiphorst, M.E., Verhoeckx, C. & Jockusch, B.M. (1982). Extrinsic and intrinsic proteins of blood platelet membranes: α -actinin is not identical with glycoprotein III. Biochim. Biophys. Acta, in press.

Other references

Bretscher, A., Vanderkerckhove, J. & Weber, K. (1979). Eur. J. Biochem., 100, 237-244.

Burridge, K. & Feramisco, J.R. (1980). Cell, 19, 587-596.

Geiger, B. (1979). Cell, 18, 193-205.

Jockusch, B.M., Griffiths, G., Veldman, H., Van Oost, B.A. & Jennekens, F.G.I. (1980). Exp. Cell Res., 127, 409-420.

Transport of plasma membrane proteins through the Golgi complex

Members: G. Warren, G. Griffiths*, P. Quinn*

Fellows: J. Armstrong*, B. Burke, P. Quinn*

Technical assistant: R. Giovanelli

When baby hamster kidney (BHK) cells are infected with Semliki Forest virus (SFV), host cell protein synthesis soon ceases and the cells are converted into factories for making more virus. Large numbers of viral membrane proteins are assembled in the rough endoplasmic reticulum (ER) and are then transported to the plasma membrane via the Golgi complex (Green et al., 1981). As they pass through the 4-6 flattened cisternae that comprise the Golgi stack they are structurally modified in a precise manner and sequence. During the last year we have been trying to dissect the Golgi stacks into discrete functional domains in an attempt to pin-point the sites of these modifications. These results will be described briefly.

Lectin labelling of Golgi membranes in thin frozen sections

The oligosaccharides on the viral membrane proteins undergo a precise sequence of structural changes during intracellular transport. The conversion of simple to complex oligosaccharides, for example, occurs in the Golgi stack (Green et al., 1981) but the precise location is unknown. We utilized the sugar specificity of plant lectins to locate the site of this oligosaccharide modification (Griffiths et al., 1982). Ricinus communis agglutinin I (RCA), for example, specifically recognizes D-galactose, one of the sugars needed to construct complex oligosaccharides. Thin frozen sections of infected BHK cells were labelled with RCA followed by an antibody to this lectin and protein A gold. RCA divided the Golgi stack into two approximately equal halves each comprising 2-3 cisternae. The cisternae on the trans side were heavily labelled; those on the cis side were unlabelled. RCA binds to the isolated viral membrane proteins only after they have acquired complex sugars. Furthermore, about 50% of the RCA was bound to viral membrane proteins in thin frozen sections. Taken together we can conclude that the construction of complex oligosaccharides is restricted to the trans half of the Golgi stack and this is indirect evidence that the enzyme that transfers galactose to the

growing complex oligosaccharide, galactosyl transferase, is also restricted to this half. Since viral membrane proteins are found in all Golgi cisternae (Green *et al.*, 1981) we can also conclude that the movement of these proteins is from the cis to the trans side. If it were the reverse it would be difficult to explain why the entire stack is not labelled by RCA; the proteins entering the cis side from the trans side would bear galactose that should then bind this lectin.

Separation of cis and trans Golgi cisternae

When SFV-infected BHK cells are treated with monensin (Tartakoff & Vassalli, 1978), intracellular transport of viral membrane proteins ceases but synthesis continues (Kääriäinen *et al.*, 1980). The proteins accumulate in swollen Golgi cisternae before the monensin block and in consequence they bind viral nucleocapsids. This distinguishes them from those swollen but smooth Golgi cisternae after the block. Using a variety of cytochemical, immunocytochemical and biochemical techniques we have located the site of the block to the middle of the Golgi stack so that the intracellular capsid-binding membranes (ICBMs) are derived from cis Golgi cisternae. ICBMs should also have markedly different physical properties from trans Golgi cisternae and we have been able to separate them from each other on density gradients. Several Golgi functions are also separated as a result. Galactosyl transferase is restricted to trans Golgi cisternae confirming the results from lectin-binding studies. The viral membrane proteins in the ICBMs were rapidly labelled by ³H-palmitate suggesting that fatty acid acylation (Schmidt *et al.*, 1979) is restricted to cis Golgi cisternae or the transitional elements of ER. We are at present trying to determine the location of α -mannosidase, one of the enzymes that trims simple oligosaccharides.

Monoclonal antibodies to Golgi membranes

In collaboration with D. Louvard's group we previously reported that polyclonal antibodies could be raised that were specific for a single protein present in the Golgi complex (Louvard *et al.*, 1982). We have continued this work by trying to raise monoclonal antibodies to Golgi membrane fractions. Preliminary results are very encouraging. The supernatants from several uncloned hybridomas gave fluorescent labelling patterns very similar to those obtained using the polyclonal antibodies and strikingly similar to the patterns originally observed by Camillo

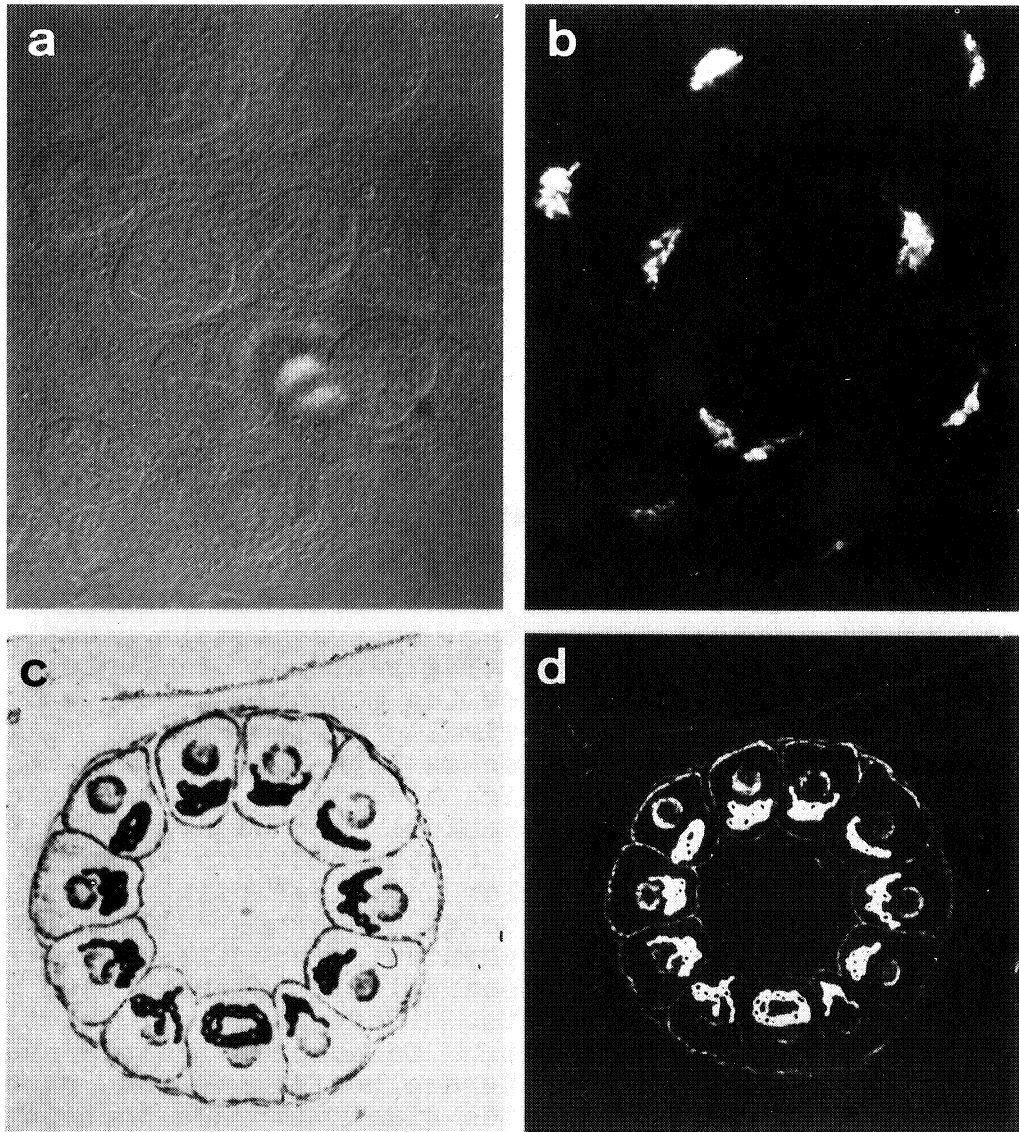


PLATE 17

The Golgi Complex

(a, b). Antibodies against the Golgi complex were used to label kidney cells that had been briefly treated with Triton X-100 to make them permeable to antibodies. The first antibody was visualized using a fluorescently-labelled, second antibody. (a) Nomarski Interference Contrast (b) Fluorescence.

(c,d). Copies of pictures published by Camillo Golgi (1898) using a silver stain to locate the organelle in kidney cells. (c) Original picture. (d) Reverse contrast so that a direct comparison can be made with (b). Note the striking similarities between the structure revealed more than 80 years ago by silver staining and that revealed by monoclonal antibodies.

Golgi (1898) (see Plate 17). Though there is still a number of technical problems we hope that we can prepare antibodies that recognize different parts of the Golgi complex. This should allow us to determine the minimum number of antigenically distinct compartments.

Primary structure of clathrin

Clathrin is found in close association with the Golgi complex (see D. Louvard's 1980 Research Report) presumably as coated pits and coated vesicles (Pearse, 1975). The latter are thought to convey newly-synthesized plasma membrane proteins, in separate stages, from the ER to the Golgi complex and thence to the plasma membrane (Rothman & Fine, 1980). In addition, the participation of clathrin-coated vesicles in endocytosis is well documented (Goldstein et al., 1979). Thus clathrin plays an important part in several processes of intracellular transport. As a first step in understanding this function at the molecular level, the primary structure of the protein is being determined via sequence determination of cloned clathrin cDNA. This project is described in detail in a separate report. Our contribution will be to obtain partial amino-acid sequences to specify the synthesis of a nucleotide probe. The impressive insolubility of the isolated protein, and the large numbers of fragments coming from a molecule of this size, have caused some problems, but several peptides have now been purified and N-terminal sequence analysis is in progress. Short portions of the sequences will be chosen, and mixtures of oligonucleotides will be synthesized corresponding to all possible codons for these sequences. These will be used as hybridization probes to screen a recombinant library for clones containing sequences representing clathrin cDNA (Suggs et al., 1981).

Publications during the year

Green, J., Griffiths, G., Louvard, D., Quinn, P. and Warren, G. (1981). Passage of viral membrane proteins through the Golgi complex. J. Mol. Biol., 152, 663-698.

Griffiths, G., Warren, G., Stuhlfauth, I. and Jockusch, B. (1981). The role of clathrin-coated vesicles in acrosome formation. Eur. J. Cell Biol., 26, 52-60.

Louvard, D., Reggio, H. and Warren, G. (1982). Antibodies to the Golgi complex and the rough endoplasmic reticulum. J. Cell Biol., 92, 92-107.

Warren, G. (1981). Membrane proteins: structure and assembly. In Comprehensive Biochemistry: ed. Finean, B. & Michell, R.; Elsevier/North-Holland, Amsterdam, Ch. 6, p. 216-257.

Other references

Goldstein, J.-L., Anderson, R.G.W. & Brown, M.S. (1979). Nature, 279, 679-685.

Golgi, C. (1898). Arch. Ital. Biol., 30, 60-71.

Griffiths, G., Brand, R., Louvard, D. and Warren, G. (1982). J. Cell Biol. submitted.

Kääriäinen, L., Hashimoto, K., Saraste, J., Virtanen, I. and Penttinen, K. (1980). J. Cell Biol., 87, 783-791.

Kraehenbuhl, J.L., Racine, L. and Griffiths, G.W. (1980). Histochem. J., 12, 317-332.

Pearse, B. (1975). J. Mol. Biol., 97, 93-98.

Rothman, J. and Fine, R. (1980). Proc. Natl. Acad. Sci., U.S.A., 77, 780-784.

Schmidt, M., Bracha, M. and Sclessinger, M. (1979). Proc. Natl. Acad. Sci., U.S.A., 76, 1687-1691.

Suggs, S.V., Wallace, R.B., Hirose, T., Kawashima, E.H. & Itakura, K. (1981). Proc. Natl. Acad. Sci., 78, 6613-6617.

Tartakoff, A. and Vassalli, P. (1978). J. Cell Biol., 79, 694-707.

Mitochondrial electron transfer enzymes

Members: H. Weiss, P. Wingfield*

Fellow: Y. Li*

Visiting workers: B. Karlsson*, P. Riccio*

Technical assistants: B. Juchs*, A. Probst*, A. Scharm*, M. Slaughter

The process of mitochondrial oxidative phosphorylation is catalysed by three electron-transfer enzymes, NADH:ubiquinone reductase, ubiquinol:cytochrome c reductase and cytochrome c: O₂ oxidase, and by ATP synthase. The electron-transfer enzymes transduce oxidative energy into the energy of a transmembrane proton gradient and ATP synthase uses this gradient to drive the formation of ATP from ADP and inorganic phosphate. The electron transfer enzymes and ATP synthase are composed of a number of different subunits. The enzymes span the phospholipid bilayer of the mitochondrial inner membrane and protrude considerably into the aqueous spaces on both sides of the membrane. They account for most of the protein of the mitochondrial inner membrane.

We have continued our structural studies on ubiquinol: cytochrome c reductase (E.C. 1.10.2.2.) from mitochondria of Neurospora crassa. Four different routes have been taken.

1. Gradual cleavage of the enzyme and biochemical characterization of subunit complexes, single subunits and subunit domains

The enzyme was dissociated under mild conditions and the preparations obtained were characterized as hydrophilic, hydrophobic or amphiphilic, according to their solubility in aqueous buffers or detergent solutions. The hydrophilic preparations are water-soluble without detergent and are assumed to lie outside the membrane. The hydrophobic preparations are soluble in detergent solution and are assumed to lie in the membrane. The amphiphilic preparations are soluble in monodisperse state only in detergent solution. These subunits, however, become water-soluble without detergent when a hydrophobic protein stretch is cleaved off by proteolysis. Amphiphilic preparations are therefore assumed to extend mainly into the aqueous phase and to

be anchored to the membrane by a hydrophobic protein stretch. This classification procedure assisted in the assignments of most of the protein to the membranous or aqueous sections of the enzyme. The preparations have also been investigated for their affinity to ferri-cytochrome c, a substrate of cytochrome reductase which is located on the outer surface of the mitochondrial inner membrane. This lead to a first assignment of protein within either of the two aqueous sections. The preparations which have been isolated and characterized so far are summarized in Table 1.

2. Neutron scattering studies

In collaboration with S. Perkins (EMBL, Grenoble), neutron scattering experiments have been performed with whole cytochrome reductase, the cytochrome bc_1 subunit complex and the complex of the subunits I and II (see Table 1). Hydrogenated Triton (an alkylphenyl polyoxyethylene ether, abbreviated formula $\text{tert } C_{80}E_{9-10}$) and deuterated Cemulsol (an alkyl polyoxyethylene ether, $C_{12}E_{8-10}$) were used as detergents. The results can be summarized as follows: the molecular weight values obtained for the proteins alone and protein-detergent complexes confirm the values determined by ultracentrifugation and detergent-binding studies. The distances between the scattering densities of protein and protein-bound detergent micelle are $38 \pm 8 \text{ \AA}$ and $23 \pm 3 \text{ \AA}$ for the cytochrome reductase and the cytochrome bc_1 subunit complex respectively. The whole enzyme is 175 \AA long. It spans the protein-bound detergent micelle and protrudes to different extents on the two sides of the micelle into the aqueous phase. The cytochrome bc_1 subunit complex is only about 90 \AA long. It protrudes only from one side of the detergent micelle. Wide-angle scattering curves showed spacings which account for the dimeric state of the preparations and the detergent-bound micelle. The whole enzyme has an unusually low protein match-point of 37% D_2O which indicates the non-exchange of 60% of the exchangeable protons (given the proton translocating function of cytochrome reductase this discovery raises the question of the role of unexchanged protons in the function). The protein matchpoint of the two parts of the enzyme, the cytochrome bc_1 subunit complex and the subunit I and II complex, are between 41-42%. Comparison of the radial distributions of scattering density fluctuations indicate a higher ratio of surface polar residues to buried non-polar residues in the cytochrome bc_1 complex

Table 2

Properties of preparations obtained by gradual cleavage of cytochrome reductase

Preparation	Subunits present	State	Molecular weight ($\times 10^{-3}$)	Solubility	Cytochrome c binding	Location
Cytochrome reductase	I-IX	dimeric	550	hydrophobic	+	Membrane, matrix and intermembrane space
Cytochrome bc_1 complex	III, IV, VI-IX	dimeric	250	hydrophobic	+	Membrane and intermembrane space
Complex without redox centres	I, II	monomeric (or dimeric)	170	hydrophilic	-	Matrix space
Subunit I	I	monomeric	50	hydrophilic	-	Matrix space
Subunit II	II	dimeric	90	hydrophilic		Matrix space
Cytochrome b	III	dimeric (or tetrameric)	80	hydrophobic		Membrane space
Cytochrome c_1	IV	monomeric	31	amphiphilic	+	Intermembrane and membrane space
Cytochrome c_1 domain	IV*	monomeric	25	hydrophilic	+	Intermembrane space
Iron-sulphur subunit	V	monomeric	25	amphiphilic	-	Intermembrane space
Iron-sulphur domain	V*	monomeric	16	hydrophilic	-	Intermembrane space

* obtained by proteolysis

and the subunit I and II complex as compared to the whole enzyme.

3. Electron microscopy of two-dimensional crystals

Membrane crystals have been prepared from the whole cytochrome reductase and the cytochrome bc_1 subunit complex by adding mixed phospholipid-detergent¹ micelles to the protein-detergent complexes and subsequently removing the detergent. In collaboration with the group of K. Leonard the low resolution three-dimensional structures of these two preparations have been reconstructed from tilted views. The following results were obtained: cytochrome reductase is dimeric with a 2-fold axis running perpendicular to the membrane. The monomeric unit has an elongated structure and extends 15 nm through the membrane. The protein is unequally distributed; 30% is located in the membrane, 50% in a section which extends 70 Å into the matrix space of the mitochondria and 20% in a section which extends 30 Å into the intermembrane space. The two monomeric units are in contact essentially only in the membrane space. The cytochrome bc_1 subunit complex is also dimeric, with 2-fold axis perpendicular to the membrane plane. The structure of the subunit complex, as compared to the structure of the whole enzyme, has a length of only about 80 Å and lacks the large peripheral section which extends 70 Å from the membrane. Furthermore that section which extends 30 Å from the membrane is smaller in the subunit complex than in the whole enzyme, and the distance between the mass centres of the two related sections of one dimer is shorter, namely 74 Å for the whole enzyme and 60 Å for the subunit complex.

4. X-ray analysis of the three-dimensional crystals

Three-dimensional microcrystals have been prepared from the hydrophilic 50,000 M_r and 45,000 M_r subunits and the hydrophilic 16,000 M_r domain of the iron-sulphur subunit. Larger crystals must be grown before an x-ray analysis can be undertaken.

Conclusion

By combining the data available so far a 25 Å structure of cytochrome reductase has been obtained. The location of this structure in the bilayer of the mitochondrial inner membrane and the topography of most of the subunits within

this structure are now known. The project is on the way towards a higher resolution of parts of the enzyme. It is hoped that more detailed structural information will lead to biochemical and/or genetic experiments which will give a clearer understanding of the molecular mechanisms of oxidative phosphorylation.

Publications during the year

Hovmöller, S. Leonard, K. & Weiss, H. (1981). Membrane crystals of a subunit complex of mitochondrial cytochrome reductase containing the cytochromes b and c₁. FEBS Lett., 123, 118-122.

Leonard, K., Hovmöller, S. Karlsson, B., Wingfield, P., Li, Y., Perkins, S. & Weiss, H. (1981). The structure of mitochondrial cytochrome reductase. In Vectorial Reactions in Electron and Ion Transport. F. Palmieri et al., eds.; Elsevier North-Holland, p. 121-137.

Leonard, K. & Weiss, H. (1981a). The structure of mitochondrial ubiquinol:cytochrome c reductase. In Membrane and Transport. Martonosi, A.N., ed.; Plenum (in press).

Leonard, K. & Weiss, H. (1981b). Electron microscopy and computer image reconstruction of membrane crystals. Membrane and Transport, Martonosi, A.N., ed.; Plenum (in press).

Leonard, K., Wingfield, P., Arad, T. & Weiss, H. (1981). Three-dimensional structure of ubiquinol:cytochrome c reductase from Neurospora mitochondria determined by electron microscopy of membrane crystals. J. Mol. Biol., 149, 259-274.

Lepault, J., Weiss, H., Homo, J.-C. & Leonard, K. (1981). Comparative electron microscopic studies of partially negatively stained, freeze-dried and freeze-fractured cytochrome reductase membrane crystals. J. Mol. Biol., 149, 275-284.

Li, Y., Leonard, K. & Weiss, H. (1981). Membrane-bound and water-soluble cytochrome c₁ from Neurospora mitochondria. Eur. J. Biochem., 116, 199-205.

Li, Y., de Vries, S., Leonard, K. & Weiss, H. (1981). Topography of the iron-sulphur subunit in mitochondrial ubiquinol:cytochrome c reductase. FEBS Lett., 135, 277-280.

Wingfield, P. & Weiss, H. (1981). Enzymology of succinate: ubiquinone reductase in detergent solution and reconstituted membranes. In Membrane Proteins. Azzi, A. et al., eds.; Springer Heidelberg, p. 128-134.

Biogenesis of cell surface domains displayed by epithelial cells

Members: D. Louvard, H. Reggio

Fellows: E. Coudrier, K. Soderberg

Visiting workers: J. Gabrion^{*}, B. Rossi^{*}

Technical assistants: B. Juchs^{*}, S. Robinson^{*}, P. Webster^{*}

This group is interested in studying the mechanisms by which membrane components are segregated into particular organelles or areas of membrane. Such a sorting-out mechanism is required to create the specialized functional domains evident at the plasma membrane of epithelial cells. An established cell line (MDCK) forms a differentiated transporting epithelium in culture and is being used by the group as a model system to study the biogenesis of the cell surface (see Research Reports 1978-1980).

Studies on intracellular membranes

One working hypothesis predicts that the segregation of cell surface membrane proteins would occur inside the cell during transport between the site of their synthesis and the cell surface. The Golgi complex, an organelle involved in the intracellular transport of secretory and membrane proteins, could act as a cross-road for control of this membrane traffic. Therefore a precise structural and functional analysis of this set of internal membranes is desirable. Unfortunately the heterogeneity of Golgi membranes, and of intracellular smooth membranes in general, has made it difficult to pursue such studies using the classical approaches of subcellular fractionation and enzymatic analysis.

During the past two years we have attempted to characterize intracellular membranes using an immunological approach, whereby smooth membranes are defined on the basis of their major antigens. Several sera have been raised in rabbits against purified membrane fractions isolated from rat liver homogenates, e.g. rough endoplasmic reticulum (RER), Golgi complex and lysosomes. After an appropriate adsorption to remove unwanted specificities, these sera are used for immunofluorescent studies of cells in culture or sections

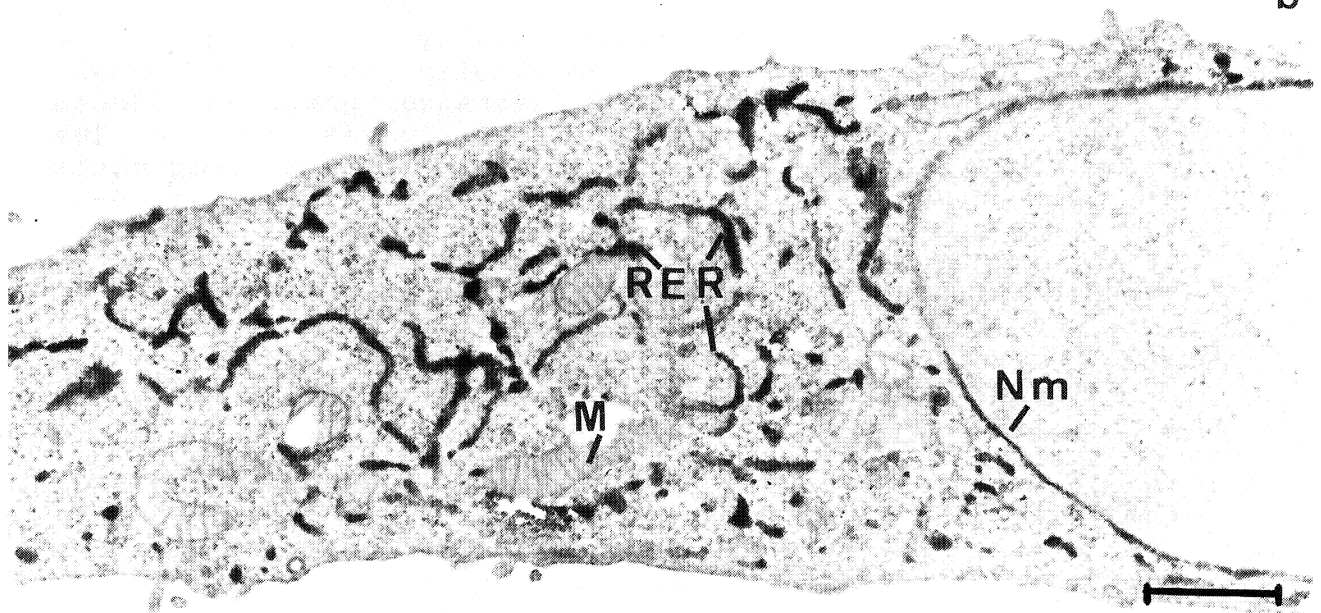
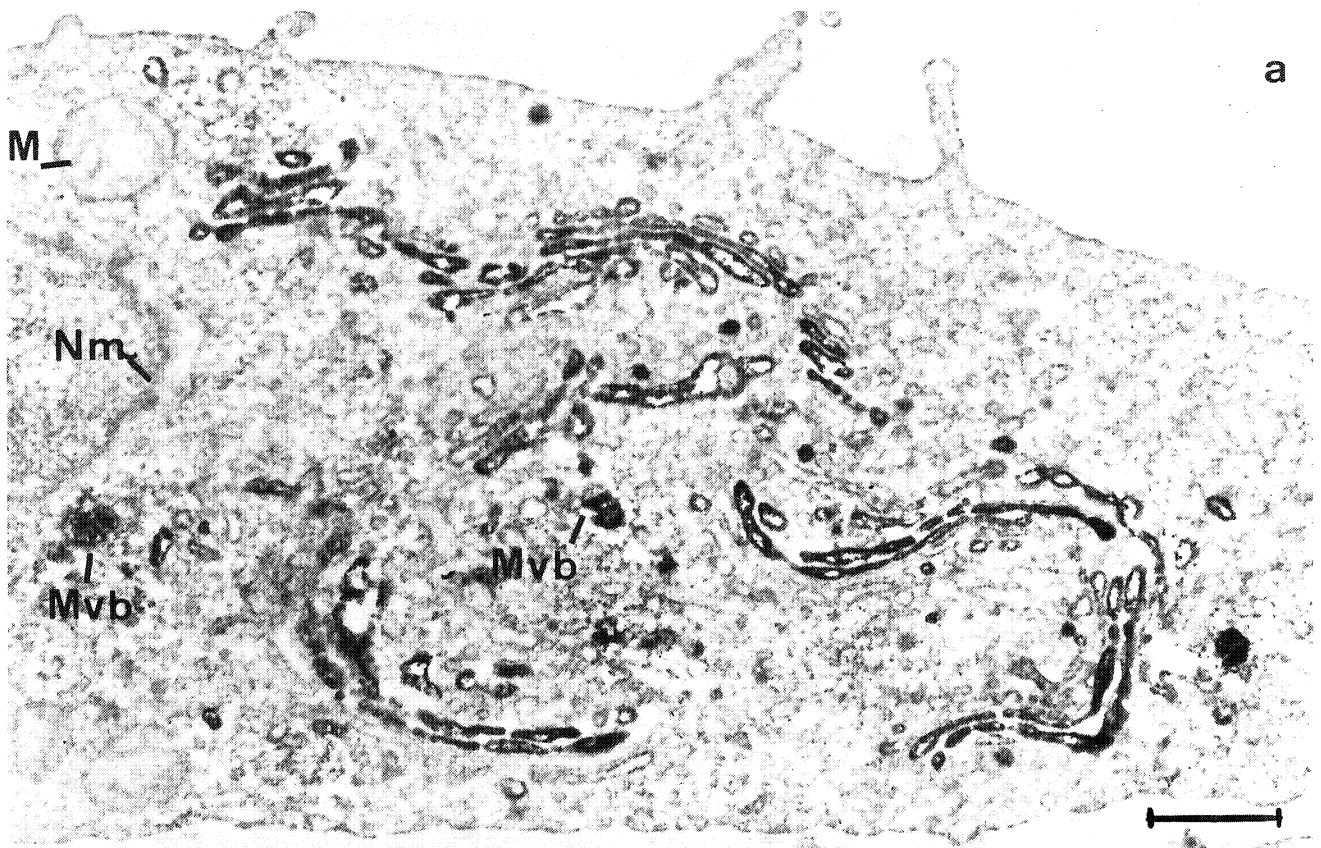
PLATE 18

- a) Immunoperoxidase labelling of NRK cells (unstained sections) using anti-Golgi antibodies.

An overview of the Golgi complex in NRK cells. Note the labelling of the Golgi cisternae and many of the small vesicles in the Golgi region. Many small vesicles were not labelled, and unlabelled Golgi cisternae were most often found on one side of the Golgi stacks. There was no labelling of the nuclear membrane (Nm), the RER, the mitochondria (M) or the nuclei. The plasma membrane was mostly free of labelling and the only labelling of the cell cytoplasm was that caused by occasional leakage from labelled multivesicular bodies (Mvb). Magnification is 15,000 bar 0.5 μm .

- b) Immunoperoxidase labelling of NRK cells (unstained sections) using anti-RER antibodies.

The anti-RER antibodies labelled the tubular network of ER throughout the cell cytoplasm and the nuclear membrane (Nm). Mitochondria (M), plasma membranes, the nuclear matrix and the cell cytoplasm were not labelled. Magnification is 15,000 bar 1 μm .



of frozen tissue at the light microscopic level, or for immunoperoxidase studies at the electron microscope level.

Work on Golgi and RER membranes was performed in collaboration with G.B. Warren's group (see his Annual Report). Recently, in collaboration with E. Harms (Universität Kinder-Klinik, Heidelberg), we have extended this approach to lysosomal membranes.

Immunoprecipitation studies of purified membrane fractions from rat liver or total extract of cells in culture labelled with ^{35}S -methionine have been performed to identify the antigens recognized by each serum.

As reported last year the serum specific for the Golgi complex (Plate 18a) precipitates a 135 k polypeptide. The serum reacting with the endoplasmic reticulum (Plate 18b) precipitates mainly four antigens (Louvard *et al.*, 1982). Antibodies prepared against lysosomal membranes precipitate essentially two polypeptides (68 k and 65 k); full characterization is now in progress.

These antibodies and the antibodies raised against clathrin (reported last year) should provide a very useful set of reagents to analyse biochemically and at the ultrastructural level the intracellular pathway of newly synthesized membrane bound or secreted proteins (Green *et al.*, 1981). Studies on the fate of ligands bound to the cell surface or the recycling of cell surface components can also be monitored with these organelle-specific probes. In collaboration with G. Warren's group we are now attempting to obtain monoclonal antibodies in order to dissect further the intracellular membrane compartments.

Studies on membrane-cytoskeleton interactions in intestinal microvilli

As discussed previously (see Research Reports 1978-1980) the cell surface of epithelial cells is divided into specialized membrane domains containing specific membrane proteins. In addition, an asymmetric distribution of specific cytoskeletal structures associated with these membrane domains is observed (Reggio *et al.*, 1982). The apical membrane is arranged as numerous microvilli containing well-organized filamentous bundles attached at the tip of the microvilli and also connected laterally

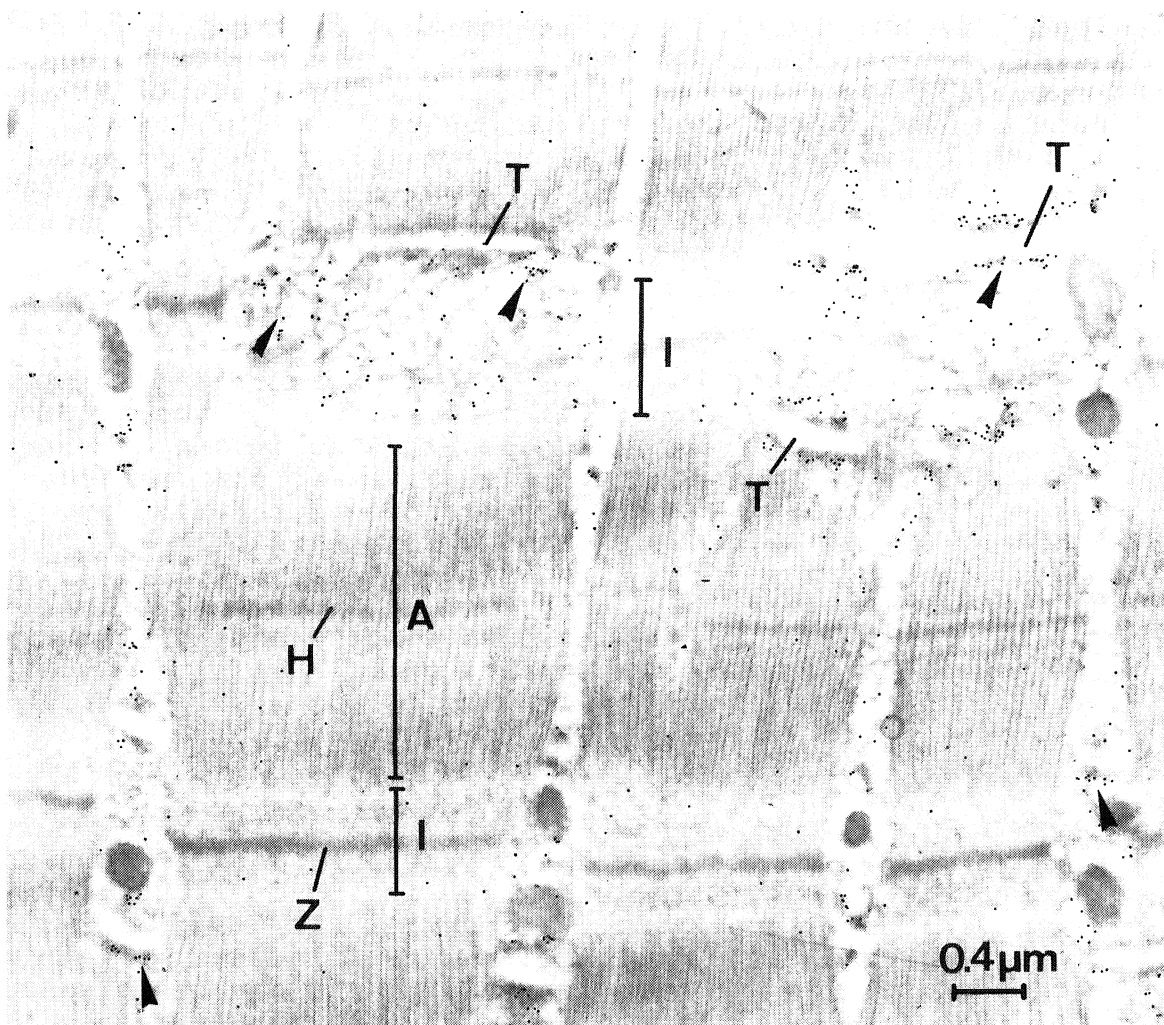


PLATE 19

Electron micrograph of a thin frozen section from rat skeletal muscle labelled with anti-140 k followed by protein A-gold conjugate.

Longitudinal section of rat posterior leg skeletal muscle (semitendinosus). The labelling is found primarily at the periphery of the I band (arrow heads) and corresponds to the periodic staining observed by immunofluorescence. The Z, A and H bands are not labelled. The labelling is localized to the periphery of the myofibrils and seems to be associated with the membrane of the sarcoplasmic reticulum. A tangential section through the fenestrae part of the sarcoplasmic reticulum indicates a strong labelling of this membrane (arrows) particularly at points adjacent to the tubules (T). Magnification is 23,000 bar 0.4 μ m.

along the long axis of each microvillus to the membrane. These actin-containing bundles resemble actomyosin filaments, but the usually associated actin-binding proteins of microfilaments are absent. The filaments of microvilli contain a special set of proteins, primarily calmodulin (17 k), actin (43 k), fimbrin (68 k), villin (95 k) and a 110 k protein. Villin acts to bundle actin filaments together (Bretscher & Weber, 1980) while the 110 k protein appears to connect the actin bundles laterally to the membrane (Matsudaira & Burgess, 1979). Using immunological techniques we have studied the properties and the localization of the 110 k protein (Coudrier et al., 1981). An antigen immunologically related to the 110 k protein has been shown to be concentrated in the I band areas of skeletal muscle. It is localized at the periphery of the myofibrils where the sarcoplasmic reticulum is abundant (Plate 19). The pattern of staining observed has led us to propose that a protein similar to the 110 k protein of microvilli must be present around the myofibrils and involved in the association of actomyosin filaments with their surrounding membranes (Coudrier et al., 1982). Identification and characterization of the muscle antigen analogous to the 110 k protein of intestinal microvilli is now in progress.

We have also demonstrated the presence of a 140 k glycoprotein tightly associated with isolated cytoskeletal elements from intestinal microvilli. The strong interaction with the microvillar microfilaments of this surface protein is dependent on calcium and can be released with EGTA. This protein lacks all previously reported enzymatic activities usually associated with intestinal microvilli it has been purified to homogeneity and its topological relationship with the membrane bilayer established. Most of the protein emerges on the external face of the microvillar membrane and it can be released by various proteases. The solubilized form of this protein has a molecular weight analogous to the uncleaved protein. A short cytoplasmic fragment might account for its lipophilic character and may be involved in anchoring this protein to the membrane. Such properties are very similar to those described a few years ago for several membrane bound hydrolases of intestinal microvilli (Louvard et al., 1976). A specific antiserum allowed us to localize it at the ultrastructural level in intestinal epithelium.

We have also shown, just as in the case of the 110 k protein, the presence in skeletal muscle of an antigen crossreacting with the antiserum raised against the 140 k

glycoprotein from intestine. Its localization is closely related to the distribution of the sarcoplasmic reticulum around the myofibrils (Coudrier et al., 1982). The identification and further characterization of the muscle antigen is now being pursued. Work in progress should also provide information concerning the interaction between the 140 k glycoprotein and cytoskeletal components. Our working hypothesis postulates that the 140 k glycoprotein may interact directly or indirectly with the cross-bridges (containing the 110 k protein) and provide lateral attachment between actin-containing microfilaments and the microvillus membranes. Analogous antigens could play a similar role in skeletal muscle providing a connecting network between the actin filaments and the sarcoplasmic reticulum membrane.

Studies on cell-cell interactions in epithelia

Several types of mutants resistant to ouabain, obtained from the MDCK cell-line, have been well characterized in collaboration with B. Rossi from Dr. Lazdunski's group (Univ. of Nice, France). These mutants have been used to study some aspects of the interactions between these cells when grown in monolayer. A mixed culture of MDCK wild-type cells and mutants resistant to ouabain exhibit an unusual case of cellular cooperation. Once grown together in the presence of ouabain a quantitative recovery of each cell type can be achieved. However confluent cultures of MDCK cells are neither electrically nor dye coupled. Moreover at confluency a metabolic cooperation in HAT medium cannot be demonstrated using co-culture of wild-type MDCK cells and HPRT-deficient mutant cells. Finally in confluent monolayers gap junctions have not been observed by freeze fracture studies.

These data taken together strongly suggest that it is unlikely that the rescue phenomenon observed can be explained, as proposed in other cellular systems, by means of the cytoplasmic bridges formed by gap junctions.

As a working hypothesis we have postulated that a continuity of cell membranes, especially at the level of the apical junctional complex (the tight junction is an area of the epithelium where membrane bilayers seem to fuse), might allow exchange of lipids and possibly membrane proteins between neighbouring cells. Such properties would then provide an explanation for our observations. This

hypothesis as well as the properties of tight junctions in MDCK cells are now being investigated in further detail.

Publications during the year

Coudrier, E., Reggio, H. & Louvard, D. (1981). Immunolocalization of the 100,000 molecular weight cytoskeletal protein of intestinal microvilli. J. Mol. Biol., 152, 49-66.

Coudrier, E., Reggio, H. & Louvard, D. (1982). The cytoskeleton of intestinal microvilli contains two polypeptides immunologically related to proteins of striated muscle. In 46th Cold Spring Harbor Symposium "Organisation of the Cytoplasm", (in press).

Green, J., Griffiths, G., Louvard, D., Quinn, P. & Warren, G. (1981). Passage of viral membrane proteins through the Golgi complex. J. Mol. Biol., 152, 663-698.

Louvard, D. & Reggio, H. (1982). Rôle des microtubules dans l'organisation du complexe de Golgi. Annales d'Endocrinologie, (in press).

Louvard, D., Reggio, H. & Warren, G. (1982). Antibodies to the Golgi complex and the rough endoplasmic reticulum. J. Cell. Biol., 82, 92-107.

Marsh, M., Matlin, K., Simons, K., Reggio, H., White, J., Kartenbeck, J. & Helenius, A. (1981). Are lysosomes a site of enveloped virus penetration? 46th Cold Spring Harbour Symposium "Organisation of the cytoplasm", (in press).

Matlin, K., Reggio, H., Helenius, A. & Simons, K. Infectious entry pathway of influenza virus in a canine kidney cell line (1981). J. Cell. Biol., 91, 601-613.

Matlin, K., Reggio, H., Helenius, A. & Simons, K. (1981). The entry of enveloped viruses into an epithelial cell line. In Membranes in Growth and Development: ed. Giebisch, G.; Alan Liss, New York, (in press).

Matlin, K., Reggio, H., Helenius, A. & Simons, K. (1982). The pathway of vesicular stomatitis virus entry leading to infection. J. Mol. Biol., (in press).

Meyer, D.I., Louvard, D. & Dobberstein, B. (1982). Characterization of molecules involved in protein on translocating using a specific antibody. Rapid communication. J. Cell Biol., (in press).

Reggio, H., Coudrier, E. & Louvard, D. (1982). Surface and cytoplasmic domains in polarized epithelial cells. International Conference on Biological Membranes, Crans-sur-Sierre, Switzerland, (in press).

Other references

Bretscher, A. & Weber, K. (1980). Cell, 20, 839.

Louvard, D., Sémériva, M. & Maroux, S. (1976). J. Mol. Biol., 106, 1023-1038.

Matsudaira, P.T. & Burgess, D.R. (1979) J. Cell Biol., 83, 667.

Electron microscopy of nucleic acids

Members: H. Delius, B. Koller

Fellow: H.J. Bohnert^{*}

Visiting workers: C. Astier^{*}, I. Kiss^{*}, H. Schnabel^{*}

Technical assistants: J. Clarke, C. Michalowski^{*}

In collaboration with T.H. Dyer, C. Bowman, C. Howe and J. Gray from the Plant Breeding Institute in Cambridge, the analysis of wheat chloroplast DNA was continued. A plasmid which contains the DCCD-(dicyclohexylcarbodiimide)-binding protein was constructed in Cambridge. Using histograms of the partial denaturation pattern and of E.coli RNA polymerase binding sites, and transcription-translation analysis, the gene was mapped at a well-defined position between two RNA polymerase binding sites.

The chloroplast DNAs (cpDNA) of the green algae Euglena gracilis strain Z and strain bacillaris were studied in detail. Single-stranded circular molecules of the cpDNA from the Z strain display two short inverted repeat structures of about 125 ntd, called I1 and I2. By electron microscopic analysis of heteroduplexes with the E.coli fragment, cloned in the plasmid pBK8, which contains the rrnB operon, we could demonstrate that I1 is localized between the 3'-end of the extra 16S rRNA gene and the 5'-end of the 16S rRNA gene in the first of the three tandemly arranged complete operons (Jenni & Stutz, 1979). The inverted repeat I2 is located upstream of the extra 16S rRNA gene (Plate 20a and b).

The bacillaris strain of the same species was thought to have a similar arrangement of three tandem rRNA operons. To analyse whether it may have the same inverted repeat structure close to a possible extra 16S rRNA gene, heteroduplexes between cpDNA of this strain and the pBK8 fragment were also prepared. Measurements of these heteroduplexes are shown in Plate 21a and the histogram derived from these molecules is drawn in Plate 21b. It is apparent that the cpDNA of the bacillaris strain contains five complete rRNA operons and two extra 16S rRNA genes, each one upstream of an inverted repeat.

To prove that this map is correct, partial denaturation maps were prepared for both strains (Plate 21c, e and f). While the Z strain has four pronounced double-stranded regions, representing the three complete rRNA operons and the extra 16S rRNA gene, with the inverted repeat I1, the bacillaris strain has seven double-stranded regions representing five complete rRNA operons, two extra 16S rRNA genes with two I1 sequences.

It is not known whether these extra 16S rRNA genes are functional and what may be the role of the inverted repeats. Heteroduplexes obtained by re-annealing different fragments from the same cpDNA with each other showed that one modified and possibly a second partial 5S rRNA sequence is found in the region surrounding I1. A short homology between the leader sequence of the normal and the extra 16S rRNA genes was also demonstrated.

A region of variable size (± 400 ntd) in cpDNA of the Z strain was described (Jenni et al., 1979). In collaboration with E. Stutz and B. Schlunegger (Neuchatel) two clones (pEgch1 and pEgch2) which contain a HindIII fragment from the same position in the cpDNA, but which differ in size by about 200 ntd, were analysed. Self-annealing of single-stranded fragments showed that both clones contain the inverted repeat I2. The loop formed by self-annealing of the two inverted sequences was 200 ntd longer in the plasmid pEgch2 than in pEgch1. The heteroduplex between the two plasmid DNAs (Plate 20c), prepared with the mica technique, shows the non-homology, and the position was mapped almost in the middle between the two inverted sequences I2.

In extension of the work on chloroplast DNA the DNA of another organism, Cyanophora paradoxa, was studied. This flagellate contains so-called cyanelles which could be regarded as endosymbiotic cyanobacteria. Unlike "modern" chloroplasts cyanelles contain a rudimentary cell wall. In collaboration with W. Loeffelhardt (Wien) the DNA components from Cyanophora were characterized. The cyanelle DNA has a complexity of 127 kb which is in the order of the size of a chloroplast DNA. A map was established for this DNA, and several genes were located on this map by hybridization with plasmid clones carrying the corresponding genes from spinach chloroplast DNA (16S, 23S, 5S rRNA genes, large subunit of RubP-carboxylase, 32 kd thylakoid membrane protein, α , β and ϵ subunit proteins of the ATPase complex). It could also be demonstrated that

PLATE 20

- a) and
- b) Cytochrome spreadings of heteroduplexes between Euglena gracilis strain Z chloroplast DNA (cpDNA) and a fragment from the plasmid pBK8 which contains the E.coli rrnB operon. The short single-stranded end indicates the 5'-end of the 16S rRNA gene and the long single-stranded end the sequence downstream of the 3'-end of the 23S rRNA gene in the pBK8 fragment. (a) Two pBK8 fragments have re-annealed with the first two of the three tandemly arranged and complete rRNA operons. Two small inverted repeat structures (I1 and I2) are indicated. (b) One pBK8 fragment re-annealed with the extra 16S rRNA gene alone, while a second fragment annealed to the first complete rRNA operon. The inverted repeat I1 is located between the two 16S rRNA genes.
- c) A mica adsorption of a heteroduplex between the two plasmids pEgcH1 and pEgcH0. Both clones contain a HindIII fragment from the same position in the cpDNA of Euglena gracilis strain Z. Single strands were complexed with T4 gene 32 protein and appear as thick complexes. The arrow points to the non-homology, indicating the region of variable size in the HindIII fragments. This region was mapped between the positions of the inverted sequences I2.
- d) Electron micrograph of a heteroduplex between two plasmid clones containing different restriction fragments from Epstein-Barr virus DNA. The transition between vector and insert DNA is marked by arrows. A hairpin structure caused by an inverted repeat is marked with an "x". An extended region of homology between the two insert DNAs can be observed in the middle of the heteroduplex.
- e) The same heteroduplex as shown in d) but prepared using the mica adsorption method. Within the region which appeared homologous in d) a row of tandemly repeated partially homologous sequences can be detected at the higher resolution as a series of substitution loops (open arrow).

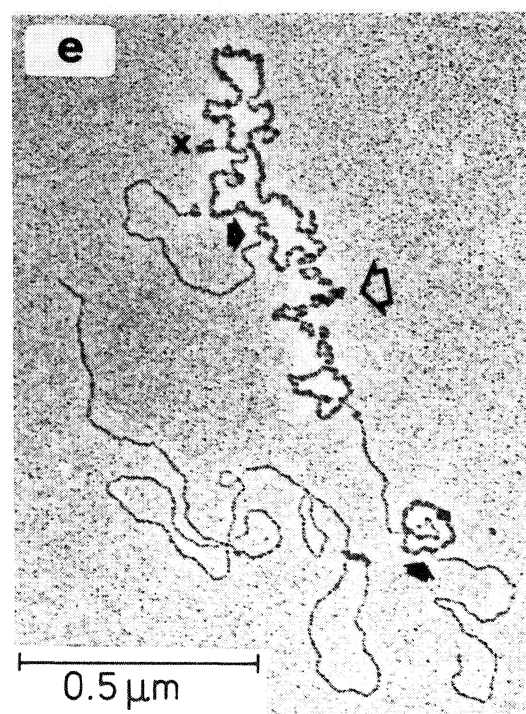
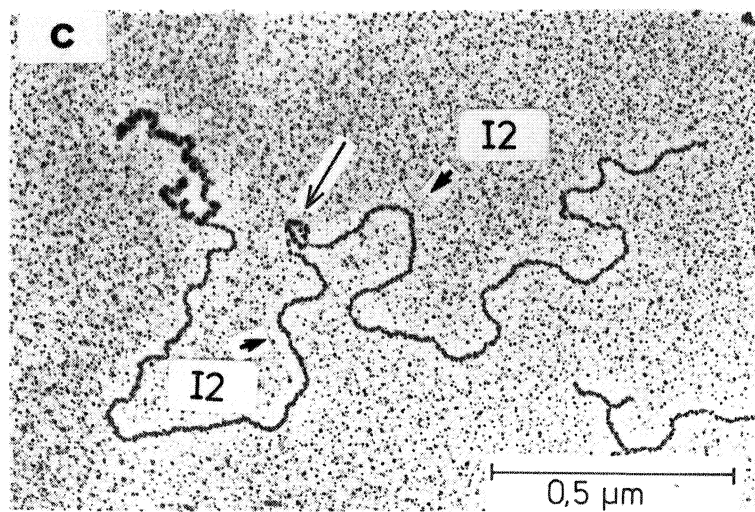
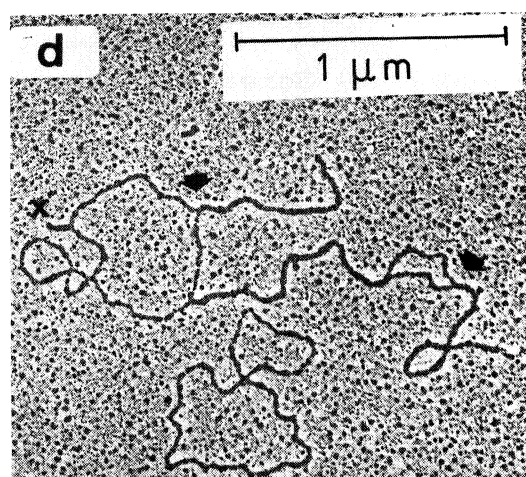
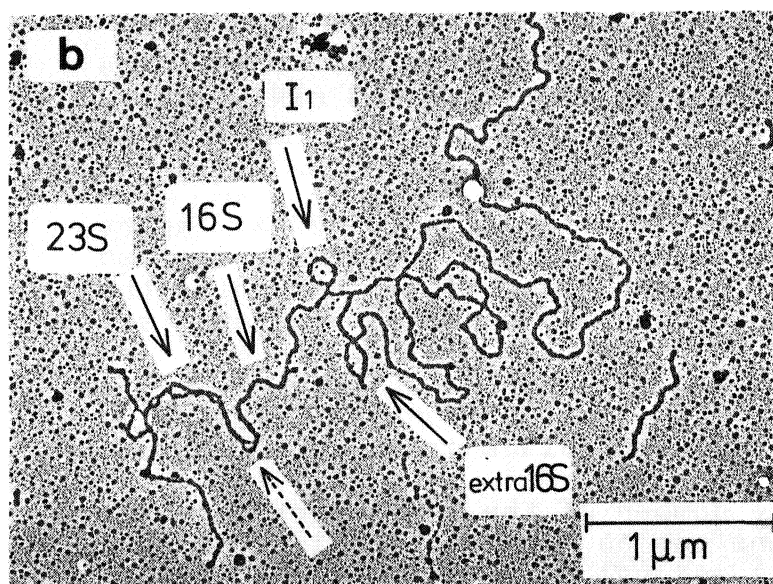
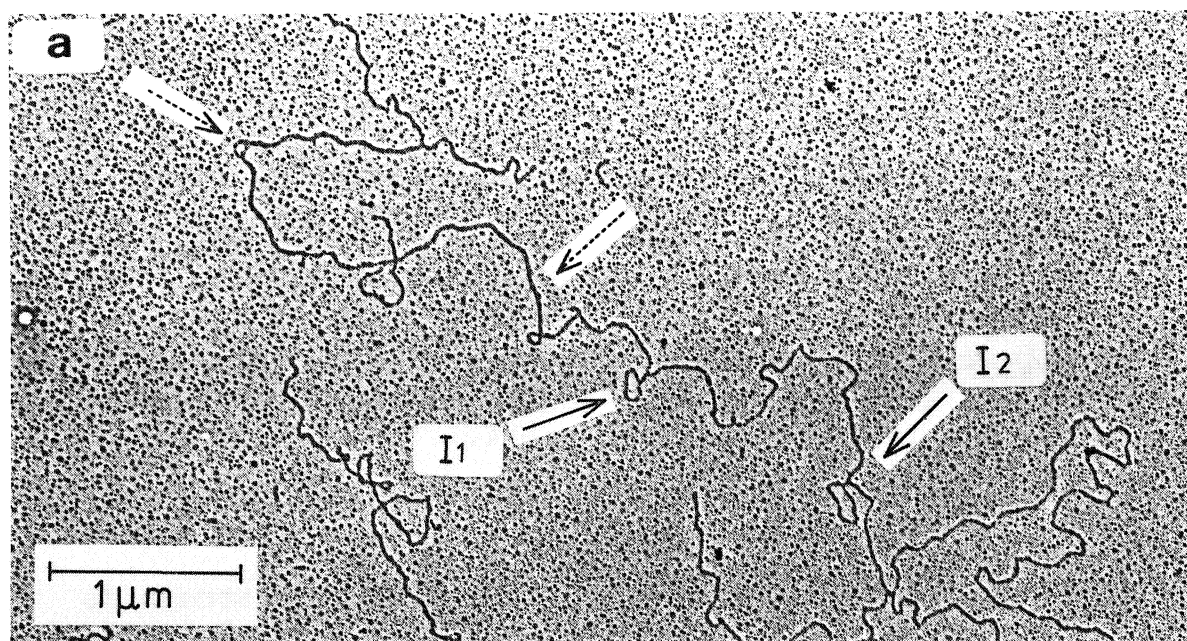


PLATE 21

Measurements on heteroduplexes prepared by cytochrome spreadings between cpDNA of Euglena gracilis strain bacillaris and the pBK8 fragment (a and b), and a comparison with partial denaturation maps from cpDNA of the bacillaris and the Z strain (c, e and f).

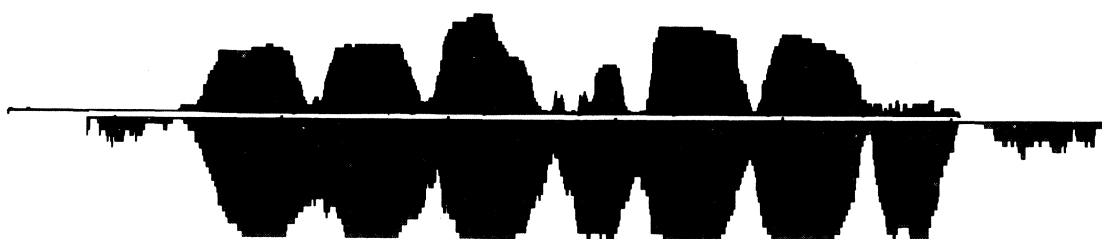
- a) Measurements of individual heteroduplex molecules. The black bars indicate the double strands, the thin lines the single strands of the cpDNA.
- b) A histogram derived from the measurements shown in (a). The black areas represent the double-stranded regions.
- c) Partial denaturation map of the bacillaris strain as in (e) but drawn to the same scale as the heteroduplex histogram and with the double-stranded regions as black areas.
- d) Schematic drawing of the arrangement of the five complete rRNA operons and the two extra 16S rRNA genes, and the two inverted repeats (I1) in the bacillaris strain.
- e) Partial denaturation map of the bacillaris cpDNA. Apart from the rRNA genes the rest of the molecule was so highly denatured that no map was obtained and only the rRNA gene region was measured. Denatured regions are drawn as black areas.
- f) Partial denaturation map of cpDNA from the Z strain. Denatured regions are drawn as black areas.

The difference in the number of the GC-rich rRNA genes between the two strains can be easily recognized in the comparison between (e) and (f).

a



b



c

d

23	16	23	16	23	16		23	16	23	16	
5		4		3		I ₁ extra 16S	2		1		I ₁ extra 16S

strain bacillaris

e



152 Kb
146 Kb

f



strain Z

related sequences exist in the genomic DNA from the free-living cyanobacteria Anacystis and Aphanocapsa (with C. Astier, Gif-s.-Yvette) In collaboration with the group of J. Weil (Strasbourg) several tRNAs were identified and located on restriction fragments of cyanobacterial DNA.

In collaboration with G. Bornkamm (Freiburg) plasmid clones containing restriction fragments from Epstein-Barr virus DNA were analysed by heteroduplex methods. Restriction analysis had shown that a row of short terminal repeats is present near the right end of the DNA, and that DNA sequences farther to the left show cross-hybridization to this region. The heteroduplexes made clear that this region also contains a series of short tandem repeats of partial homology to the right stretch of repeat sequences resulting in a row of small substitution loops. These could not be detected in a cytochrome preparation, but are visualized in the electron micrograph obtained by mica adsorption (Plate 20d and e). This region becomes actively transcribed upon TPA induction of the virus, and is, therefore, of special interest.

Together with D. Bruehl (Nürnberg) a new instrument for length measurements has been developed. A new projector has been built to combine the manual measuring stage with the computer-controlled step motor stage. With the help of the electronic workshop a device has been built which allows a vector scan using the random access camera to speed up the automatic line following process. All the hardware is now installed and the programming to provide an easy switching between manual and automatic measurements is under development.

Various collaborative work:

- plasmids containing sequences derived from both ends of phage μ were analysed by heteroduplex analysis to determine the extent and the relative orientation of the insertions (with the group of E. Bade, Konstanz);
- together with I. Kiss (Szeged) heteroduplexes between different recombinant DNAs carrying Drosophila heat shock genes were analysed;

- in collaboration with the groups of Dobberstein and Lehrach hybrids between recombinant β DNA containing genes from the histocompatibility region of mouse and mRNA were measured and the extent and position of intron loops was determined;
- together with H. Schnabel (Zillig, Martinsried) DNA from a phage infecting an Archaeobacterium was self-annealed and shown to possess a restricted circular permutation and terminal redundancy.

Publications during the year

Bowman, C. M., Koller, B., Delius, H., & Dyer, T. (1981). A physical map of wheat chloroplast DNA showing the location of the structural genes for the ribosomal RNAs and the large subunit of ribulose 1,5-bisphosphate carboxylase. Mol. Gen. Genet., 183, 93-101.

Darai, G., Fluegel, R. M., Zoeller, L., Matz, B., Krieg, A., Gelderblom, H., Delius, H. & Leach, R. H. (1981). The plaque-forming factor for mink lung cells present in Cytomegalovirus and Herpes-Zoster virus stocks identified as Mycoplasma hyorhinis. J. Gen. Virology, 55, 201-205.

Hudewentz, J., Delius, H., Freese, U.K., Zimmer, U., & Bornkamm, G.W. Two distant regions of the Epstein-Barr virus genome with sequence homologies have the same orientation and involve small tandem repeats. EMBO Journal, (in press).

Koller, B., Delius, H. & Dyer, T.A. (1981). The organization of the chloroplast DNA in wheat and maize in the region containing the LS gene. Europ. J. Biochem., (in press).

Mellado, R., Delius, H., Klein, B., & Murray, K. (1981). Transcription of sea urchin histone genes in Escherichia coli. Nucl. Acids Res., 9, 3889-3906.

Schnabel, H., Zillig, W., Pfaeffle, M., Schnabel, R., Michel, H., & Delius, H. (1982). Halobacterium halobium phage ϕ H. EMBO Journal, (in press).

Temple, M., Antoine, G., Delius, H., Stahl, S. & Winnacker, E.-L. (1981). Replication of mouse adenovirus strain FL DNA. Virology, 109, 1-12.

Other references

Jenni, B. & Stutz, E. (1979). FEBS Lett., 102, 95-99.

Jenni, B., Fasnacht, M. & Stutz, E. (1981). FEBS Lett., 125, 175-179.

Electron microscopy and computer image analysis

Member: K. Leonard

Fellows: F. Booy, S. Hovmöller*, B. Karlsson*

Visiting workers: A. Cremer*, S. Grundy*, D. Holmes*, J. Lake, P. Riccio, A. Yonath

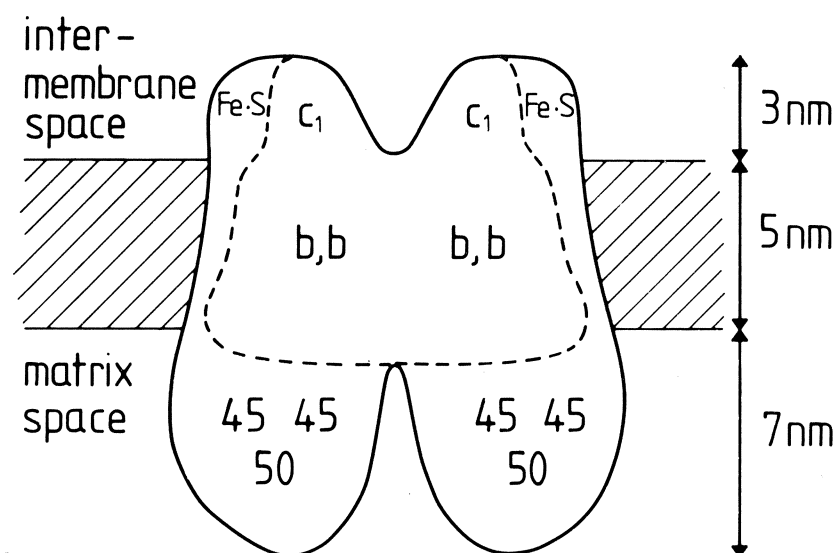
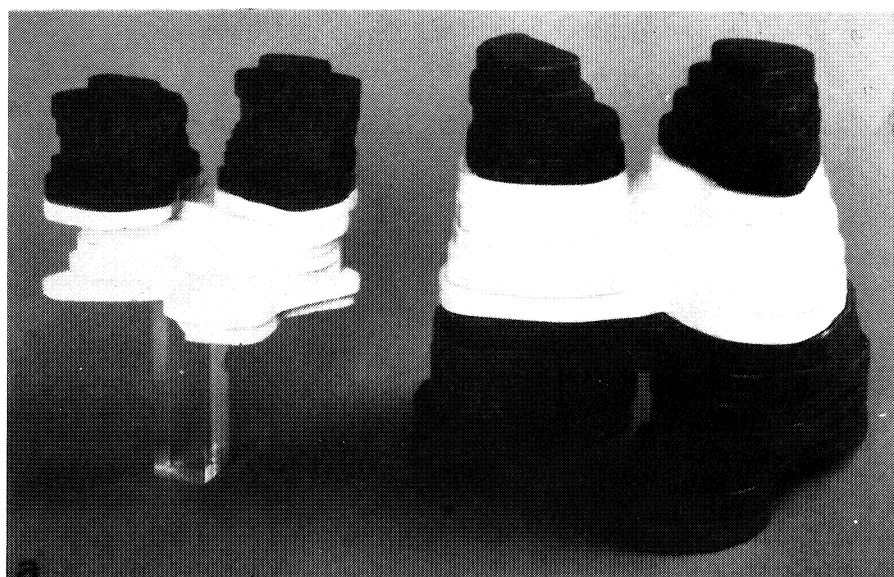
Technical assistant: T. Arad

This group has been working on the electron microscopy and computer image analysis of several periodic biological structures.

Membrane crystals

Membrane proteins are only stable in a hydrophobic environment such as the lipid bilayer or in detergent micelles. This is a disadvantage when trying to produce three-dimensional crystals for protein crystallography but can be of advantage for electron microscopy. Within the membrane bilayer, protein molecules may exist naturally as two-dimensional crystals, or may be induced to crystallize by raising the ratio of protein to lipid in protein-containing lipid vesicles. These two-dimensional membrane crystals are sufficiently thin for electron microscopy and are very suitable for analysis by Fourier methods. The effects of specimen damage can also be reduced by taking advantage of the redundancy of information in a crystalline array.

In collaboration with the group of H. Weiss and with S. Hovmöller and B. Karlsson, we have been studying the membrane protein cytochrome reductase and its sub-complex containing only the cytochromes b and c1. Both of these proteins can be obtained as two-dimensional membrane crystals. A low-resolution three-dimensional structure for the native molecule which is in good agreement with the biochemical model has been reconstructed from tilted views of the crystals. Although the membrane crystals of the cytochrome bc₁ subcomplex are less well ordered than those of the native enzyme it has now been possible to obtain a three-dimensional reconstruction of this part of the enzyme. Comparison of this with the structure of the whole enzyme complex has confirmed the polarity and the



b

PLATE 22

- a) Models for cytochrome bc_1 complex (left) and cytochrome reductase (right). The region of each molecule thought to be within the membrane is lighter in colour, that outside the membrane is darker. The size and shape of the bc_1 reconstruction corresponds to that for the whole enzyme with the larger of the two peripheral darker sections removed.
- b) Schematic distribution of the major subunit polypeptides of cytochrome reductase based on biochemical data and on the distribution of density found in the image reconstructions (see also the Report of H. Weiss).

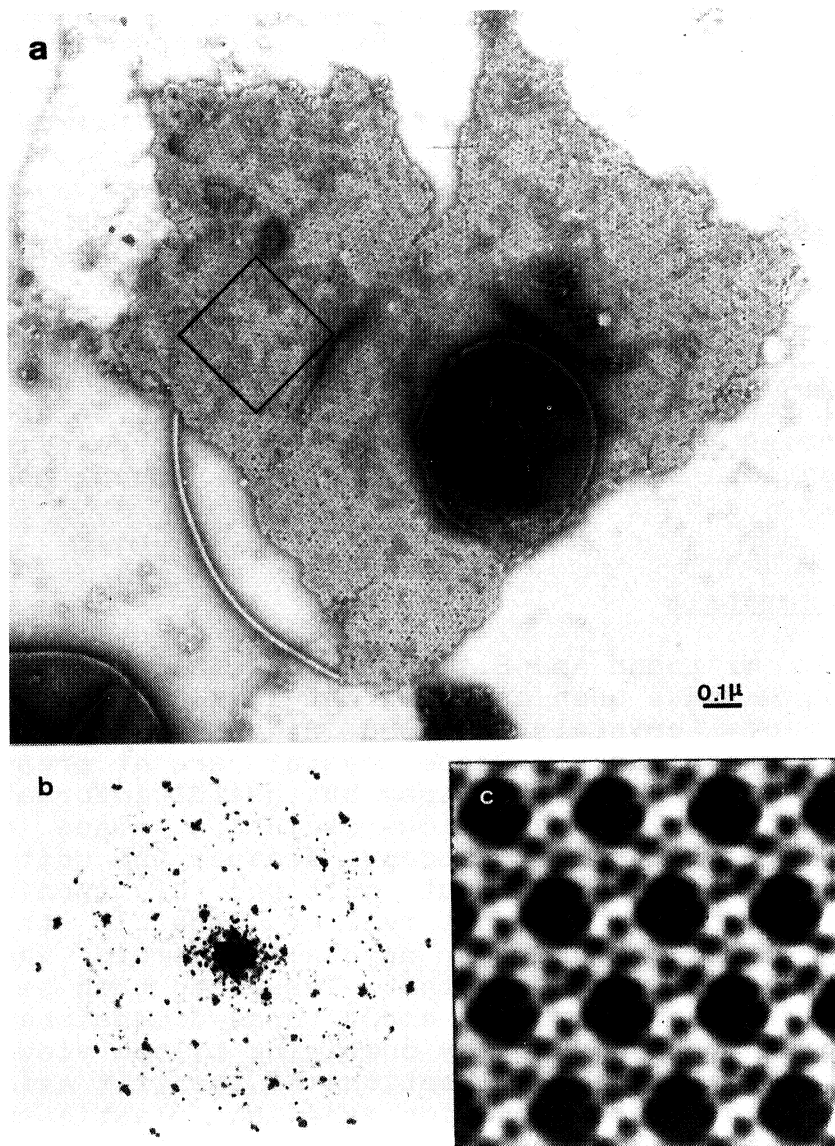


PLATE 23

- a) Cell-wall sheet of *Chlamydia trachomatis*, negatively stained with sodium phosphotungstate.
- b) Computer calculated diffraction pattern for the region outlined in black in (a).
- c) Computer noise filtered and averaged image from the same area - the lighter, stain-excluding, regions are protein.

distribution of major subunits in the native enzyme (Plate 22).

We have also been working (with J.-J. Chang) on the naturally occurring crystalline outer cell wall of Chlamydia trachomatis. It has been possible to obtain sufficiently large and well-preserved crystalline areas to carry out two-dimensional image processing that reveals the cell wall structure more clearly (Plate 23). We are now in the process of carrying out a three-dimensional reconstruction from tilted images of these cell-wall layers.

Ribosome crystals

With H.G. Wittmann and B. Tesche (Berlin) and A. Yonath (Rehovot), we have been carrying out image analysis of thin sections of crystals of 50S ribosome subunits of B.Stearothermophilus. These crystals are at present too small for x-ray crystallography but useful information on the subunit packing and low-resolution shape can be obtained from electron microscopy. Because the unit cell is large, it is possible to cut sections of epon-embedded crystals which are one unit cell or less in thickness. Grids are then searched for crystalline areas where the sectioning direction is constant. These can then be treated as two-dimensional crystals and a three-dimensional image reconstruction carried out by combining tilted views of one crystal taken at several directions of the tilt axis. Plate 24 shows such a reconstruction made on plastic-embedded, positively stained material.

With J. Lake (UCLA) we have also carried out a preliminary analysis of tilted views of negatively stained sheets of E.coli 50S ribosome subunits. This has enabled the symmetry of these sheets to be determined and could be extended to carry out a three-dimensional reconstruction.

Low temperature electron microscopy (F.P. Booy)

In collaboration with the E/M Applications Group (see Report p. 131) methods for preparing frozen hydrated specimens have been developed and tested. In particular, a method has been found for examining water-soluble fibrous specimens in the frozen hydrated state. This has been applied to specimens of DNA, hyaluronic acid and the

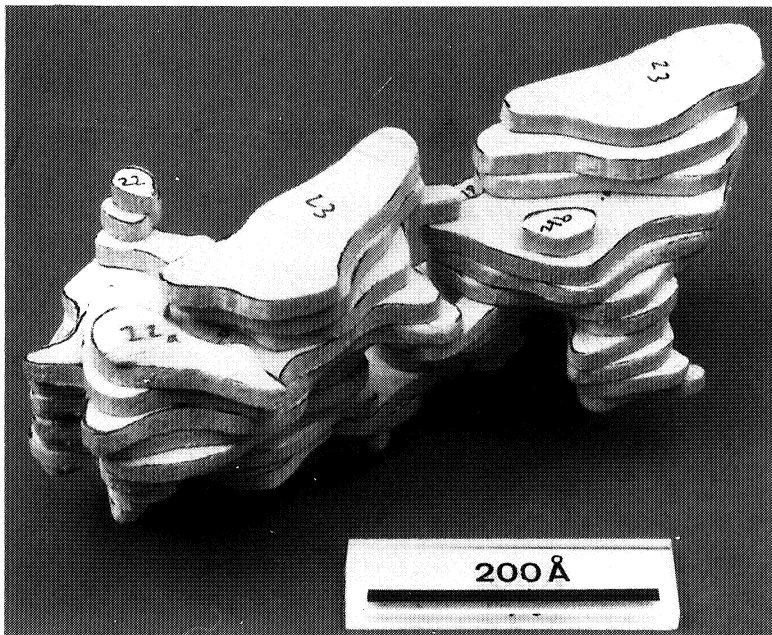
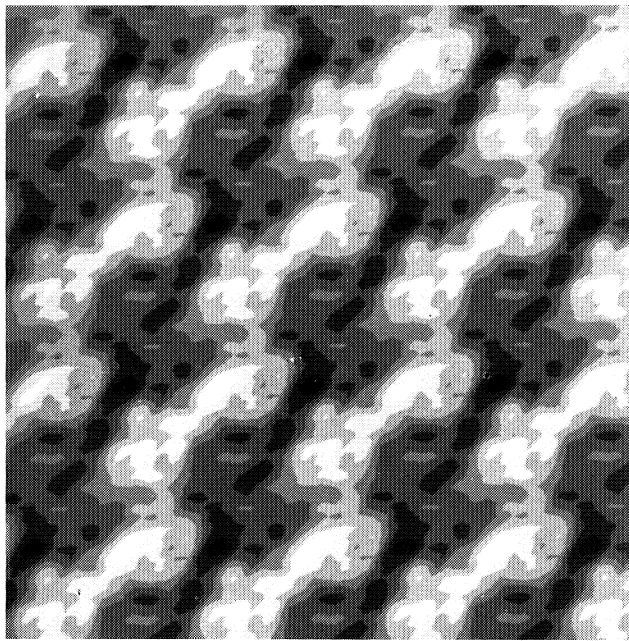
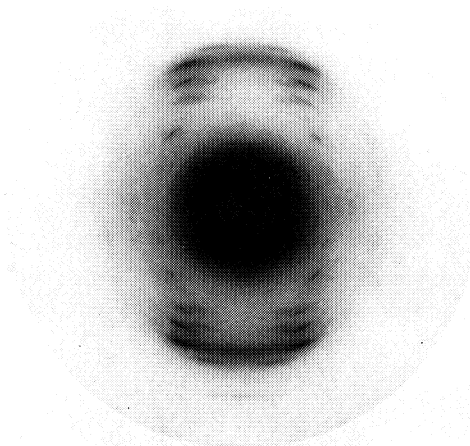
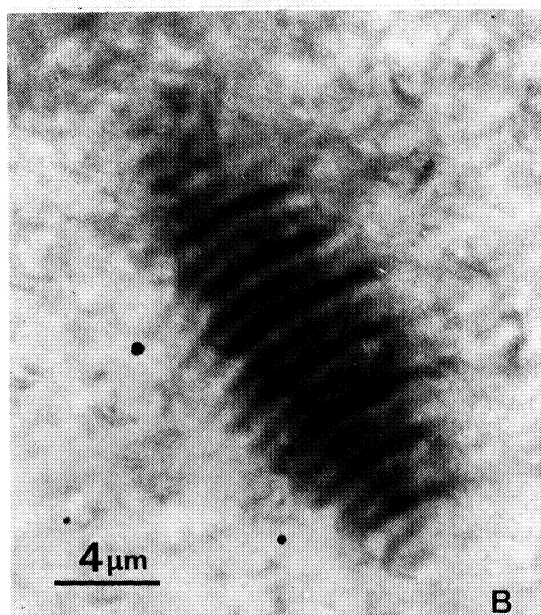


PLATE 24

- a) Density contoured, filtered image of a thin sectioned crystal of 50S ribosomal subunits. In this case, the lighter regions correspond to positively stained ribonucleoprotein.
- b) A balsa-wood model of one repeating unit of the crystal (this should be compared with the lighter area of image (a) above) showing two lobes of density, each corresponding approximately to the volume expected for two 50S subunits.



A



B

PLATE 25

- a) Electron diffraction pattern from a specimen of DNA prepared by drawing fibres and annealing at 60°C , 76% humidity for 20 h. Specimen was then quench-frozen in liquid nitrogen and examined at -160°C , 120kV. The outermost meridional spacing is 2.56 Å.
- b) Example of a mesomorphic phase structure (liquid crystal) observed in a specimen of fd filamentous bacterial virus annealed and examined as above.

filamentous bacterial viruses fd and Pf1. DNA and hyaluronic acid give high resolution fibre electron diffraction patterns (Plate 25A). For phage fd and Pf1, only poorly oriented diffraction patterns have so far been obtained. In the imaging mode, liquid crystalline structures have been clearly seen (Plate 25B) and these can be related to the degree of specimen orientation. Using this technique it would be possible to monitor, by both electron imaging and diffraction, the process of formation of highly ordered fibrous specimens (for example, under the influence of a strong magnetic field, see Report of D. Marvin's group).

Tests have also been carried out at room temperature on the new Philips EM400T microscope to determine the optimum film and magnification for low dose imaging. With crystalline specimens of the polysaccharide dextran, low dose images have been obtained which give 6 Å resolution in optical diffraction. With J.C. Homo it has been demonstrated that the Philips PW6591 cold stage on this microscope will routinely resolve 10 Å and with further modification will resolve 3.4 Å. With this cold stage it should also be possible to obtain tilted images of frozen crystalline material in order to carry out three-dimensional image analysis.

Other work

With A. Cremers (Leiden) we have been studying thin crystals of elongation factor EF-Tu and a preliminary three-dimensional reconstruction has been carried out.

With G. Isenberg (Munich) and B. Jockusch we have been using image analysis to study the interaction of actin with vinculin (see Report of B. Jockusch and Plates 15 and 16).

With D. Banner and R. Bryan we have carried out a helical reconstruction of helical particles obtained by acid treatment of filamentous phage Pf1. This used programs for helical reconstruction from noisy data developed by the Data Analysis Group (see Reports of D. Marvin and S. Provencher, also Plate 52).

With T. Pitt some preliminary work has been carried out on two-dimensional averaging of small fragmented crystals of cytochrome reductase.

With P. Riccio (University of Bari) we have been trying to obtain membrane crystals of mitochondrial ATP/ADP transport protein.

Publications during the year

Freeman, R. & Leonard, K.R. (1981). Comparative mass measurements of biological macromolecules by scanning transmission electron microscopy. J. Microscopy, 122, 275-286.

Gray, C.W., Kneale, G.G., Leonard, K.R., Siegrist, H. & Marvin, D.A. (1982). A nucleoprotein complex in bacteria infected with Pf1 filamentous virus: Identification and electron microscopic analysis. Virology, 116, 40-52.

Isenberg, G., Leonard, K.R. & Jockusch, B.M. (1982). Structural aspects of vinculin-actin interactions. J. Mol. Biol., (in press).

Leonard, K., Hovmöller, S., Karlsson, B., Wingfield, P., Li, Y., Perkins, S. & Weiss, H. (1981). The structure of mitochondrial cytochrome reductase. In Vectorial Reactions in Electron and Ion Transport in Mitochondria and Bacteria: eds. F. Palmieri et al.; Elsevier, Amsterdam, p.127-137.

Leonard, K. & Weiss, H. (1981). Electron microscopy and computer image reconstruction of membrane crystals. In Membrane and Transport: ed. Martonosi, A. N.; Plenum, New York (in press).

Leonard, K. & Weiss, H. (1982). The structure of mitochondrial ubiquinol: cytochrome c reductase. In Membrane and Transport: ed. Martonosi, A. N.; Plenum, New York (in press).

Leonard, K., Wingfield, P., Arad, T. & Weiss, H. (1981). Three-dimensional structure of ubiquinol: cytochrome c₁ reductase from Neurospora mitochondria determined by electron microscopy of membrane crystals. J. Mol. Biol., 149, 259-274.

Lepault, J., Weiss, H., Homo, J.-C. & Leonard, K. (1981). Comparative electron microscopic studies of partially negatively stained, freeze-dried and freeze-fractured cytochrome reductase membrane crystals. J. Mol. Biol., 149, 275-284.

Li, Y., DeVries, S., Leonard, K. & Weiss, H. (1981). Topography of the iron-sulphur subunit in mitochondrial ubiquinol:cytochrome c reductase. FEBS Letters, 135, 277-280.

Li, Y., Leonard, K. & Weiss, H. (1981). Membrane bound and water-soluble cytochrome c₁ from Neurospora mitochondria. Eur. J. Biochem., 116, 199-205.

Electron microscopy applications group

Members: J. Dubochet, R. Freeman, J. Lepault, C.A. Walter

Fellow: J.-J. Chang

Visiting workers: A. ^{*}Brisson, F. ^{*}Harper, H. ^{*}Heumann, G. Nicolas, A. Ollins, K.T. Tokuyasu

Technical assistants: J.A. Berriman, A.W. McDowall

Cryo-electron microscopy

The cryo-electron microscopy project will combine the advantages of the considerable reduction of electron-beam damage observed at 4 K (Knapek & Dubochet, 1980) with the improved preservation of biological structure in frozen-hydrated specimens. These two parts of the project are now ready to be combined, since the superconducting lens manufactured by the group of Dr. Dietrich from Siemens GmbH (Munich) was delivered in December of this year and is now being installed in a modified Zeiss 10A electron microscope (see also Report of E/M Development Group).

During the year the E/M Applications Group has continued the work of the previous years to develop the methodology for the preparation and observation of frozen hydrated specimens. The major finding is that liquid water or any aqueous solution can be vitrified. The freezing artefacts due to ice crystal growth can thus be suppressed. Having adapted the methods developed previously for vitrification (see Research Report 1980), we are now in a position to prepare well-prepared samples of any biological suspensions (Plate 26). We have also developed methods for the preparation and high resolution observation of frozen-hydrated thin sections (Plate 27).

Our major results are the following:

1. Pure water or any aqueous solution can be prepared simply for electron microscopy. Layers up to 1 μ m thick can be vitrified. In the electron microscope, frozen water behaves as foreseen from previous x-ray studies. In particular, sublimation rate and phase transition can be used for temperature determination.

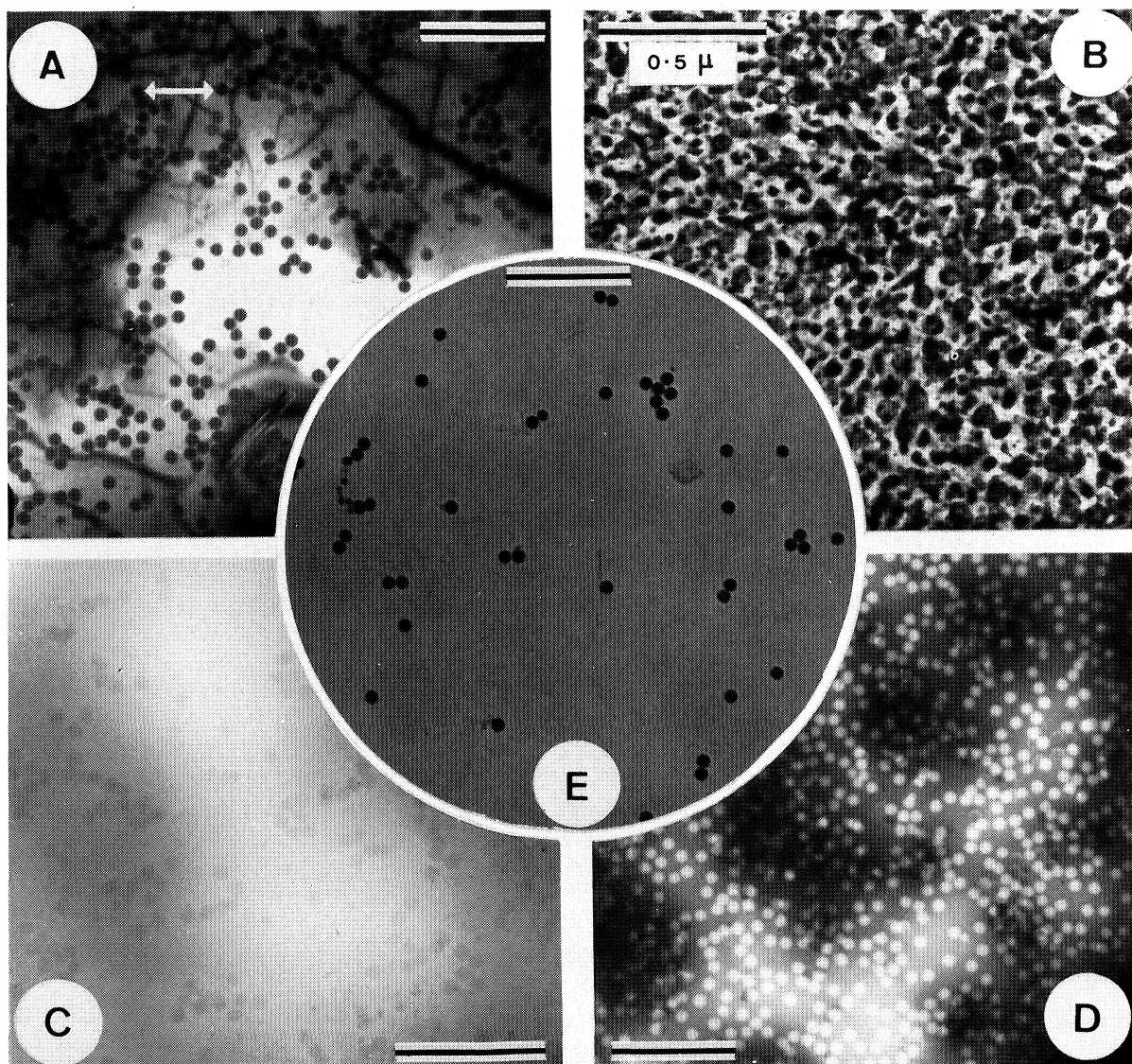


PLATE 26

Particles in frozen water observed at 110 K. Magnification: 18,000 times. (a) Polystyrene spheres in crystalline ice. Some of the spheres have been pushed above the surface of the water; they appear with higher contrast (arrows). (b) T₄ bacteriophages in 30% sodium phosphotungstate solution. On freezing ice and solute have formed two separated phases. Magnification: 48,000 times. (c) Vitrified suspension of polystyrene spheres in pure water. (d) Vitrified suspension of polystyrene spheres in 20% sodium phosphotungstate solution. (e) Dry polystyrene spheres observed at room temperature.

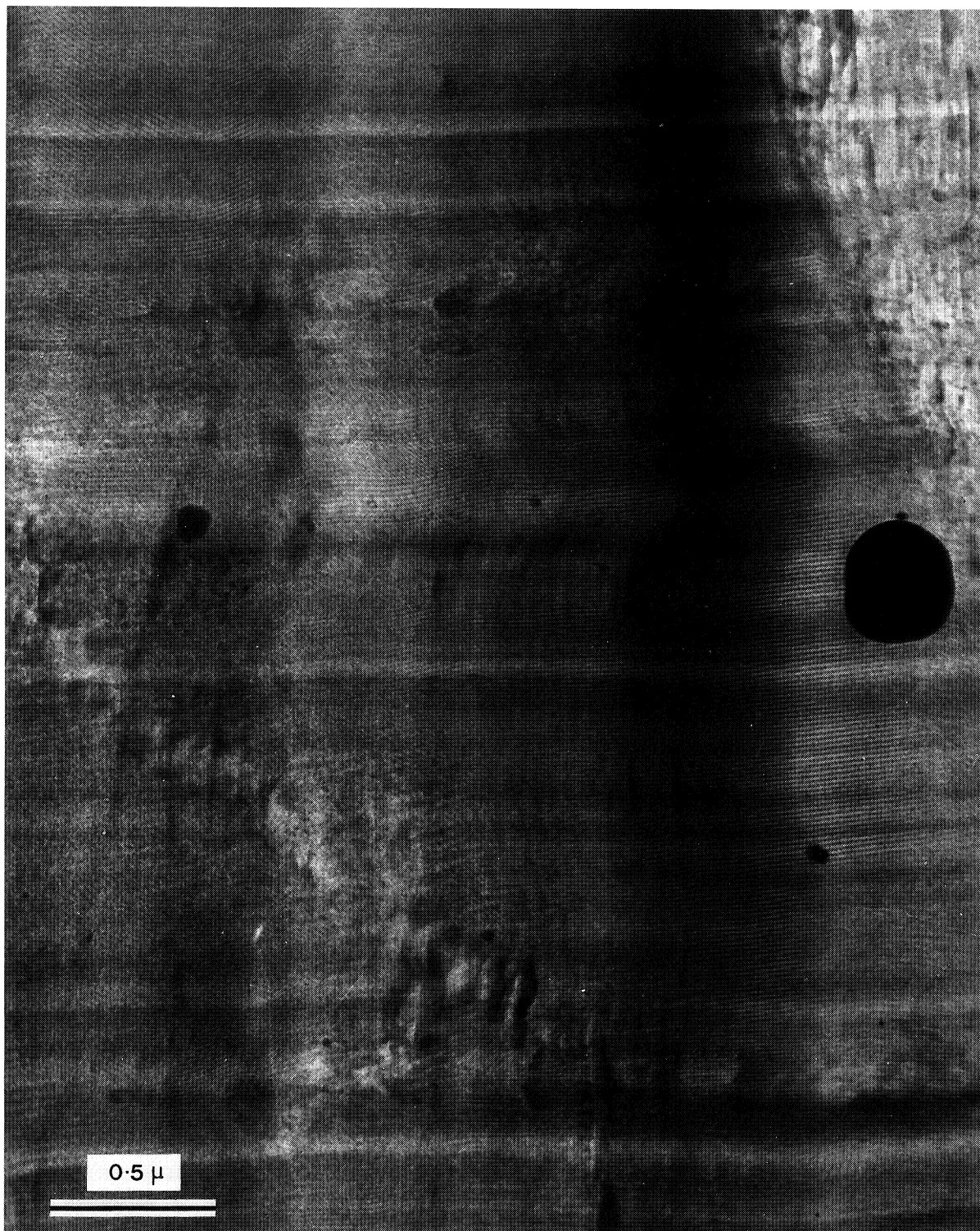


PLATE 27

Frozen hydrated section of an unfixed and unstained catalase crystal. Magnification: 54,000 times.

2. There are no visible freezing artefacts when biological suspensions are vitrified. In particular, biological structures and local solute concentrations are preserved.
3. In vitrified suspensions, the contrast of the image is directly and quantitatively related to the density of the various components. An adequate choice of the solute may lead to positive or negative staining of the structure, or alternatively permits the localization of specific components by contrast matching.
4. In general freeze-drying (even when partial) does not permit good preservation of the structure while increasing contrast by removing bulk water.
5. Thin sections in which structure is conserved at high resolution can be obtained if the material is locally vitrified. Unfortunately, a sizeable piece of biological material can only be vitrified when the biological material itself has a sufficient antifreeze effect (as may be the case in concentrated protein solutions), or by adding cryoprotectant.
6. Above 100 K, hydrated specimens are no more beam-sensitive than dry specimens. On the contrary, it is not so much the water that has a harmful effect on the irradiated biological material, but the biological material that induces damage in the water.

Service activities

The E/M Applications Group has collaborated during the year with the following scientists within the EMBL:

F. Booy, J.-E. Edström, G.G. Kneale, K.R. Leonard, D. Louvard, M.F. Moody, H. Reggio, H. Weiss.

We have collaborated with, or provided instrumental facilities for, the following outside scientists:

A. Brisson (CENG, Grenoble). Observation of frozen hydrated membranes.

J. Escaig (Univ. of Paris, Paris). Methodological developments on freeze-fracture.

H. Heumann (MPI für Biochemie, Martinsried, Munich). Attempt to measure the mass of RNA polymerase on DNA.

W. Hoffmann (MPI für Medizinische Forschung, Heidelberg). Mass measurements on amphibian muscles.

B. Martin (MPI für Kernphysik, Heidelberg). Trace elements in frozen-hydrated sections.

G. Moyne and F. Harper (CREC, Villejuif, Paris). Observation on minichromosomes of SV40.

G. Nicolas (Univ. of Paris IV, Paris). Methodology for cryo-sectioning.

A. Ollins (Oak-Ridge, Tennessee, USA). Recording of tilt-series of embedded chromatin.

P. Oudet (University of Strasbourg). Operation of the STEM.

M. Takahashi (University of Toulouse). cAMP and RNA polymerase binding to DNA.

K.T. Tokuyasu (Univ. of California, La Jolla, San Diego). Development of methodology for cryo-sectioning.

Zhang You Kun (Peking Institute of Ophthalmology, Peking, China). Three-dimensional reconstruction of Chlamydia trachomatis envelope.

Publications during the year

Chang, J.-J., Dubochet, J., Baudras, A., Blazy, B. & Takahashi, (1981). Electron microscope observation of a fibre structure formed by non-specific binding of cAMP receptor protein to DNA. J. Mol. Biol., 150, 435-439.

Deimann, W., Freeman, R. & Fahimi, H.D. (1981). Improved contrast in cytochemistry of dehydrogenase by scanning transmission electron microscopy. J. Histochem. Cytochem., 29, 678-681.

Dubochet, J., Lepault, J., Freeman, R., Berriman, J.A. & Homo, J.-Cl. (1982). Electron microscopy of frozen water and aqueous solutions. J. Microsc., (in press).

Freeman, R. & Leonard, K.R. (1981). Comparative mass measurements of biological macromolecules by scanning transmission electron microscopy. J. Microscopy, 122, 275-286.

Homo, J.-C., Freeman, R., Walter, C.A. & Dubochet, J. (1981). STEM à basses températures. Mesure de la température du specimen. Transfert et observations des specimens biologiques hydrates congelés. Proc. of Meeting of Société Française de Microscopie Electronique: Besançon, (in press).

Kneale, G.G., Freeman, R. & Marvin, D.A. (1982). The Pf1 bacteriophage replication-assembly complex: x-ray fibre diffraction and scanning transmission electron microscopy. J. Mol. Biol., (in press).

Lepault, J. (1981). Thèse de doctorat d'état ès-Sciences Naturelles. Université Paris VI, Paris. Contribution à l'étude du cryodécapage appliqué aux suspensions biologiques.

Lepault, J., Freeman, R. & Dubochet, J. (1982). Microscopie électronique de haute résolution à basse température. Journal de Physique, (in press).

Lepault, J., Weiss, H., Homo, J.-C. & Leonard, K. (1981). Comparative electron microscopic studies of partially negatively stained, freeze-dried and freeze-fractured cytochrome reductase membrane crystals. J. Mol. Biol., 149, 275-284.

Moyne, G., Freeman, R., Saragosti, S. & Yaniv, M. (1981). A high-resolution electron microscopy study of nucleosomes from Simian Virus 40 chromatin. J. Mol. Biol. 149, 735-744.

Reference

Knapek, E. & Dubochet, J. (1980). J. Mol. Biol., 141, 147-161.

Structure and assembly of filamentous bacterial viruses

Members: D.A. Marvin, D.W. Banner^{*}, G.G. Kneale, C. Nave

Fellows: M. Bansal^{*}, W. Folkhard^{*}

Students: T. Watts^{*}, K. Zimmermann^{*}

Visiting workers: T. Cross^{*}, S. McGavin^{*}, A. Prieler^{*}

Technical assistant: K. Nilsson

One important general question in structural molecular biology is how the function of macromolecular assemblies emerges from the structure of the component subunits. Just as all information necessary to define the tertiary structure of a protein is present in the amino-acid sequence, so must all information for functional interactions between molecules be present in the tertiary structure of the molecules. Genetic engineers who wish to define desirable changes in DNA sequence must know the rules by which these changes are expressed in function. Since these rules are likely to be complicated, it is preferable to study simple systems.

The filamentous bacterial viruses use small proteins to carry out many basic biological functions such as transport of proteins across membranes and manipulation of DNA by proteins. This makes them ideal systems in which to use the techniques and concepts of physical science to study fundamental questions of biology. Several structures that are present at various stages in the virus life-cycle are suitable for study by x-ray fibre diffraction. Fibre diffraction has one great advantage over single-crystal crystallography: structurally meaningful periodicities are detected directly on the diffraction pattern, and changes in these periodicities can be read off the pattern almost by inspection. Although even the best fibre data do not approach the best single-crystal data in quality, almost any long macromolecule will give some kind of fibre pattern.

Structure of the Pf1 virion

We have had several experimental successes with the Pf1 virion project in the past few years. Specific chemical reactions were used to prepare and characterize an iodine

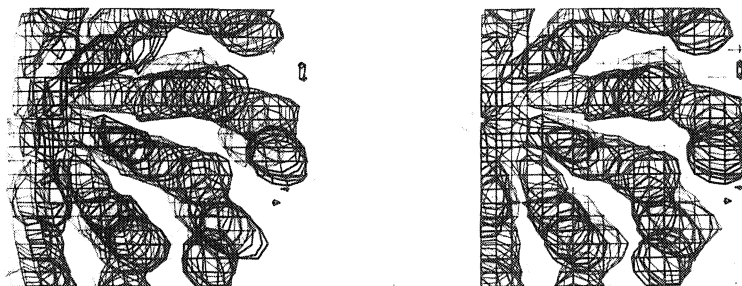


PLATE 28

Electron density distribution of Pf1 virions, calculated using isomorphous replacement and solvent flattening. Stereo pair of a view down the helix axis, showing one quadrant of the circular cross-section.

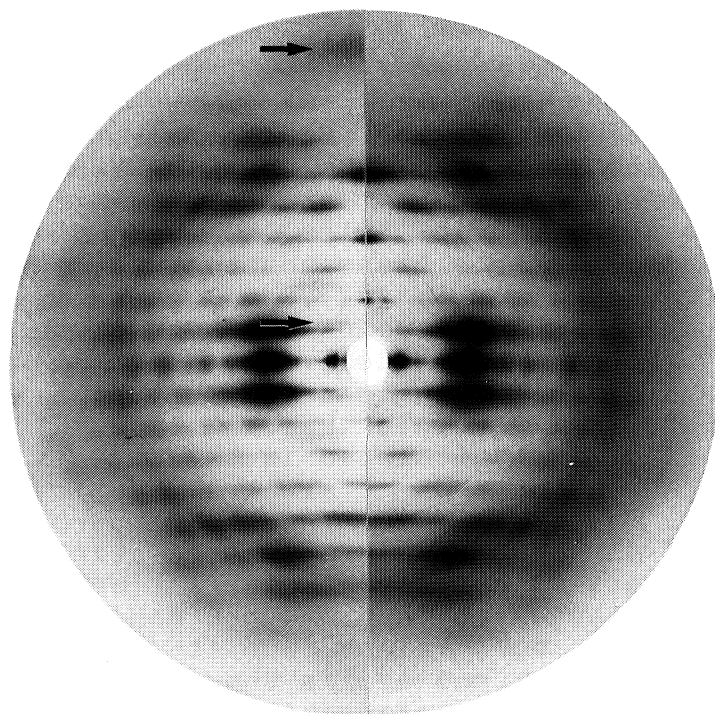


PLATE 29

X-ray fibre diffraction patterns of fd virions. Fibre axis vertical. Left: native virions, showing layer lines attributed to DNA (arrows). Right: virions after acid degradation; DNA layer lines are absent.

and a mercury derivative of Pf1; high quality fibre diffraction patterns were obtained using a strong magnetic field to orient the virions during preparation of fibres; and Bessel functions were resolved by preparing fibres at 4°C to induce a slight change in virion symmetry, giving three-dimensional data to 4 Å resolution (Nave et al., 1981). The success of these experiments has led us to concentrate on a detailed analysis of the Pf1 virion.

In order to make full use of our high quality fibre diffraction data, we must solve several computational problems. One problem is to reduce the data on the x-ray film to a form that can be used for further calculation. We are making use of a regularized inverse method developed by R. Bryan (see Research Report of the Data Analysis Group). A second problem is to calculate electron density distributions from the diffraction data. In principle two heavy-atom derivatives should be sufficient to determine phases of resolved Bessel functions, but in fact the position of the mercury is closely related to the position of the iodine by the helix symmetry of the virion. Therefore the two heavy-atom derivatives do not give independent phase information. Further constraints can be used in the calculation to resolve phase ambiguity: for instance the electron density cannot be negative, and it must be flat outside the molecular envelope. Two different methods were used to apply these constraints. In the first method (Marvin & Nave, 1982), a phase probability distribution was calculated point-by-point along the layer lines using the native and derivative data, and refined with techniques used in single-crystal studies where non-crystallographic symmetry is present. A preliminary electron density map calculated in this way is shown in Plate 28. The map shows rods of electron density which can be interpreted as α -helices. Another approach to the calculation of electron density has been developed by R. Bryan, using a maximum entropy regularization method. This method includes heavy-atom data and the non-negativity and molecular boundary constraints, but it also includes a smoothness constraint and avoids the termination errors inherent in Fourier transformations. A more detailed description with an electron density map of Pf1 calculated by this method is given in the Research Report of the Data Analysis Group.

The ultimate goal of the structure analysis is to build a molecular model of the virion. Such a model not only should predict the diffraction data, but also should be consistent with the important stereochemical constraints imposed by

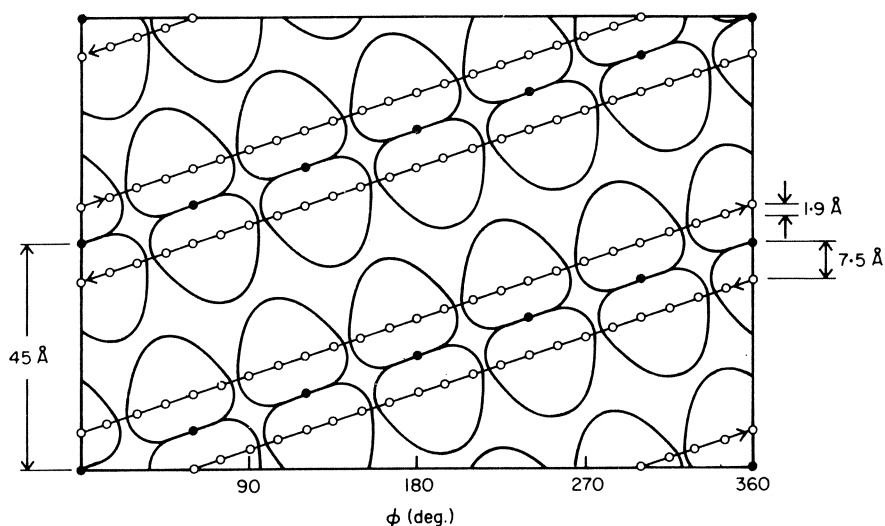


PLATE 30

Surface lattice of Pf1 replication-assembly complex, drawn at a radius of 21 Å. The helix pitch is 45 Å. The line joining the open circles represents the DNA helix with 24 nucleotides per turn along each of the two anti-parallel DNA strands. The protein subunits are drawn schematically. Dimers are formed from subunits related by a two-fold symmetry axis (filled circles) corresponding to the proposed two-fold symmetry relating the anti-parallel DNA strands. Each subunit interacts with 4 nucleotides of one DNA strand, and there are 6 dimers/turn.

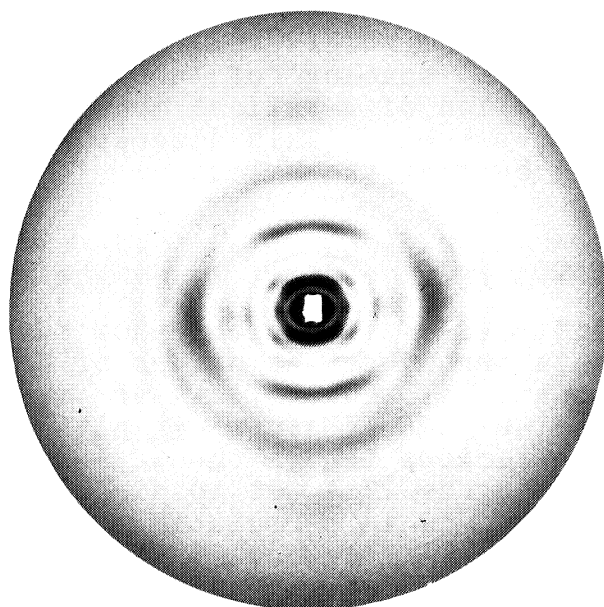


PLATE 31

X-ray fibre diffraction pattern of Pf1 replication-assembly complex at high water content. Compare with Plate 22 of the 1980 Research Reports.

the sequence of the protein, and the constraints defined by accessibility studies and heavy-atom substitution. An electron density map can help to define the model, but if the subunit is small, features of the fibre pattern can be interpreted directly in terms of periodicities in the structure. It is therefore feasible to define a model by direct comparison of the calculated diffraction with the observed native and derivative data. The operation of constructing a model on the basis of an electron density map is sometimes called "interpreting the map", and the operation of constructing a model that predicts the diffraction data is sometimes called "model-building", but both operations lead to the same result from the same data.

We are using the molecular graphics system FRODO. This enables us to display a model and the corresponding difference electron density map as a step in refining the model. It also enables us to display 5.40 and 5.46 subunits/turn models, in order to explore the molecular details of the temperature-induced structural transformation (see below).

Our model-building studies (Marvin *et al.*, 1981; Marvin & Nave, 1982) have shown that the general features of the diffraction pattern are consistent with a single slightly curved α -helical subunit, but one persistent discrepancy between calculated and observed diffraction is found near the meridian at a spacing of about 15 Å, where the calculated diffraction of α -helical models is substantially larger than the observed. This discrepancy can be removed by stretching or bending the helix.

DNA in the virion

Highly ordered fibres of fd virions show two distinct sets of layer lines: a strong set at orders of 32 Å, due to the protein coat, and a weaker set at orders of 27 Å, attributed to the DNA (Banner *et al.*, 1981). Acid treatment of the virions leaves the 32 Å set of layer lines intact, but causes the 27 Å set to disappear (Plate 29), and this disappearance is correlated with degradation of the viral DNA to small fragments. Gel electrophoresis on parallel acid-treated fd and Pf1 virions shows that Pf1 DNA undergoes a similar acid degradation. Although there are no distinct layer lines attributable to DNA on Pf1 diffraction patterns, a comparison of the Pf1 layer lines before and after DNA degradation should give information about the structure of DNA in the Pf1 virion.

Polymorphism of the virion

The Pf1 virion can be transformed into other forms without being degraded (Marvin et al., 1981). The simplest and best-studied transformation is the temperature-induced transformation between 5.40 and 5.46 subunits/turn. O. Greulich in the group of R. Wijnaendts has studied this transformation using fluorescence measurements to study changes in the tyrosine environment (see the Research Report of R. Wijnaendts), and using partial specific volume measurements to study the effect of solvent.

We have also found a more dramatic change in virion structure that is induced by a combination of acid and heat: the virions are transformed into twisted ribbon structures. These structures have been studied by image reconstruction of electron micrographs, in collaboration with K. Leonard, T. Arad and R. Bryan. An electron micrograph of a ribbon and the corresponding reconstructed image are shown in Plate 29 of the Research Report of the Data Analysis Group. Understanding these different kinds of polymorphism at the molecular level should give insight into the laws governing motion of subunits within a molecular assembly.

The replication-assembly complex

The gene 5 DNA-binding protein of filamentous bacterial viruses is involved in replication of viral DNA and in subsequent assembly of virions at the bacterial cell membrane. This protein binds to viral DNA to form a helical intracellular complex about 100 Å in diameter and 1 µm long. The fd complex and the Pf1 complex are superficially similar, but they differ in some significant respects. The fd gene 5 protein has a molecular weight of 9,690, whereas the corresponding protein of Pf1 has a molecular weight of 15,400 and an entirely different amino-acid sequence (determined in collaboration with the group of A. Tsugita; Maeda et al., 1982). The fd complex has a 90 Å pitch, whereas the Pf1 complex has a 60 Å pitch, as seen by electron microscopy (Gray et al., 1982). X-ray fibre patterns of the Pf1 complex show a 45 Å helix pitch, and STEM measurements (in collaboration with R. Freeman) show that within this pitch there are six protein dimers, with four nucleotides per monomer (Plate 30; Kneale et al.,

1982). The structure of the Pf1 complex changes substantially with conditions such as water content, and these changes are reflected in the x-ray fibre patterns (Plate 31). Detailed analysis of these fibre patterns may lead to a better understanding of the dynamics of DNA-protein interactions.

Pili structure

PAK pili are the bacterial organelles to which the Pf1 virion adsorbs. The fibre diffraction patterns of PAK pili (Folkhard et al., 1981) indicate that much of the protein subunit is α -helical, with the long axis of the helix roughly parallel to the long axis of the pilus. Hydrodynamic studies on soluble pilin by T. Watts (Edmonton) suggest that the axial ratio of the pilin monomer is about 4:1. A computer model-building approach was used to study in more detail the orientation of the subunit within the pilus and the orientation of the helices within the subunit. A class of models could be defined which are consistent with the observed diffraction pattern.

Myosin and intermediate filaments

The technique of magnetic orientation developed for filamentous bacterial viruses should be applicable to other assemblies of α -helices such as myosin thick filaments and intermediate filaments. We have tried to use our cryomagnet to orient fibres of reconstituted myosin thick filaments (supplied by J. Davis, Johannesburg) and eukaryotic intermediate (or 100 Å) filaments. In both cases it became clear that further biochemical studies are necessary to determine conditions for formation of liquid crystalline arrays which respond to the magnetic field. This end might be gained by removing non-helical portions of the filaments using specific enzymatic degradation, and/or by exploring the effect of changing solvent, ionic strength, pH, temperature, or other conditions.

Publications during the year

Banner, D. W., Nave, C. & Marvin, D. A. (1981). Structure of the protein and DNA in fd filamentous bacterial virus. Nature (London), 289, 814-816.

Folkhard, W., Marvin, D. A., Watts, T. H. & Paranchych, W. (1981). Structure of polar pili from Pseudomonas aeruginosa strains K and O. J. Mol. Biol., 149, 79-93.

Gray, C. W., Brown, R. S. & Marvin, D. A. (1981). Adsorption complex of filamentous fd virus. J. Mol. Biol., 146, 621-627.

Gray, C.W., Kneale, G.G., Leonard, K.R., Siegrist, H. & Marvin, D.A. (1982). A nucleoprotein complex in bacteria infected with Pf1 filamentous virus: Identification and electron microscopic analysis. Virology, 116, 40-52.

Maeda, K., Kneale, G.G., Tsugita, A., Short, N.J., Perham, R.N., Hill, D.F. & Peterson, G.B. (1982). The DNA-binding protein of Pf1 filamentous bacteriophage: amino acid sequence and structure of the gene. EMBO J., (in press).

Kneale, G.G., Freeman, R. & Marvin, D.A. (1982). The Pf1 bacteriophage replication-assembly complex: x-ray fibre diffraction and scanning transmission electron microscopy. J. Mol. Biol., (in press).

Kneale, G.G. & Marvin, D.A. (1982). A nucleoprotein complex in bacteria infected with Pf1 filamentous virus: isolation and biochemical characterization. Virology, 116, 53-60.

Marsh, M., Matlin, K., Simons, K., Reggio, H., White, J., Kartenbeck, J. & Helenius, A. (1981). Are lysosomes a site of enveloped virus penetration? Cold Spring Harbour Symp. Quant. Biol., 46, "Organisation of the Cytoplasm", (in press).

Marvin, D.A. & Nave, C. (1982). X-ray fibre diffraction. In Structural Molecular Biology: Methods and Applications, Plenum Press, New York, (in press).

Marvin, D. A., Nave, C., Ladner, J. E., Fowler, A. G., Brown, R. S. & Wachtel, E. J. (1981). Macromolecular structural transitions in Pf1 filamentous bacterial virus. In Structural Aspects of Recognition and Assembly in Biological Macromolecules: eds. Balaban, M., Sussman, J., Traub, W. & Jonath, A.; Balaban ISS, Rehovot and Philadelphia, p.891-910.

Nave, C., Brown, R. S., Fowler, A. G., Ladner, J. E., Marvin, D. A., Provencher, S. W., Tsugita, A., Armstrong, J. & Perham, R. N. (1981). Pf1 filamentous bacterial virus. X-ray fibre diffraction analysis of two heavy-atom derivatives. J. Mol. Biol., 149, 675-707.

Torbet, J., Gray, D. M., Gray, C. W., Marvin, D. A. & Siegrist, H. (1981). Structure of the fd DNA-gene 5 protein complex in solution. J. Mol. Biol., 146, 305-320.

Structural studies on clathrin coats and on proteins interacting with nucleic acids

Members: F.K. Winkler, K. Stanley

Technical assistants: A. D'Arcy, R. Brown

Clathrin coats

The transport of lipid membrane between organelles in eukaryotic cells has been shown in most cases to occur by a process involving the formation of a protein coat of clathrin and associated molecules. The coat shows a regular weblike surface structure and its principal component is clathrin, a polypeptide of M_r 180,000. In vitro, the coat can be reversibly dissociated into trimeric units that consist of three clathrin molecules ('heavy chains') and three polypeptide chains of smaller molecular weight ('light chains'). Depending on the source of material the two kinds of light chains that are usually found associated with clathrin have molecular weights between 30 and 40,000. During coated pit formation, their transformation into coated vesicles and subsequent disassembly the trimeric units must make, rearrange and break contacts with themselves and with other proteins in a coordinated fashion.

In the electron microscope they appear as three-legged structures which associate into cages in such a way that each unit occupies a vertex of the polygonal structure. As proposed by Crowther & Pearse (1981) each leg probably extends over two edges. This crude picture leaves many questions open, among them those concerning the function, location and stoichiometry of the two kinds of light chains in these assemblies. In this context we have devoted a major effort to seeking conditions under which light chains could be dissociated and separated from heavy chains without causing irreversible denaturation. This became possible by using chaotropic agents under specific conditions. It could be shown that heavy chains in the absence of light chains retain the three-legged structure (Plate 32a) and also assemble into cages (Plate 32b). Such heavy chain cages rebind light chains with high affinity. The kinetics of rebinding can now be followed for the first time in a well characterized system.

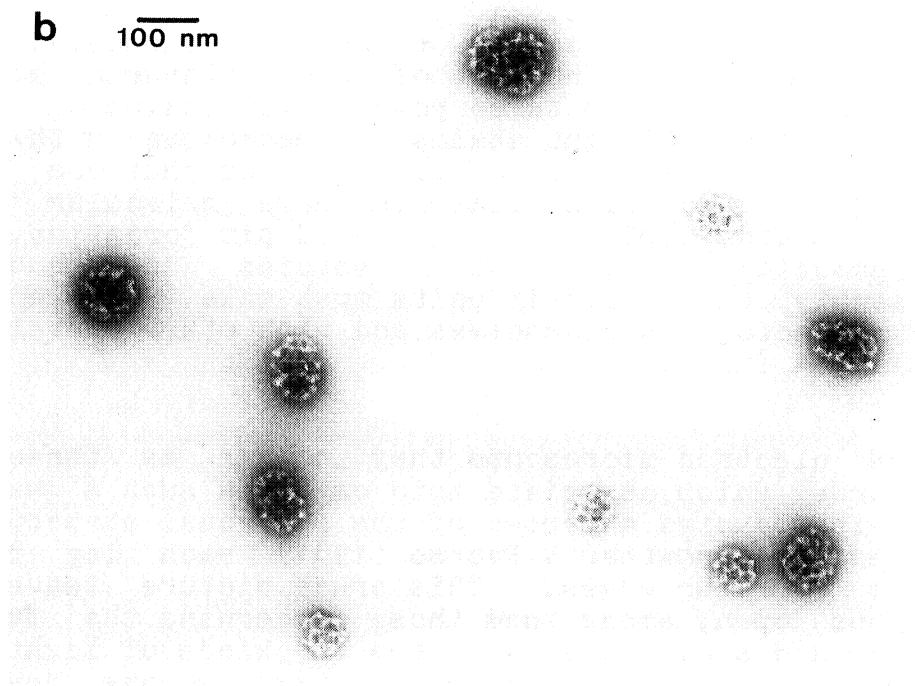
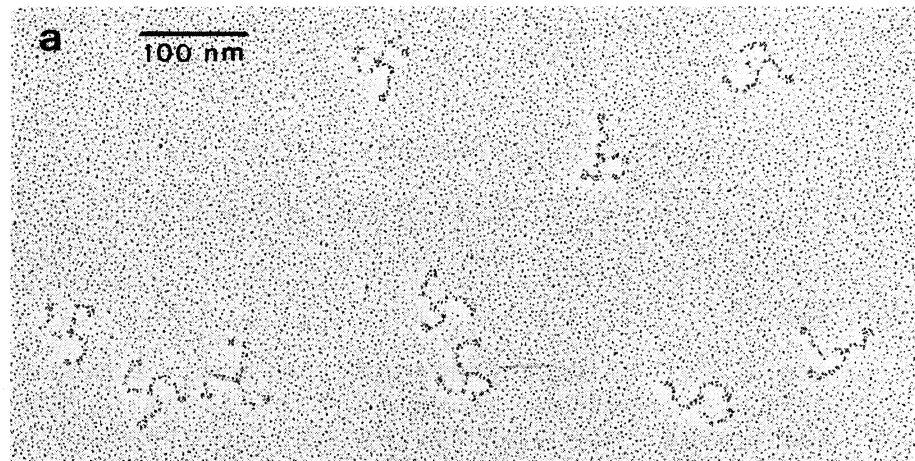


PLATE 32

- a) Electron micrograph of renatured clathrin trimers (heavy chain only) after rotary shadowing as described by Ungewickell and Branton (1981).
- b) Electron micrograph of clathrin cages reassembled from heavy chain trimers after negative staining with uranyl acetate.

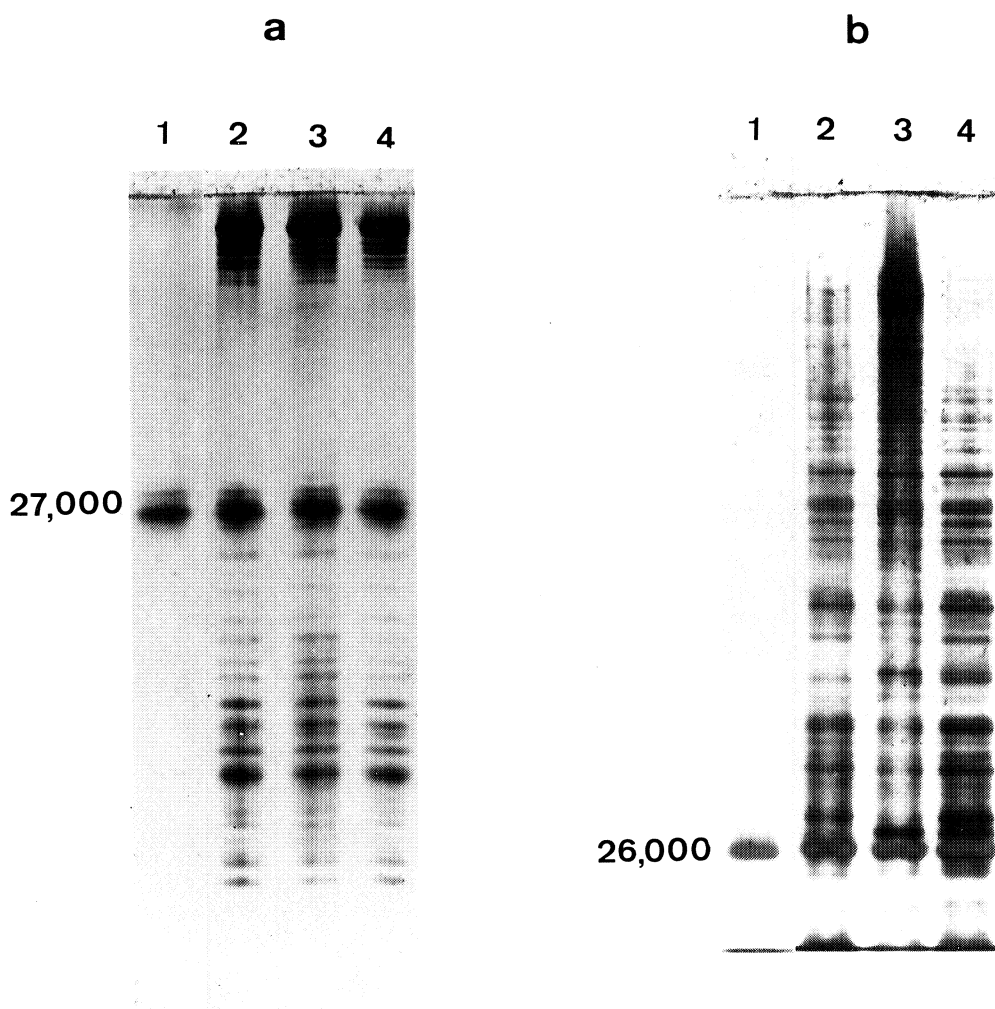


PLATE 33

Proteolytic cleavage patterns of clathrin isolated from pig brain, rat liver and SL2 cells. Clathrin bands (10-15 μ g of protein) were cut out from SDS gels, placed in the sample well of a second SDS gel and overlayed with protease solution as described by Cleveland *et al.* (1977). The second gel was stained with silver.

- a) VB protease, 16% polyacrylamide gel. Lanes 1-4: VB protease (1), digests of rat liver clathrin (2), SL2 clathrin (3), pig brain clathrin (4).
- b) Elastase, 10% polyacrylamide gel. Lanes 1-4: Elastase (1), digests as under (a).

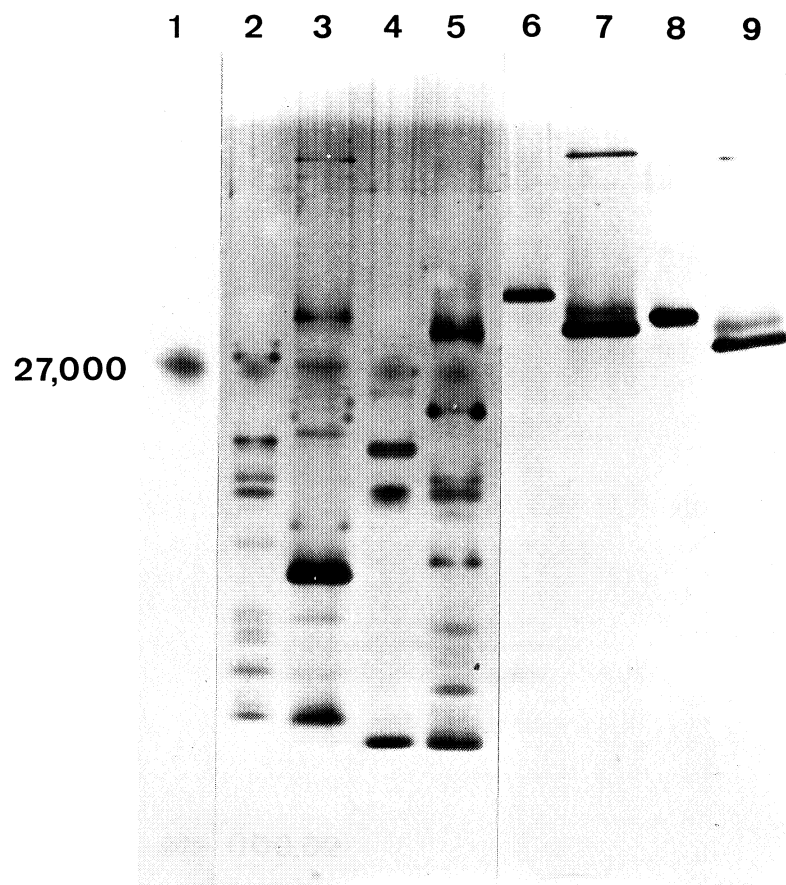


PLATE 34

VB protease cleavage patterns of light chains isolated from pig brain and rat liver. Method as described for Plate 33, 5-10 μ g protein per band, 20% polyacrylamide gel. Lane 1: VB protease. Lanes 2-5: digests of pig brain light chain A, rat liver light chain A, pig brain light chain B and rat liver light chain B. Lanes 6-9: undigested light chains in same order as lanes 2-5.

Another important question now being investigated is whether the two kinds of light chains that can be separated compete for the same binding sites on clathrin. Furthermore, we will examine whether light chains isolated from one kind of tissue can bind equally well to clathrin from another source. We have isolated clathrin from pig brain, rat liver and SL2 cells (a mouse lymphoma cell line) and have compared their cleavage patterns in one dimension using the proteases V8, subtilisin, chymotrypsin, elastase and papain (Plate 33). The almost identical patterns suggest that the amino-acid sequence of clathrin has been highly conserved. One might therefore expect that different clathrins can substitute for each other in binding one specific light chain. In a similar analysis of light chain protease cleavage patterns the differences are more striking than the similarities (Plate 34). This by no means implies that these different light chains cannot have a common heavy chain interaction site but simply that they are not extensively homologous.

The fact remains that no function has yet been established for the light chains. Certainly they are not needed for the formation of clathrin cages and do not appear to be involved in cage-specific contacts. The possibility of getting pure heavy chains in the state of trimers or cages will allow newly proposed functions to be tested in vitro by biochemical and physical techniques if such techniques are adequate for a functional test. As more detailed structural information becomes available, there will be a need to relate this information to the amino acid sequence of clathrin. As a major activity therefore, the group has engaged in a collaborative project (see Report on p. 153) to clone cDNA from clathrin mRNA and determine its sequence.

Proteins interacting with nucleic acids

Our knowledge about the structural details of specific protein-nucleic acid interactions is still very limited and there is a great need to determine a number of representative complexes at high resolution before common patterns or rules governing these interactions can be established.

We have continued to prepare the two enzymes T4 DNA ligase and EcoRI methylase in amounts and purity sufficient for crystallization attempts (see Research Reports 1980). Neither enzyme has so far crystallized under a large

variety of conditions including the addition of cofactors or inhibitors. We hope that crystals can be obtained in the presence of suitable DNA substrates. For this purpose oligonucleotides have been synthesized for us by the group of J.V. Boom (University of Leiden, The Netherlands). The T4 ligase substrate synthesized consists of the octamer dCGCTTCGG and the two tetramers dGCGA and dpAGCG. Unfortunately we were unable to ligate this substrate under a variety of ligation conditions. Recent circular dichroism studies (carried out by D. Dornboos, Leiden) shows that no duplex can be detected at concentrations around 10^{-5} M down to 0°C. As co-crystallization attempts are made at higher concentrations we are at present testing substrate binding and ligation under these conditions. It may however be necessary to use longer nicked duplexes whose synthesis has been initiated. EcoRI methylase has been shown to methylate an octamer duplex (Greene et al., 1975). We have just obtained the octamer dCGAATTCG and have started binding studies and cocrystallization attempts.

Contribution to other projects

We are also collaborating with the group of M. Moody on the crystal structure determination of the catalytic chain trimers from the enzyme aspartate transcarbamylase (see Report by M. Moody).

References

- Cleveland, D.W., Fischer, S.G., Kirschner, M.W. & Laemmli, U.K. (1977). J. Biol. Chem., 252, 1102-1106.
- Crowther, R.A. & Pearse, B.M.F. (1981). J. Cell Biol. 91, 790-797.
- Greene, P.J., Poonian, M.S., Nussbaum, A.L., Tobias, L., garfin, D.E., Boyer, H.W. & Goodman, H.M. (1975). J. Mol. Biol., 99, 237-261.
- Ungewickell, E. & Branton, D. (1981). Nature, 289, 420-422.

Cloning of the clathrin gene

Members: K. Stanley, M. Zabeau, F. Winkler, D. Louvard, G. Warren

Fellow: J. Armstrong

This joint report describes the collaborative effort of a number of groups to clone the cDNA coding for the protein clathrin. Clathrin is a cytoskeletal protein which is found in close association with restricted areas of most eukaryotic membranes, giving them a "coated" appearance in transmission electron micrographs. The areas of membrane which are coated correlate with areas which are engaged in the uptake and transport of membrane through the cell. During this process individual types of membrane proteins are segregated in the bilayer, some being accumulated in coated pits so that they are preferentially taken up into coated vesicles (Wall & Hubbard, 1981), others being specifically excluded (Bretscher & Thompson, 1981). Once in a coated vesicle the membrane proteins may be taken to a variety of sites in the cell. However, specificity is retained during this sorting phase of membrane transport so that, for instance, coated vesicles containing proteins endocytosed at the cell surface remain separate from coated vesicles containing newly synthesized protein in the secretory pathway. The observation of clathrin coats at the suspected sites of segregation and sorting has led to the suggestion that the proteins of the clathrin coat might be responsible for these processes. One way in which the coat structure might direct the movement of membrane vesicles in the cell is via pathway-specific components. Thus multiple forms should be present. The aim of the present study is to test this prediction using recombinant DNA techniques. In addition the cloned DNA coding for clathrin will be used to derive an amino-acid sequence for the protein. Two approaches are being taken in an attempt to isolate a cDNA clone coding for clathrin. In the first approach, cyanogen bromide fragments of clathrin purified from pig brain are being subjected to limited amino-acid sequencing in order to prepare an oligonucleotide probe with which to screen a cDNA library. This amino-acid sequence information will also be essential to determine the correct reading frame of the base sequence of the cDNA. The second approach is described in detail below.

A new cloning strategy for rare mRNA molecules

Cloning of the clathrin gene from partially purified mRNA presents two problems; one is the very low abundance of the mRNA; the other is the large size of the protein. These factors complicate the in vitro manipulations required in using hybrid-selected translation as a method of screening a library of cDNA clones, to a point where confident identification of positive clones is extremely difficult. A similar problem is encountered when trying to clone any protein for which the mRNA is present in low abundance or is not efficiently translated in existing in vitro translation systems. It therefore seemed worthwhile to develop a general strategy for the cloning of rare cDNA molecules for which an antibody to the corresponding protein is available. In essence this involves the in vivo expression of the cDNA library as fusion proteins with the E.coli protein β -galactosidase followed by a two-site immunoradiometric assay which monitors both the β -galactosidase and the foreign domain of the fusion protein. In this manner fusion domains retaining antigenic determinants of the parent molecule may be identified.

The first goal was to develop a vector in which efficient expression of any inserted DNA could be achieved. Since we intended to express pieces of cDNA derived at random from the mRNA sequence it was necessary to modify the existing expression vectors so that all the required signals for transcription and translation were present. This was done by fusing to the 3' end of the lac Z gene a portion of DNA from phage that contained the P_R promoter, ribosome binding site, and DNA sequence coding for the amino-terminus of cro (see page 66 for details of this construction). The result was a family of plasmids with the general structure shown in Plate 35. The use of the P_R promoter enabled us to retain control over the expression of fusion protein using host strains containing a Ts C1 repressor. Thus plasmids containing DNA sequences coding for lethal fusion proteins could be transformed at 30°C and transient expression assayed after a shift to 42°C.

Using this system we have found that all cro-lac Z fusions that produce high levels of β -galactosidase fusion proteins are lethal to the cell. However, by deleting DNA sequences beyond the 3' end of the lac Z gene (derived from lac Y and phage λ) this killing effect was removed allowing continued expression of β -galactosidase (Plate 36). The final level of expression in these cells was not very high, however, owing to the loss of plasmid from these cultures when grown

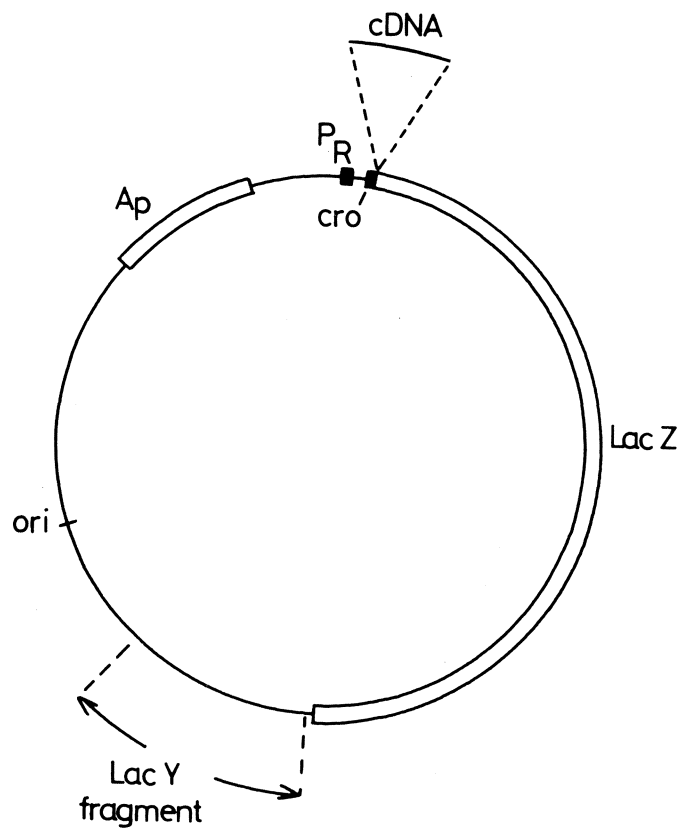


PLATE 35

Structure of the *cro-lac* fusion vectors.

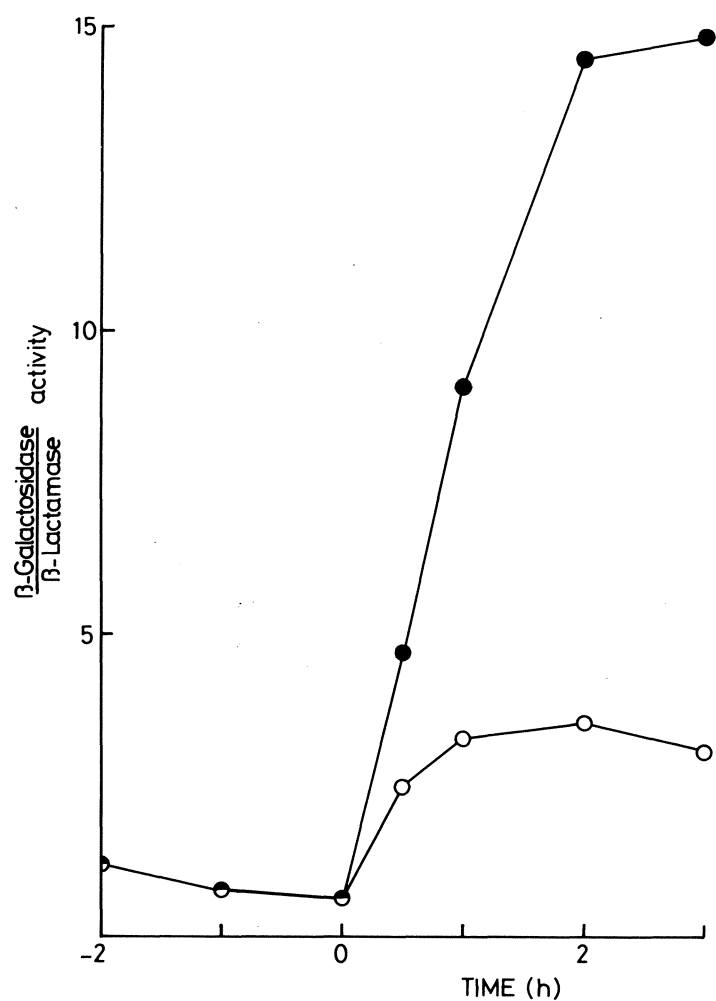


PLATE 36

Expression of β -galactosidase activity by cro-lac fusion vectors. Two cultures of E.coli NF₁ cells transformed with cro-lac fusion vector were maintained in culture at 10^8 - 10^9 cells/ml. At intervals, samples were withdrawn for assay of β -galactosidase and β -lactamase activity. The ratio of these two activities is used here as a measure of fusion protein expressed per copy of plasmid DNA. (O) cro-lac vector before deletion of lac y fragment, (●) cro-lac vector after deletion of lac Y fragment. Cultures were shifted from 30°C to 42°C at time 0.

in non-selective medium. On the hypothesis that this loss of plasmid was due to interference between transcription of the plasmid DNA and plasmid replication, we inserted transcription terminator sequences in between the lac Z gene and the origin of replication of the plasmid. The result was a much lower rate of plasmid curing and concomitantly higher levels of cro-lac Z fusion protein synthesis.

Alongside the development of efficient vectors for the expression of foreign segments of DNA we have developed a sensitive 2-site immunoradiometric assay for detecting fusion protein synthesis. In this solid phase assay fusion proteins from a bacterial lysate are immun-affinity purified on guinea-pig anti-(E.coli β -galactosidase) antibodies bound to a plastic micro-titre plate. The presence of fusion domain derived from cDNA coding for clathrin is then tested using indirectly radiolabelled rabbit anti-(pig brain clathrin) antibodies. This is a very specific assay since both the β -galactosidase and clathrin domains have to be present in order to give a positive result. It is, however, easily adapted to other proteins simply by using a different second antibody.

When foreign pieces of cDNA are inserted at a unique restriction enzyme site between the cro terminus and lac Z segments of the fusion vector only one in 18 fusions would be expected to give rise to the correct reading frame and orientation in both the inserted DNA and lac Z gene. In order that these in-phase fusions might be selected, the starting vector is used in a derivative form in which the lac Z gene is in a different reading frame from the AUG of the cro segment. High levels of β -galactosidase expression, only occur, therefore, if the inserted DNA restores the reading frame of the lac Z gene and itself contains no stop codons. Furthermore, since the lac Z gene is downstream of the inserted DNA, the presence of a lac Z phenotype is a good marker for screening for recombinants which contain expressed inserted DNA.

Each part of this cloning strategy now works, and the combined operation of all aspects is at present being tested by inserting cDNA from Semliki Forest virus into the vector and assaying fusion protein synthesis with an anti-(virus spike protein) antibody.

References

Bretscher, M.S., Thompson, J.N. & Pearse, B.M.F. (1981).
Proc. Natl. Acad. Sci., 77, 4156-4159.

Wall, D.A. & Hubbard, A.L. (1981). J.Cell Biol., 90, 687-696.

Structure of bacterial polypeptide elongation factors

Members: R. Leberman, D. Suck

Technical assistant: B. Antonsson

These studies are being carried out in collaboration with the following staff of the Max-Planck-Institut für medizinische Forschung in Heidelberg.

W. Kabsch, G.E. Schulz, A. Wittinghofer, U. Schmidt, R. Schumann

Throughout the year data collection and processing for the two crystallographic projects have continued. For the trypsinized EF-Tu.GDP crystals a complete set of data to 2.4 Å of the mercury-bicine derivative has been collected at the Hamburg Outstation. This has been scaled against the native and methyl mercury data and a 2.7 Å electron density map is in the process of being produced. For the EF-Tu.EF-Ts complex data collection to 6 Å has been proceeding using a diffractometer and a complete set of native data is now available.

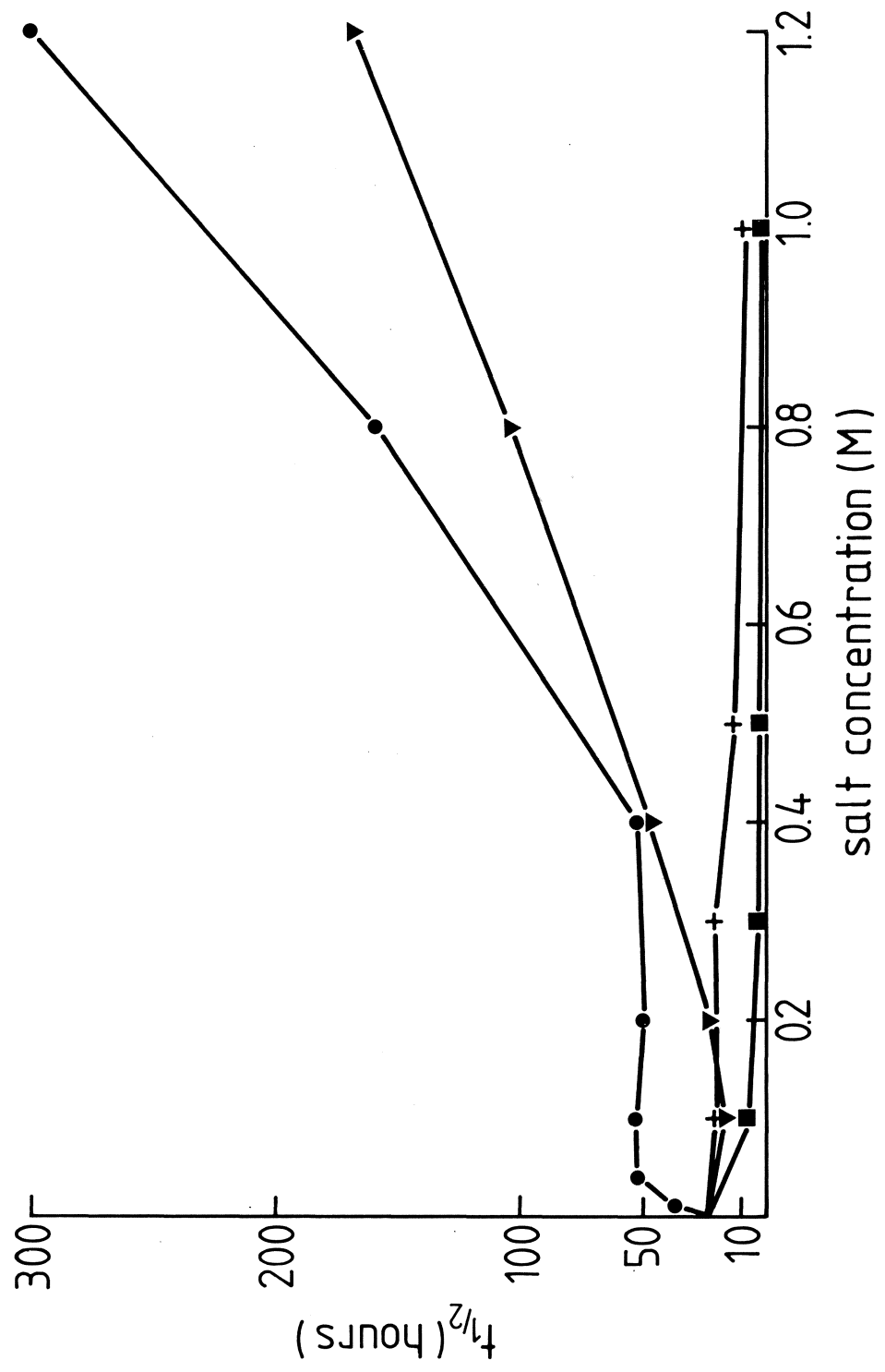
In the search for conditions under which aminoacyl-tRNA is stabilized, some unexpected effects of ammonium salts on the stability of the EF-Tu.GTP aminoacyl-tRNA ternary complex have been found (similar observations have been made for the interaction of tRNAs with their cognate aminoacyl-tRNA synthetases by Giége, R., Lorber, B., Ebel, J.-P., Moras, D., Thierry, J.-C., Jacrot, B. & Zaccari, G., personal communication). It has been known for some time that the rate of non-enzymatic hydrolysis of aminoacyl-tRNA is reduced on complex formation with EF-Tu.GTP, and this effect was used by Pingoud *et al.* (1977) to estimate the binding constants between EF-Tu and various aminoacyl-tRNAs. A study has been made of the hydrolysis rate of valyl-tRNA^{Val} complexed to EF-Tu.GTP in the presence of various additives which might stabilize it, or be used for its eventual crystallization. These additives included organic solvents, polyethylene glycol, deuterium oxide, and a selection of salts.

Conventionally it was to be expected that the addition of salt to the nucleoprotein complex would lead to a reduction in its stability and thus to a decrease in the half-life of

PLATE 37

Effect of various salts on the half-life of valyl-tRNA^{val} complexed with EF-Tu.GTP.

□ sodium chloride, + potassium chloride, • ammonium sulphate, ▽ ammonium citrate.



the complexed aminoacyl-tRNA, and this is indeed observed with e.g. sodium chloride. However, ammonium sulphate and ammonium citrate have the opposite effect, in that the half-life is increased in the presence of these salts, and this is to be interpreted as a consequence of an increase in the stability of the complex. These effects have been observed at high concentrations of the salts (Plate 37) but at the moment there is no completely adequate theoretical treatment of such solutions to provide a physico-chemical explanation of the results. Nevertheless, some general observations may be made about results and their possible relevance to the other nucleoprotein complexes.

In that sodium chloride and ammonium sulphate exert such opposite effects on this nucleoprotein complex it is clear that the two salt effects cannot be simply discussed in terms of "ionic strength". This concept only applies to dilute salt solutions, and in this and other situations where concentrated salt solutions are used (e.g. crystallization of macromolecules, lithium chloride degradation of ribosomes), it is probably the nature of the salt and its concentration which are important.

The effects appear to be strongly associated with the ammonium ion and are accentuated on combination with sulphate or citrate anions. These separate ionic effects cannot be correlated with the lyotropic properties of the ions as described by the Hofmeister series, according to which the ammonium ion would act in opposition to the effects of the multivalent anions.

It is very probable that the high concentrations of ammonium sulphate and citrate exert some direct effects on the structure of the solvent, and in doing so reinforce the hydrophobic interactions between the aminoacyl-tRNA and the protein. A possible thermodynamic description of the phenomenon may be similar to that given by Gekko & Timasheff (1981) for the stabilizing effect of glycerol on proteins. They find that glycerol is excluded from the protein domains and that this imposes a more compact structure on the protein; these authors indicate that similar observations have been made for ammonium sulphate.

The goal of these solution studies has been to find crystallization conditions for the ternary complex. Contrary to expectation, it would appear that ammonium

sulphate and citrate are likely candidates as crystallizing agents and trials are under way using these two salts.

Publications during the year

Antonsson, B., Kalbitzer, H.R. & Wittinghofer, A. (1981). The binding of nucleotides and metal ions to elongation factor Tu from Bacillus stearothermophilus as studied by equilibrium dialysis. Z. Physiol. Chem., 362, 735-743.

Leberman, R., Schulz, G.E. & Suck, D. (1981). Crystallization and preliminary x-ray diffraction data on the EF-Tu.EF-Ts (EF-T) complex of E.coli. FEBS Lett., 124, 279-281.

Suck, D. & Kabsch, W. (1981). X-ray determination of the GDP-binding site of E.coli elongation factor Tu by substitution with ppGpp. FEBS Lett., 126, 120-122.

Other references

Gekko, K. & Timasheff, S.N. (1981). Biochemistry, 20, 4667-4676 and 4677-4686.

Pingoud, A., Urbanke, C., Krauss, G., Peters, F. & Maass, G. (1977). Eur. J. Biochem., 78, 403-409.

X-ray analysis of DNAase I and the actin:DNAase I complex

Member: D. Suck

Technical assistant: H. Lahm (part-time)*, H. Pfrang (from the MPI für medizinische Forschung)

These studies were carried out in the Biophysics Department of the MPI für medizinische Forschung, Heidelberg.

X-ray structure determination of the actin:DNAase I complex (in collaboration with W. Kabsch, MPI für medizinische Forschung and H.G. Mannherz, University of Marburg).

Rabbit skeletal muscle actin in its monomeric G-form and bovine pancreatic deoxyribonuclease I (DNAase I) form a high affinity 1:1 complex ($K_B = 5 \times 10^8 \text{ M}^{-1}$). Filamentous F-actin, which is the main constituent of the thin filaments of muscle fibres, is completely depolymerized by DNAase I. Besides the possible physiological importance of this interaction for the regulation of the degree of polymerization of actin, this complex formation provides a way of keeping actin in its monomeric form in crystallization experiments. Crystals of the actin:DNAase I complex suitable for a high resolution x-ray study have been obtained and the structure has been solved at 6 Å resolution by the multiple isomorphous replacement method using six heavy atom derivatives. The 6 Å electron density map clearly shows the boundary of the complex and in most regions allows the separation of the actin and the DNAase I density. Contrary to earlier assumptions, actin is a rather elongated molecule with overall dimensions 67 x 40 x 37 Å and can be described as consisting of two domains of different sizes (see Plate 38). The point of highest density in the actin part probably indicates the ATP-binding site located in the cleft between the two domains. Within the crystal the actin molecules form a helical array which resembles the arrangement of monomers in the F-actin filament (Plate 39). Although the diameter of the crystal "filament" is larger than the diameter of the F-actin filament as determined from electron microscopy and x-ray fibre diffraction, the repeat distances are very similar in the two cases.

The identification of certain residues in the actin molecule, as for example the most reactive cysteine (Cys 373), will give us important information about the

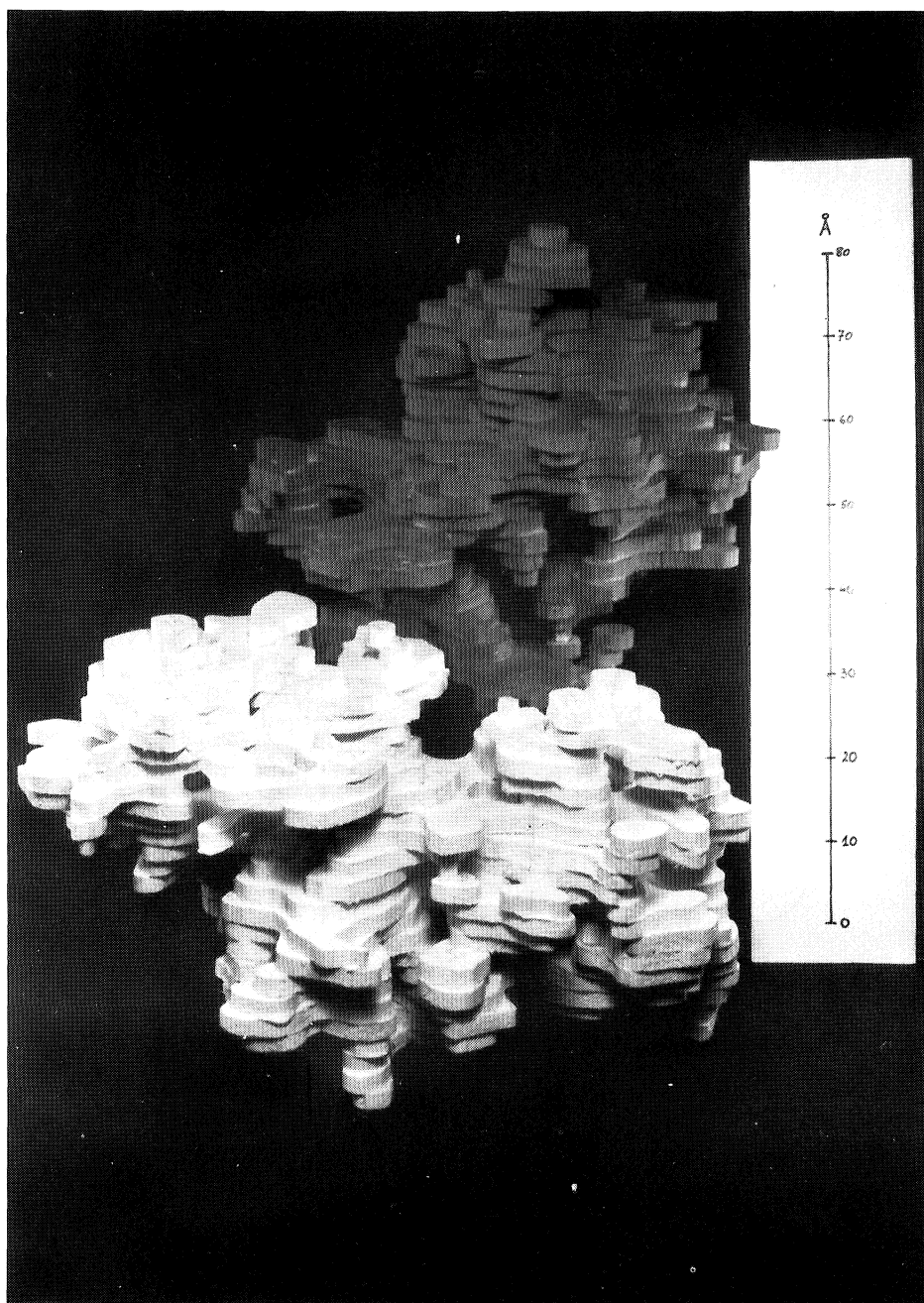


PLATE 38

Balsa-wood model of the actin:DNAase I complex. The lower part of the model represents actin. The cut-off level is 10% of the maximum electron density. Overall dimensions are 87 Å x 67 Å x 43 Å.

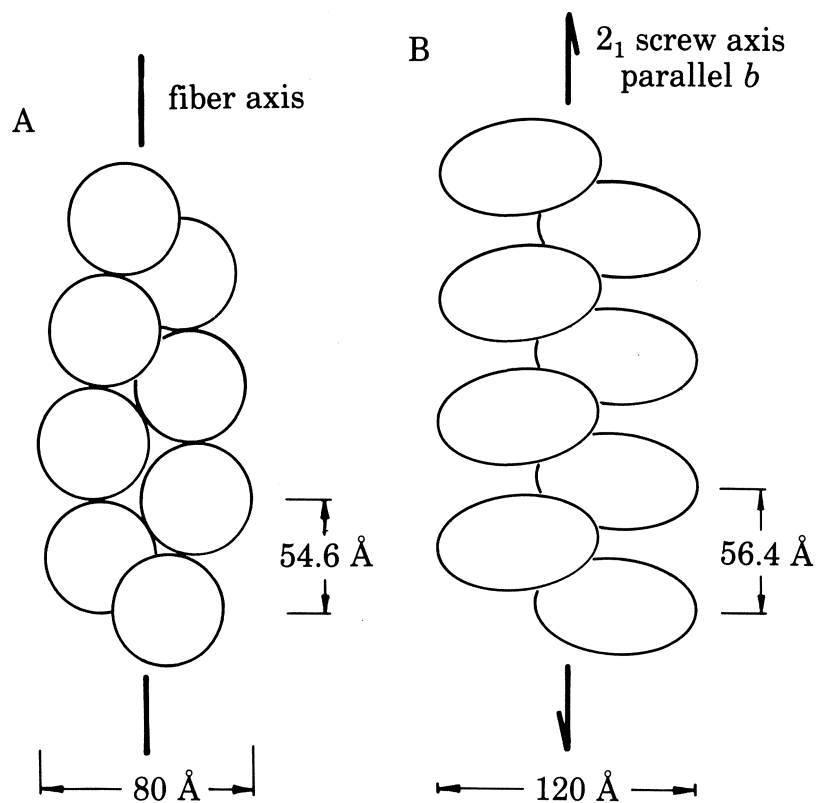


PLATE 9

Comparison of the packing of G-actin in the crystal with the F-actin filament. (A) F-actin filament, (B) crystal packing.

interaction between actin monomers in the F-actin filament. We hope to be able to locate Cys 373 even at low resolution, since we have crystals of the trypsin-treated complex (lacking three residues from the C-terminus of actin, including Cys 373) and also of the untreated complex, which seem to be isomorphous. A complete native film-data set, to a nominal resolution of 2 Å, and part of the mercury derivative data set, have been collected at the Hamburg Outstation using synchrotron radiation. The search for further heavy atom derivatives continues, but so far only the mercury derivative is isomorphous at high resolution. Recently the x-ray analysis of DNAase I crystals (see below) was begun. Once we have a high resolution electron density map of DNAase I, this can be used for the solution of the actin:DNAase I complex, since it represents about 40% of the density.

Crystallization and x-ray structure analysis of DNAase I

Single crystals of deoxyribonuclease I (DNAase I) from bovine pancreas have been obtained from protein solutions containing PEG 6000 as precipitating agent. The crystals are of space group $C2$ with one molecule of molecular weight 31,000 in the asymmetric unit and cell constants $a = 131.7$ Å, $b = 54.9$ Å, $c = 38.4$ Å, $\beta = 91.3^\circ$. They diffract to at least 1.8 Å and are very stable in the x-ray beam. A complete native set to 2.5 Å resolution (9,000 reflexions) has been collected from one crystal within 6 days using a 4-circle diffractometer. Two heavy atom derivatives ($TbCl_3$ and K_2PtCl_4) have been analysed by difference Patterson and Fourier techniques. Co-crystallization experiments of DNAase I with short, self-complementary oligodeoxynucleotides have been started.

In collaboration with R. Leberman and W. Kabsch we are also working on the high resolution structure of E.coli elongation factor Tu (see Report on the structure of bacterial polypeptide elongation factors).

Publications during the year

Leberman, R., Schulz, G. & Suck, D. (1981). Crystallization and preliminary x-ray diffraction data of the EF-Tu.EF-Ts (EF-T) complex of E.coli. FEBS Lett., 124, 279-281.

Suck, D. & Kabsch, W. (1981). X-ray determination of the GDP-binding site of E.coli elongation factor Tu by substitution with ppGpp. FEBS Lett., 126, 120-122.

Suck, D., Kabsch, W. & Mannherz, H.G. (1981). Three-dimensional structure of the complex of skeletal muscle actin and bovine pancreatic DNAase I at 6 Å resolution. Proc. Natl. Acad. Sci., USA, 78, 4319-4323.

Structural basis of allosteric control in aspartate trans-carbamylase (ATCase)

Member: M.F. Moody

Fellows: H. Kihara^{*}, P. Vachette^{*}

Technical assistants: A.G. Fowler (Instrumentation Division), P.T. Jones

The goal of this project is to explain the different allosteric control features of ATCase in terms of its molecular structure. Control in this enzyme appears to involve a relatively large conformational change, so its study may also contribute something to understanding motility at the molecular level. Our investigations are following two paths. We are trying to determine the molecular details of the large conformational change, and we are also studying how the conformational states relate to the properties of the enzyme in solution.

1. Structural details of the conformational change

We have suggested that the homotropic effects may involve a jaw-like closing of the active site cleft, the movements of the 6 different clefts being coupled by a mechanism in which the regulatory subunits form hinges (Foote *et al.*, 1981). Structural data to test this idea come from three sources.

a) Solution scattering

The changes in the x-ray solution scattering pattern following the binding of substrate analogues (Moody *et al.*, 1979) can give us some information about the movements of the subunits. We are examining which different configurations of ATCase are compatible both with the known structures of the subunits (using the structure of the unligated form: Monaco *et al.*, 1978), and also with the scattering pattern of the ligated enzyme. To supplement that pattern, a collaboration has been initiated with H. Stührmann (now at the University of Mainz) to study the anomalous solution scattering of ATCase; the data are being analysed.

b) X-ray crystallography (in collaboration with F. Winkler)

We are studying crystals of the unligated catalytic trimer (Foote *et al.*, 1981, and last year's Report). Progress here has been slow, mainly because of the low yield, slow growth and variable quality of the crystals. Data to 4 Å resolution have been collected, partly in Heidelberg, and partly at the EMBL outstation at DESY (in collaboration with H. Bartunik). The data have been processed, and structure analysis will start as soon as the necessary crystallographic programs have been implemented on the new VAX computer system.

c) Electron diffraction (in collaboration with J.-J. Chang, J. Dubochet and J. Lepault)

When the catalytic trimer is ligated with the transition state analogue PALA, only fine needle-shaped crystals have been obtained. These crystals, though useless for x-ray crystallography, have been found to give electron diffraction patterns that extend to about 4 Å resolution (Plate 40). The intensities of the spots show serious departures from Friedel symmetry and from the *mm* symmetry that appears to be present. If better patterns should become available, however, it might be possible to investigate what subunit movements of the catalytic chains might explain them. Meanwhile, the excellent negatively-stained images that these crystals also give (Plate 41) are being used to obtain a low-resolution three-dimensional image of the ligated catalytic chain and of its packing.

2. Role of conformational states in solution

X-ray scattering allows us to find, for any solution, the proportion of ATCase molecules with each of the two conformations. Furthermore, the scattering pattern can be analysed to see if any further conformational states can be detected.

a) Static x-ray scattering experiments

Qualitative studies have shown that the scattering patterns in the presence and absence of PALA are identical, despite an apparent loss of cooperativity, over the pH range 6 to 10.2, and also when the enzyme has been grown in the presence of 2-thiouracil (see

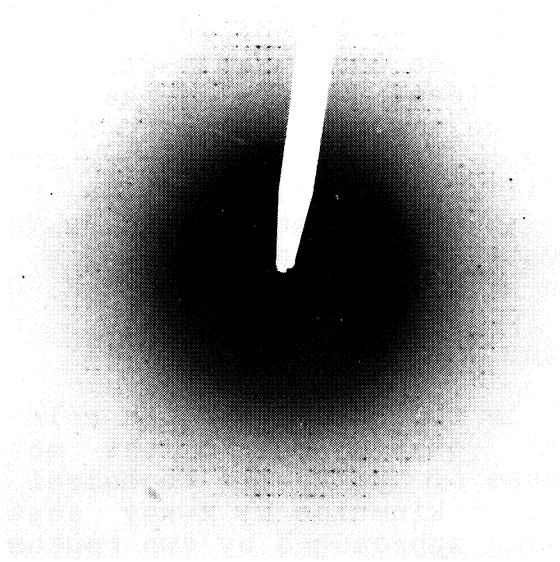


PLATE 40

Electron diffraction pattern from a frozen, hydrated crystal of the ATCase catalytic subunit ligated with PALA. 1 cm is equivalent to $1/(12 \text{ \AA})$.

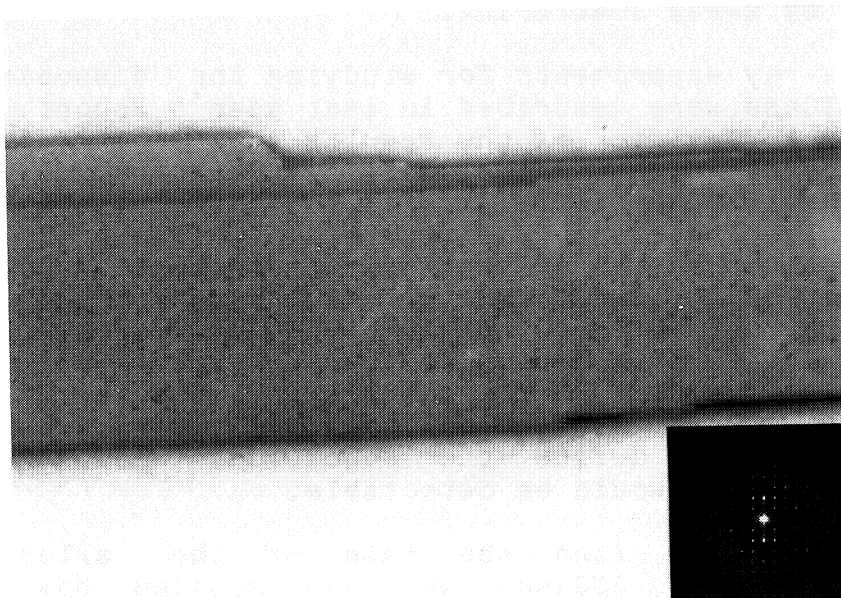


PLATE 41

A crystal of the ATCase catalytic subunit, ligated with PALA, after negative staining with 2% uranyl acetate. Times 162,000. Insert: optical diffraction pattern of part of the image. 2mm are equivalent to $1/(80 \text{ \AA})$.

last year's Report). Hensley et al. (1981) claim that the apparent loss of cooperativity of ATCase can be explained by the Monod-Wyman-Changeux theory if there are significant amounts of the T state present in solution. We are attempting to test this by recording x-ray scattering patterns from solutions containing different concentrations of effectors (experiments in collaboration with P. Vachette, now at LURE, Orsay.) These data are being analysed in collaboration with S. Provencher and J. Glöckner.

b) Kinetic studies

The main goal is to investigate the role of the large conformational change during the activation of ATCase. Because of the severe technical difficulties of studying fast kinetics by x-ray scattering, the problem is being approached by two routes. Apparatus and techniques are being developed for the much easier x-ray kinetic study of the dissociation of ATCase; and the kinetics of the allosteric transition of ATCase are being studied by conventional techniques, both for their own sake, and in the hope that conditions can be found that would permit their study by x-ray scattering.

The x-ray experiments for studying the dissociation of ATCase were described in last year's Report. A puzzling feature of the results was the apparent absence of intermediates, despite the known presence of the intermediate c_6r_4 (Subramani & Schachman, 1980). Presumably the intermediate cannot be detected because its scattering pattern is too similar to that of the native enzyme. This is being checked by the use of a pulsed-quench-flow machine to determine the composition of the solutions as a function of time. The results will be used to simulate the x-ray data, and we hope it will then be possible to define the conditions under which intermediates would be detectable.

In order to find the rate of the allosteric transition of ATCase, we have studied how the reaction rate changes after substrates are added to the enzyme. These experiments (in collaboration with T. Barman, CNRS, Montpellier) have shown, under some conditions, the presence of a lag (roughly 10 msec long) before enzyme activity reaches its steady-state level (Plate 42). Since this lag is absent when the catalytic trimer is used, it presumably represents the time needed for the allosteric transition. There

are also indications that the duration of the lag depends on substrate concentrations and on the presence of CTP. These data need to be confirmed and extended.

Publications during the year

Moody, M.F. & Makowski, L. (1981). X-ray diffraction study of tail-tubes from bacteriophage T2L. J. Mol. Biol., 150, 217-244.

Phillips, J.C., Bordas, J., Foote, A.M., Koch, M.H.J. & Moody, M.F. (1982). The zinc-sulphur bonds of aspartate transcarbamylase studied by x-ray absorption spectroscopy. Biochemistry, (in press).

Other references

Foote, A.M., Winkler, F.K. & Moody, M.F. (1981). J. Mol. Biol., 146, 389-391.

Hensley, P., Yang, Y.R. & Schachman, H.K. (1981). J. Mol. Biol., 152, 131-152.

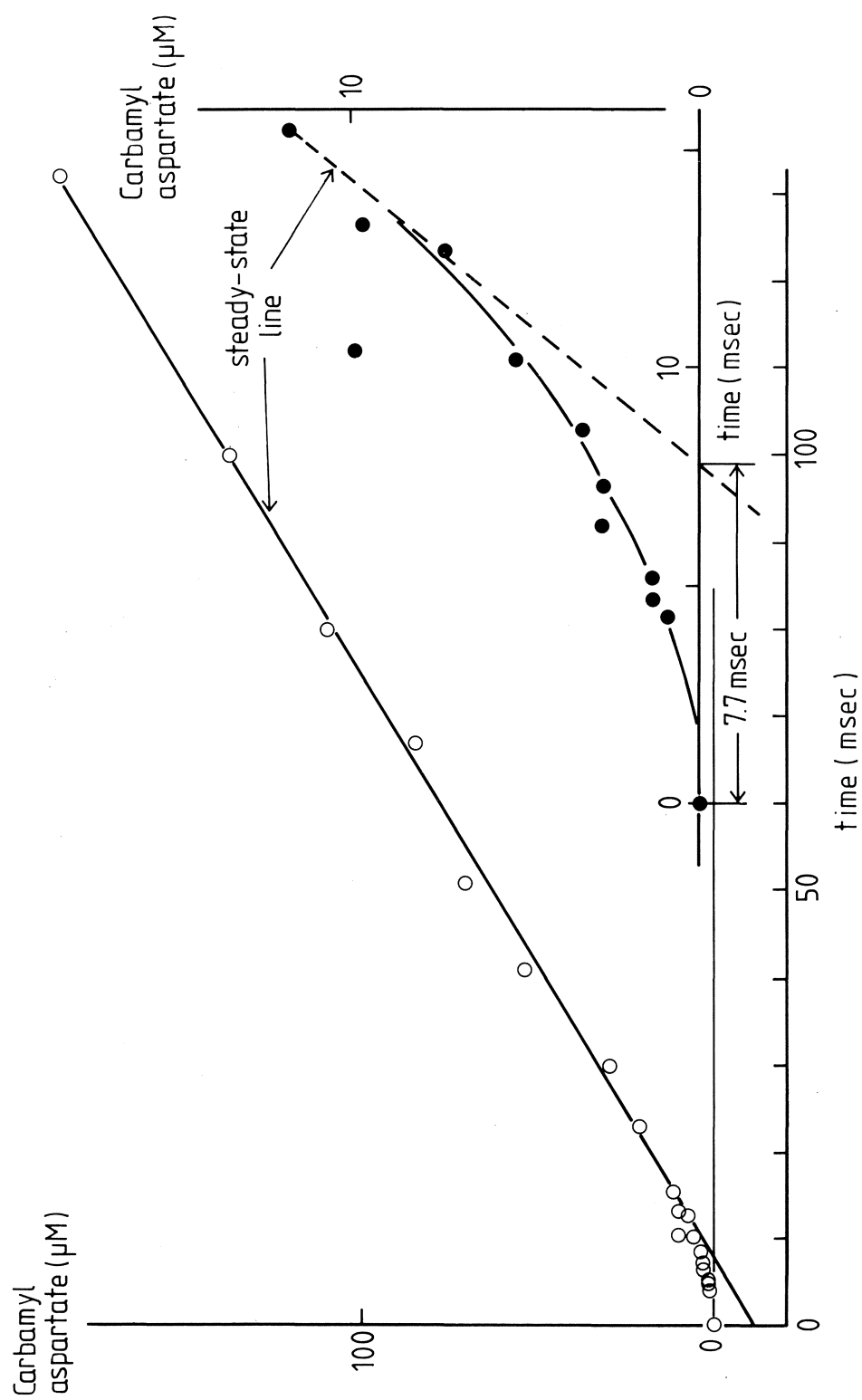
Monaco, H.L., Crawford, J.L. & Lipscomb, W.N. (1978). Proc. Natl. Acad. Sci., USA, 75, 5276-5280.

Moody, M.F., Vachette, P. & Foote, A.M. (1979). J. Mol. Biol., 133, 517-532.

Subramani, S. & Schachman, H.K. (1981). J. Biol. Chem., 256, 1255-1262.

PLATE 42

Chemical quench data showing a lag before the steady-state reaction rate is reached. ATCase (7.5 mg/ml, at pH 7 in phosphate buffer, plus 1 mM CTP) was mixed with an equal volume of a solution containing 60 mM aspartate, 10 mM carbamyl phosphate and 1 mM CTP. The mixture was aged at 4°C for 4 - 130 msec before quenching with trichloroacetic acid, and then assayed for carbamyl aspartate. The inset (bottom right) shows an enlarged copy of the data near the origin.



X-ray crystallography of insecticyanin

Member: D. Tsernoglou*

Fellow: K. Petratos*

The work described here was performed during the summer of 1981 while D. Tsernoglou was on sabbatical leave from Wayne State University. The protein studied was provided by Dr. P. Cherbas of Harvard University who isolated it from the insect Manduca sexta. Here, because of its bluish-green colour, it is used by the caterpillars for camouflage. The colour of the protein is due to the presence of biliverdin which is a product of the breakdown of haem. It is a precursor of bilirubin which is medically very important (jaundice in the newborn, etc.). Bilirubin is carried by plasma proteins but little is known about its mode of binding. Insecticyanin forms hexagonal crystals (Plate 43) with cell constants $a = b = 79 \text{ \AA}$, $c = 312 \text{ \AA}$.

Systematic absences indicate that the space group is $P6_122$. The density of the crystals, 1.26 g/cm^3 , was determined by the use of a density gradient consisting of chlorobenzene and carbon tetrachloride. The water content is about 37% by volume and the crystal asymmetric unit appears to be a trimer (3 x 24,000 daltons). The latter is in agreement with Cherbas's observation (1973) for the behaviour of the protein in solution.

The length of the c axis makes it difficult to measure diffraction intensities in a conventional crystallographic set-up. However, it was possible to take good photographs at the Hamburg Outstation with the assistance of H. Bartunik. An example is shown in Plate 44. The limit of the resolution is 2.5 \AA .

We shall search for heavy atom derivatives by means of the rotation camera in Heidelberg where with good collimation we should be able to obtain low resolution data. Once the heavy atom derivative is found, high resolution data can be measured in Hamburg. The derivative needs only provide sufficient information to enable us to determine the molecular envelope. After that use of the local symmetry of the trimer should provide sufficient phasing information for the entire structure determination (Rossmann & Blow, 1962; Bricogne, 1974).

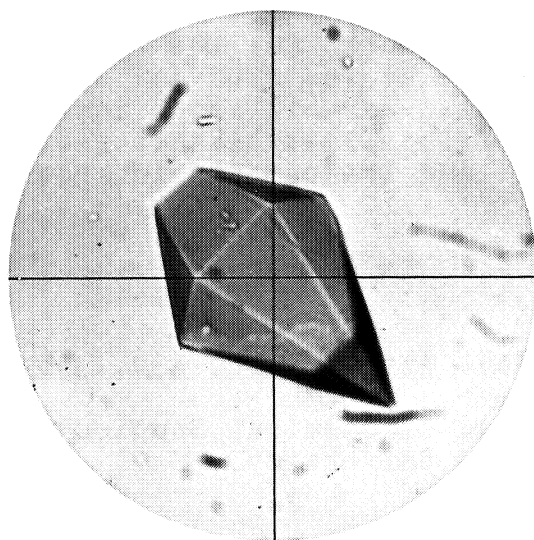


PLATE 43

Crystals of insecticyanin. The long dimension is 0.8 mm.

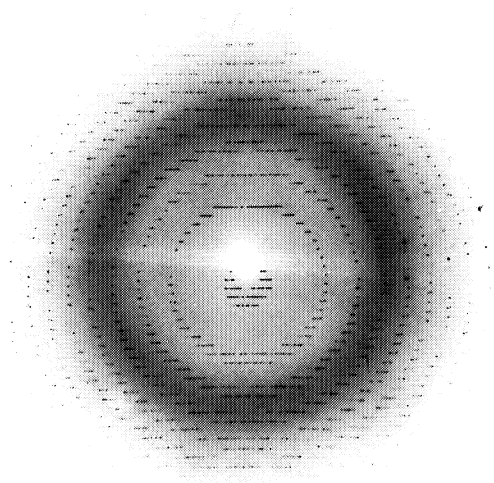


PLATE 44

Rotation photograph of insecticyanin extending to a resolution of 2.5 Å.

In addition to the above project we hope during the coming year to undertake work in low temperature protein crystallography aimed at the study of enzyme mechanism and structural dynamics, as well as to initiate work on the crystallization of locally available proteins involved in membrane structure and DNA-protein interactions.

References

Bricogne, G. (1974). Acta Cryst., A30, 395-405.

Cherbas, P. (1973). Biochemical Studies of Insecticyanin, Ph.D Thesis, Harvard University.

Rossmann, M.G. & Blow, D.M. (1962). Acta Cryst., 15, 24-31.

Protein sequencing

Member: A. Tsugita

Fellows: C. Alvino^{*}, A.C. Dianoux^{*}, S. Fischer^{*}, K. Maeda

Visiting workers: Y. Nozu^{*}, S. Sasada^{*}

Technical assistants: R. v.d. Broek, J.-J. Scheffler, D. Woodland

A major preoccupation of the group has been the development of techniques for the sequencing of membrane proteins and DNA-binding proteins, and the actual determination of the sequences of proteins of these types. A rapid hydrolysis method has been extensively studied (Tsugita & Scheffler, 1981 a and b), as has a sensitive method of analysis for tryptophan (Tsugita, 1982). A method of extracting proteins from conventional sodium dodecyl sulphate polyacrylamide electrophoresis gels has been developed so that the proteins can be further investigated chemically (Dianoux et al., 1981); and a new polyacrylamide gel electrophoresis method has been developed which is capable of separating peptides and proteins in the range from 200 to 10^5 daltons (Tsugita, 1982 a and c). A new N- and C-terminal sequencing method has been developed, based on exopeptidase digestion and field desorption mass spectrometry (Tsugita, 1982 a and b).

Turning to actual sequence determination, spinach chloroplast thioredoxins have been divided into two classes (f and m), and class m has been further subdivided into three N-terminal redundant isomers (Schürmann et al., 1981 and in press), and all the isomers of classes f and m were found to complement to T7 gene 5 for DNA polymerase activity to an equal extent (Harth et al., in press); a beef heart mitochondrial ATPase inhibitor (IF1) was partially digested with proteases and the region involving the inhibitory activity was sequenced (Dianoux et al., 1981), and later the sequence was almost completed revealing homology with the yeast inhibitor (Matsubara et al., 1981); and finally a DNA-binding protein from Pf1 has been sequenced, the work being cross-checked from the DNA sequence (G.B. Peterson and D.F. Hill, MRC, Cambridge, N. Short and R.N. Perham, Univ. of Cambridge).

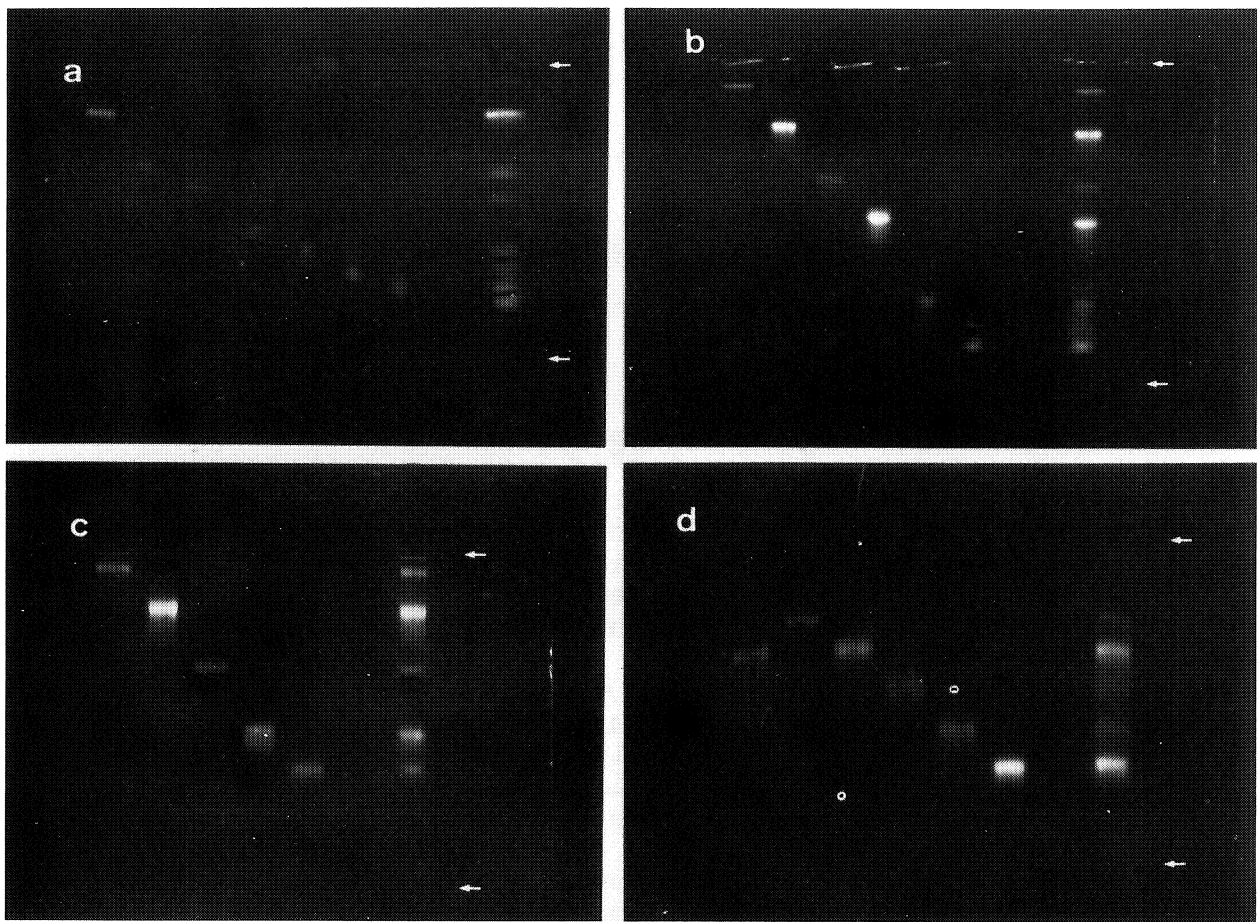


PLATE 45A

Typical fluorescence patterns obtained with the new acrylamide gel electrophoresis technique. Names of samples are from right to left and the numbers in parenthesis are the corresponding molecular weights. The upper arrows are at the top of the lower gel and the lower ones are at the front of the migration

(a) 32% acrylamide; Phe-Ala (236), Leu-Trp (317), Leu-Trp-Met (449), Ala₃-Pro-Tyr-Ala₃ (705), angiotensin II (1046), angiotensin I (1297), glucagon (3483).

(b) 20% acrylamide; Ala₃-Pro-Tyr-Ala₃ (705), angiotensin II (1046), glucagon (3483), ACTH fragment (18-39) (2466), aprotinin (6500), lysozyme (14400).

(c) 10% acrylamide; glucagon (3483), aprotinin (6500), lysozyme (14400), myoglobin (17200), ovalbumin (45000).

(d) 5% acrylamide; myoglobin (17200), chymotrypsinogen A (25000), ovalbumin (45000), albumin (68000), phosphorylase b (92500), catalase (60000).

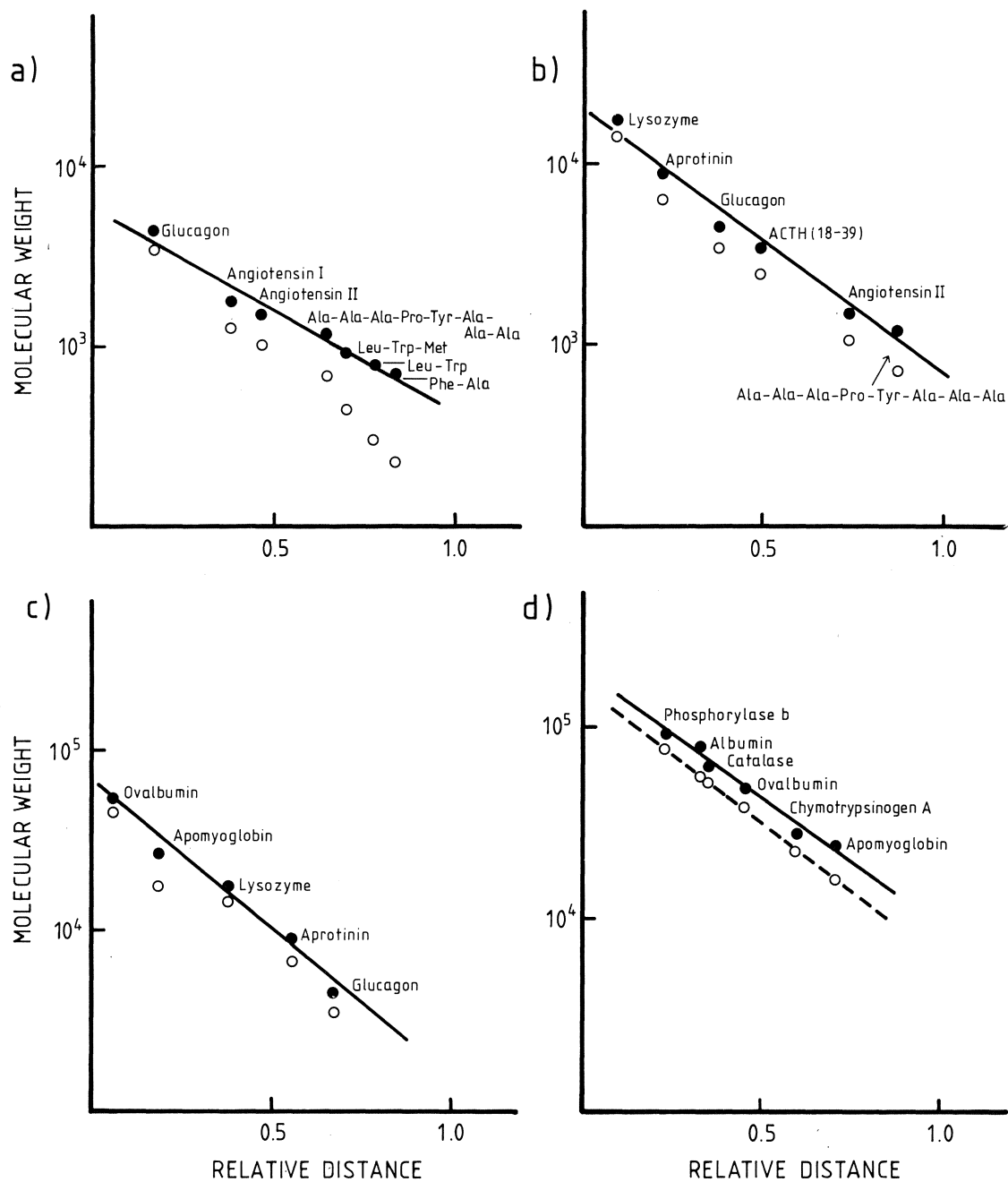


PLATE 45B

Relationships between migration distance and molecular weight. The data are taken from Plate 45A (a) for 32%, (b) for 20%, (c) for 10%, and (d) for 5% polyacrylamide gels. ○ molecular weights; ● modified molecular weights.

These projects are described in more detail below.

Protein hydrolysis

Conditions for hydrolysis were further studied and optimized on the basis of the degree of hydrolysis of hydrophobic peptide bonds and on the yields of the unstable amino-acids. 8N HCl in 30% trifluoroacetic acid containing 0.005% phenol at 166°C for 25 and 50 min yielded an amino-acid composition identical to, or better than, that given by conventional methods, particularly for hydrophobic proteins (Tsugita & Scheffler, in press a). The minimum amount of acid for 5 µg protein was found to be 20 µl (Tsugita & Scheffler, in press b). In this method tryptophan is not recovered, but by reducing the volume of 3N mercaptoethanesulphonic acid (Penke *et al.*, 1974) to 25 µl, 5 µg of protein can be hydrolysed without destroying tryptophan, and the hydrolysate analysed in the usual way. This modification permits tryptophan analysis from a reasonably small amount of protein (Tsugita, in press).

Extraction from SDS electrophoresis gel

Removal of SDS from protein-SDS complexes has been achieved by dialysis against strong organic acids such as 50% trifluoroacetic acid or 70% formic acid (Tsugita, in press). The same procedure has been applied to the extraction of proteins from SDS gels and to the removal of SDS, dye and buffer from proteins. After staining with Coomassie blue, the protein band is cut out and diced, and then soaked in 70% formic acid overnight with gentle stirring. The extract is evaporated and put into a Biogel P2 column with 70% formic acid. The initial fractions before the dye are collected, and contain protein free from SDS and other non-volatile salts. The recovery starting from 5 µg of protein is 50-90% and the protein is ready for further chemical studies (Dianoux *et al.*, 1981).

A new acrylamide gel electrophoresis system for proteins

Instead of using an SDS-protein complex, the NH₂ groups of the protein (or peptide) are covalently modified with the strongly acidic and fluorescent Edman reagent trisulphonate-pyren thioisocyanate, and the reaction mixture is applied directly to a polyacrylamide gel containing a volatile buffer of pH 11.7. After electrophoresis and without fixing and staining, proteins and peptides are observed under UV light as fluorescent

bands. Proteins and peptides migrate as a function of molecular weight in the range 200 to 10^5 ; sensitivity is about 50x greater than with Coomassie blue and resolution is better than 50 daltons (Plates 45A and 45B; Tsugita, in press).

A new method for terminal sequence determination

The conventional method using carboxypeptidases or aminopeptidases has limited applicability owing to the nature of the linear sequential kinetics and to contamination and autodigestion of the enzymes. In our method, after exopeptidase digestion in pyridine acetate buffer, one aliquot of digest is analysed with an amino-acid analyser to test the extent of digestion, and another is subjected after evaporation to field desorption (FD) mass spectrometry. In FD mass spectrometry molecular ions (including H^+) derived from the residual molecules after liberation of amino-acids from the terminus can be measured. Pyridine acetate buffer is important because it gives only H^+ but no other cations. The spectrum shows various molecular ions corresponding to the peptides that have lost amino-acids one by one from the terminus. The sensitivity is better than 100 pmol. Several digests mixed, or if necessary separate, can be analysed, but the limit of molecular weight is 3000 (Tsugita, in press).

Spinach chloroplast thioredoxins

Preliminary protein chemical studies distinguished two classes of thioredoxin, f and m, and class m could be subdivided into two N-terminal redundant isomers (Schürmann *et al.*, 1981). Further sequencing studies of class m revealed 3 different terminal redundant isomers (Schürmann *et al.*, in press). In order to investigate biological differences between the latter, which were identical in enzymatic activity, we tested their complementation activity to T7 gene 5 protein for DNA polymerase; like *E.coli* thioredoxin all 4 spinach thioredoxins had complementation activity. This was the first demonstration that plant thioredoxins complement to T7 DNA polymerization activity, and it provides a new tool for studying protein-protein interactions in DNA polymerization reactions (Harth *et al.*, 1981).

Beef heart mitochondrial ATPase inhibitor (IF1)

IF1 was digested to the limit both with trypsin and

chymotrypsin; the former gave an active fragment and the latter an inactive one. The fragments were extracted from the gel after SDS electrophoresis. The sequence of the active fragment has been determined (Dianoux et al., 1981), and more recently that of almost the whole IF1, which turns out to be homologous to yeast inhibitors (Matsubara et al., 1981).

DNA-binding protein of Pf1 bacteriophage

The sequence was determined of a protein coded by Pf1 which binds single-stranded phage DNA in the host cell. The DNA sequence of the coding region has also been determined by G.B. Peterson and his colleagues (Cambridge). The two sequences coincide almost completely, and a minor discrepancy is being investigated. There is no obvious homology to other similar proteins coded by Pf1 or M13 gene 5; however, a high content of 3 β -sheet is common²¹ to the two, and the binding region is probably around Tyr²¹.

Bacterial FDP aldolase

The amino-acid compositions of five class I staphylococcal FDP aldolases have been determined and compared. The phylogenetic relationships between the different bacterial strains have been studied using a divergence matrix, and the sequences of the active centres of two of the aldolases have been determined (Fischer, 1981).

Publications during the year

Bozzaro, S., Tsugita, A., Fromme, I., Janku, M., Monok, G., Opatz, K. & Gerisch, G. (1981). Characterization of a purified cell surface glycoprotein as a contact site in polysphondylium pallidum. Exp. Cell Biol., **134**, 181-191.

Dianoux, A.-C., Vignais, P.V. & Tsugita, A. (1981). Partial proteolysis of the nature ATPase inhibitor from beef heart mitochondria. FEBS Lett., **130**, 119-123.

Fischer, S. (1981). Comparative (biochemical immunological and protein chemical) studies on the class 1 fructosebisphosphate aldolases from Staphylococci. Dissertation, Technical University Munich.

Harth, G., Geider, K., Schürmann, P. & Tsugita, A. (1981). Thioredoxins from spinach chloroplasts supplement phage T7 gene 5 protein for DNA polymerase activity. FEBS Lett., 136, 37-40.

Maeda, K., Kneale, G.G., Tsugita, A., Short, N.J., Perham, R.N., Hill, D.F. & Peterson, G.B. (1982). The DNA-binding protein of Pf1 filamentous bacteriophage: amino acid sequence and structure of the gene. EMBO J., (in press).

Nave, C., Brown, R.S., Fowler, A.G., Ladner, J.E., Marvin, D.A., Provencher, S.W., Tsugita, A., Armstrong, J. & Perham, R.N. (1981). Pf1 filamentous bacterial virus. X-ray fibre diffraction analysis of two heavy-atom derivatives. J. Mol. Biol., 149, 675-707.

Schürmann, P., Maeda, K. & Tsugita, A. (1981). Isomers in thioredoxins of spinach chloroplasts. Eur. J. Biochem., 116, 37-45.

Schürmann, P., Maeda, K., Woodland, D., Tsugita, A., Harth, G. & Geider, K. (1982). Isomers in thioredoxins of spinach chloroplasts. Proc. Intern. Conf. on Thioredoxins, (in press).

Tadros, M. (1981). Isolierung, Charakterisierung, enzymatischer Abbau und Ermittlung der C-terminalen Sequenz der Lipoproteins aus der äusseren Membran von Proteus mirabilis D52. Dissertation zur Erlangung des Grades eines Doktors der Naturwissenschaften von der Universität Kaiserslautern.

Tsugita, A. (1982 a). New method for purification and sequence of (insoluble) proteins. Protein, Nucleic Acid and Enzyme, (Symposium on new aspects of protein structure and function, Protein Research Inst. of Osaka, Japan) (in press).

Tsugita, A., v.d. Brock, R. & M. Przybylski (1982 b). Exopeptidase digestion in combination with field desorption mass spectrometry for amino-acid sequence determination. FEBS Lett., 137, 19-24.

Tsugita, A. & Scheffler, J.-J. (1982). A new rapid method for acid hydrolysis of protein. Japan. Acad. Sci., 58B, 1-4.

Tsugita, A. & Scheffler, J.-J. (1982). A rapid method for acid hydrolysis of protein with a mixture of trifluoroacetic acid and hydrochloric acid. Eur. J. Biochem., (in press).

Tsugita, A., Sasada, R., v.d. Broek, R. & Scheffler, J.-J. (1982 c). A new polyacrylamide gel electrophoresis system: Separation of small peptides and proteins in a volatile buffer system after modification with a strongly acidic fluorescent NH_2 -reagent. Eur. J. Biochem., (in press).

Maeda, K., Tsugita, A., Kneale, G.G., Short, N., Perham R.N., Hill, D.F. & Peterson, G.B. (1982). The DNA-binding protein of Pf1 filamentous bacteriophage: amino-acid sequence and structure of the gene. J. EMBO, (in press).

Other references

Matsubara, H., Hase, T., Hashimoto, T. & Tagawa, K. (1981). J. Biochem., 90, 1159-1165.

Penke, B., Ferenczi, R. & Kovacs, K. (1974). Anal. Biochem., 60, 45-50.

Nucleotide sequence data base group

Member: G. Hamm

Visiting worker: K. Stüber*

Nucleotide sequence data library

Substantial progress was made during the year in the development of a data base. This will make possible the inauguration in early 1982 of the EMBL Nucleotide Sequence Data Library. The library is being established to provide a unified collection of sequence data at little or no cost to scientists in Europe and elsewhere. We hope that, once established, the library will also encourage standardization among users of sequence data, and provide a basis for the exchange of useful and transportable computer programs among people with similar interests. The library will of course also serve the EMBL staff and visiting scientists.

The first edition of the data base is planned for the beginning of March 1982. The data will be available for distribution on tape, and, somewhat later, via dial-up access to the Laboratory's VAX 11/780 computer system. A news-letter will be sent out which will describe the data base and procedures for its distribution. Subsequent editions of the news-letter will be distributed for each major update of the data base.

Much of the effort this year was directed toward the design of a flexible organization for the published nucleotide sequence data and the refinement of the existing data in accordance with the resulting design. The goal has been to produce a data base which could meet requirements at two levels. At the first level (which might be termed a "low-technology" data base system), the sequence data and associated taxonomic, bibliographic, and cross-reference data are used much as one uses a reference book: the data are systematically accessible, but the mode of use (and writing of the associated programs) is left to each user. At the second level, the data base must also be useful as the input to a "high-technology" data base system, which would allow extremely flexible use of the data in conjunction with a tailored set of tools. A data base usable in both environments will be more widely usable by scientists in different computing environments, and will

ID MMIG20 MUS.MUSCUL.IG.MOPC41; DNA; L; 350BP.
 XX
 DT 82.01.01 (first entry)
 XX
 DE First two exons in immunoglobulin light chain genes from
 DE cell line MOPC41.
 XX
 KW differentiated gene; immunoglobulin.
 XX
 OS Mus musculus (house mouse, souris domestique, Hausmaus)
 OC Eukaryota; Metazoa; Chordata; Vertebrata; Tetrapoda;
 OC Mammalia; Eutheria; Rodentia.
 XX
 SQ Sequence 350bp: 80 A; 82 C; 122 T; 66 G.
 CGTGACCAAT CCTAACTGCT TCTTAATAAT TTGCATACCC TCACTGCATC GCCTTGGGGA
 CTTCTTTTATA TAACAGTCAA ACATATCCTG TGCCATTGTC ATTGCAGTCA GGA CTCAGCA
 TGGACATGAG GGCTCCTGCA CAGATTTTTG GCTTCTTGTT GCTCTTGTTT CAAGGTAAAA
 ATGAAACTTA AAATTGGGAA TTTTCCACTG TTTCCAAC TGTTAGTGT TGA CTGGCAT
 TTGGGGGATG TCCTCTTTA TCATGCTTAT CTATGTGGAT ATTCATTATG TCTCCACTCC
 TAGGTACCAG ATGTGACATC CAGATGACCC AGTCTCCATC CTCCTTATCT
 XX
 FT Key From To Description
 FT
 FT CDS 126 176 first exon (leader peptide)
 FT CDS 303 >350 second exon (variable part)
 XX
 RN [1] (bases 1-350)
 RA Altenburger W., Steinmetz M., Zachau H.G.;
 RT "Functional and non-functional joining in immunoglobulin light
 RT chain genes of a mouse myeloma";
 RL Nature 287:603-607(1980).
 //

PLATE 46

facilitate the incremental growth of capability we envision for the system at EMBL.

The basic design has now been completed, although it will certainly evolve after some use and comment. Much of the work has involved problems of nomenclature and taxonomy, and to the extent that these remain scientifically unresolved, they of course remain so within the data base design. The key feature of the organization chosen is that it is suited for use by humans; even a simple print-out of the data (with no further processing) will be a useful and cross-referenced data collection. At the same time, the organization is systematic enough to allow simple programs to be written for search and analysis, and to permit the incorporation of the data into more sophisticated data base systems, including that to be developed here.

Plate 46 shows the format and information for a single entry in the data base. Note that the inclusion of taxonomic (lines OS and OC), keyword (KW), and bibliographic (lines RN through RL) information allows computer programs to generate indexes to the sequence entries automatically.

Computer-assisted gel reading

A separate task completed during the year was the installation of a computer-assisted gel reading station for use with radioautographs of DNA sequencing gels, similar to that described by Gingeras & Roberts (1980). The station consists of a translucent, backlighted digitizing tablet connected to a NORD-10S computer system. A moderate-sized interactive Pascal program was developed to control the tablet and user dialogue. The user is guided through the reading process, and thus requires little other instruction to use the system. At each step in the process, a variety of editing and user assistance is available to allow corrections and back-tracking during the reading. To minimize error, each gel film is read twice; the two readings are then compared and the discrepancies are edited (using a separate program) while the film is still on the tablet.

Reference

Gingeras, T. & Roberts, R. (1980). Science, 209, 1322-1328.

DIVISION OF INSTRUMENTATION

Electron microscope development group

Members: A.V. Jones, J.-C. Homo^{*}, B.M. Unitt

Technical assistants: C. Eavis, H.J. Elema, P. Labouesse, N. Webster

As in the previous year, the major activities of the group centred on the construction of the two cryo-microscopes.

Cryo-TEM

To recapitulate, this microscope is based on a modified Zeiss 10A electron microscope with the original objective lens replaced by a superconducting objective lens and intermediate lens assembly, designed and constructed under contract by the Siemens Research Laboratories in Munich. This lens was originally due for delivery in April/May but, owing mainly to problems in testing in Munich, was finally delivered only in December. In the intervening period, the Zeiss 10A electron microscope was extensively modified to accommodate the new objective lens.

Because of its low operating temperature the cryo-lens acts as a sink for residual contamination in the microscope. To reduce this contamination it was necessary to redesign the vacuum system of the microscope (Plate 47). The figure shows the flanges to which additional pumps could be fitted should an even lower operating pressure become necessary.

Since the cryo-lens operates in a persistent current mode it can no longer be used to focus the microscope. This function is therefore exercised by varying the energy of the electron beam. To maintain constant magnification during focussing, it is necessary to vary simultaneously the excitation of all other lenses. The normal magnification control of the Zeiss 10A electron microscope can not, of course, be used since a new set of operating conditions must be determined after installation of the cryo-lens. The imaging lenses were therefore converted for independent operation. The control electronics are based on digital techniques so that automatic operation under microprocessor control can be introduced at a later stage of development. The circuitry for carrying out these functions is shown on the right-hand side of the optical column in Plate 48. The left-hand console contains the

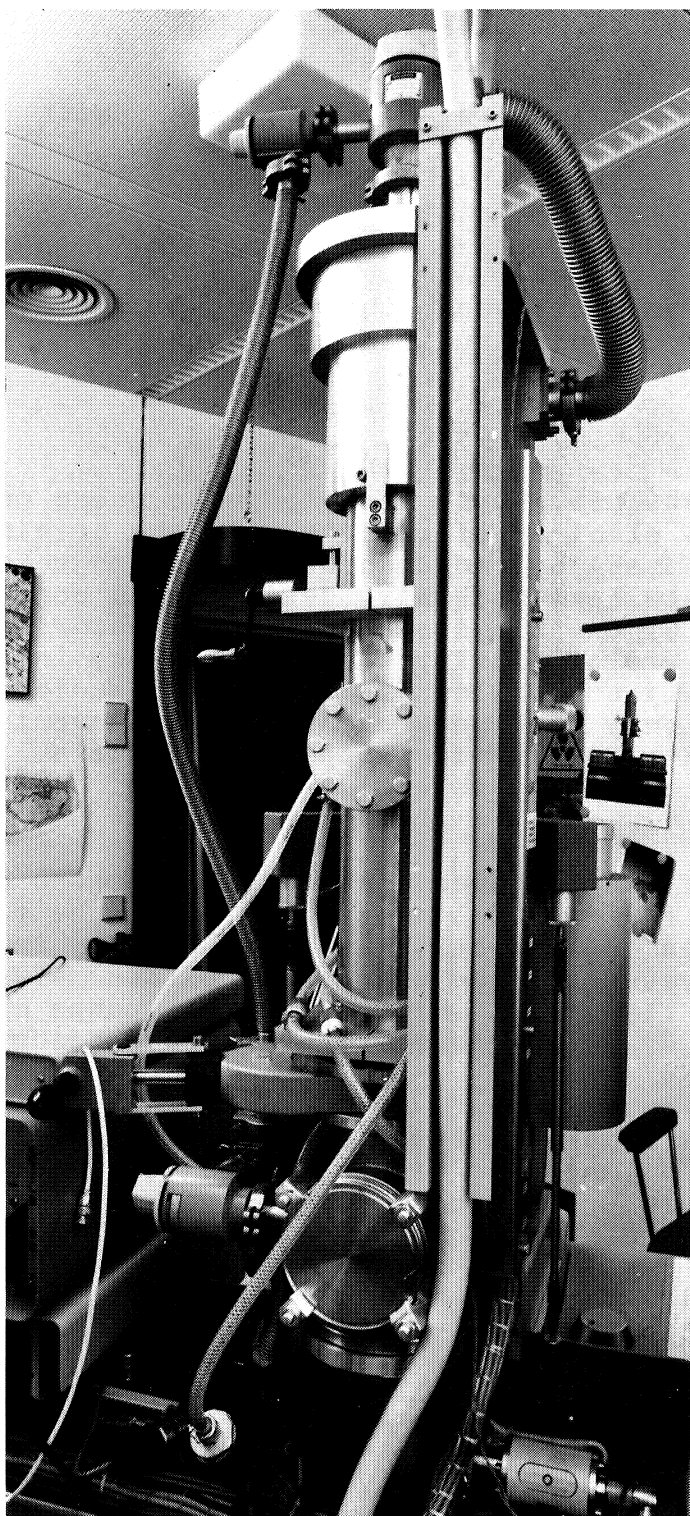


PLATE 47

Redesigned vacuum system of cryo-TEM.

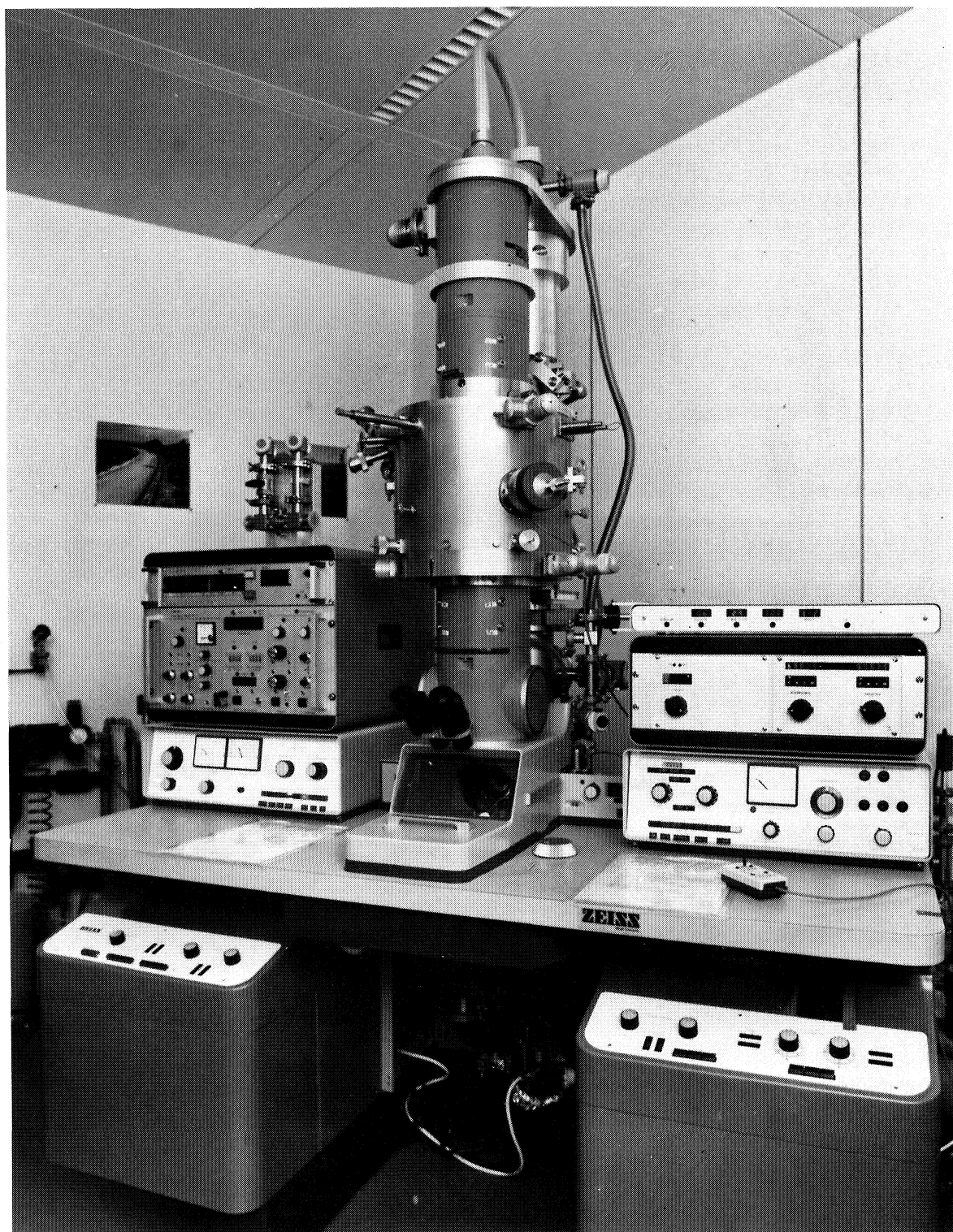


PLATE 48

Modified Zeiss 10A electron microscope showing additional electronics for operation with the cryo-lens.

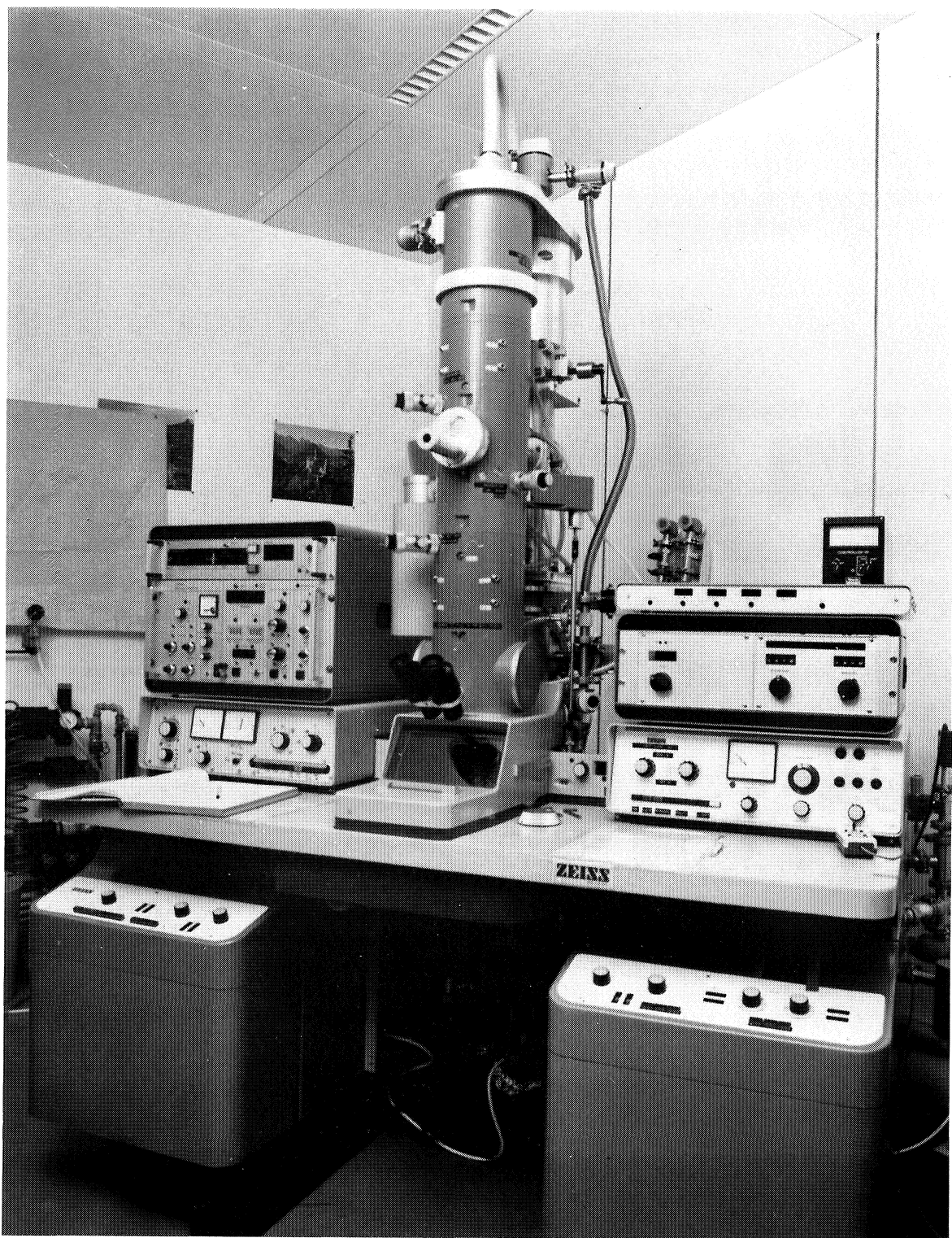


PLATE 49

Completed cryo-TEM.

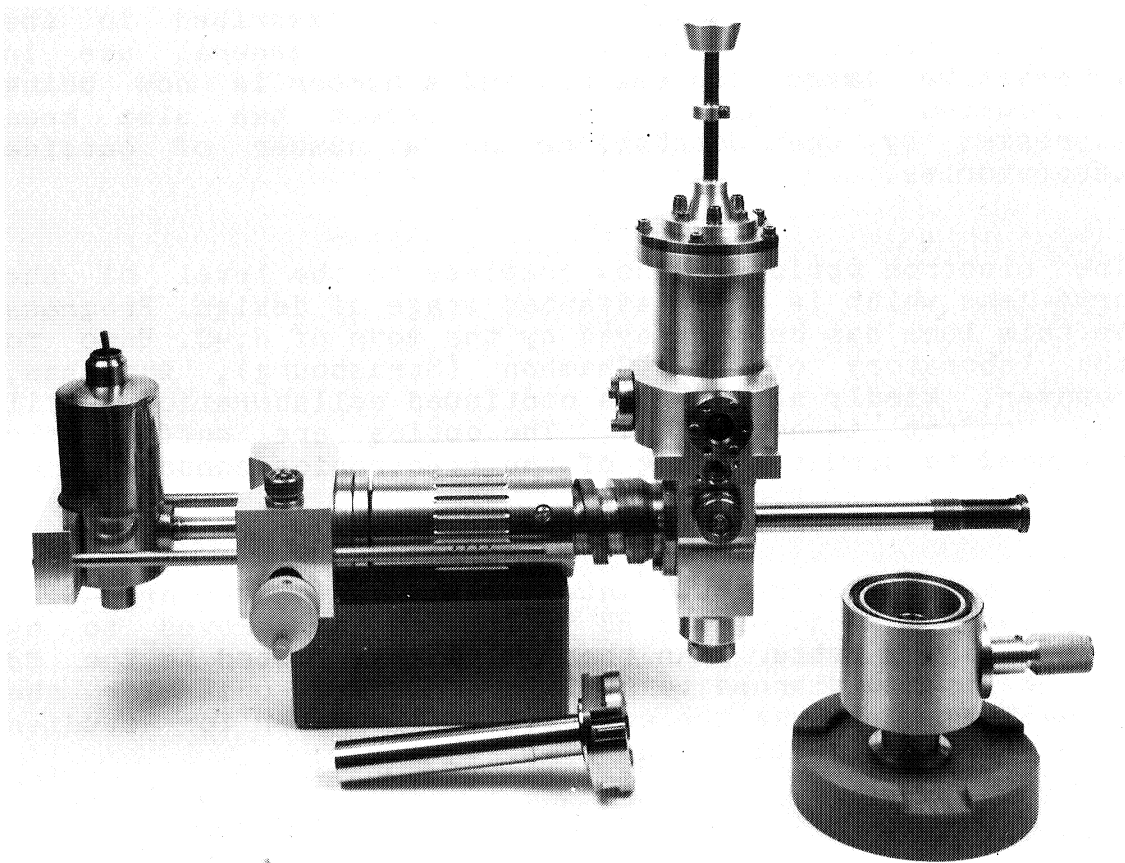


PLATE 50

Portable airlock system for the transfer of prefrozen specimens into the HB5 STEM.

electronics for control of the cryo-lens together with its liquid helium supply.

Plate 49 shows the complete cryo-TEM with the lens installed. The microscope is now ready for test.

Cryo-STEM

The electronics for the cryo-STEM are now about 80% complete and the tedious and time-consuming task of assembling the individual units into a functional system is in progress. The digital frame store described in the previous Report has proved to be of general use in interactive image processing, and a number is now being constructed for this purpose. Interest has also been expressed by the Outstations and a number of outside laboratories.

The electron optics are now complete to the level of the cryo-lens which is at an advanced stage of design. Progress on this lens has been delayed by the move of J.-C. Homo to the laboratory of Prof. Chambon (Strasbourg), who has, however, kindly agreed to a continued collaboration until the project is completed. The optics are sufficiently advanced to permit testing of the electronics console when assembly is complete.

The electron spectrometer intended for use on the cryo-STEM has been tested on the HB 5 STEM and has proved to be significantly better than that originally fitted to the HB 5. It is now planned to build a duplicate unit for the cryo-STEM and to use the existing spectrometer for studies of new imaging modes on the HB 5.

STEM

The cryo-stage on the HB 5 STEM has been further improved to lower the attainable temperature from 20°K to about 10°K. The prototype of the new stage has been supplied to the laboratory of Prof. Chambon which is also equipped with a HB 5. When tests are complete a duplicate stage will be fitted to our STEM.

The handling of frozen specimens has also been improved by the development of a transportable airlock system (Plate 50) which contains its own cryogenic pumping system and refrigerated specimen holder, to minimize contamination and frost build-up during transport between the preparative system and the microscope.

Publications during the year

Dubochet, J., Lepault, J., Freeman, R., Berriman, J.A. & Homo, J.-C. (1982). Electron microscopy of frozen water and aqueous solutions. J. Microsc., (in press).

Homo, J.-C., Freeman, R., Walter, C.A. & Dubochet, J. (1981). STEM à basses températures. Mesure de la température du spécimen. Transfert et observations des spécimens biologiques hydratés congelés. Proc. of Meeting of Société Française de Microscopie Electronique: Besançon, (in press).

Lepault, J., Weiss, H., Homo, J.-C. & Leonard, K. (1981). Comparative electron microscopic studies of partially negatively stained, freeze-dried and freeze-fractured cytochrome reductase membrane crystals. J. Mol. Biol., 149, 275-284.

Data analysis group

Members:: S.W. Provencher, R.K. Bryan, V.G. Dovi*, P.T. Speck, R.H. Vogel

Students: J. Glöckner, R. Metzger*

Visiting workers: U. Hopfer*, H. Ruf*, J. Smith*, H.-J. Wagner

Unstable data inversion problems

S.W. Provencher and J. Glöckner

CONTIN, the portable Fortran package for the regularized solution of unstable linear data inversion problems, has been distributed to 90 laboratories. Most are applying CONTIN in areas mentioned in the 1979 and 1980 Reports. However, some other applications being investigated are the analysis of data from studies of (1) dynamic processes in proteins using flash photolysis (H. Frauenfelder, University of Illinois, Urbana) and hydrogen exchange (A. Rosenberg, University of Minnesota, Minneapolis); (2) mass transport in cells using laser-Doppler microscopy (J.C. Earnshaw, Queen's University, Belfast and R. Johnson, University of Aberdeen); (3) globular protein secondary structure using laser-Raman spectroscopy (R.W. Williams, Naval Research Laboratory, Washington) and using circular dichroism to wavelengths below 180 nm with synchrotron radiation (J.C. Sutherland, Brookhaven National Laboratory); (4) NMR spin lattice relaxation in tissue (S.K. Mun, Georgetown University, Washington and P.C. Lauterbur, State University of New York, Stony Brook).

In collaborations with E. Stelzer, H. Ruf, and U. Hopfer (Max-Planck-Institut für Biophysik, Frankfurt) and L. De Maeyer (Max-Planck-Institut für biophysikalische Chemie, Göttingen), CONTIN has been applied to the estimation of size distributions of various preparations of liposomes, zymogen granules, and vesicles using dynamic laser light scattering. The method was verified by detailed studies of suspensions of well characterized latex spheres. Even bimodal distributions could be reproducibly determined if the ratio of the radii of the two components exceeded two.

Such rapid and reliable estimates are often prerequisites to the proper interpretation of data from other studies (Hopfer, 1981). For example, after the size distributions of vesicles from rabbit renal cortical and small intestinal brush border membranes had been estimated, CONTIN was then used to obtain continuous estimates of the distributions of rate constants for Na-dependent D-glucose transport across these membranes from equilibrium isotopic exchange data (with U. Hopfer). The estimated distributions were reproducible and very broad, covering two orders of magnitude. As a by-product, CONTIN computes initial rates directly from the first moment of the normalized distribution, and this is much more reliable than the usual procedures, which use only the early part of the data.

In other collaborations, CONTIN was applied to the analysis of multicomponent energy spectra of radioisotope mixtures used in physiological studies (with M.C. Trachtenberg, University of Texas Medical Branch, Galveston) and to the estimation of the secondary structure content of several crystallins (with R. Siezen, Australian National University, Canberra) and cytotoxins (with W.R. Kem, University of Florida, Gainesville) from circular dichroism data that could not be satisfactorily analysed by previous methods.

Automatic analysis of multicomponent data

R.H. Vogel and S.W. Provencher

The method for the automatic analysis of data represented by a sum of one-parameter functions mentioned in last year's Report has been implemented in a portable Fortran package by R.H. Vogel. It has been intensively used in the analysis of fluorescence lifetime measurements in collaboration with R.W. Wijnaendts van Resandt. This has led to the addition of new features and strategies in both the measurement and program. For example, it was found that the serious difficulties due to the wavelength and count rate dependence of the photomultiplier response could be avoided by replacing the response function with a reference one-component decay curve (similar to the strategy of Gauduchon & Wahl, 1978) that was measured simultaneously with the same detector using an optical delay (Wijnaendts van Resandt & De Maeyer, 1981). This makes possible reliable lifetime estimates even in the region from 1 ns down to about 100 ps, a time range where reproducibility problems have been apparent in the literature. This reference technique is being extended to the analysis of

depolarization data, and as soon as this has been tested and incorporated into the users manual, the program will be distributed.

Neurographics

P.T. Speck

A users' manual and a programmers' reference manual have been prepared for the neurographics system to document both its usage and functional design. The program together with its full documentation has been distributed to several laboratories to serve as an implementation kernel for installations outside the EMBL.

Together with some minor but useful improvements in the handling of interactive graphical data acquisition, the representation of transparent outlines mixed with opaque surface contours has been added to the graphical data rendition program of the neurographics system.

Structural analysis of chromatin structures in electron micrographs

P.T. Speck

The pattern recognition method developed for automatic length measurement of DNA strands in electron micrographs (see 1979 and 1980 Reports) is currently being extended to area measurements on digitized electron micrographs of chromatin. Its range of morphology from stretched filaments ("beads on a string") to dense clusters of particles provides an ideal range of input data for the development of a generally applicable area measurement method.

The existing system together with its extension will be implemented on a DeAnza IP8500 image processing system connected to a VAX 11/730 at the image science department of the ETH Zürich (in collaboration with O. Kübler). This highly advanced special purpose image processor should facilitate both the development and application of the method, which will hopefully become a useful tool for quantitative electron microscopy.

Large and non-linear inverse problems

R.K. Bryan

A computer program to estimate the electron density of particles with helical symmetry from their fibre diffraction patterns has been developed. Using a maximum entropy regularizer, it finds the structure with a specified maximum radius and with the smoothest non-negative electron density consistent with the statistically weighted native and heavy atom derivative data. The advantages of such an approach over conventional methods were outlined in last year's Report and have become apparent in applications this year. In particular, possibly spurious details that are not necessary to fit the (possibly incomplete) data are suppressed in the maximum entropy structure, and this tends to make the interpretation of the structure clearer and safer.

In collaboration with C. Nave and D.A. Marvin, the program was used to estimate the structure of the Pf1 virion. Fibre diffraction data were available for iodine and mercury heavy atom derivatives as well as for the native structure. However, estimates of the positions of the heavy atoms by C. Nave indicated that the mercury was in a symmetry-related position to the midpoint between the two iodine atoms, and thus would yield no additional phasing information. In addition, it was suspected that the mercury derivative was less isomorphous with the native structure than was the iodine derivative. Therefore only the native and iodine derivative data were used. Using this data to 8 Å, the solution illustrated in Plate 51 was obtained. As a check, the phased transform of the solution and the amplitudes of the derivative data were used to calculate a map of the iodine electron density. This map showed the iodine atoms to be in the input positions with virtually no spurious background density, thus confirming the consistency of the solution.

Classical phasing procedures require at least two heavy atom derivatives. In this particular case it was possible to obtain a reasonable structure with only one derivative, starting the maximum entropy optimization from a completely uniform electron density (i.e., with no initial bias toward a detailed structure). However, the contribution of non-negativity and smoothness constraints to alleviating non-uniqueness due to the phase problem still needs much study.

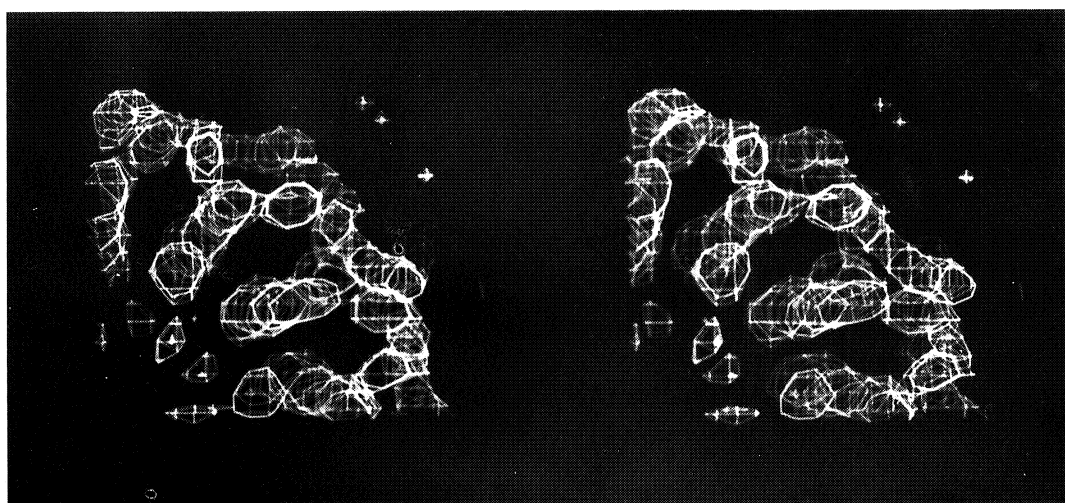


PLATE 51

Stereo-pair of one quarter of the maximum entropy reconstruction of the electron density of the Pf1 virion (displayed as a surface contour image on the Evans & Sutherland graphics system, with H.E. Bosshard). This represents a length of 40 Å of the virion, with the helix axis at the lower right. The rods of electron density are interpretable as α -helices. The maximum entropy optimization was started from a completely uniform electron density (i.e. with no bias toward a detailed structure) and used fibre diffraction intensity data to 8 Å. from only the native and one heavy atom (iodine) derivative.

The fit to the layer line data was good, but there were indications that some of the misfit could be attributed to layer line broadening causing some of the stronger layer lines to spill over onto adjacent ones. Therefore, in order to make full use of the high resolution data, work has started on estimating layer line intensities from the diffraction pattern, taking into account the broadening due to disorientation and finite coherence length of the particles. The program will use the routines of Provencher & Glöckner (1982) and perform the analysis globally over the entire diffraction pattern, using an appropriate form of the maximum entropy algorithm (Bryan, 1980). Preliminary simulations have been encouraging.

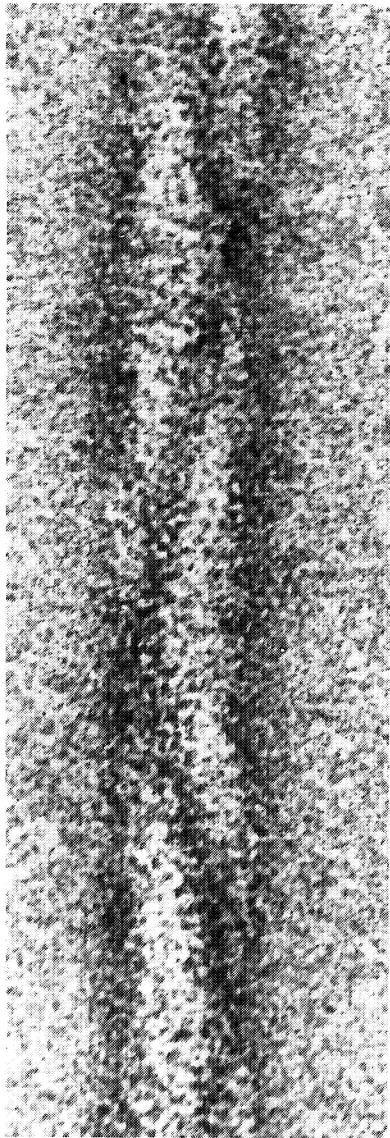
The program was also modified to reconstruct the three-dimensional structure of helical particles from a single projection. The Fourier transform of a projection perpendicular to the helical axis is an axial section of the Fourier transform of the whole particle and thus contains all the (phased) layer line information necessary to reconstruct the whole particle. In collaboration with D.W. Banner and K.R. Leonard, this program was applied to the thick ribbon-like structures that are visible in electron micrographs of negatively stained, acid denatured Pf1 particles (Plate 52a). If the stain on either side of the particle is assumed to be nearly uniform along the length of the particle, its contribution can be approximately eliminated by using only the four non-equatorial layer lines available. The projection of the solution thus obtained is shown in Plate 52c, which may be compared with the original micrograph. The reconstruction (Plate 52b) clearly shows a groove, which when filled with stain gives the black zigzag line on the projections. However, the detailed interpretation of the rest of the structure would probably require data from a tilt series, since the particle may be flattened on the microscope grid and the assumption of helical symmetry would no longer apply strictly.

Other possible applications include the analysis of x-ray and neutron solution scattering from particles with assumed spherical symmetry, the quantitative analysis of complex two-dimensional gel electrophoresis images, and large scale energy minimization problems that require optimization of a large number of nonlinear parameters with a very efficient algorithm (Skilling & Bryan, 1982).

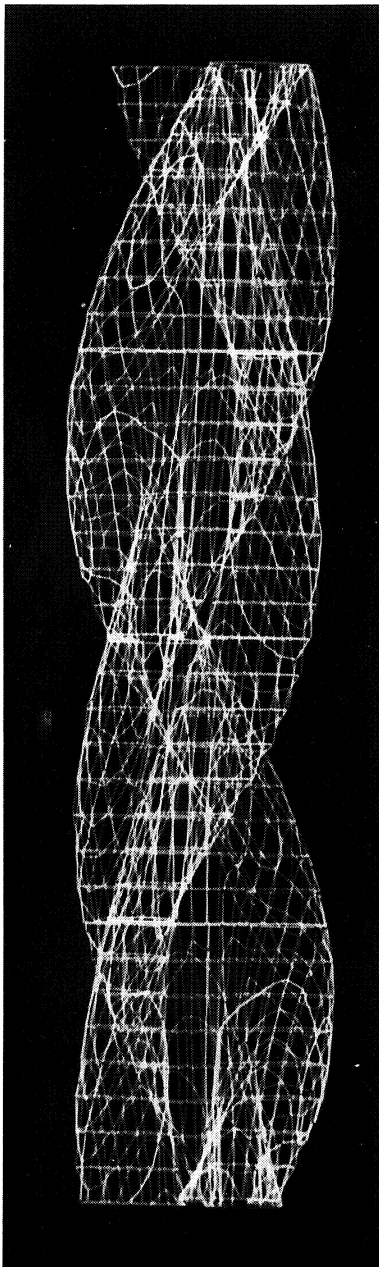
PLATE 52

An example of a three-dimensional reconstruction of a particle with helical symmetry from limited data on a single projection using the maximum entropy method.

- (a) A length of the "thick-ribbon" structure of acid-denatured Pf1, selected from a larger electron micrograph.
- (b) Three-dimensional reconstruction of one turn of the helix (displayed as in Plate 51) showing an approximately "V"-shaped cross-section.
- (c) Transaxial projection of the reconstruction, which may be compared with the original image (a). The background level has changed because the equator of the Fourier transform of (b) was not used in the reconstruction in order to suppress the effects of the negative stain.



a)



b)



c)

Publications during the year

Nave, C., Brown, R.S., Fowler, A.G., Ladner, J.E., Marvin, D.A., Provencher, S.W., Tsugita, A., Armstrong, J. & Perham, R.N. (1981). Pf1 filamentous bacterial virus. X-ray fibre diffraction analysis of two heavy-atom derivatives. J. Mol. Biol., 149, 575-707.

Provencher, S.W. (1982). A general-purpose constrained regularization program for inverting noisy linear algebraic and integral equations. Comput. Phys. Commun., (in press).

Provencher, S.W. & Glöckner, J. (1981). Estimation of globular protein secondary structure from circular dichroism. Biochemistry, 20, 33-37.

Provencher, S.W. & Glöckner, J. (1982). Rapid analytic approximations for disorientation integrals in fibre diffraction. J. Appl. Cryst., (in press).

Speck, P.T. (1981). Automatische Darstellung und Interpretation von Linien- und Kantenstrukturen in Digitalbildern. Informatik-Fachberichte, 49, 151-157.

Speck, P.T. (1981). NEU User's Manual. EMBL Technical Report DA03.

Speck, P.T. (1981). NEU Program Reference Manual. EMBL Technical Report DA04.

Other references

Bryan, R.K. (1980). Ph.D. dissertation, University of Cambridge.

Gauduchon, P. & Wahl, Ph. (1978). Biophys. Chem., 8, 87-104.

Hopfer, U. (1981). Federation Proc., 40, 2480-2485.

Skilling, J. & Bryan, R.K. (1982). Math. Programming, (in press).

Wijnaendts van Resandt, R.W. & De Maeyer, L. (1981). Chem. Phys. Lett., 78, 219-223.

Computer group

Members: M. Albrecht, H. Bosshard, C. Boulín, D. Iversen, R. Kempf, T. Pitt, H. Struve, W. Winkler

Student: P. Koenig*

The year 1981 has seen some expansion of the Group's activities in providing computing facilities for the Laboratory, particularly through the installation of a VAX-11/780 midicomputer. However, this extra work-load, combined with shortage of staff, has led to a near stand-still as far as software development is concerned. The situation will improve somewhat in 1982.

The central computers

The demand for computer resources has - not surprisingly - surpassed that of previous years, and large processing power was demanded particularly for crystallographic work and molecular modelling. We also welcomed many new users of the computers, particularly in the area of DNA sequence analysis (see G. Hamm's Report).

The Laboratory is now well equipped to meet these demands following the installation of the VAX-11/780 in May and June 1981. This machine has 4 Mbyte of main memory and has two 300 Mbyte disk drives, two 27 Mbyte disks (for user packs), and a fast magnetic tape station for densities up to 6250 bpi.

To facilitate exchange of information with other installations, e.g. for the nucleotide sequence data base, four modems have been installed (two 300 and two 1200 baud). This modest installation is the best available in Germany at a reasonable price.

Major tasks during the year were the definition of tentative operating procedures for the VAX, its integration with the existing Nord computers, and the solution of hardware problems. The computer room was reorganized and the cables renewed in preparation for the installation of a port contention unit. This unit (an Upnod TCS 2000) will allow most of the 60 terminals scattered in the Laboratory

to connect to any of the in-house computers, as well as to the network of the Max-Planck Institutes.

Computer graphics

H. Bosshard

In connection with the move to the VAX-11/780 the Evans and Sutherland Picture System 2 used for molecular modelling was upgraded to a multi-picture system with extended memory. This MPS supports multiple work stations and reduces the load on the host (interrupt service etc.) so that a dedicated computer is no longer required. The system will be expanded with the addition of a colour monitor in the spring of 1982. This calligraphic display uses 64 different hues with 8 levels of saturation for each, thus offering unique possibilities for visualizing complex structures.

A VAX version of A. Jones' modelling program, FRODO, was imported from Merck, Sharp and Dohme, and after incorporation of some improvements (extended memory, auxiliary software from the old Nord-10 version) the system has been extensively used by in-house and visiting groups.

In addition a structure refinement program, CORELS (written by J. Sussman, Weizmann Institute), was implemented. Some modifications of the IBM version were needed but more must be done to reduce the impact of this program on other users of the VAX.

Frame store interfacing

M. Albrecht, D. Iversen

The connection between the Nord computers and the frame store (reported by the E/M development group) was established and implemented in the SEMPER image processing package. A CAMAC module was developed which sends the control sequences to the microprocessor in the frame store, validates its responses, and transfers (and unpacks) image data at up to 1.2 Mbyte/s. Support software was written for maximum speed and reliability using request buffering, CPU/DMA overlap, and interrupt suppression. A shared driver segment controls all frame stores installed using semaphores for critical sequences.

Detector read-out system

C. Boulin, R. Kempf

Following last year's success with linear wire detectors, work has concentrated on improving the set-up for 2-dimensional detectors. Because of cross-correlation problems with the system described in last year's Report (plate 39), each of the two delay lines is now read out with a set of digitizers (CERN DTD 211 and DTD 164) as in the linear detectors, using the anode pulse as a common trigger. The results of the trial experiments with this system are reported by the Hamburg Outstation.

At present work is in progress on applying the fast encoding TDC 4201 from LeCroy instead of the CERN digitizers. This new module is superior to the others both in resolution and in function, and will be used both for linear and 2-dimensional detectors.

In order to perform kinetic experiments with these 2-dimensional detectors large storage capacity is required since each frame takes 64 k words of histogram memory for a resolution of 256 x 256. A CAMAC Memory Access Controller was designed to extend the memory capacity to 512 k words, and was used in the experiments of H. Riedl & T. Nemetschek (1981) (personal communication).

The classical method of calculating and displaying a histogram proved too slow for alignment of the 2-dimensional detectors. A simple display was built using two digital-to-analogue converters to control the X and Y deflection of an oscilloscope. Although of poor quality, this system has provided quite spectacular dynamic images, e.g. the Ewald sphere of a slowly turning crystal.

Acquisition module for synchrotron radiation

The existing unit counts data from 6 channels by incrementing a shared histogram memory, thereby causing band-width problems. A new module has been designed capable of counting at up to 10 MHz on 16 channels, using 4 k words of 32-bit memory.

Microcomputer-based pulse processor

A student, from the Institut Universitaire de Technologie, Mulhouse, built an intelligent CAMAC module (based on a Z80 microprocessor) for semi-automatic recording of pulse data. This module permits print-out of frequencies, differences etc. of the counts on 8 independant channels.

Stop flow data acquisition

A CAMAC module used for x-ray data acquisition was developed for M. Moody's group. It uses a 12-bit digitizer (2 μ s/word) and has a 1 k word memory. This module replaces a digital storage oscilloscope which did not provide data transfer capabilities.

Reading of electrophoresis gels

After the initial trials on reading radioactively-marked gels it was decided that A. Gabriel (Grenoble) should build a larger detector. This has now been tested and will arrive in Heidelberg in February 1982. Work has started on the scanning system and the pre-processing programs.

Support provided to outside groups

Dr. Stewart McGavin, University of Dundee, Scotland: Used the MPS for theoretical models of 4-strand DNA.

Dr. Dino Moras' group, CNRS, Strasbourg: Used MPS and VAX for modelling of asp-tRNA.

Department of Chemistry, University of Groningen, The Netherlands: Purchased EMBL modules for STEM data acquisition.

JET Cudas division, Abingdon, UK: Purchased 24 bit CAMAC data expanders.

Publications during the year

Boulin, C. A 16-channel data acquisition module with autonomous memory. Nucl. Instr. Meth. (in press).

Geiger, G., Boulin, C. & Bucher, R. (1981). How the two eyes add together: monocular properties of the visually guided orientation behaviour of flies. Biol. Cybern., 41, 71-78.

Pitt, T. J. (1982). Application of digital computer techniques to aid the interpretation of electron microscope images. Journal de Microscopie et de Spectroscopie Electroniques, 7 (in press).

Pitt, T.J. (1982). Application of an array processor to image processing in electron microscopy. Journal of Microscopy, (in press).

Other references

Hendrix, J., Weber, W. (1982). IEEE Trans. Nucl. Sc., (in press).

Position-sensitive detectors

Member: A. Gabriel

Technical assistant: F. Dauvergne

X-ray detectors

Begun in 1972, the use of a gas chamber as position-sensitive detector continues to be a most powerful tool for x-ray diffraction and kinetic experiments.

Plate 53 shows patterns recorded by two-dimensional, circular and linear detectors, as routinely used at the EMBL. Kinetic experiments could be carried out with about 1 ms time resolution.

Electron microscopy

The use of semiconductor detectors in electron microscopy is now under investigation. With the help of ENERTEC (Schlumberger), first results were recently obtained which seem very promising. A counting rate of 3.5 MHz was attained and it is possible that this figure will be exceeded.

A microstrip semiconductor will be mounted in the STEM. Such a detector can measure the electron distribution as a function of the radius of the beam. In view of recent technological progress it is probable that new detection methods in electron microscopy need careful review, e.g. very fast photomultiplier tubes and semiconducting single electron counters.

References

Mandelkow, E.M., Harmsen, A., Mandelkow, E., Koch, M.H.J. & Bordas, J. (1980). Nature (London), **287**, 595-599.

Moody, M.F., Vachette, P., Foote, A.M., Tardieu, A., Koch, M.H.J. & Bordas, J. (1980). Proc. Nat. Acad. Sci. USA, **77**, 4040-4043.

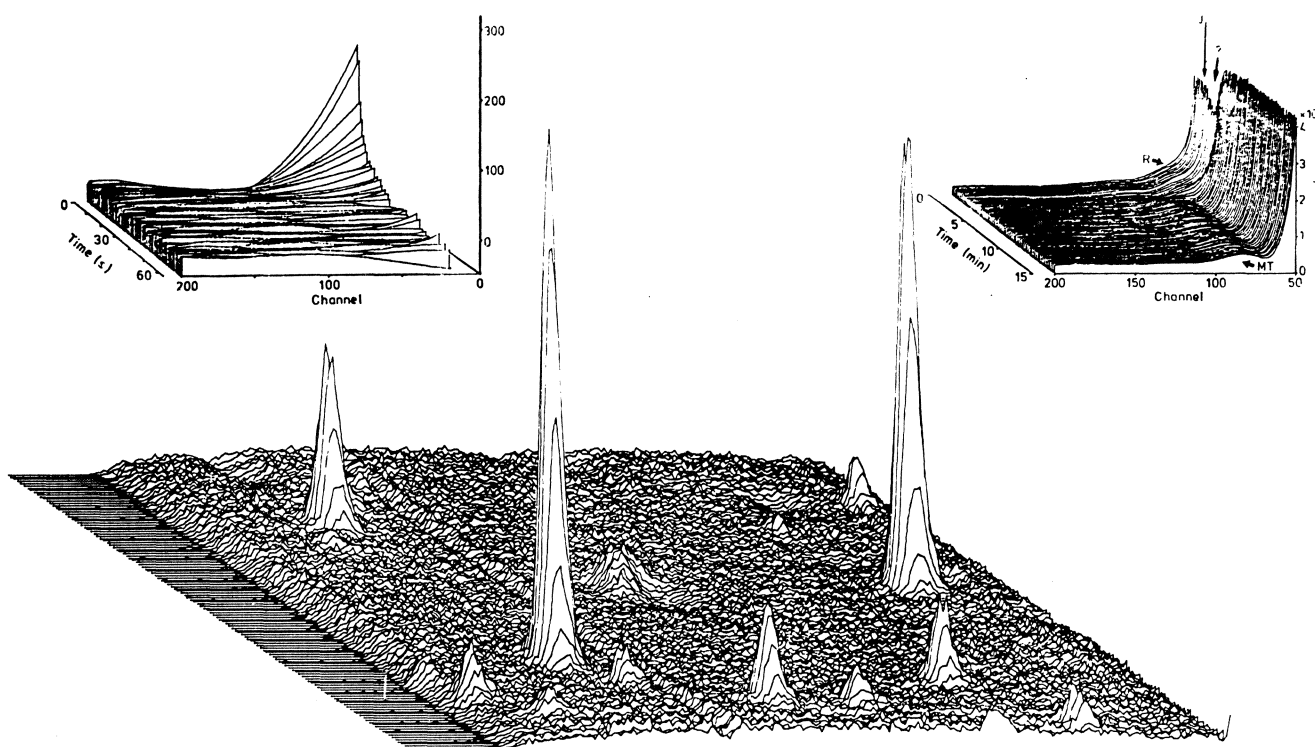


PLATE 53

Patterns recorded by two-dimensional, circular and linear detectors. Kinetic experiments were carried out with about 1 ms time resolution.

Upper left. Circular detector; time course of the dissociation of the enzyme ATCase (Moody et al., 1980).

Upper right. Linear detector; scattering pattern of a solution of tubulin as a function of time (Mandelkow et al., 1980).

Below. Two-dimensional detector; part of diffraction pattern from crystal of CO-myoglobin.

Applications of lasers

Member: R.W. Wijnaendts van Resandt

Fellow: K.-O. Greulich (part-time)

Technical assistants: D. Layer^{*}, H.J. Marsman, R. Stricker^{*}

The group is working on the applications of a synchronously pumped, mode locked, cavity dumped dye laser. This source delivers pico-second pulses (about 10 ps) with variable repetition rates (up to 82 MHz) and relatively high power (up to 2 kW) in the visible region of the optical spectrum and, via frequency doubling, in the ultraviolet range (280-310 nm).

1. Fluorescence depolarization and lifetime measurements

The dynamic fluorescence depolarization method, using an optical delay line to measure two events simultaneously with the same detection equipment, has been expanded to include the measurement of long rotational correlation times and the fluorescence lifetime itself. We are now able to measure rotational correlation times up to 10 to 20 times the fluorescence lifetime. This is particularly useful for the measurement of the rotational diffusion of proteins in solution. Using a Hamamatsu channel-plate photomultiplier we were able to achieve a total resolution of the single photon counting system of 150 ps (FWHM). The multi-exponential analysis of the data has been developed with programs of R. Vogel and S.W. Provencher. Further details of the method and the data analysis, together with a test experiment on the fluorescence decay of aqueous tryptophan, will be published (R.W. Wijnaendts van Resandt, R. Vogel & S.W. Provencher, in preparation). There have been indications that tryptophan decays with two lifetimes, of 3.1 ns and less than 0.6 ns respectively (Szabo & Rayner, 1980; Robbins et al., 1980). Our measurements confirm these results beyond any doubt.

A number of more biological applications have been started or completed:

1.1. Fluorescence properties of Pf1, fd-virus and their gene 5-DNA complexes (K.-O. Greulich, with D.A. Marvin and G.G. Kneale).

Fluorescence-lifetime quenching has been used to localize tryptophans and tyrosines in the filamentous phages Pf1 and fd and in the gene 5 protein of Pf1. The interpretation of lifetime quenching has turned out to be somewhat more straightforward than the interpretation of intensity quenching (Eftink & Ghiron, 1981). By the use of differently charged quenchers (I^- , Cs^+) charged groups in the neighbourhood of the aromatic amino acids have been detected. This information may be used for the prediction of secondary structures around the aromatic amino acids. The fd phage reveals "hydrophobic fluorescence" (i.e. an emission maximum at 330 nm). Following normal interpretations, one would conclude that the tryptophan is buried in the interior of the phage. However, fd fluorescence is quenchable by KI, which is a surface quencher (Lehrer & Learis, 1978). Probably the peak position is not suitable for predictions on the exposure of the fd tryptophan to the solvent. If this finding is generally true for proteins, one can explain why most tryptophan-containing proteins reveal "hydrophobic fluorescence", whereas x-ray crystallographic results indicate that only 114 of the tryptophans are buried (Chothia, 1975).

Fluorescence lifetime measurements have been applied to observe a reversible structural transition of Pf1 phage. This transition can be described by a simple thermodynamic concept (Hinz et al., 1980) and may serve as a model for transitions in other biological systems, for example chromatin. Fluorescence is a particularly valuable tool to study such transitions, since only very small protein concentrations are necessary and thus macroscopic effects (for example phase transitions of the whole solution) can be excluded.

Information on DNA-protein interaction has been deduced from the fluorescence of the Pf1 gene 5 protein-DNA complex. The main fluorescence of the free protein has a very long lifetime of 8.2 ns (possibly the microenvironment of the fluorescing tryptophan is highly alkaline). In the complex with DNA the lifetime is somewhat shorter (6.5 ns). This might be caused by a structural change of the protein

during DNA binding or by energy transfer from the Trp to the DNA. The fact that the fluorescence lifetime remains relatively long indicates that the tryptophan does not intercalate with the DNA, i.e. Trp is not directly involved in DNA binding.

1.2. Fluorescence properties of EcoRI methylase (with F. Winkler and R. Brown)

In a first experiment only the wavelength dependence of the fluorescence lifetime was monitored in various situations. In this way the fluorescence of the tyrosines of the enzyme can be separated from the tryptophan contribution. This was important since it was expected that tyrosine fluorescence would be particularly sensitive to DNA binding (as was found to be in the case of the fd gene 5-DNA complex for example). However, only very small changes could be detected. Further experiments are in preparation, where the rotational correlation time of the enzyme will be used as a monitor of the enzyme-DNA binding.

1.3. Alfalfa mosaic virus (with J.H. Kan and J.E. Mellema, Leiden, and H. Salzer, Heidelberg)

The coat protein of this RNA virus, which is also involved in the infection process, consists of 220 amino acids of which at least the first 25 residues form a "tail". There have been indications from NMR measurements that this "tail" is highly flexible (Andree *et al.*, 1981). First attempts to observe this mobility from the depolarization of the emission from Tyr²¹ failed, since the fluorescence is dominated by the two tryptophan residues. However the rotational correlation time of the coat protein (MW 25,000) which occurs only as dimers, was found to be 39nsec. Using a fluorescent dye (POP) which mainly reacted with the lysine residues in the flexible tail, we could observe a rapid motion of less than 1 ns over a very large angle. Further measurements to verify the rigid binding of the dye to the lysines are in progress.

1.4. Further experiments were performed for J. Kruse (Strasbourg) on the fluorescence of turnip yellow mosaic virus and tomato bushy stunt virus, to study the swelling behaviour and the interaction between the protein coat and the RNA core of these viruses. The depolarization of a POP dye attached to actin was

measured for H. Salzer, Dept. of Biochemistry, University of Heidelberg).

2. Laser microprobe

The mechanical design (with G. Brakenhoff, University of Amsterdam) and construction (in the EMBL workshop) have been completed and the instrument has been tested at various wavelengths (628, 600, 514 and 280 nm). The resolution was measured by scanning over a razor blade and was found to be as theoretically expected (97 nm at an excitation wavelength of 280 nm). The design and the construction of the electronic part of the instrument have been delayed somewhat but will consist of a CAMAC memory and a frame buffer as used for electron microscopy. It will be possible to accumulate a sequence of images from, for instance, a photo-bleaching experiment. Two initial applications have been tested in principle. The first was the scanning of chromosome bands using unstained chromosomes with high resolution. With the data processing equipment that will be constructed very high resolution and accurate measurement of the optical density against position will be possible.

The second application is the measurement of the lateral and rotational diffusion of macromolecules in membranes, using photo-bleaching and intensity correlation. Preliminary experiments were very promising. We intend to compare bleaching measurements with correlation measurements of the same objects, in order to study possible experimental artifacts in the widely used photo-bleaching method (see, for example, Bretscher, 1980).

References

- Andree, P.J., Kan, J.H. & Mellema, J.E. (1981). FEBS Lett., 130, 265.
- Bretscher, M.S. (1980). TIBS.
- Chothia, C. (1975). Nature, 254, 304.
- Eftink, M.R. & Ghiron, C.H. (1981). Anal. Biochem., 114, 199.

Hinz, H.J., Greulich, K.O., Ludwig, H. & Marvin, D.A. (1980). J. Mol. Biol., 144, 281.

Lehrer, S.S. & Learis, P.C. (1978). Meth. Enzymol., 49, 222.

Robbins, R.J., Fleming, G.R., Beddar, G.S., Robinson, G.W., Thistlethwaite, P.J. & Woolfe, G.J. (1980). J. Am. Chem. Soc., 102, 6271.

Szabo, A.G. & Rayner, D.M. (1980). J. Am. Chem. Soc., 102, 554.

Development of microanalytical techniques

Member: W. Ansorge

Fellow: T. Knott^{*}

Student: P. Kollenz^{*}

Visiting* workers: M.P. Gaub^{*}, J.M. Jeltsch^{*}, C. Krüger^{*},
P. Oudet

Technical assistants: R. Barker, J. Dickson

Microinjection into living cells

A technique for microinjection into cells was developed with several simplifications of the procedures for the preparation and handling of micropipettes, sample filling and the injecting system. The simplified procedure enables us to pull and fill capillaries in an easy, reproducible and fast way, taking only about one minute. The injecting system uses three positive pressure levels (high, injecting, holding) controlled by one button. It provides for quick and reproducible changes between the three pressures. Furthermore, it limits the chances of clogging the microcapillary by elimination of the temporary negative pressure (suction at its tip) which would normally occur when the pressure is reduced from the injecting pressure to a zero (atmospheric) pressure value. The estimated sample ejection rate achievable with this system corresponds to 10^{-11} - 10^{-13} ml per second. Compared to other known techniques using pressurized gas in bottles, this ejected volume is three orders of magnitude smaller and makes the system of interest for work with cells smaller than 50 μ m. While the sample volume injected into cells is reproducible, further improvement in the control of the amount actually injected may be desirable. The manipulation of the sample ejection system is very easy and no time is needed to learn it. The user can inject the sample volume either in the cytoplasm or the nucleus, as desired, by manipulating a single button.

To test the viability of the system, DNA of simian virus 40 (SV40) was injected into the nucleus of monkey (CV1) cells. As is known (Graessmann *et al.*, 1980), the early phase of infection with SV40 is marked by the synthesis of a tumour antigen (T-antigen) which is accumulated in the cell nucleus. Cells were fixed 24 hours after they were

injected, exposed to anti-T antibody and then to a second fluorescently labelled antibody. Fluorescence is visible only in the nuclei, indicating the presence of T-antigen. The T-antigen was observed in 70-80% of the injected cells.

Thymidine kinase deficient rat cells were co-transformed by microinjection of genetically linked SV40 and TK DNAs by A. Dunn using this system. Cells could be injected at an initial rate of about 600-800 per hour, the actual number of cells injected in one hour being about 400. A system for microinjection and follow-up of fluorescently labelled proteins into cells was set up in collaboration with D. Louvard.

The above improvements make the injection technique easily accessible to molecular biologists who need to screen for expression of the recombinants made in vitro, or to study the distribution of fluorescently labelled structural proteins.

The pressure, the valves and the penetration of the cell (piezo driver) may be regulated electronically. The system would be of interest for any automated injection process.

System for DNA sequencing with resolution up to 600 base pairs

Tests and studies on further optimization of resolution on DNA sequencing gels have been continued. We have been working on the problem of sample quality. After discussion and collaboration with H. Garoff and S. Kvist we were able to prepare samples of sufficiently good quality, apparently giving proper labelling even around 1000 base pairs. The effect of the physico-chemical properties of gels and buffers on resolution were tested e.g. ionic strength and pH of buffers, different buffer systems, acrylamide concentration, crosslinker concentration, type of crosslinker, temperature of polymerization, denaturing conditions (urea vs. no urea, formamide, SDS), gel length and thickness. Tested also were different running conditions like electric field, gel temperature and dimension of sample slots. Gels 0.1 mm - 0.2 mm thick and up to 1.2 m long were cast and tested routinely.

We were able to count up to 600 base pairs in the new system using 1m long gels (Ansorge & Barker, to be submitted). At present the resolution is no longer limited by the quality of the sample but by the resolving power of the polyacrylamide gel.

Protein separation and visualization by impregnation in potassium permanganate and silver nitrate

This new technique for the visualization of proteins separated by gel electrophoresis was developed in the group and in collaboration with G. Warren, applied both to the very thin (thickness 0.1 - 0.2 mm) and to the usual 1 mm thick gels (Ansorge, 1981). It is reproducible, only stable chemicals are used and the time can be shortened to about one hour even for the 1 mm thick gel. The amount of silver used is very small, the most expensive chemical in the procedure being trichloroacetic acid. An interesting feature is the resulting different colours of the protein bands.

The technique has been used with success in the continuous, discontinuous and two-dimensional gel systems. Amounts as low as 5×10^{-10} g of protein per band were resolved (Ansorge, in preparation). In collaboration with the clinics in Neukoelln (W. Berlin) we have tested our isoelectric focussing, SDS separation and the two-dimensional techniques with the aim of finding fast and very sensitive diagnostic tools for pre-natal diseases and cancer. New protein bands were correlated with some diseases, using the above technique.

Publications during the year

Ansorge, W. (1981). Preparation of ultrathin (0.01 - 0.2 mm) gels. Application to protein separation with a new silver stain. Proceedings of the 3rd Int. Conference on Electrophoresis, Charleston 1981, (in press).

Ansorge, W. (1982). Improved system for capillary microinjection into living cells. Exp. Cell Research, (in press).

Ansorge, W. & Garoff, H. (1981). DNA sequencing on very thin (0.2 mm) gels. In Electrophoresis 1981: eds. Allen, R.C., Arnaud, P.. Walter de Gruyter & Co., p. 635-646.

Garoff, H. & Ansorge, W. (1981). Improvements of DNA sequencing gels. Anal. Biochem., 115, 450-457.

Other references

Graessmann, A., Graessmann, M. & Müller, C. (1980). Methods in Enzymology, 65, 816-825.

Operating principle of a self-pumping continuous-flow centrifuge

Member: L.-S. Kim

The basic operating principles of self-pumping continuous-flow centrifugation have been studied. When an open bent tube with one limb vertical rotates around the vertical axis with the bottom end in a liquid, the liquid will be pumped up and ejected above a certain speed (see Plate 54). If the central part of the vertical limb is widened to form a rotor chamber, and liquid is supplied continuously, sedimentation takes place in the rotor chamber (see Plate 55). In this self-pumping continuous-flow centrifugation (SPCFC), under certain conditions, the sedimentation coefficient depends only on the geometrical design of the rotor and the properties of the suspension, but not on rotor speed or flow rate, i.e. there is a compensating effect between rotor speed and flow rate.

If the flow is confined to a narrow space perpendicular to the centrifugal field, a laminar flow region required for sedimentation field flow fractionation may be maintained in a simple manner. The stability of the flow region and the geometric factors influencing the performance of a self-pumping continuous-flow centrifuge have been studied in preliminary experiments.

Such centrifugation methods can be used in the design of both preparative centrifuges and analytical fractionation centrifuges with separations better than in hitherto existing centrifuges.

An apparatus employing SPCFC and several test rotors have been designed and constructed, and the operating principles have been tested in preliminary experimental studies during this year.

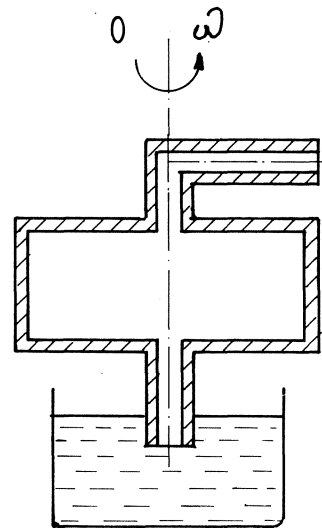
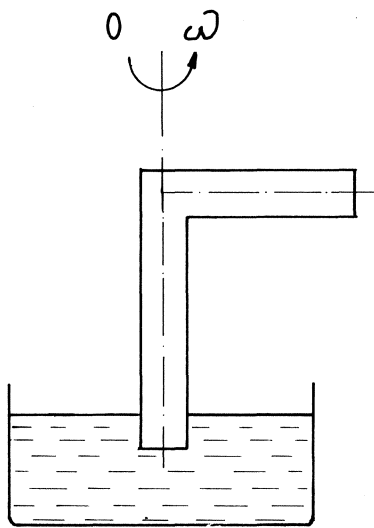


PLATE 54

Sketch of a device illustrating the principle of self-pumping continuous-flow.

PLATE 55

Modification of the device to include a centrifuge rotor.

Cell separations using magnetically manipulated adsorption media

Member: T. Reed

Technical assistant: A. Cockcroft

The pseudo-first-order binding kinetics for the interaction of biological cells with sensitized adsorption beads at low bead concentrations (3.3 vol% to 14 vol%), as well as the relatively high rate constants of such reactions, have been established by work already reported. Although preliminary studies had shown this behavior to be independent of the presence of non-binding cells, a careful repetition of the work was undertaken with kinetics and microscopy to establish the degree of non-specific binding shown by the inert cells. The NS-1 myeloma cells used as "null targets" were inactivated by fixing with formaldehyde, equilibration with succinyl concanavalin A and subsequent refixation with formaldehyde. Kinetic experiments included the simultaneous measurement of rate constants for pure target cells (HeLa, S-3), "null target" cells (inactivated NS-1), and a mixture of approximately equal numbers of both cell types. To calculate the binding rate-constant in the case of the mixture, the number of null target cells is subtracted from the total number of cells and the binding calculations are based on the difference. This method assumes that the null target cells do not bind to the sensitized adsorption beads. A false assumption would manifest itself as an abnormally high rate constant for the reaction of the target cells with the beads in the presence of null target cells, or the direct observation of non-specific binding in microscopic examination. Both the similarity of rate constants in binding experiments with and without null target cells, and the low binding rate of null target cells (Plate 56), confirm the lack of non-specific binding and the independence of the binding reaction from interference by non-binding cells.

Cells bound to beads from binding experiments with target and null-target cells were examined by fluorescence microscopy. Two-step staining was used. The cells were first treated with anti-mouse rabbit IgG (cross incubated with HeLa cells) and then with anti-rabbit goat IgG coupled to rhodamine. In this way the null target NS-1 cells were specifically stained and non-specific binding could be clearly observed in the fluorescent microscope (Plate 57). Fluorescence microscopic studies showed non-specific

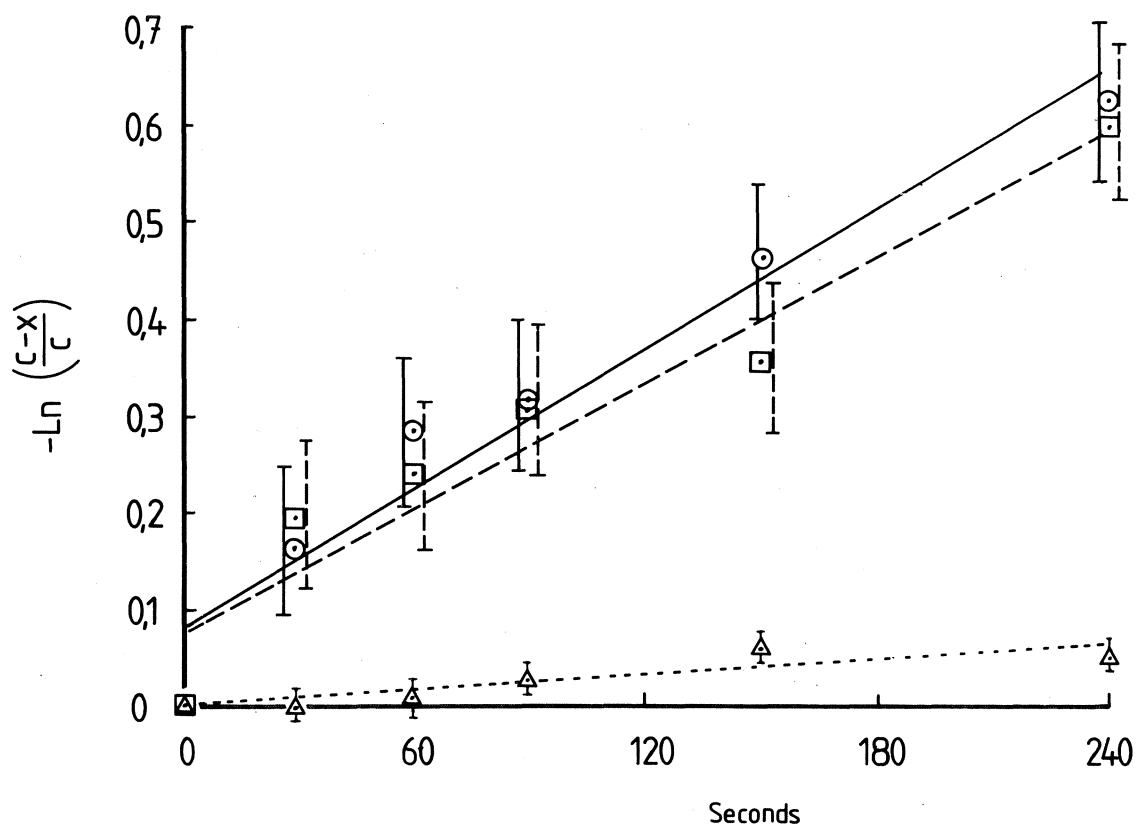
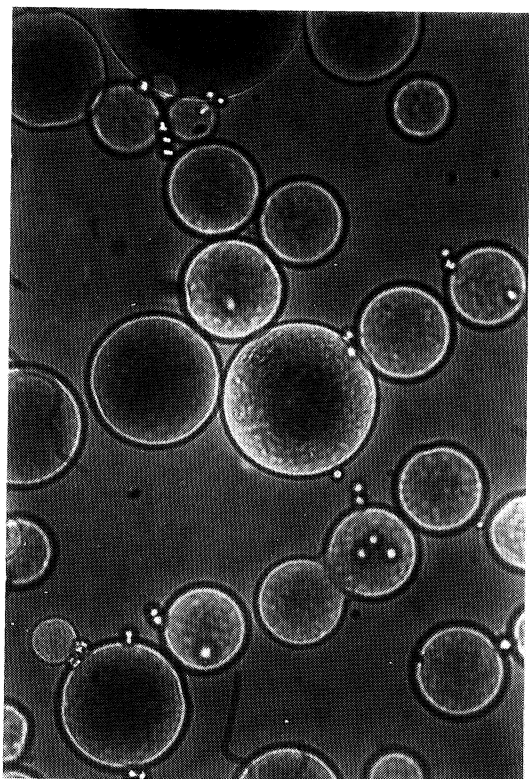
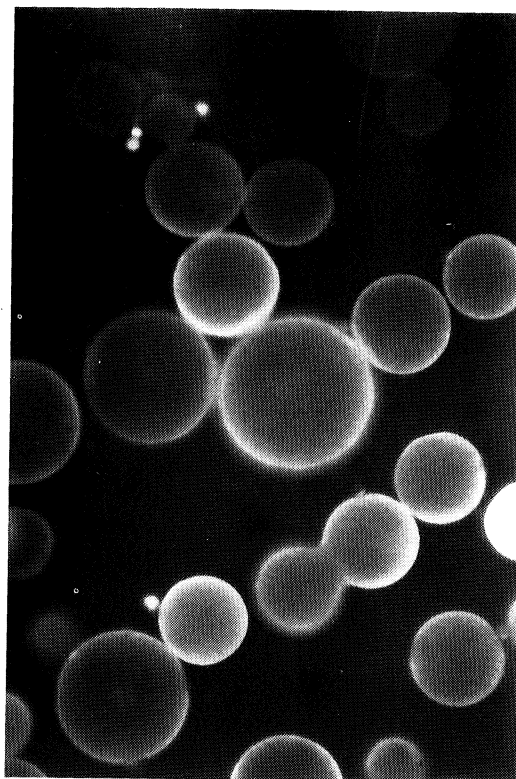


PLATE 56

A kinetic study of cell binding in mixtures containing inert cells. The points are averages of those from two complete experiments. Each experiment consisted of a determination of the binding rate of pure HeLa cells ($2 \cdot 10^5$ per ml) shown as circular points with a solid line, the binding rate of a 50:50 mixture of HeLa and blocked NS-1 cells ($4 \cdot 10^5$ total cells per ml) shown as square points with a dashed line, and the binding rate of blocked NS-1 cells ($2 \cdot 10^5$ per ml) shown as triangles with a dotted line. Both studies used Magnogel-44 at 3.3 vol%. In one case the conA concentration was 5.0 mg per ml beads and in the other it was 5.8 mg per ml. The correlation coefficient for pure HeLa and mixture plots is 0.97.



Transmission



Fluorescence (Ploem)

PLATE 57

Photographic determination of non-specifically bound cells. Both views of the same microscopic field show Sepharose beads (4 mg conA per ml) which have been exposed to mixed NS-1 (blocked) and HeLa cells for 2.5 min under roller-bottle conditions. In the transmission micrograph the focus has been arranged to produce internal reflection in the cells. It shows a total of 32 cells. In the fluorescence micrograph excitation (Ploem) at 530-560 nm (green) and observation at >580 nm (red) shows stained NS-1 cells non-specifically bound (4 cells). Fluorescence in the Sepharose beads is due to non-specific absorbance of the antibody stain.

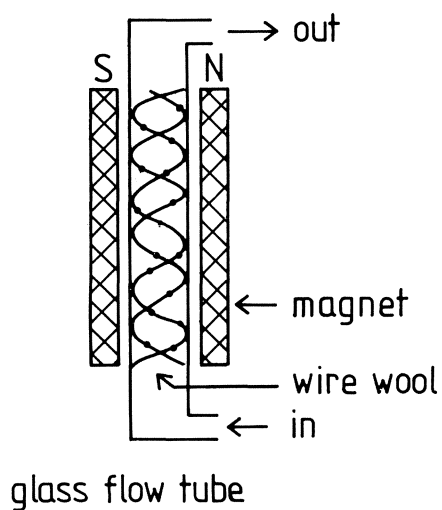
binding levels of about 10% which is in agreement with the kinetic control experiments. These results compare favorably with the level of non-specific binding (21% to 38%) obtained using antibodies bound to Magnogel 44 in adsorption column experiments (Antoine et al., 1978).

Two types of flow system have been devised which make use of the open array technology. To test these systems a pumping system was constructed in which a constant flow of suspended cells could be alternated with a constant flow of cell-free buffer. Piston displacement pumps were used for this purpose to avoid cell damage by the "roller elements" of peristaltic pumps. Simple valving systems were designed to permit interruption-free change from cell suspension to buffer, and to avoid the introduction of bubbles. After passing through the flow reactor, the flowing liquid passed into a conventional fraction collector for analysis by cell-count and microscopic examination. Beads could be removed by turning off the magnetic field and collecting them at the bottom of the column.

In the static array system (Plate 58) ferromagnetic wire wool is placed in the flow tube, which is between the poles of a conventional electromagnet. The beads are held at the surface of the wire by magnetic gradients produced there by interaction with the magnetic field. The system proved capable of holding a sufficient number of beads. In preliminary studies, the amount of non-specific binding caused by cells caught in the interstices between beads on the wires was too high. Although a detailed treatment of bead surface chemistry and wire geometry might have solved this problem, this was felt to be a relatively non-productive line of research and further development in this direction was discontinued.

In the dynamic array system (Plate 58) field gradients are used to contain the beads in what is effectively a magnetic bottle. In order to improve the slope of the end gradients, a magnetic "return circuit" with appropriately shaped pole-pieces may be placed around the solenoid. Such a flow system with removable pole pieces and return circuit was constructed and tested. The volume of the system was 100 ml, although the actual working volume was probably more like 50 ml. Containment of the beads was significantly improved by the return circuit and pole pieces. At higher fields (1000 gauss) beads binding to the walls of the flow chamber became an important factor. The return circuit and associated higher end gradients permitted operation at significantly lower field strengths (500 gauss). The

Static System



Dynamic System

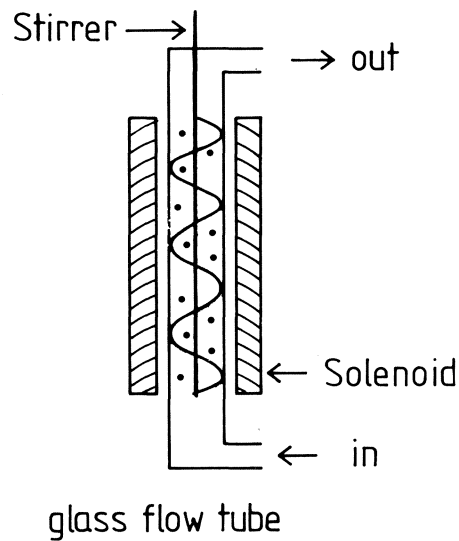


PLATE 58

Geometry of the open array devices. In the static system, 100 gauss - 300 gauss is sufficient field strength to cause bead-binding. In the dynamic system, 800 gauss - 1000 gauss is sufficient to contain the beads. With a return circuit and shaped pole pieces (not shown) the field requirement is considerably lower.

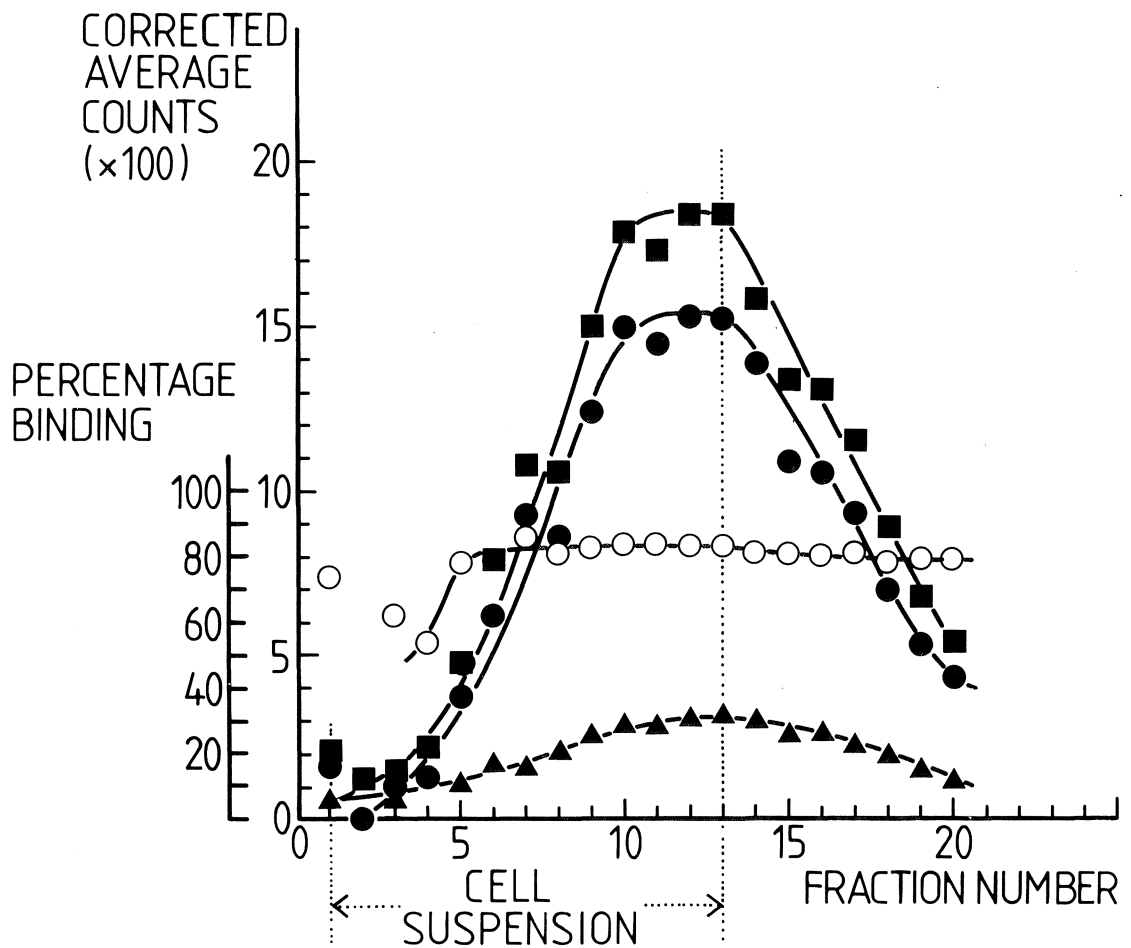


PLATE 59

Flow study of cell binding₅ in a dynamic array. A suspension of HeLa cells ($2 \cdot 10^5$ per ml) was caused to flow (5 ml per min) through the column containing 10 ml of magnetic Sepharose (3.8 mg conA per ml). Stirring was 30 rev min. Fractions were taken every 3 minutes (15 ml). Squares show the count of control cells (inactive beads). Triangles show the cell count for cells which have passed through the column with active beads in place. Solid circles show the total cells bound by difference. Open circles show the percentage of presented cells binding.

higher magnetic susceptibility and higher density of Magnogel 44 relative to magnetic Sepharose made it relatively unacceptable as a support medium in this system under conditions which we attempted. This was due to excessive amounts of "wall binding" which always occurred. The preferred system used shaped pole pieces and a return circuit on the solenoid in conjunction with magnetic Sepharose as the substrate. Under these and similar conditions, cells binding varied from 80% at 5 ml min (Plate 59) to 25% at 20 ml min.

Since the possibility of kinetic separation had been established with conA in roller-bottle systems, the magnetic bottle unit had been shown to contain magnetic adsorption beads properly in flowing systems, and cell binding had been demonstrated in flowing systems, it seemed appropriate to repeat the results with an antibody system to demonstrate an application to cell separation directly. The necessary knowledge of the growth, characterization and isolation of monoclonal antibodies is being developed within the group. A suitable system of monoclonal antibodies, cultured target cells, and cultured null target cells, has been obtained from Dr. Robert Hyman (Salk Institute). Antibody binding studies should be under way early in 1982.

Reference

Antoine, J. C., Ternynck, T. Rodrigot, M. & Avrameas, S. (1978). Innunochemistry, 15, 443-452.

Isolation of organelles with antibodies

Member: K. Howell

Fellow: A. Harel-Bellan^{*}

Student: E. Sztul^{*}

Visiting worker : A. Ito^{*}

Technical assistants: S. Massardo, A. Scharm^{*}

A major aim of the group is to develop efficient cell fractionation techniques using antibodies, to select from a cellular homogenate all the membranes or vesicles which contain a specific antigen.

An immunological-affinity separation technique is desirable, because when a cell is homogenized, the subcellular compartments fragment and form small vesicles. These vesicles, derived from different organelles, may have the same size and density and it would not be possible to separate them by conventional techniques. As an example, an electron micrograph of a fraction of rat liver homogenate which has the density of 1.15 g/cm^3 is shown in Plate 60. The major component of the fraction is small, smooth membrane vesicles derived from smooth endoplasmic reticulum and plasma membrane; but it also contains components of the Golgi apparatus, rough endoplasmic reticulum and fragments of mitochondria. Using an antibody against the enzyme NADPH cytochrome P 450 reductase and binding this antibody to a 2μ acrylamide bead, we were able to isolate from the total fraction those vesicles which contained the enzyme accessible on their outer surface. The bead illustrated in Plate 61 shows that only the small, smooth membrane vesicles were isolated by this immuno-absorbant. It is important to note that the rough endoplasmic reticulum also contains the enzyme, but it was not accessible to the antibody bound to the bead.

In collaboration with A. Ito we continued to use the immuno-bead system with antibody to NADPH cytochrome P 450 reductase to show the heterogeneity of isolated Golgi derived vesicles (Ito & Palade, 1978).

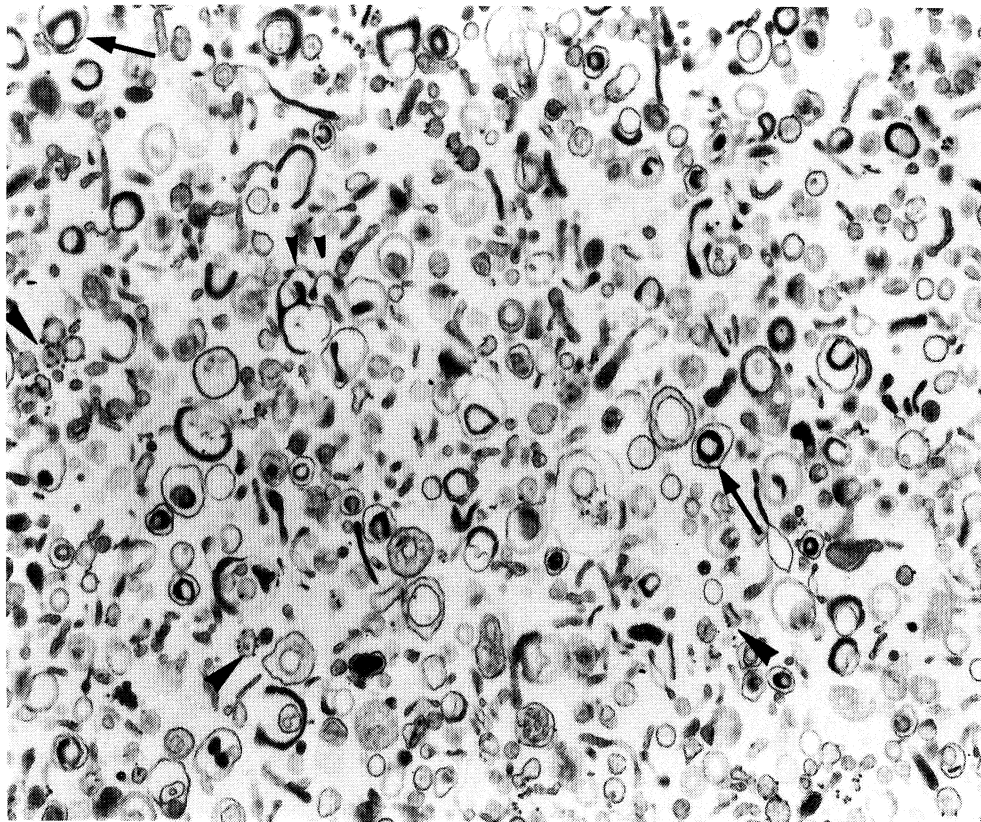


PLATE 60

Electron micrograph of all components of rat liver homogenate of density 1.15 g/cm^3 . The fraction was isolated in a sucrose density gradient. The major component of the fraction is small, smooth membrane vesicles. Rough endoplasmic reticulum is marked with large arrow heads, Golgi elements are marked with small arrow heads, and mitochondrial fragments with arrows. Magnification: 25,300 times.

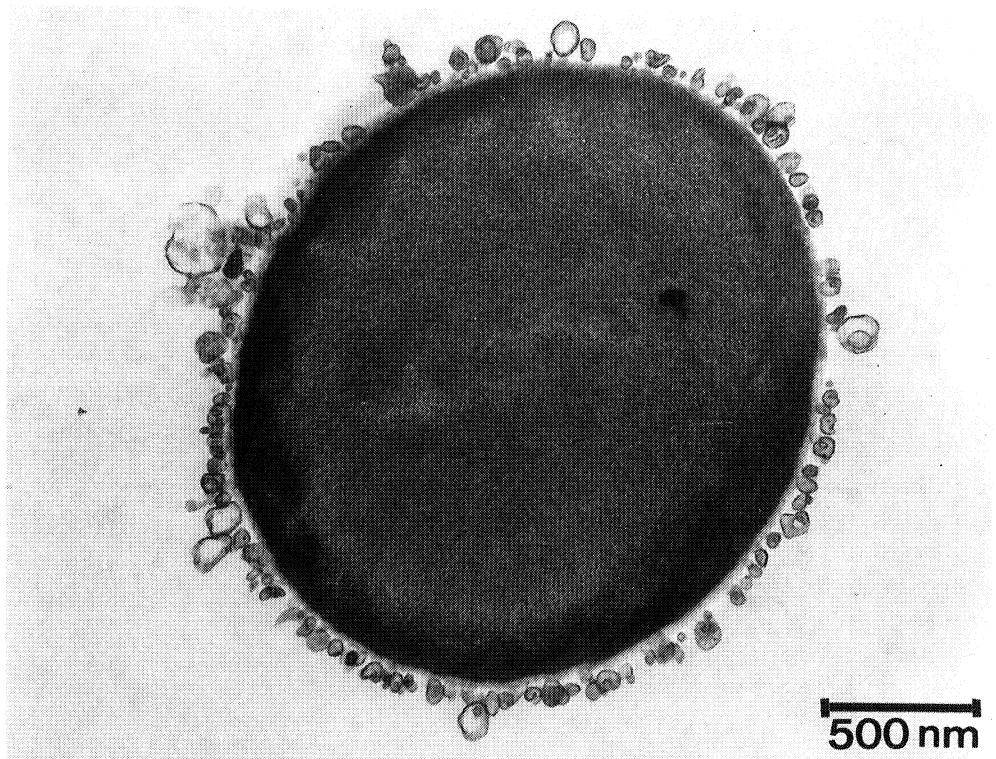


PLATE 61

Electron micrograph of vesicles of the fraction shown in Plate 60 which bound to anti-NADPH cytochrome P 450 antibody bound to an acrylamide bead. Magnification: 37,500 times.

In order for this isolation system to have widespread applicability, a large bank of antibodies, specific for each organelle or transport vesicle, needs to be produced. Other requirements of the antibodies are that they must recognize determinants exposed to the outer (cytoplasmic) surface of the membrane vesicle, must be of high enough affinity to pick up vesicles present in the total population in low concentrations, and must be available in large quantities.

Our group and others working on cellular membranes have put considerable effort into raising these antibodies. It is envisioned that the antibodies produced according to the strategy of D. Louvard (see Report of the Louvard group and Louvard et al., 1982), will produce the affinity reagents required. Louvard has been successful in raising organelle-specific antibodies to endoplasmic reticulum, Golgi, and lysosomes. Both Louvard and B. Burke are raising organelle-specific monoclonal antibodies and members of K. Simons' group are raising monoclonal antibodies to the plasma membrane enzymes aminopeptidase (apical plasma membrane) and $\text{Na}^+\text{K}^+\text{ATPase}$ (basolateral plasma membrane). All of these antibodies would be available for this project. A. Harel-Bellan has screened a large number of the available antibodies but unfortunately none of them meets the above requirements.

In addition to raising organelle-specific antibodies, we have also raised antibodies to rat serum apo-lipoproteins. With these antibodies we have been able to isolate forming lipoproteins from the compartments of the intracellular secretory pathway - rough and smooth endoplasmic reticulum, Golgi, and secretory vesicles - using the same immuno-affinity technique. This isolation technique will be used to characterize further the intracellular, i.e. newly synthesized, lipoproteins and provide additional markers for the vesicles of the secretory and degradative pathways in the hepatocyte (Howell & Palade, 1982 a, b).

In addition, effort has been placed on designing an instrument to improve the isolation procedure. The isolation system must permit rapid and complete separation of the bound from the unbound vesicles and the process should leave the vesicles intact so that procedures for characterization and identification can be carried out. These include a morphological survey and assays for other antigens, functional criteria, or enzymatic activities. T. Reed has designed a magnetic system, similar to the one he

has successfully used to isolate cells, and we will be testing this soon (see Report of the Reed group).

References

Howell, K.E. & Palade, G.E. (1982a). J. Cell Biol., 92, 822-832.

Howell, K.E. & Palade, G.E. (1982b). J. Cell Biol., 92, 833-845.

Ito, A. & Palade, G.E. (1978). J. Cell Biol., 79, 590-597.

Louvard, D., Reggio, H. & Warren, G. (1982). J. Cell Biol., 92, 92-107.

THE OUTSTATIONS

The Outstation at the DESY, Hamburg

Head: H.B. Stuhrmann*

Acting joint heads: J. Bordas*, M. Koch*

Members: K.-S. Bartels, H.-D. Bartunik, J. Bordas, D. Dainton, J. Hendrix, C. Hermes, M. Koch, P. Laggner, J. Phillips

Fellows: Y. Inoko*, L. Lijk*

Trainees: R. Dimper*, J. Heuer, E. Jerzembek

Visiting workers: R. Aasa*, M. Adams*, D. Albrecht*, R. Bauer, C. Boulin, W. Carson, C. Chen, D. Collins, O. Dideberg, J. Drenth, G. Elsner, K.-E. Falk, A. Faruqi, M. Feiters, A. Gabriel, M. Garavito, W. Gaykema, I. Glover, J. Goodfellow, R. Goody, H. Grewe, K. Güth, M. Guss, H.J. Hartmann, G. Henkel, C. Hermes, W. Hol, K. Hornbech-Svendsen, G. Huber, H.F. Huxley, K. Jellinek, J. Jenkins, M. Just, W. Kabsch, C. Kalk, H. Kihara, H.J. Korte, M. Kress, R. Ladenstein, P.F. Lindley, J. Lowy, Y. Maeda, E. Mandelkow, E.M. Mandelkow, M. Marden, E. Meyer, M. Moody, R. Padron, F. Parak, K. Petratos, F. Poulsen, L. Prespa, W. Prieske, D. Pruss, R. Pufall, Sir John Randall, W. Renner, H. Riedl, R. Rigler, W. Sängler, M. Sandom, B. Schmelezer, T.M. Schuster, Z. Sayers, U. Simones, B. Simmons, L. Skolyokke, J. Slappendale, D. Spohr, P. Studerus, D. Suck, L. Summers, B. Torensma, D. Tsernoglou, W. Turnell, P. Vachette, T. Vängaard, J. Walter, K. Wilson, F. Winkler

Technicians and engineers: P. Bendall, H. Borgwardt, E. Dorrington, P. Gill, R. Kläring, J. Kühl, H. Ludwig, P. Moir-Riches, V. Renkowitz, B. Robrahn, H. Sammet, K.-H. Sönnholz (part-time), W. Weber.

During 1981 the storage ring DORIS was used exclusively as a dedicated source of synchrotron radiation. Main user shifts in Laboratory IV, on the positron ring, amounted to 53 twelve-hour shifts, whereas a total of 209 shifts was available in HASYLAB, on the electron ring.

With respect to beam time, 1981 was a year of transition with HASYLAB producing an increasing share of the dedicated beam time.

After the shutdown of DORIS, which is planned to end in May 1982, the machine will be considerably upgraded and should run for approximately 10 months each year. One third of this time will consist of dedicated beam periods for synchrotron radiation research in HASYLAB. The remaining two-thirds are reserved for colliding beam experiments during which the machine will be run in the "single bunch" mode at 5 GeV with expected currents around 20 mA, and under these conditions useful beam should be available both in HASYLAB and in Laboratory IV.

Despite the fact that this evolution, which will lead in the future to a transfer of the main experimental activity of the Outstation to HASYLAB, was planned, a difficult balance had to be found between the requirements of the development of the new instruments and the efficient use of the available dedicated beam time for experiments in Laboratory IV.

Nevertheless, the construction of the beam path for two instruments was completed and the optical components and controls of the double-focussing monochromator-mirror camera were installed and tested. Plate 62 shows a general view of this new installation.

It can be realistically expected that the optical components (cylindrical mirror and double monochromator) for the second instrument will also be installed by the end of the DORIS shutdown.

Detailed design and planning for the third instrument, which will be equipped with a cylindrical mirror and a double monochromator for x-ray spectroscopy (EXAFS), are under way. No definitive schedule can, however, be made, as this task is complicated not only by the fact that this beamline has to be installed in the very narrow space between existing devices, but also because at this stage of operation of HASYLAB, construction is only possible during shutdowns.

Instruments and developments

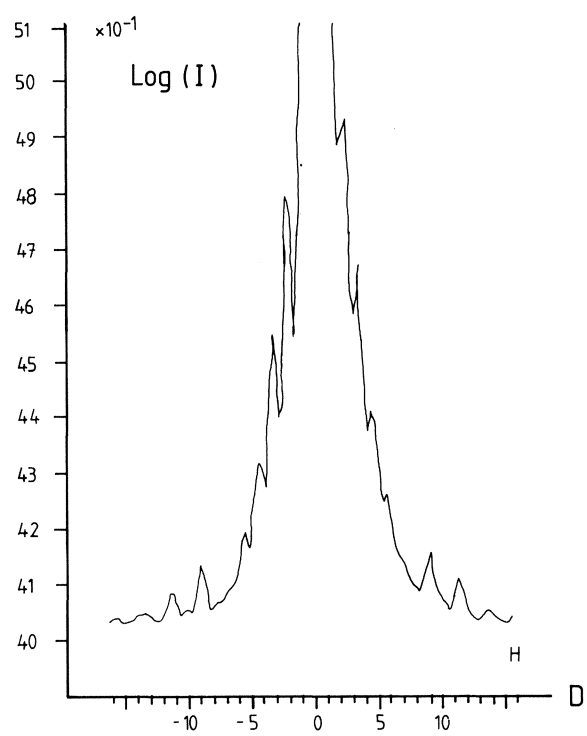
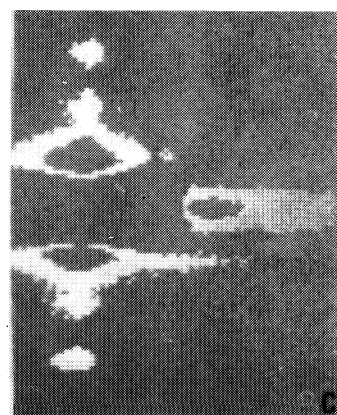
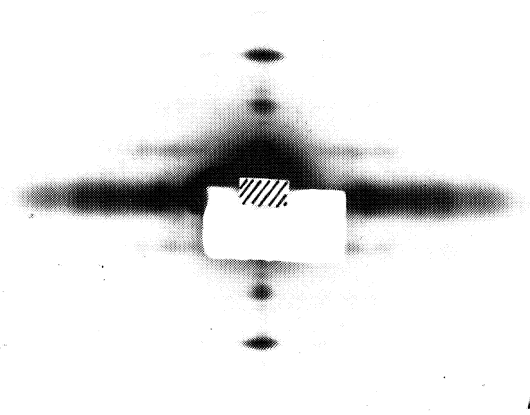
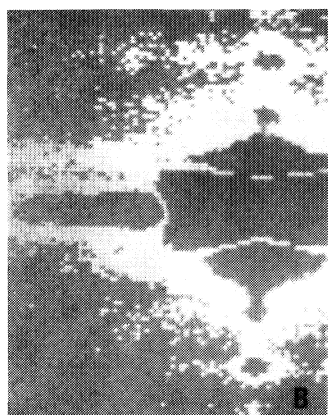
PLATE 62

General view of HASYLAB taken in August 1981. The two arrows indicate the location of the new EMBL instruments
A: Time-resolved measurement (X33) and B: protein crystallography (S31).



PLATE 63

Film exposure of frog sartorius muscle taken on the new camera for time-resolved measurements (X33). [A], [B] and [C] show the display of a similar pattern obtained with an area detector. Two different intensity windows were used for the display, i.e. only the parts of the picture where the intensity is above the lower level and below the upper level are shown. In [B] the very strong equatorial reflexion appears as a hole, whereas the meridional reflexions are clearly resolved. In [C] both limits of the window are lowered and all strong reflexions appear as holes, whereas the layer lines are clearly recognizable. [D] illustrates the meridional diffraction pattern of frog sartorius muscle as seen in the ultra-small-angle scattering camera. The abscissa corresponds to the orders of the sarcomere repeat (2.5 μm). Note that this entire pattern is contained inside the hatched area in [A].



a) Instruments in Laboratory IV

The instruments in Laboratory IV, X11, X13, X15, S11 and P11, which are described in the 1978 Research Report, were in routine use throughout the year for time-resolved measurements, protein crystallography, EXAFS and anomalous small-angle scattering.

The first results obtained with the ultra small-angle scattering camera X12, which is now complete, were very encouraging and of a quite unique nature.

Although the optics of the instrument remained unchanged, several improvements and developments were made at the back end of the experiments. Some of these developments are indicated below under specific research topics.

Obviously, P11 (Mössbauer spectroscopy), which requires the single-bunch mode only available during parasitic shifts when DORIS is used for colliding beam experiments, could not be used for actual measurements, but the visiting group responsible for this instrument performed useful calibration measurements.

b) Instruments in HASYLAB

V. Renkowitz, R. Kläring, H. Borgwardt, B. Robrahn.
Technical coordination: H. Ludwig.

A few weeks before the DORIS shutdown, the new fixed wavelength camera for time-resolved measurements (X33) was successfully tested. The first measurements indicate that with the new arrangement of the optical elements (i.e. with the triangular focussing monochromator in front of the segmented mirror) allowed by the geography of HASYLAB, an increase in intensity of about three times has been achieved together with a considerable reduction in background and improvement in resolution as illustrated by a typical film recorded from frog sartorius muscle on X33 (Plate 63). The instrument is driven by a new CAMAC stepping motor control system designed at the Outstation. This very flexible system, which can control up to 63 motors and contains its own memory to protect the alignment of the instrument from power failures, will also be used on the two other new instruments in HASYLAB.

c) Detectors

The higher intensities to be expected after the current improvements of DORIS will, it is hoped, result in time-resolved measurements with higher accuracy and time resolution. This will, however, only be possible if the detectors can cope with the higher fluxes. The efforts in detector development have thus to be pursued and expanded. Gaseous position-sensitive detectors, the basis of the systems so far successfully applied, are limited in their count-rate capability for two reasons. The first is the so-called space-charge effect which tends to reduce the signal amplitudes below the threshold of detection. The second is the dead time of the electronic system associated with the localization of a photon impact.

There are several approaches to the solution of the count-rate problem. One is to divide the detector into separate elements which are able to count individually. This concept has been adopted for a linear system with parallel read-out. The other approach is to make use of new electronic circuits to reduce the dead time. As a result of efforts undertaken along this line a new extremely fast time digitizer has been produced as well as a read-out system based on priority encoding.

1) The linear detector with parallel read-out: wire-per-wire detector

J. Hendrix

This system, illustrated in Plate 64, consists of a linear array of 128 anode wires, each with an individual amplifier-discriminator and a fast-counting channel. By subdivision into separate counting elements the space charge effect is reduced by the number of wires. This concept is inherently limited to one-dimensional applications with a relatively low number of resolution elements because of the amount of electronics needed. During operation, the scaler channels are read out, and their contents are dumped into a buffer-memory with an interruption of the accumulation of data of less than 100 μ s. The count-rate capability exceeds 2×10^5 counts per wire, or 2.5×10^7 counts/s for the entire detector. The system has been used for time-resolved measurements on frog sartorius equatorial reflexions.

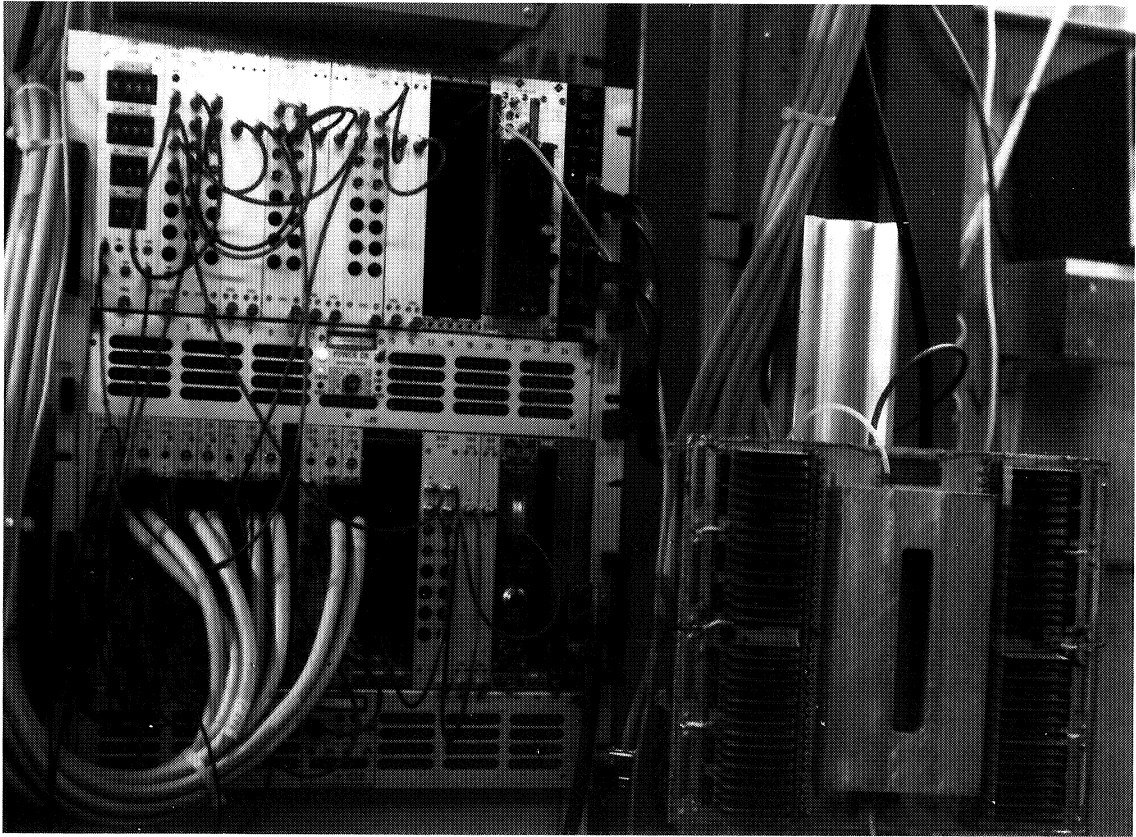


PLATE 64

The wire-per-wire detector system: the linear detector with its preamplifier-discriminators is at the right and the 128 scalers and the buffer memory are on the left.

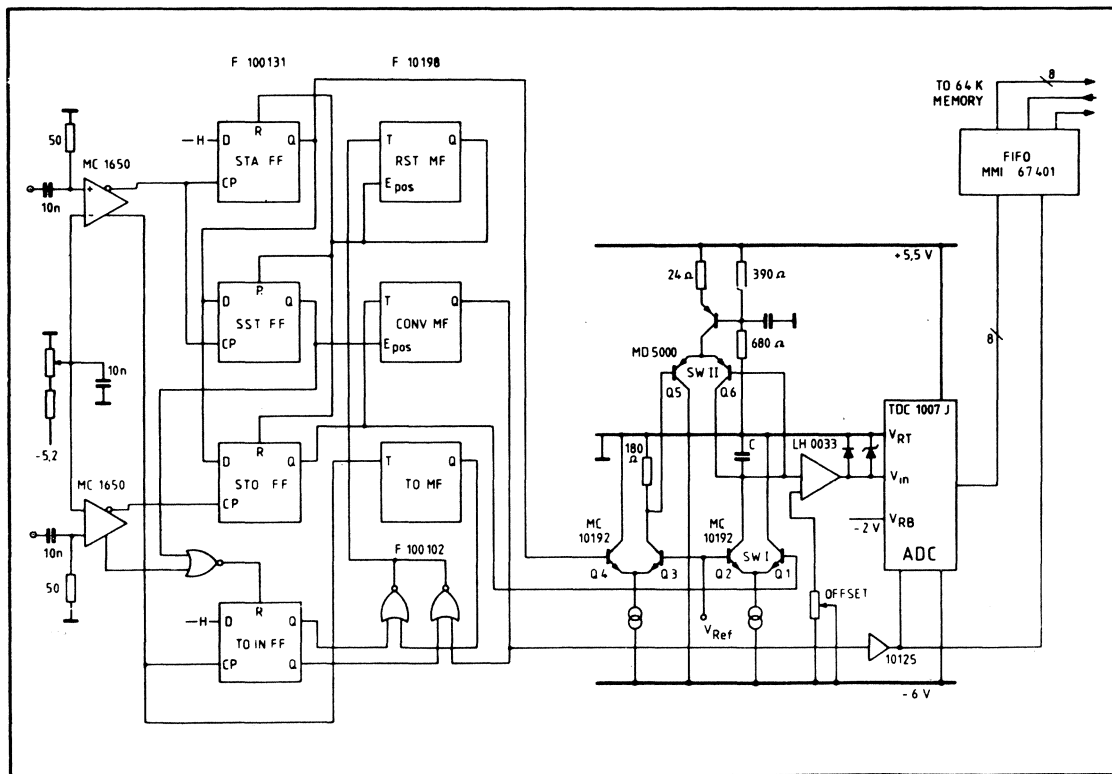


PLATE 65

The fast time digitizer basic circuit diagram. The circuit consists of a pre-processing logic (flip-flops F100131, monoflops F10198) to prevent the conversion of multiple events, a fast time-to-amplitude converter (Q1 to Q6), and a flash - ADC (TDC 1007J).

2) A very fast time-digitizer system

J. Hendrix.

Multiwire proportional chambers, as they are used at the Outstation, deliver their positional information as a time difference between two signals, propagating through a delay line. The total propagation delay plus the digitization of the time difference constitute the dead time of such a system. A time-digitizer system which minimizes both factors has been developed. The circuit is based on a novel time-to-amplitude convertor and an 8-bit (later 9-bit) flash analogue-to-digital convertor (Plate 65). The new device combines two advantages: a very high time resolution (50 psec), resulting in a shorter propagation delay, and an extremely short conversion time (<50 ns).

The dead time per event is 100 ns at most for a delay line length of 50 ns, corresponding to a peak count-rate of 10^7 cps i.e. 20 times faster than the hitherto available units.

3) Priority encoding data acquisition system for a linear multiwire detector

P. Gill and A. Gabriel.

A conceptually elegant and inexpensive system based on the use of priority encoders, capable of count-rates up to 2×10^7 counts/s, was tested with satisfactory results. The device is now fully operational and will be used mainly for solution scattering work in the time-resolved mode and for time-resolved x-ray fluorescence experiments on the new experimental station in HASYLAB.

Besides these developments, new approaches to the reduction of the space-charge effect which should lead to an increased count-rate capability and resolution have been explored.

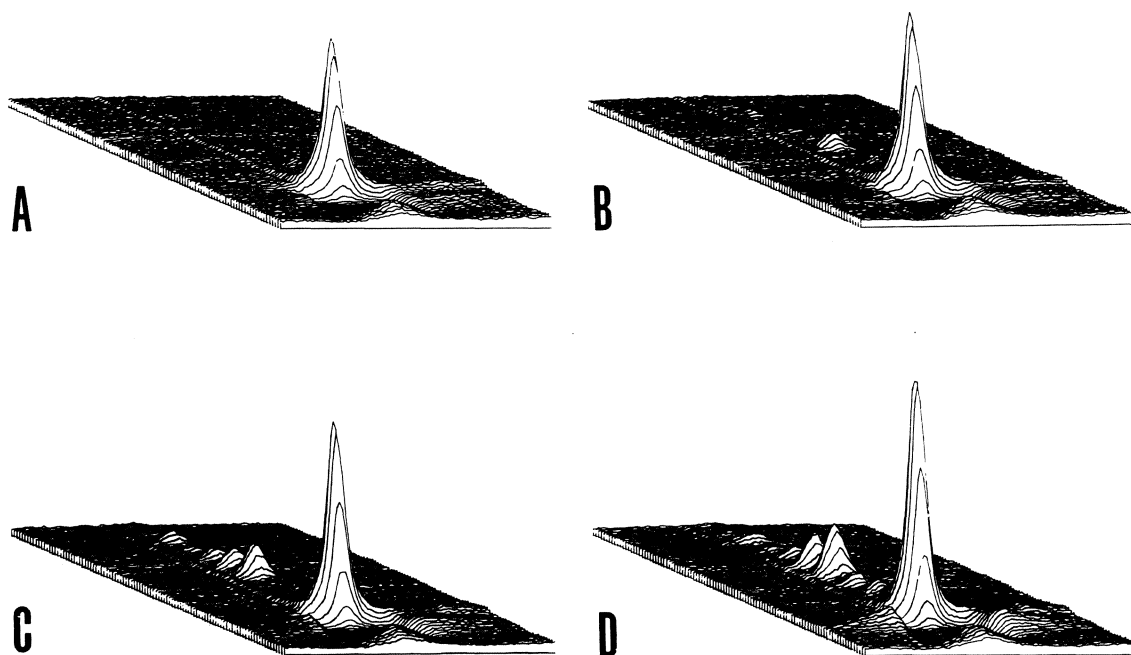


PLATE 66

Evolution of the diffraction pattern of collagen after incubation with phosphotungstic acid (H. Riedl & Th. Nemetschek, Heidelberg) as followed with an area detector. (A: after 30 s, B after 60 s, C after 90 s, D after 8 min).

4) Area detector for solution and fibre work

A. Gabriel (EMBL, Grenoble); C. Boulin (EMBL, Heidelberg); D. Dainton, M.H.J. Koch, J. Bordas.

A detector with an active area of 100 cm^2 with delay line read-out and time-to-digital conversion was tested for static measurements and preliminary time-resolved work.

The detector was flushed with argon/ CO_2 so that its efficiency was comparable to film. The efficiency could, however, be substantially improved by the use of xenon.

Examples of static patterns of frog sartorius muscle displayed with two different intensity windows are shown in Plate 63, and should be compared with the corresponding film pattern. The first few frames taken with a time-resolution of 20 s during the incubation of a single collagen fibre with phosphotungstic acid are shown in Plate 66. The system still needs development but should be available for specific experiments after the DORIS shutdown.

5) Area detector and data acquisition system for protein crystallography

A. Gabriel (EMBL, Grenoble); C. Boulin (EMBL, Heidelberg); K.S. Bartels, H.D. Bartunik, L. Lijk.

Software for static and time-resolved protein data collection using a multiwire area detector with a fast read-out and data compression hardware is being written. It is based on the Cambridge, Bristol and Munich film evaluation programs.

Computing and Data Acquisition

D. Dainton, M.H.J. Koch, P. Bendall, E. Dorrington, B. Robrahn, P. Gill.

Apart from actively participating in the developments already mentioned in connection with detectors and control systems for instruments, the computer electronics group has further enhanced the existing installations and provided,

whenever necessary, direct support for the experiments. In particular, a number of modules for the control of time-resolved experiments was designed or modified.

Hardware

A new serial highway was installed on the PDP 11/45 to control the instruments in HASYLAB. The connection between the PDP 11/45 and the DESY IBM computing centre was implemented and has been heavily used throughout the year.

Software

The CAMAC driver was extended to support the third serial branch and the necessary software for the new Tektronix 4663 plotter was produced. Floating point arithmetic facilities and graphics routines were added to the CATY language. Development of additional routines is still in progress. Software has also been written to allow easy transfer of data files and graphic output between the DESY IBM and the PDP 11/45. Further, a major effort has been undertaken to document both the data acquisition and data evaluation software. A complete set of users' manuals should be available by the beginning of the next measurement period.

Application software for protein crystallography

K.S. Bartels

The Martinsried PROTEIN program package for film evaluation was adapted to the PDP 11/45 to circumvent the problems arising from the slow turn-round time on the DESY IBM. Further, various improvements were made to the existing set of programs for the IBM including the possibility of scaling Bijvoet reflexions independently. A full description and users' manual for the film evaluation programs is available (Internal Report - EMBL-HH 81002/01).

Film data were evaluated at the Outstation for lysozyme B (collaborative project with the University of Paris), catalase (collaborative project with the Academy of Sciences, Moscow), crystallin II and avian pancreatic polypeptide (in collaboration with Birkbeck College, London).

Selected research projects

The complete list of projects is given in Table 2 and a full account of the research projects is to be found in the references.

EXAFS

Studies on the metal environment in zinc proteins and their model compounds

H. Grewe, B. Krebs (Münster); J. Randall (Edinburgh); G. Dodson (York); J. Bordas, M.H.J. Koch

The x-ray spectroscopy project on the structural characterization of zinc sites in proteins, initiated some time ago, came to fruition this year.

The results of this very comprehensive investigation of the structure of the environment of zinc, an atom to which other spectroscopic techniques are "blind", have now been fully analysed and the manuscripts are either in press or in the final stage of preparation.

It is gratifying to realize that it is possible to interpret very complex local structures with a high degree of accuracy using the first principle calculations approach chosen, which is based on the theory described in the now classical paper of Lee & Pendry (1975).

An optimized set of data reduction procedures has been implemented and the techniques for correctly evaluating the several functions needed to obtain reliable results from the theory have been mastered.

The EXAFS equipment, which shares a beamline with the ultra-small-angle scattering camera X12, was fully used during every hour of available beam time, resulting in the accumulation of a large amount of data which are now being interpreted at the Outstation. In this respect the temporary closure of DORIS came as a not totally unwelcome break.

Selected examples of the spectroscopic results on model compounds are shown in Plate 67 a-c. The full lines correspond to the EXAFS oscillations extracted from the new data whereas the theoretical fit is indicated by the broken lines. The structures of the model compounds are also depicted.

The insulin data were also fitted in order to compare the relative performances of EXAFS and x-ray diffraction.

Clearly EXAFS is a very favourable technique for the solution of biochemical problems which require knowledge of the structure around a metal site for their solution.

A new biochemical result has been the elucidation of the structure around the Zn sites in sheep liver metallothionein (in collaboration with D. Garner et al., Manchester).

Besides Zn centres other metal environments have been studied. Among the results for the metal site of copper proteins those for Cu-thionein have already been interpreted and are illustrated in Plate 67d (in collaboration with H.J. Hartmann and U. Wesor, Tübingen). They provide information about the mechanism by which this protein binds copper. A very large number of high quality data sets was also obtained for the blue copper proteins laccase and stellacyanin. Lack of time has, however, prevented their interpretation.

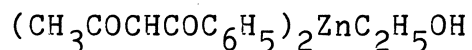
Protein crystallography

Low-temperature crystallographic study of trypsinogen

J. Walter and W. Steigemann (MPI of Biochemistry, Martinsried); T.P. Singh (Dept. of Physics, University of Indore, India); H.D. Bartunik; W. Bode and R. Huber (MPI of Biochemistry, Martinsried).

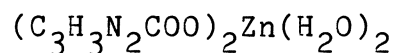
Intramolecular dynamics in trypsinogen, in particular flexibility of the activation domain, were investigated on the basis of crystallographic data extending to 1.7 Å resolution collected at 170 K and 100 K, using a cooling device developed at the Outstation.

PLATE 67a

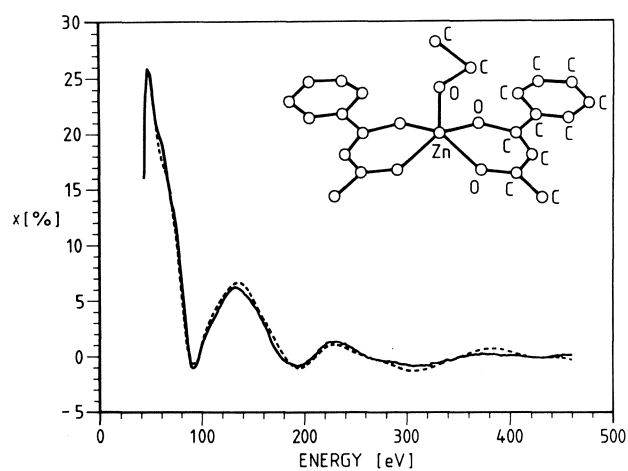


In this and the following diagrams the experimental EXAFS spectrum (full line) and the result of the theoretical fits using first-principle calculations (dotted line) are compared. The table on the right gives a comparison of the results obtained by x-ray diffraction and by EXAFS. Note the sensitivity of the method to changes in the coordination of the metal atom.

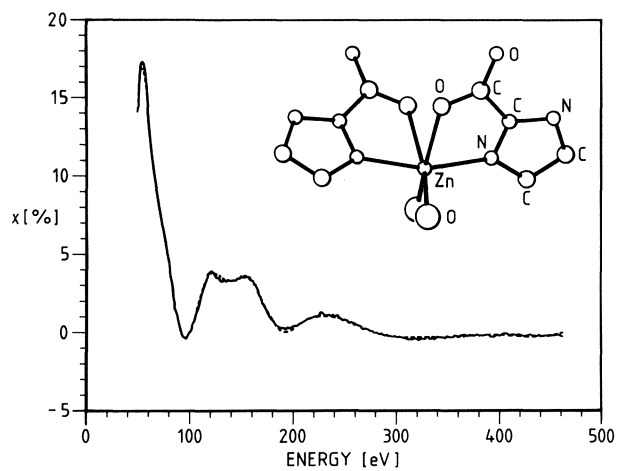
PLATE 67b



The EXAFS spectrum of this model compound, in which Zn^{2+} is bound to two imidazoles, shows the typical "camel back" around 130 eV characteristic of imidazole ligands. This feature is also present in the spectrum of $[\text{Zn}(\text{imidazole})_6]^{2+}$ shown below.

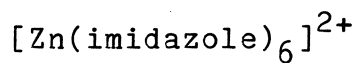


Shell	atom	coordination number	D (Å) x-ray	D (Å) EXAFS
1	O	4	1.987	2.02
2	O	1	2.061	2.09
3	C	4	2.946	2.88
4	C	3	3.255	3.08
5	C	3	3.739	3.78



Shell	atom	coordination number	D (Å) x-ray	D (Å) EXAFS
1	N	2	2.027	2.00
2	O	2	2.078	2.06
3	O	2	2.327	2.22
4	C	2	2.857	2.88
5	C	2	3.018	3.03
6	C	2	3.178	3.21

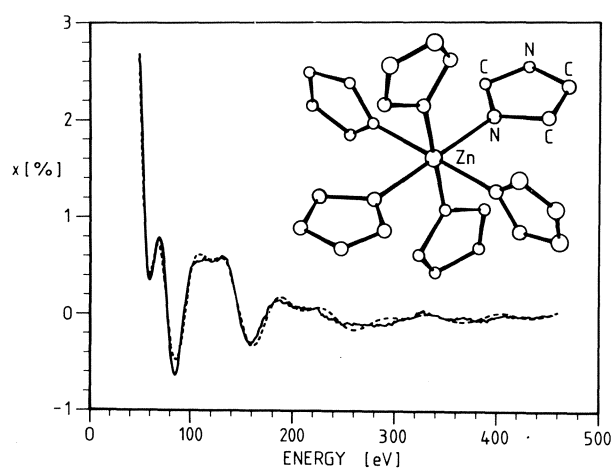
PLATE 67c



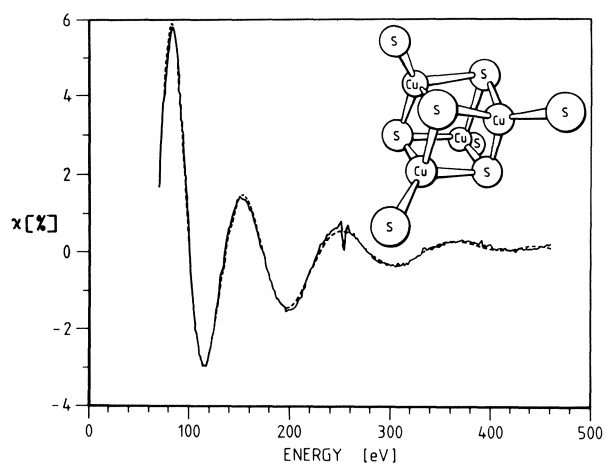
The Zn-complex with imidazole ligands alone has three main shells.

PLATE 67d

Cu site of yeast Cu-thionein showing the cubane-type arrangement of copper and sulphur atoms in this protein inferred from chemical information and EXAFS results.



Shell	atom	coordination number	D (Å) x-ray	D (Å) EXAFS
1	N	6	2.204	2.20
2	C	6	3.224	3.15
3	C	6		3.35
4	C	6	4.1	4.15
	N	6		



Shell	atom	coordination number	D (Å) EXAFS
1	S	2	2.22
2	S	2	2.36

The low-temperature structures were refined to R -factors of 18.7% (170 K) and 20.9% (100 K). The overall temperature factor decreased from 16.1 \AA^2 at room temperature to 11.6 \AA^2 at 170 K; cooling to 100 K did not cause a further change in the overall temperature factor (11.5 \AA^2). Analysis of the main-chain temperature factors (Plate 68) and of Fourier maps (Plate 69) indicates that the flexible segments (N-terminus to Gly 19, Gly 142-Pro 152, Gly 184-Gly 193, Gly 216-Asn 223) in the trypsinogen structure remain disordered even at 100 K except for the N-terminal region. At room temperature, no electron density is observed in the Fourier map between the N-terminus and Gly 19. At 170 K there is density for Gly 18, at 100 K for Gly 18 and Val 17. This demonstrates for the first time that collective internal motions occur in a crystalline protein even at very low temperatures. (A detailed description of the experiments and results is in press.)

Time-resolved crystallographic study of ligand-rebinding for CO-myoglobin following photolysis

H.D. Bartunik and E. Jerzembek (EMBL, Hamburg); D. Pruss and G. Huber (Inst. Appl. Physics, University of Hamburg).

The 3-dimensional structure of haem proteins, in particular in the vicinity of the haem, depends on the ligation state. The project aims to determine structural changes in MbCO which occur during ligand rebinding following pulse photolysis, by means of time-resolved crystallography (at low temperatures) on a $\mu\text{s/ms}$ time scale. The feasibility of such studies has been demonstrated by measuring the time course of approximately 30 Bragg reflexions from a small MbCO crystal (size $200 \times 200 \times 20 \mu\text{m}^3$) before and after photolysis of the ligand by a 10 ns laser pulse with a time resolution of 500 μs using a linear detector (A. Gabriel) and a modified data acquisition system for time-resolved measurements (B. Robrahn). Plate 70 shows the experimental set-up together with the time course (insert B) observed for three simultaneously recorded reflexions. Several reflexion intensities increased or decreased immediately after the flash. At room temperature these intensities displayed exponential relaxation with a lifetime of 3 ms, which is in good agreement with the results from optical transmission studies of ligand rebinding in MbCO in solution. The time-resolved x-ray results can be interpreted as indicative of the production of a transient deoxy-Mb state immediately after the flash followed by statistical rebinding of the ligand. This view is supported by the results of time-resolved optical transmission studies of ligand rebinding in single crystals of MbCO.

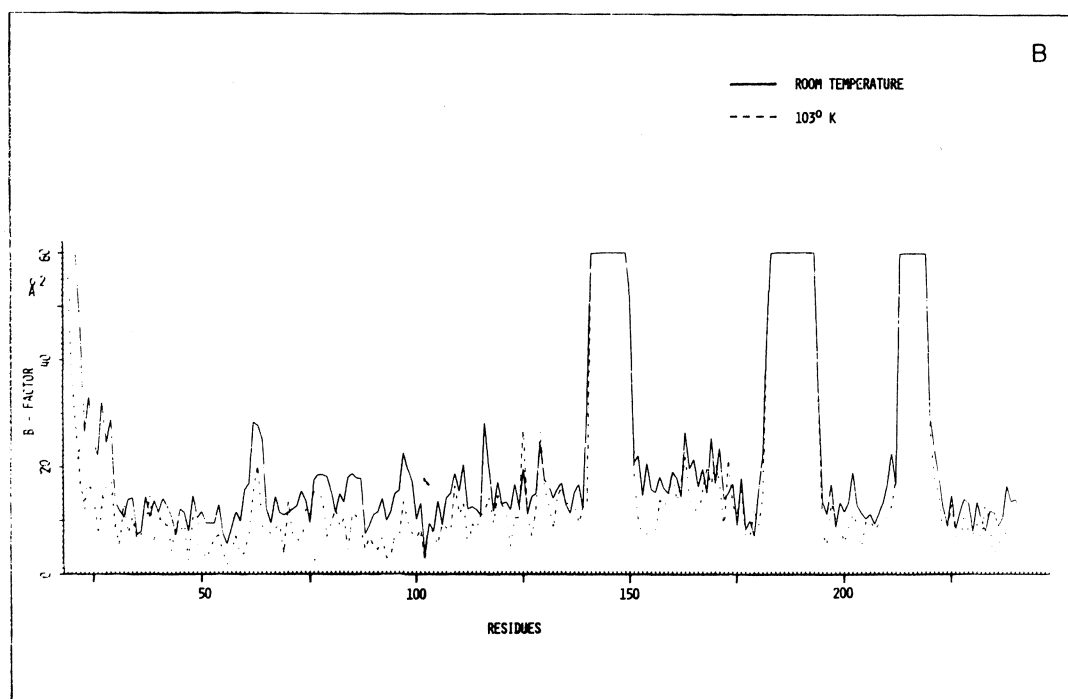
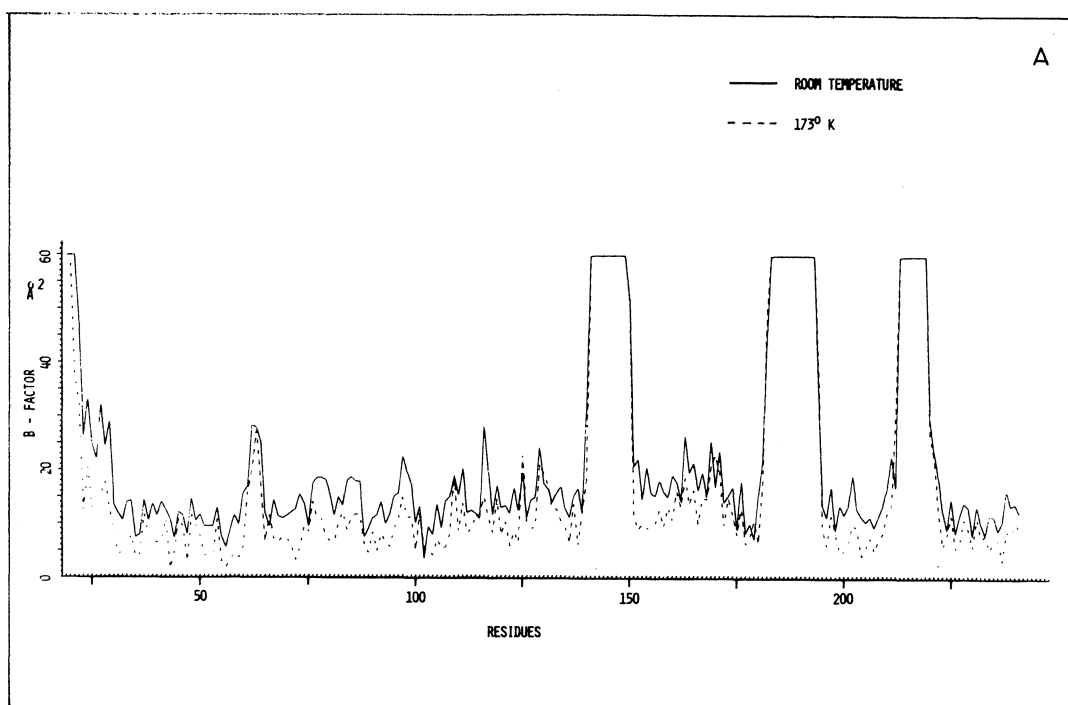


PLATE 68

Temperature behaviour of the crystallographic B-factors of the main chain atoms (including C β) of trypsinogen at room temperature, 173 K (A) and 103 K (B). Residues 10-19, 142-152, 184-193 and 216-223 correspond to "flexible" segments of the structure which are not visible in the Fourier map obtained from data collected at room temperature. Besides a decrease in the overall B-factor, cooling particularly affects the degree of ordering of residues 17 and 18 near the N-terminus (see Plate 69).

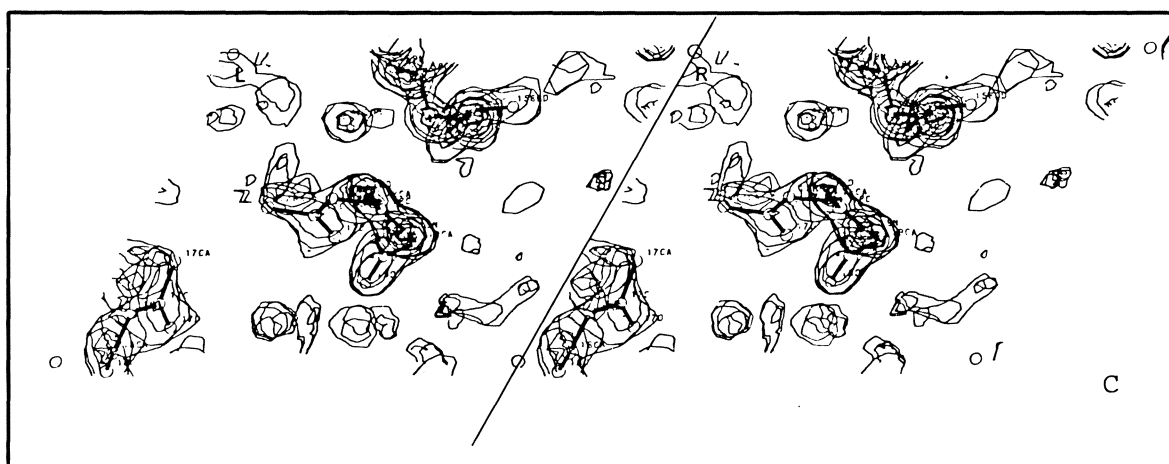
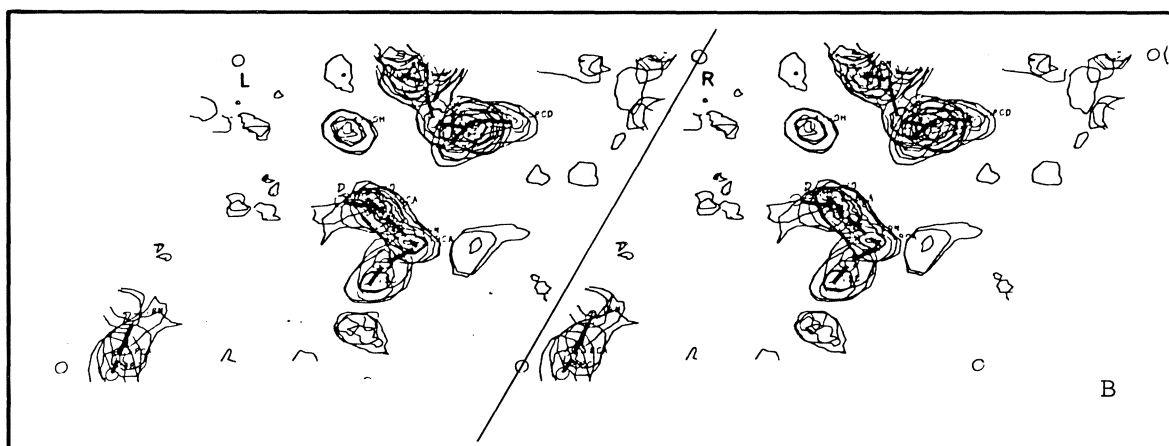
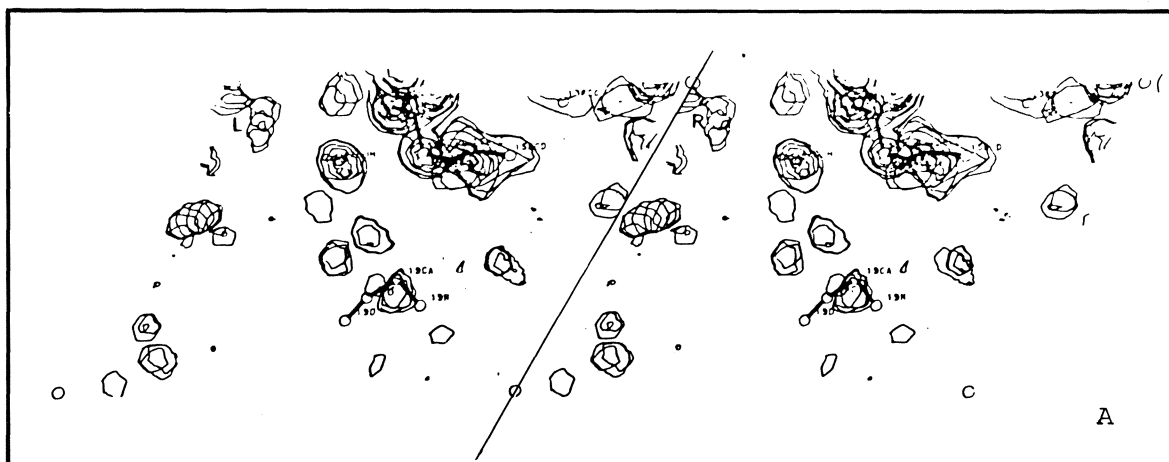
PLATE 69

Stereo-pairs of a section of the Fourier map and the refined model of trypsinogen around Gly 19 near the N-terminus at room temperature (A) 173 K (B) and 103 K (C). Contours are drawn starting from σ (standard deviation of the electron density) in steps of σ . Residues 10-19 are not ordered at room temperature. Gly 18 is visible in the Fourier map at 173 K (B), Gly 18 and Val 17 at 103 K (C).

A. A section of the final Fourier map and the refined model of trypsinogen around Gly 19 at room temperature.

B. A section of the final Fourier map and the refined model of trypsinogen around Gly 19 at 173 K.

C. A section of the final Fourier map and the refined model of trypsinogen around Gly 19 at 103 K.



Further work is required, including measurements made at very low temperatures to slow down internal motions in the proteins.

Time-resolved measurements

Time-resolved measurements were carried out to study assembly processes in solution on a variety of systems (tubulin, actin, tobacco mosaic virus coat protein, haemoglobin) in the time range from a few 100 ms to a few seconds.

The experimental data for most of these projects are still being analysed.

The studies on muscle contraction were pursued on several systems: arthropod muscle (Y. Maeda et al., MPI für Medizinische Forschung, Heidelberg), insect flight muscle (K.C. Holmes et al., MPI für Medizinische Forschung, Heidelberg) and frog sartorius muscle. A brief account of the latter project is given below.

X-ray diffraction studies of contracting frog muscle

H.E. Huxley, A.R. Faruqi, M. Kress (MRC, Cambridge); R.M. Simmons (University College, London); J. Bordas, M.H.J. Koch.

These studies are directed at finding out what are the structural changes in the cross-bridges between actin and myosin filaments in muscle which bring about contraction. The problem is being approached by applying small but very rapid length changes to an otherwise isometrically contracting muscle, so that a temporary synchronization of cross-bridge movements is produced and can be detected as changes in the low-angle x-ray diffraction diagram, provided these can be recorded quickly enough. As indicated briefly in last year's Report, it was found possible using the high flux from DORIS to record changes in the 143 Å meridional reflexion (which arises from the groups of cross-bridges which occur with this periodicity along the myosin filaments) with a time resolution of 1 millisecond or less. It has now been possible to analyse these changes in some detail.

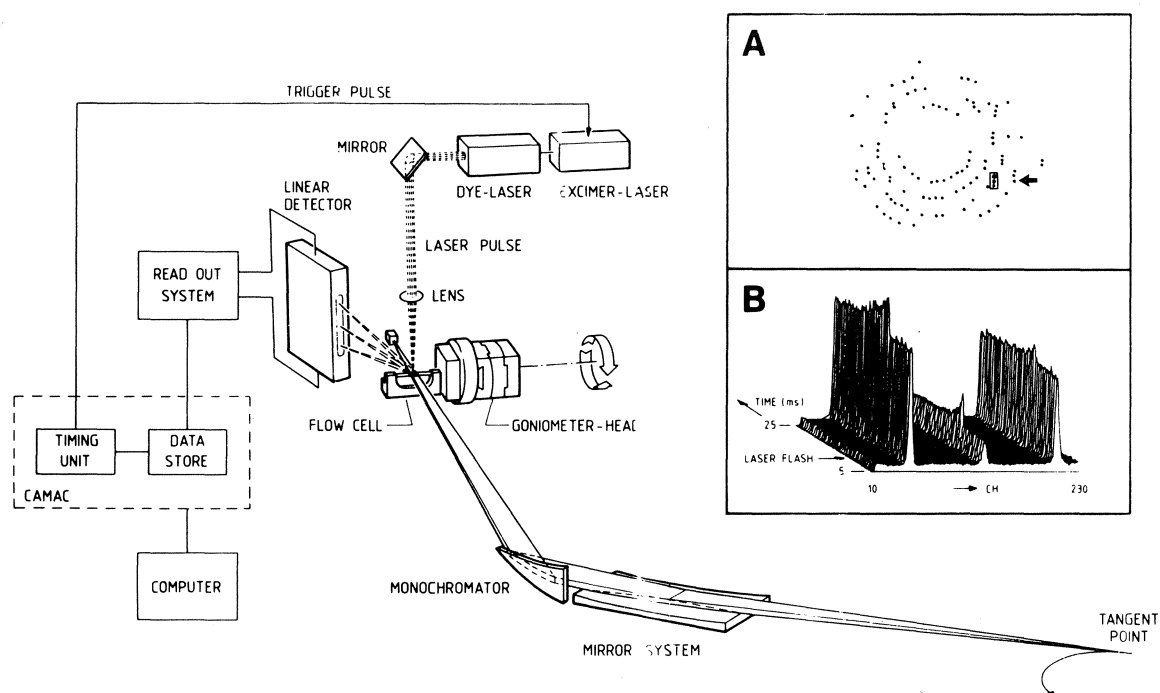


PLATE 70

Time-resolved crystallographic data collection from MbCO before and after laser pulse photolysis of the ligand. The time course of the intensity of the three Bragg reflexions indicated in the box in insert A, recorded with a linear detector, is illustrated in insert B. One time frame corresponds to 500 μ s. The data were accumulated at room temperature over 500 repetitions (flashes).

It was found that changes in muscle length representing a movement of adjacent actin and myosin filaments past each other by 100 Å or less produced a very large drop in intensity (to one quarter or less) of the 143 Å meridional reflexion without any change in the width or the spacing of the reflexion. If the length change was a quick release, the intensity decrease was delayed by approximately half a millisecond relative to the tension and length changes (which were essentially synchronous with each other) and was followed by a rapid partial recovery of intensity, lasting about 6 milliseconds, even though there was little tension recovery during this short time. This was followed by a much slower recovery of the rest of the intensity, accompanied by the usual tension recovery. During the time following a quick release when the 143 Å intensity was very low, there was a small increase of intensity in the 214 Å 'forbidden' meridional reflexion. If the length change was a quick stretch, the drop in intensity was more nearly synchronous with the tension and length change, and no rapid recovery of intensity took place, only a slow one having a similar course to the progressive return of tension to its steady value. If the length changes were reversed within a millisecond or so of their initial application, the intensity immediately returned to near its original value. However, if 5 or 6 milliseconds of delay were interposed between a release and a re-stretch, during which time the rapid phase of intensity recovery occurred, then the restretch was accompanied by a further large decrease in intensity. These observations are not readily explained by some non-specific disordering of the cross-bridges by the sudden length change. They do, however, give an indication of a specific structural change, reversible immediately after it has happened. This change in bridge configuration then leads, in the case of quick release, to some further step in the cross-bridge cycle - possibly detachment followed by reattachment to a different point on the actin filament, with tension development happening later - which partially restores the intensity.

It was very gratifying to find that such large and reproducible changes in x-ray pattern did indeed take place on this time scale and could be studied using a storage ring as an intense x-ray source. The changes show that very drastic alterations in the organization or structure of the cross-bridges occur when actin and myosin filaments move rapidly past each other by about 100 Å during contraction, i.e. by the amount that might be associated with one cross-bridge 'throw'. This provides direct structural evidence, hitherto unavailable, of a direct physical link between an axial change in the structure or positioning of cross-

bridges and the axial movement of actin filaments past myosin filaments. However, the position has not yet been reached where these large changes in pattern can be fully understood in terms of a detailed model of cross-bridge behaviour. Nevertheless, the approach is revealing new and well-defined structural phenomena during the cross-bridge cycle which it is planned to explore further in the future and which, combined with other types of information about muscle structure and chemistry, should provide direct information about the energy-transducing events. Details are described in several recent publications.

Anomalous small-angle scattering

Resonant scattering

H.B. Stuhrmann.

A systematic exploration of the potential offered by this new technique (see 1980 Report) has been started. Measurements have been carried out on a variety of systems including metalloenzymes, synthetic polyelectrolytes, ribosomes and membrane model systems. Procedures for data reduction and analysis, including corrections for fluorescence and absorption, are being developed.

Anomalous dispersion of barium and europium ions absorbed to the surface of lipoproteins and phospholipid vesicles

P. Laggner, H.B. Stuhrmann.

Small-angle scattering measurements were carried out on the X15 camera at the wavelengths of the L_{III} absorption edges of Ba^{2+} and Eu^{3+} ions, which had been added to solutions of lipoproteins (HDL and LDL) and to phosphatidylcholine (DPPC) vesicles. These experiments aimed at obtaining otherwise inaccessible information on the structure and ionic shell of these lipid-water interfaces. In the case of the DPPC vesicles, measurements were taken at different temperatures to study the effects of the chain-melting transition on the ionic surface layer. In both systems the anomalous dispersion approach is facilitated by the relatively high contribution of the anomalous scatterers resulting from the intrinsically low scattering contrast of the particles. Furthermore, the symmetry properties of the particles facilitate the isolation of the anomalous scattering term.

Ultra small-angle scattering (USAX)

Although other cameras to perform scattering work at small angles exist at the Outstation, none of them are suitable for the study of structures much larger than about 1000 Å in their largest dimension.

It has been recognized for some time that the characteristics of synchrotron radiation combined with suitable x-ray optics can lead to resolutions in angle such that the measured scattering patterns can complement and in some cases improve the results obtained with optical microscopy, electron microscopy and light scattering methods. Plate 63D shows the meridional diffraction pattern obtained with the new camera X12 from a specimen of frog sartorius muscle. The reflexions are characteristic of the distribution of mass within a sarcomere. The first Bragg peak corresponds to the second order of the sarcomere repeat of 2500 Å. The investigation of this superstructure of muscle is still in progress.

To give an indication of the resolving power of the instrument, Plate 63A shows a muscle diffraction pattern obtained with the new time-resolved small-angle diffraction instrument in HASYLAB (X33). The diffraction pattern measured on the USAX camera is contained within the box shown in the inset, i.e. well within the beam stop. One can notice the wealth of structural detail which is hidden in this region of the scattering pattern which so far could not be recorded by x-ray diffraction methods.

Other systems than muscle have also been investigated using this new device. This includes study of the variation of the interfibrillar spacing in cornea as a function of hydration as well as a variety of experiments on protein solutions. It is hoped to use the device for the study of slow assembly process after the DORIS shutdown.

Publications during the year

Bartunik, H. D., Clout, P. N. & Robrahn, B. (1981). Rotation data collection for protein crystallography with time-variable intensity from synchrotron radiation sources. J. Appl. Cryst., 14, 134-136.

Bartunik, H.-D. & Schubert, P. (1982). Crystal cooling for protein crystallography with synchrotron radiation. J. Appl. Cryst. 15, (in press).

Bordas J., (1982). Applications of x-ray spectroscopy to biochemical problems. In Uses of Synchrotron Radiation in Biology: ed. Stuhmann, H. B.; Academic Press, London (in press).

Bordas, J. & Mandelkow, E. (1982). Time resolved X-ray scattering from solutions using synchrotron Radiation. In Fast methods in Physical Biochemistry and Cell Biology: ed. Shaafi, R. I. & Fernandez, S. M.; Elsevier/North Holland Biomedical Press, Amsterdam, (in press).

Garner, C.D., Hasnain, S.S., Bremner, I. & Bordas, J. (1982). An EXAFS study of the zinc sites in sheep liver metallothionein. J. Inorg. Biochem., (in press).

Golding, F., Bendall, P.J. & Dainton, D.M. (1981). The addition of auxillary processors to a CAMAC data collection system without changes to the user software. Proc. of the Digital Equipment Computer Users Society, 8, 261-264.

Hendrix, J. & Weber, W. (1982). A 10 MHz conversion rate time digitizer for delay-line read-out systems. IEEE Trans. on Nucl. Sci. (in press).

Huxley, H. E., Simmons, R. M., Faruqi, A. R., Kress, M., Bordas, J. & Koch, M. J. H. (1980). Millisecond time-resolved changes in x-ray reflections from contracting muscle during rapid mechanical transients, recorded using synchrotron radiation. Proc. Nat. Acad. Sci., USA., 78, 2297-2300.

Huxley, H.E., Faruqi, A.R., Kress, M., Bordas, J. & Koch, M.H.J. (1982). Time resolved x-ray diffraction studies of the myosin layer-line reflections during muscle contraction. J. Mol. Biol., (in press).

Jürgens, G., Knipping, G. M. J., Zipper, P., Kayushina, R., Degovies, C. & Laggner, P. (1981). Structure of two subfractions of normal porcine (sus domesticus) serum low-density lipoproteins. X-ray small-angle scattering studies. Biochemistry, 20, 3231-3237.

Kam, Z., Koch, M. H. J. & Bordas, J. (1981). Fluctuation x-ray scattering from particles in frozen solution using synchrotron radiation. Proc. Nat. Acad. Sci., USA, 78, 3559-3562.

Knoll, W., Haas, J., Stuhmann, H.B., Földner, H.-H., Vogel, H. & Sackmann, E. (1981). Small-angle neutron scattering of aqueous dispersions of lipids and lipid mixtures. A contrast variation study. J. Appl. Cryst., **14**, 191-202.

Koch, M. H. J. & Bendall, P. J. (1981). INSCOM: an interactive data evaluation program for multichannel analyses-type date. In DECUS UK Conference proceedings 1981, p.13-16.

Koch, M.H.J. & Tardieu, A. (1981). Quand les rayons x voient les mouvements moléculaires. La Recherche, **128**, 1438-1440.

Laggner, P. (1981). Lateral diffusion of lipids in sarcoplasmic reticulum membranes is area-limited. Nature (London), **294**, 373-374.

Laggner, P. (1981). Lipids, lipoproteins and membranes. In X-ray Small Angle Scattering: ed. Kratky, O. & Glatter, O.; Academic Press, New York (in press).

Laggner, P. (1981). X-ray and neutron small-angle scattering on plasma lipoproteins. In Supramolecular Structure and Function: ed. Pifat, G.; Plenum Press, London (in press).

Laggner, P. (1981). Physicochemical characterization of high density lipoproteins. In High Density Lipoproteins, ed. Day, C. E.; Marcel Dekker, New York, p.43-72.

Laggner, P., Kostner, G., Rakusch, U. & Worcester D. (1981). Neutron small-angle scattering on selectively deuterated human plasma low-density lipoproteins: the location of polar phospholipid head-groups. J. Biol. Chem., **256**, 11832-11839.

Laggner, P., Suko, J., Punzengruber, C. & Prager, R. (1981). Electron spin resonance studies on conformational changes of the sarcoplasmic reticulum Ca^{++} ATPase induced by synergistic action of Ca and ATP. Z. Naturforsch., **36b**, 1136-1143.

Mandelkow, E., Mandelkow, E.M. & Bordas, J. (1981). Stages of tubulin assembly studied by time resolved x-ray scattering. Europ. J. Cell Biol. **24**, 336.

Mazid, M. A., Razi, T., Sadler, J., Greaves, G. N., Gurman, S. J., Koch, M. H. J. & Phillips, J. C. (1981). An EXAFS study of gold co-ordination in the anti-arthritis drugs "myocrisin" and "solganol". J. Chem. Soc. Chem. Commun., (1980), 1261-1263.

Meek, K. M., Elliot, G. F., Sayers, Z., Whitburn, S. B. & Koch, M. H. J. (1981). Interpretation of the meridional x-ray diffraction pattern from collagen fibrils in corneal stroma. J. Mol. Biol., 149, 477-488.

Phillips, J. C. (1981). Fluorescence EXAFS detection at the EMBL synchrotron radiation outstation, Hamburg: hardware, software and operational experience. J. Phys. E: Sci. Instrum., 14, 1425-1428.

Phillips, J.C., Bordas, J., Foote, A.M., Koch, M.H.J. & Moody, M.F. (1982). The zinc-sulphur bonds of aspartate transcarbamylase studied by x-ray absorption spectroscopy. Biochemistry, (in press).

Sayers, Z., Whitburn, S.B., Koch, M.H.J., Meek, K.M., Elliott, G. & Harmsen, A. (1982). A synchrotron x-ray diffraction study of corneal stroma. J. Mol. Biol., (in press).

Stuhrmann, H.B. (1982). Anomale Röntgenstreuung zur Erforschung makromolekularer Strukturen. Die Makromolekulare Chemie, (in press).

Stuhrmann, H. B. (1981). Anomalous small-angle scattering. Quart. Rev. Biophys., 14, 433-462.

Stuhrmann, H.B. (1982). Anomalous x-ray scattering from macromolecular structures using synchrotron radiation. (in russian) Kristallografiya (in press).

Stuhrmann, H.B. (1982). Contrast variation. In Small-angle x-ray scattering: ed. Kratky, O. & Glatter, O.; Academic Press, London, (in press).

Stuhrmann, H. B. & Notbohm, H. (1981). Configuration of the four iron atoms in dissolved human hemoglobin as studied by anomalous dispersion. Proc. Nat. Acad. Sci., USA, 78, 6216-6220.

Torensma, R. & Phillips, J. C. (1981). A comparison of the copper sites in arthropod and mollusc oxyhemocyanins. FEBS Letters, 130, 314-316.

Walter, J., Steigemann, W., Singh, T.P., Bartunik, H.D., Bode, W. & Huber, R. (1982). On the disordered activation domain in trypsinogen: Chemical labelling and low temperature crystallography. Acta Cryst., (in press).

Reference

Lee, P.A. & Pendry, J.E. (1975). Phys. Rev., B11, 2795.

Table 2

List of projects

Projects on X11

a) Protein crystallography ⁺

Low temperature study of trypsinogen at 100 K	W. Bode, R. Huber, J. Walter (MPI für Biochemie, Martinsried)
Time-resolved study of ligand rebinding in MbCO following laser pulse photolysis	H.D. Bartunik, E. Jerzempek (EMBL, Hamburg), D. Pruss, G. Huber (University Hamburg)
Crystallographic structure of porin, an integral membrane protein from <u>E.coli</u>	R.M. Garavito, J.A. Jenkins, J.N. Jansonius, R. Karlsson, J.P. Rosenbusch (Biozentrum Basel)
Structure determination of ascorbate oxidase including anomalous techniques	R. Huber, R. Ladenstein (MPI für Biochemie, Martinsried)
High-resolution study of haemocyanin near the Cu K-edge	J. Drenth, W. Haygema, W. Hol, C. Kalk (Univ. Groningen)
High-resolution study of actin-DNAase	W. Kabsch (MPI für Med. Forschung, Heidelberg), D. Suck (EMBL, Heidelberg)
Structure determination of kallikrein	W. Bode, Z. Chen, R. Huber (MPI für Biochemie, Martinsried)
Crystallographic structure of phosphorylase B	L.N. Johnson, K.S. Wilson (Univ. Oxford)
Structure determination of insecticynanin (biliverdin carrier protein)	K. Petratos, D. Tsernoglou (Wayne State University)
Very high resolution study of ribonuclease A at -30 °C	K. Petratos, D. Tsernoglou (Wayne State University)

Very high resolution study of plas-
tocyanin

M. Guss, H.C. Freeman
(University of Sydney)

Structure determination of aspartate
transcarbamylase catalytic subunit

M. Moody, F. Winkler
(EMBL, Heidelberg)

⁺ in collaboration with K.S. Bartels and H.D. Bartunik

b) Time-resolved muscle diffraction ⁺

Time-resolved study of contracting
live crab leg muscle

Y. Maeda, K.C. Holmes
(MPI für Med. Forschung,
Heidelberg)

Time-resolved study of contracting
live lobster muscle

Y. Maeda, K.C. Holmes
(MPI für Med. Forschung,
Heidelberg)

Time-resolved study of stretch-
activated glycerinated insect
flight muscle

R.S. Goody, K.C. Holmes
(MPI für Med. Forschung,
Heidelberg) K. Güth, M. Just
(Universität Heidelberg)

⁺ in collaboration with H.D. Bartunik

Projects on X13 ⁺

a) Small-angle diffraction

X-ray diffraction from corneal
collagen

G. Elliott, Z. Sayers,
S. Whitburn, K. Meek
(Oxford)

Intermolecular crosslinking of
bovine collagen

K. Hornbech-Svendson
(Copenhagen)

b) Time-resolved measurements

Muscle

Time-resolved studies on contrac-
ting frog muscle

H.E. Huxley, A.R. Faruqi,
M. Kress (Cambridge),
R.M. Simmons (London)

Time-resolved x-ray diffraction
from thin filaments in contrac-
ting frog muscle

M. Kress (Cambridge)

Collagen

Small-angle scattering from native
and stained collagen fibres

T. Nemetschek, H. Riedl
(Heidelberg)

Solutions

Polymerization of actin

J. Bordas, M. Koch
(EMBL, Hamburg)

Structural transitions in microtubule
assembly

E. Mandelkow, E.M. Mandelkow
(MPI, Heidelberg)

Time-resolved solution scattering
studies of TMV coat protein assembly

T.M. Schuster (Connecticut)

Stopped flow studies on the recons-
titution of carboxyhaemoglobin from
isolated subunits

Y. Inoko (Osaka)

⁺ in collaboration with J. Bordas and M. Koch

EXAFS projects on S11⁺

X-ray absorption experiments on
2 Zn and 4 Zn insulin, carboxy-
peptidase A and model compounds

J. Randall (Edinburgh),
G. Dodson (York)

X-ray absorption spectroscopy
of copper proteins

T. Vanngard, K.E. Falk,
B. Reinhammar (Göteborg)

EXAFS investigation of the iron
centres of soy bean lipxygenase

M. Feiters (Utrecht)

EXAFS study on Cu-thionein from
yeast

U. Weser, H.-J. Hartmann
(Tübingen)

EXAFS study of the stereochemistry
of model complexes for Zn enzymes

B. Krebs, H. Grewe
(Münster)

⁺ in collaboration with J. Bordas and M. Koch

Projects on X15 ⁺

Counter-ion distribution in the 50S subunit of E.coli ribosomes

K. Nierhaus (MPI für Molekulare Genetik, Berlin)

Phase determination of Bragg reflexions of DPPC membranes by anomalous scattering of erbium

G. Büldt (Biozentrum, Basel)

The location of iron atoms in human oxyhaemoglobin as seen by anomalous scattering of iron at the K-absorption edge

H. Notbohm (Med. Hochschule, Lübeck)

Iron-iron distances in catalase as seen by resonant scattering of iron at the K-absorption edge

F. Parak (TU München)

Anomalous scattering of zinc and mercury in aspartate transcarbamylase

M. Moody (EMBL, Heidelberg),
P. Vachette (CNRS Gif-sur-Yvette)

Distance between mercury atoms in the α -chains of haemoglobin as seen by anomalous scattering of mercury at the L_{III} -absorption edge

Y. Inoko (Osaka)

Binding sites of terbium ions in t-RNA from anomalous scattering of terbium at the L_{III} -absorption edge

R. Rigler (Stockholm)

Binding of barium ions to low density and high density lipoprotein at various temperatures

P. Laggner (EMBL, Hamburg)

Decoration of DPPC-vesicle suspension with europium ions studied by anomalous scattering of europium at its L_{III} -absorption edge

P. Laggner (EMBL, Hamburg)

⁺ in collaboration with H.B. Stuhmann

The Outstation at the ILL, Grenoble

Head: B. Jacrot

Members: C. Berthet, F. Borrás-Cuesta, S. Cusack, A. Gabriel*, J.-C. J  sior, R. Leberman, B. Schoot, K. Simpson, C. Wolff (part-time), M. Zulauf

Fellows: J.* Chroboczek*, M. Cuillel, M. Katouzian-Safadi*, S. Perkins

Students: A. Foote, J.-Y. Sgro*

Visiting workers: J.* Baldwin*, W. Baranow*, C. Blake*, A. Briss  n, S. Burley, D.L.D. Caspar*, A.F.M. Cremers*, C. Crifo, S. Coniglio, M.* Corti, V. Degiorgio*, H. Eisenberg*, H. Frauenfelder, R.* Giege, D.* Herbage, P. Krijgsman*, C. Kroon, J.* Kruse, D. Maras, J. Mellema, A. Miller*, K. Nierhaus, J.A. Odell*, R.E. Offord, C. Oostergetel*, F. Podo*, M.C. Ronziera*, J. Rosenbusch, D.M. S  dler, I. Serdyuk, J.J. Skehel*, H. Soderlund, A. Spirin, R. Strom, D. Wade, J. Witz

Technical assistants: J.-M. Bois, H. Bono*, B. Dal'Zotto*, F. Dauvergne, M.-T. Dauvergne, J. Sedita, E. Truche

The deuteration laboratory (R. Leberman, technical assistants: M.-T. Dauvergne, A. Foote)

1981 has been a year of major change for the laboratory with the installation of new staff and the introduction of a defined programme for the deuteration of a simple eukaryote.

Bacterial systems (M-Th. Dauvergne, R. Leberman)

During the year systematic basic studies on the growth of bacteria during adaptation to high concentrations of D₂O and variations in growth media have been carried out. Since the deuteration of bacteria requires the use of artificial media for culture, this information is required for various reasons; to increase yields of bacteria in the minimal media used for the D₂O cultures, to define conditions for the continuous culture production of large quantities of deuterated bacteria, to study the effect under deuteration conditions of different carbon sources on the incorporation of deuterium into bacterial proteins and nucleic acids.

The present in-house requirements for deuterated bacteria are all involved with neutron and NMR studies on components of the bacterial protein biosynthetic pathway. As the fractionation of the bacterial extracts will be carried out exclusively in this laboratory other deuterated bacterial products can be made available to other laboratories on demand.

An example of the customer-contractor service that the laboratory can offer is the production of E.coli IC 100 grown in 80% D₂O for the group of K. Kirschner (Biozentrum, Basel). This strain of E.coli K12 is an overproducer of tryptophan synthetase, a tetrameric $\alpha_2\beta_2$ enzyme. Preliminary neutron scattering measurements on the enzyme have been made at the ILL by R. May and K. Ibel, but progress in the structure determination requires deuterated enzyme for the production of deuterated-protonated hybrids. The bacteria were progressively adapted to growth in 80% D₂O in a minimal medium supplemented with L-tryptophan (medium 4C) with continual monitoring of dependence on tryptophan and the presence of the enzyme by analytical PAGE. Eventually 3 x 10 litre batches of the bacteria were grown in 80% D₂O yielding 220 g bacteria and 250 mg enzyme with a deuteration level of about 62% (NMR determination by A. Foote).

An internal service is the production of deuterated bacteria to be fed to Physarum polycephalum (see below).

Physarum polycephalum (A. Foote, R. Leberman)

This project is primarily concerned with the production of deuterated histones for neutron scattering studies on higher order chromatin structure and core particles in collaboration with J. Baldwin and B. Carpenter (Portsmouth). However, since the isolation of the histones will be carried out in this laboratory, it is conceivable that the procedures could be adapted for the simultaneous isolation of other deuterated cell components (e.g. actin) for other laboratories. With these aims the slime mould Physarum polycephalum is being grown. This organism has been extensively studied, being of particular interest as a means to investigate changes in cellular biochemistry during the cell cycle since it forms large synchronous multinucleate macroplasmodia.

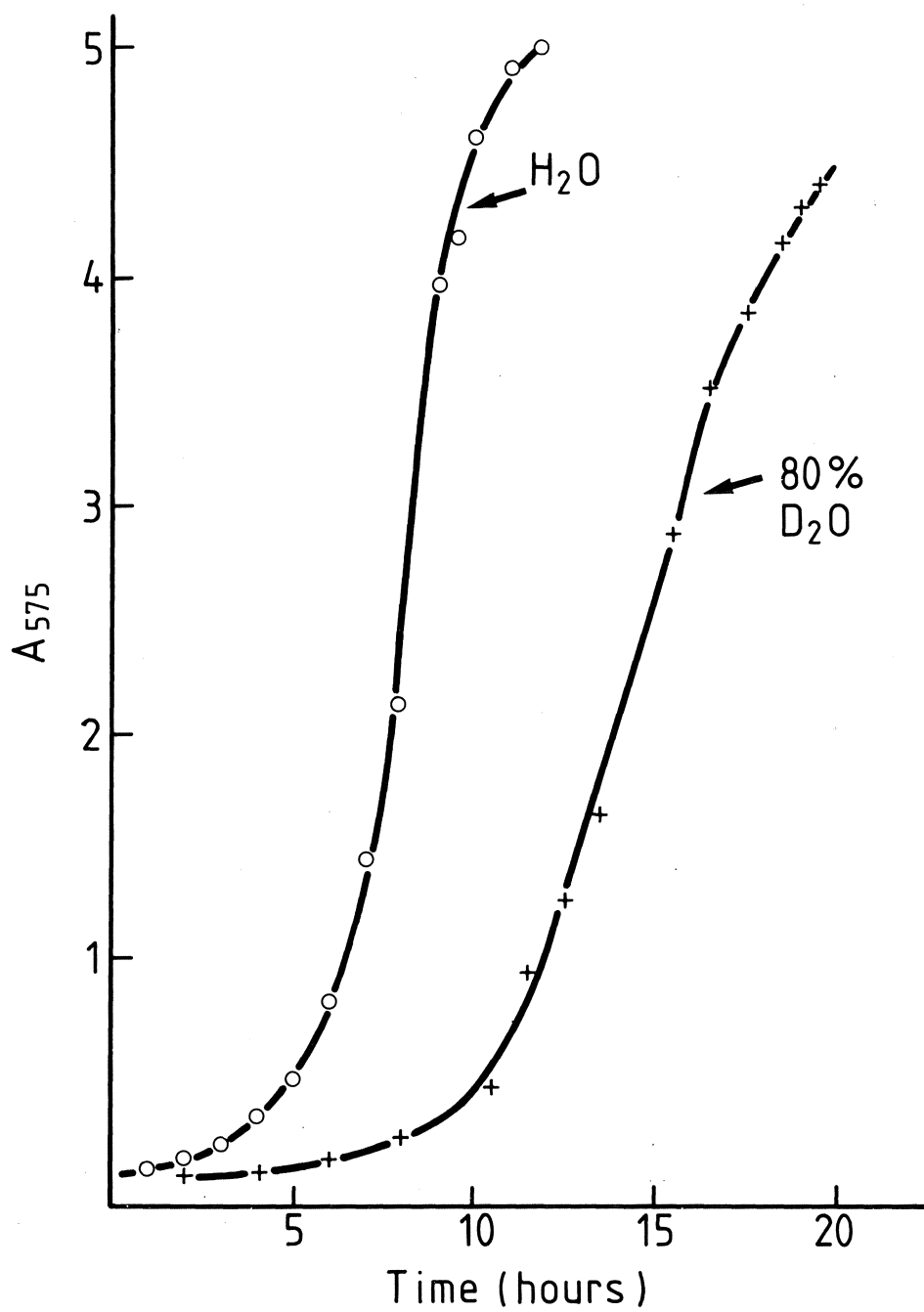


PLATE 71

Growth curves for *E. coli* IC 100 in minimal medium 4C;
 o-----o in H_2O , +-----+ in 80% D_2O .

Unlike bacteria, Physarum polycephalum cannot be grown on a minimum medium nor can it tolerate a D₂O level exceeding 30%. By growing in normal media but replacing the usual peptone by 0.4% (w/v) deuterated amino-acids (from deuterated blue-green algae) cultures with a deuteration level of 25-50% have been obtained (B. Carpenter and F. Sewell, personal communication). At present we are growing the mould in its microplasmodial form in liquid culture. Deuteration is being carried out by supplying only two carbon sources to the culture medium in 25% D₂O; glucose at 50% of the usual concentration and heat-denatured deuterated (70 - 80%) bacteria or bacterial residues.

In conjunction with the production of deuterated histones, NMR methods are being developed for the estimation of the level of deuteration in specific proteins and nucleic acids. By recording spectra of acid-hydrolysed proteins it may also be possible to identify the level of deuteration in specific amino-acid residues.

The collagen of cartilage (C. Berthet in collaboration with D. Herbage, Université de Lyon, and M.C. Ronzières, Université de Saint-Etienne)

We have continued our project on the structure of cartilage. The aim of this work is to understand if the special features of the x-ray diffraction pattern are due to the presence of collagen type II or to a periodic organization of other components.

We have been able to reconstitute collagen type II in the presence of a small amount of proteoglycans (1% by weight). This fact demonstrates the participation of proteoglycans in collagen fibrillogenesis, as has been pointed out by several authors using various techniques. At low resolution the x-ray diffraction pattern from this reconstituted type II collagen is different from that obtained from cartilage but similar to that obtained from collagenous tissues constituted of type I collagen. This indicates that the modification to the diffraction pattern from the nucleus pulposus of the intervertebral disc is not due to a structural change in collagen but to some other molecule related to the 670Å periodicity.

X-ray studies on cartilage from which the proteoglycans have been extracted is another way to understand the behaviour of the collagen in this tissue. The x-ray pattern

changes as a function of the percentage of the proteoglycans extracted, becoming more and more similar to that of type I collagen tissue.

The study of collagen hydration using Brillouin light scattering (S. Cusack, EMBL, and S. Lees, Forsyth Dental Center, Boston)

Brillouin light scattering is a technique which enables the sound velocity of a transparent material in the gigahertz frequency range to be measured. In principle this information can be interpreted in terms of the inter- and intra-molecular forces which govern the elasticity of the material. In the past measurements have been made on collagen fibres demonstrating their anisotropic elastic properties (Cusack & Miller, 1979). More recently we have measured the longitudinal acoustic velocity along the fibre axis of rat-tail tendon as a function of relative humidity (Cusack & Lees, submitted for publication). The velocity increases sharply between 95% and 84% relative humidity and subsequently increases linearly at a more modest rate reaching a maximum value of 3.9 km/sec at 0% r.h. Using the desorption isotherm of collagen (Pineri *et al.*, 1978) these results have been interpreted in terms of the amount and nature of the adsorbed water. Below 84% r.h. most of the variation of the velocity can be accounted for by the additional weighting of the collagen by 'structural' and 'bound' water, the remainder being due to changes in the elastic coupling between molecules. At high humidities the additional adsorbed water has the properties of bulk liquid and the steep decrease in acoustic velocity in this region is ascribed to the diminution of the electrostatic component of the intermolecular elastic coupling due to the high dielectric constant of bulk water. On the assumption that in the native wet state the inter-molecular cross-links dominate the elastic coupling, it has been possible to estimate the relative contributions of cross-links and non-bonded interactions to the elasticity at lower water contents.

References

- Cusack, S. & Miller, A. (1979). J. Mol. Biol., 135, 39-51.
- Pineri, M.H., Escoubes, M. & Roche, G. (1978). Biopolymers, 17, 2799-2815.

Structural studies of influenza virus (S. Cusack, EMBL, J.E. Mellema, P.C.J. Krijgsman & R.W.H. Ruigrok, Leiden, the Netherlands)

We are able to report considerable progress in our investigation of the low resolution structure of influenza virus. Interesting results have been derived from three sets of neutron scattering data obtained at the ILL, Grenoble, complemented by electron microscopy and biochemical work carried out at the University of Leiden, the Netherlands.

The structure of influenza virus strain B/Hong Kong

Last year we presented a contrast variation set of neutron scattering curves measured for influenza virus strain B/Hong Kong/5/72 (Mellema *et al.*, 1981). To aid interpretation of these data we subsequently measured the neutron scattering curves of 'spikeless' influenza virus obtained by proteolytic cleavage of the glycoprotein spikes. In most contrasts the scattering curves of the two particles are very different. However in 41% D₂O (when the protein is matched and the scattering is given only by the lipid) the scattering curves are very similar, indicating that the bilayer is not disrupted by the removal of the spikes (see Plate 72). Use of the two sets of data provides a unique means of deriving certain structural information. For instance, simply from the radius of gyration at infinite contrast (which is 393 Å for the spikeless particle and 447 Å for the intact particle) it is possible to deduce that the mass of the spikes is close to 45% of the total viral mass. This figure is significantly higher than previously thought, but is in agreement with the values of 180×10^6 and 95×10^6 for the molecular weights of the two particles given by STEM measurements.

The fitting of spherical shell models to the scattering curves of both the spikeless and intact particles confirms the large mass of the spikes and leads to the following model of the virus structure. The spikes occupy a shell from radius 450 Å to 590 Å, constituting about 45% of the viral mass (i.e. about 400 spikes). They are embedded in the lipid bilayer which is between 400 Å and 450 Å and represents about 25% of the viral mass. Between 360 Å and 400 Å is a layer with a matchpoint of 39% D₂O, close to that predicted from the composition of the M₂-protein. This layer constitutes about 13% of the total mass of the virus and would correspond to about 1000 molecules of M₂-protein (MW 28,000), substantially less than previously thought.

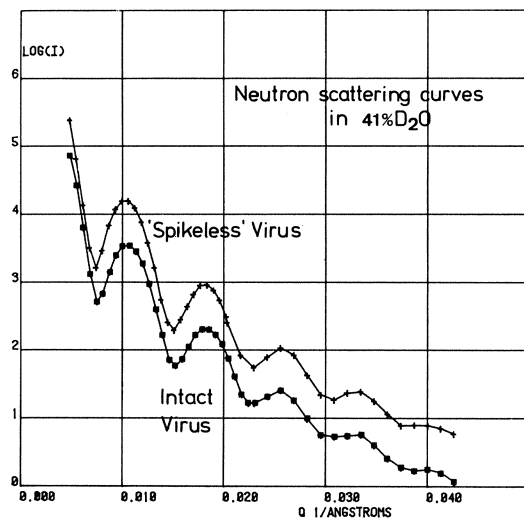
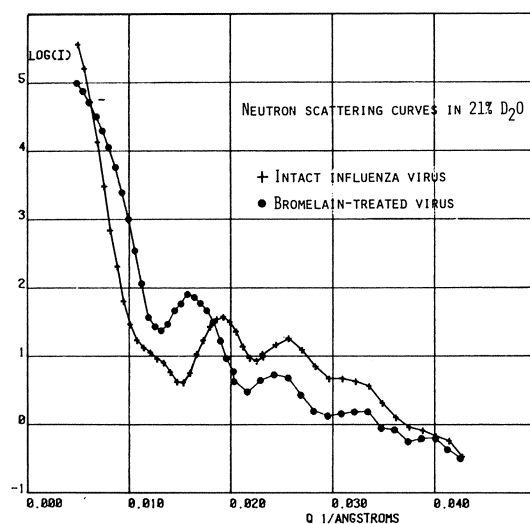


PLATE 72

A comparison of the neutron scattering curves of intact and 'spikeless' influenza virus in 21% (top) and 41% (bottom) D₂O. In 41% D₂O the two curves are very similar. Since the scattering in this case is principally due to the lipid bilayer (the protein being matched) this indicates that the bilayer is not disrupted by the removal of the spikes. In 21% D₂O the curves are very different due to the contribution of the spikes to the scattering in the intact particle.

The core of the virus (0 - 360 Å) has a match point of 47% D₂O which would be given by a complex of 88% protein (presumably principally the ribonucleoprotein) and 12% RNA.

In summary the following composition of the virus is proposed:

Component	% of total mass	Approximate number of protein subunits (total MW 200x10 ⁶)
Glycoprotein spikes	45	410
Lipid	25	
M-protein	13	930
Ribonucleoprotein	15	530
RNA	2	

A final series of experiments is planned on core particles stripped of both spikes and lipid bilayer to provide further elucidation of the structure inside the membrane.

The structure of influenza strain A/Texas

A and B strains of influenza virus are distinguished by their different antigenic determinants but it is not known whether there are any major structural differences. We have therefore measured the neutron scattering curves of the A/Texas strain to compare with those of B/Hong Kong. The preparations of A/Texas appear slightly less homogeneous than those of B/Hong Kong but the scattering curves are otherwise similar. For instance the lipid bilayer is found to be in exactly the same radial position for the two strains and the radii of gyration are very close. STEM measurements of molecular weights however suggest that the mass of A/Texas may be somewhat less than that of B/Hong Kong.

Behaviour of influenza virus at low pH

There has recently been considerable interest in the ability of influenza virus (and other enveloped viruses) to

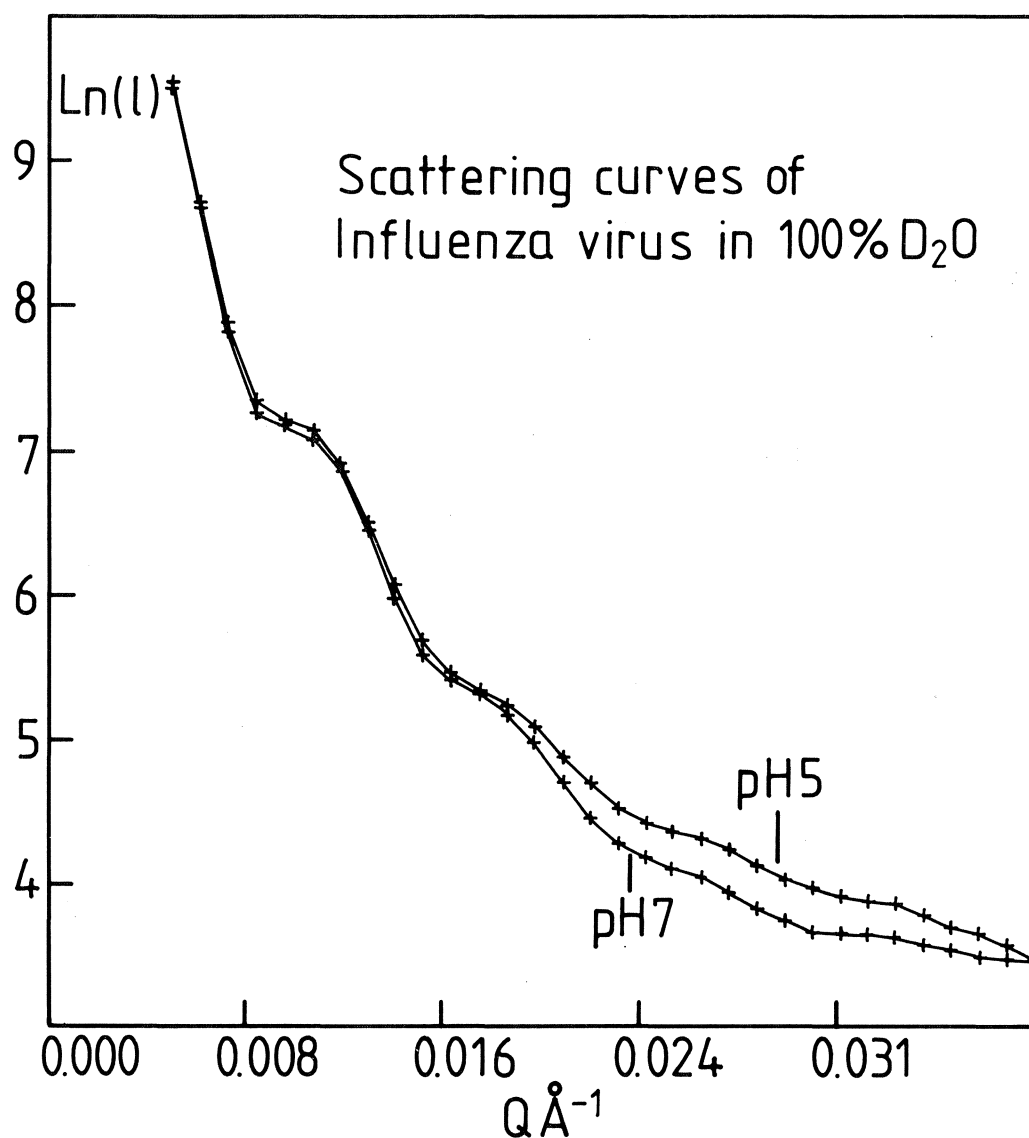


PLATE 73

Scattering curves of influenza virus in 100% D₂O.

bind lipid and induce cell-cell fusion in mildly acidic conditions (e.g. White et al., 1981). This behaviour, which may be important in the process of viral infection, is postulated to result from the loss at low pH of negative charge from the N-terminus of the HA₂ chain of haemagglutinin, thus enabling it to partake in hydrophobic interactions. We have therefore measured neutron scattering curves of both A/Texas and B/Hong Kong strains at various pHs with the aim of elucidating any structural changes that might accompany the fusion behaviour at low pH.

Plate 73 compares the scattering curves in 100% D₂O of A/Texas at pH 7.5 and pH 5.0. The difference in the curves in the vicinity of $q = 0.028 \text{ \AA}^{-1}$ is found for both virus strains below pH 5.5 and is irreversible. At low angles the curves are very similar suggesting that there is no overall change in size of the virus. The observed changes are not easy to interpret but calculations have shown that a possible explanation would be the clustering of the spikes into groups of six at low pH. Clearly further experiments are needed to test this hypothesis.

References

Mellema, J.E., Andree, P.J., Krijgsman, P.C.J., Kroon, C., Ruigrok, R.W.H., Cusack, S., Miller, A. & Zulauf, M. (1981). J. Mol. Biol., 151, 329-336.

White, J., Matlin, K. & Helenius A. (1981). J. Cell. Biol., 89, 674-679.

The structure and molecular weight of Semliki Forest virus
(M. Cuillel & B. Jacrot in collaboration with H. Soderlund, Helsinki)

A structural investigation of Semliki Forest virus has been made with neutron scattering. Both the nucleocapsid (extracted by triton) and the virus have been investigated. The main findings are the following.

- a) The nucleocapsid has a radius of 205 Å. Its molecular weight (9.46×10^6) suggests that, if this nucleocapsid is built following icosahedral symmetry, it should have 180 copies ($T=3$) of the protein subunits. The variation of the radius of gyration with contrast, which is small, indicates that this nucleocapsid is not built like a plant virus, with nucleic acid surrounded by a protein

shell, but that there is much more interpenetration of the two species.

- b) The virus. Surprisingly the molecular weight (42×10^6) found for the virus, and its protein content ($23-24 \times 10^6$), are incompatible with earlier structural analysis, based on electron microscopy, which suggested a virus built on a triangulation number $T=4$ (240 copies of the three capsid proteins). We have confirmed our molecular weight by a combination of sedimentation coefficients and diffusion coefficient D (measured with light inelastic scattering by M. Zulauf). Combining the known composition of the RNA and of the four proteins present in the virus we find the following composition:

Protein core	5.35×10^6
RNA	4.1×10^6
Lipids	12×10^6
Capsid	
Proteins	18.3×10^6
Carbohydrate	2.2×10^6

This composition is, in percentage, in agreement with published values, except for the RNA, for which we find a higher percentage. Also our virus molecular weight agrees with that determined by the STEM at Heidelberg (R. Freeman and colleagues).

The interpretation of the data in structural terms is not yet finished, but several points are suggested at the present stage of analysis. There must be more protein in the lipid bilayer than the two strands which are known to span this membrane. Also the data support the conclusion drawn from the isolated nucleocapsid that the RNA is not confined in a central hole, but interpenetrates the shell of the protein core.

The structure of adenovirus type 2 (C. Berthet, M. Zulauf, B. Jacrot & P. Timmins, ILL, in collaboration with P. Boulanger, laboratoire de Virologie, Lille, and C. Devaux, Institut Laue-Langevin and laboratoire de Virologie, Lille)

Two lines of investigation have been followed. In the first the molecular weight of the structural proteins has been studied. In the second x-ray and neutron scattering are used to obtain a low resolution model of the virion.

- a) The molecular weight of the structural oligomers (Berthet et al., in press). Neutron scattering and a combination of sedimentation and diffusion coefficients have been used. The main result is that the oligomeric protein which sits on the 12 five-fold axes, called the penton, is not a pentamer as expected but rather a trimer. The implication of this result is either that the main structural role at each apex of the particle is assumed not by the penton but by some other protein (e.g. protein IIIa, which is also located there), or that the principle of equivalent or quasi-equivalent bonds associated with the icosahedral symmetry is not strictly observed in this case.
- b) The low resolution structure of adenovirus type 2. Neutron scattering is used to determine the radial distribution of DNA and protein in the virus by contrast variation. Higher resolution data have been obtained by x-ray scattering from solution. Comparison of the scattering pattern from the complete virus with that from its intermediate components allows the investigation of details of the capsid structure and of the organization of the nucleoprotein in the core.

From the combined results obtained by the two methods we are able to draw the following conclusions:

- 1) In the main structural component of the capsid, namely the group of nine hexons, the distance between the centre of the hexons is ~ 100 Å; a value which differs from that deduced from electron microscopy (86 Å).
- 2) A maximum in intensity at 33 Å can be attributed with certainty to DNA and no other line is found which is due to DNA. This makes a nucleosome-like structure the core rather unlikely. In the mutant H2ts 104, which has the same quantity of DNA but disordered, this line is absent, showing that it must be attributed to the organization of the DNA inside the virus.

The polymerization of brome mosaic virus protein (M. Cuillel, M. Zulauf, C. Berthet, B. Schoot & B. Jacrot)

We are continuing to investigate this self-assembly process, which provides a good approach to the self-assembly of the virus itself.

The protein at high pH is in the form of low molecular weight components (dimers, in equilibrium with monomers and possibly hexamers). At low molecular weight it is associated into empty capsids. These capsids have been analysed by neutron and light scattering, and by sedimentation. The main findings are the following:

- 1) The product of assembly is dependent on the method used to go from high pH to low pH. By dialysis a capsid is formed which has a molecular weight compatible with 180 subunits, but its size is larger by 10 to 20% than the viral capsid. Its size is indeed dependent on pH and ionic strength. It is also different in H₂O and D₂O.

By a pH jump, achieved by fast mixing with a buffer, one gets a capsid which has the same size as the viral capsid, but which has a molecular weight much lower than that of 180 subunits, indeed rather that of a capsid of 120 subunits. Electron microscopy work is in progress to visualize these incomplete capsids.

These results show that BMV proteins must exist in several states, and that the high pH and low pH states polymerize differently.

- 2) We have studied (in collaboration with P. Vachette and A. Tardieu) the kinetics of this self-assembly, using the synchrotron radiation from L.U.R.E. and a stopped-flow device constructed by M. Moody. The kinetics of formation are found (in agreement with preliminary work done with neutrons) to have a very fast component. With a concentration of 8 mg/ml about 50% of the capsids are already formed in less than 1 sec. This very fast component is followed by a very slow one, during which the capsid gives the same scattering curves, but with slowly increasing intensity. This is possibly due to a partial filling of the gaps left in the capsid made at the beginning with only 120 subunits.
- 3) In cooperation with G. Zaccari (ILL) we have examined the effect of pressure on the stability of capsids. We have found that capsids are completely stable up to the highest pressure tested, namely 1800 atm. This is true even at pH 6.5 which is the boundary between stable and unstable capsids. This result is surprising.

Changes may occur in the partial specific volumes of proteins on complex formation. In these cases an effect of pressure on the dissociation constants of the complexes may be expected. The effect of pressure on the dissociation constant will give information on the forces which hold the complex together.

Structure of viral RNA in solution (B. Schoot, S. Cusack, M. Zulauf, J.Y. Sgro and B. Jacrot)

This program, begun in November 1980, has the object of examining the three-dimensional structure of RNA in solution and the factors that influence this structure. Changes in the structure will be determined by physical techniques and be confirmed by chemical means. The RNA being used for these experiments is extracted from brome mosaic virus (BMV). In particular the 280,000 dalton RNA component is being used. The choice of a plant virus as source of RNA is justified by the ease of obtaining large quantities of this virus.

The 280,000 component of the RNA molecules present (of molecular weights 280,000, 700,000, 1,000,000 and 1,100,000 daltons respectively) can easily be purified on sucrose gradients. Milligram amounts of RNA of identical size can easily be obtained. This is a prerequisite for physical measurements such as neutron scattering and light scattering.

In order to reveal possible effects of extraction on the structure, RNA is being prepared by two different methods: a classical phenol-SDS extraction and a preparation obtained after proteolytic degradation of the capsid proteins.

This project is being undertaken in cooperation with G. Oostergetel and J. Mellema of the Leiden State University (the Netherlands); their contribution will be parallel studies with a 1,000,000 dalton RNA molecule, obtained from alfalfa mosaic virus (AMV).

Results:

Neutron scattering

Experiments are performed on RNA molecules prepared by

phenol extraction. It is found, as expected, that at low ionic strength (20 mM) there is a strong interparticle interaction. This leads to a low apparent radius of gyration and molecular weight. In the presence of 200 mM KCl the data from BMV RNA give a correct molecular weight and a radius of gyration of 115 Å, both in presence of 1 mM $MgCl_2$ and 1 mM EDTA. In the presence of 500 mM KCl the apparent molecular weight is too high, which suggests some aggregation.

From these experiments we conclude that the 280,000 dalton RNA of BMV has a rather open structure in solution (a globular RNA with 50% of its volume occupied by water would have an R_g of 39 Å). However the molecule is more compact than would be predicted from a random coil configuration. Thus it must be strongly compacted by the viral proteins during the morphogenesis of the virion. Data on the 1,000,000 dalton RNA of AMV suggests an R_g around 200 Å, which also indicates a low degree of compaction. These experiments will be continued to examine various solute effects.

Inelastic light scattering

Preliminary experiments on an RNA molecule of molecular weight 700,000 have demonstrated a strong dependence of the apparent hydrodynamic radius both on RNA concentration and on the ionic strength of the solvent. A more detailed study will be undertaken with the 280,000 RNA molecule as soon as sedimentation experiments are completed. The sedimentation constants are at the moment being determined and the S values will serve, among other purposes, to calculate the molecular weight from the diffusion constants obtained by the light scattering experiments. This control is being made to check for inter-particle interactions, which could result in erroneous calculations of the hydrodynamic radius.

Chemical studies

Preliminary experiments have been done to cross-link RNA. The crosslinking reagent used is trioxalene, a psoralene derivative (Hearst, 1981). The yield of crosslinks is determined by the residual melting behaviour. The melting of non-crosslinked RNA shows a rather low increase in absorbance in the melting experiment (26 %), which confirms the rather open structure found by neutron diffraction.

Reference

Hearst, J.E., (1981). Ann. Rev. Biophys. Bioeng., 10, 69-86.

Membranes containing melittin (C. Berthet in collaboration with R. Stroom, F. Podo & C. Grifo, Rome University, and G. Zaccari, ILL)

In the earlier phases of this project, which started in June 1979, the results from various physico-chemical techniques indicated the formation of complexes between melittin (the protein of bee venom) and artificial phospholipid bilayers. The aim of the x-ray and neutron studies was to determine the phase diagram of the system in order to study the structure of the lamellar phases.

During 1981 we have obtained by x-ray diffraction the phase diagram of the system dimyristoyl phosphatidylcholine (DMPC)-melittin (MEL) as a function of DMPC: MEL ratio, water content, and temperature. A comparative study of pure DMPC under the same experimental conditions was also carried out. The determination of the structure of each phase is now in progress by x-ray and neutron diffraction. The first results allow us to conclude that when melittin interacts with the bilayer the spacing increases. The protein has an ordering effect on the lipid, the transition of the chains from gel to liquid crystal occurring at considerably higher temperatures.

At low temperatures (45°C) and reduced water content the phase diagram shows a non-lamellar crystalline structure in coexistence with the bilayer, but its composition is not yet clear.

Neutron scattering studies on cytochrome reductase (S.J. Perkins, EMBL, Grenoble, & H. Weiss, EMBL, Heidelberg)

The neutron studies on cytochrome reductase were analysed with the results given below and summarized in Table 3. In the first place, the intact reductase-detergent complex was studied with both protonated and deuterated detergents. The reductase molecule was then cleaved into two halves, the bc₁ subunit-detergent complex and the core complex. In the second study, each of these was analysed.

Table 3

	Matchpoint (% D ₂ O)	Mol. Wt.	R _c (Å)	α (x10 ⁻⁵)	∇ (Å)
Triton	16	55,000	25.0	9	-
Cemusol	81-84	54,000	22.6	1	-
Reductase-Triton	31.0-33.4	670,000	57.3	50	~35-63
Reductase-Cemusol	46.1-46.5	660,000	56.7	45	38
Reductase	37.0	-	56.4	49	-
Detergent	-	-	~48	-	-
Core complex (monomer)	-	190,000	-	-	-
Core complex (dimer)	42	340,000	50.5	12	-
bc ₁ subunit-Triton	33.2	380,000	45.4	43	49
bc ₁ subunit-Cemusol	54.6	370,000	47.0	31	46
bc ₁ subunit	41.4	-	44.0	23	-
Detergent	-	-	~32	-	-

R_c - radius of gyration at infinite contrast

α^c - radial distribution of scattering density
fluctuations about the mean value

∇ - separation between centres of protein and detergent

The detergents and the reductase-detergent complex

The low resolution structure of ubiquinol: cytochrome c reductase (E.C. 1.10.2.2) from Neurospora crassa, which had been solubilized with detergents, was studied by small-angle neutron scattering. Triton and a deuterated-hydrogenated mixture of Cemulsol were used. Contrast variation experiments on reductase-Triton and reductase-Cemulsol complexes showed that the matchpoints of reductase-Triton and reductase-Cemulsol were 31.0 - 33.4% D₂O and 46.1 - 46.5% D₂O respectively. From these values an unusually low protein matchpoint of 37.0% D₂O was determined. The matchpoint is accounted for in terms of the nonexchange of about 60% of the exchangeable protons in reductase. This finding shows that the subunit structure of reductase is strongly linked together to restrict the extent of H-D exchange, and possesses buried polar groups (in particular lysyl and arginyl residues) within the reductase which are inaccessible to solvent.

Stuhrmann plots gave the radius of gyration at infinite contrast R_G of 57.3 ± 0.2 Å for reductase-Triton and 56.7 ± 0.3 Å for reductase-Cemulsol. Combination of these two experiments leads to an R_G of 56.4 Å for reductase alone, and an R_G of about 48 Å for the detergent alone. The distance between the centres of scattering density of the protein and detergent components in the complex was best determined to be 38 ± 8 Å from the data for reductase-Cemulsol.

The R_G values were compared with the three-dimensional structure of reductase determined from electron microscopy of membrane crystals (Leonard et al., 1981). Reductase can be modelled on the basis of two ellipsoids of axes 50 Å x 90 Å x 150 Å and separated by 75 Å. The detergent micelle could be modelled as a one-molecule deep detergent bilayer of average height 50 Å and thickness 3 Å which surrounds reductase uniformly. The method of hard spheres was adapted to the electron microscopy model. The Debye calculation of the R_G is slightly less than the experimental R_G . This implies that the length of the E/M model for reductase is less than its actual length in solution; the latter was estimated to be 175 Å. Analysis of the wide-angle scattering curve of reductase accounted for peaks equivalent to Bragg spacings of 63 Å and 38 Å in terms of the dimerization of reductase and the presence of the detergent micelle, and confirmed the lengthened E/M model of reductase to a nominal resolution of 30 Å. Calculations of α on the basis of the E/M model showed

that a significant proportion of polar residues with non-exchanged protons are buried within the core of reductase.

The bc₁ subunit-detergent complex and the core complex

Mild salt treatment of cytochrome reductase in 0.02M NaCl cleaves it into two major products and one minor product. These are the dimeric cytochrome bc₁ subunit, two monomers of the core complex and two copies of the iron-sulphur subunit (MW 25,000). Small-angle neutron scattering techniques were used to study the bc₁ subunit-detergent complexes with Triton and deuterated Cemulsol, and the core complex.

From the matchpoints of the bc₁ complexes, the protein matchpoint was determined to be 41.4% D₂O. The matchpoint of the core complex was found to be 42% D₂O. In relation to intact reductase, it is concluded that many of the non-exchanged exchangeable protons in reductase are located at or near the interfaces of the bc₁ subunit, iron-sulphur subunit and core complex within the reductase.

The molecular weight of the core complex in H₂O buffers was found to be 340,000 \pm 40,000, showing that it is a dimer. On dilution or in the presence of 200 mM NaCl it dissociated into monomers. The separation between the two monomers in the dimer is 63 \pm 4 Å.

From analysis of the Stuhrmann plots, the distance between the centre of the bc₁ subunit and the Triton micelle was found to be 49 \pm 7 Å, and for the bc₁ subunit and Cemulsol was found to be 46 \pm 5 Å. The R_G for the bc₁ subunit alone was found to be 44.0 Å. That for the detergent micelle is about 30 Å. The distance between the bc₁ subunit and the core complex in intact reductase was determined to be 65 Å.

The results from neutron scattering are now being compared with the electron microscopy model of crystalline bc₁ subunit in phospholipid bilayers (Karlsson, et al., submitted for publication). It is shown that the values of R_G, α and β , and the wide-angle scattering curve, are consistent with this model if the shape of the detergent micelle is now different from that in the case of reductase. The micelle now forms a base which completely covers the interface of the bc₁ subunit that previously was in contact with the core complex. It is concluded that the

core complex is located on the side of the reductase that protrudes by 70 Å from the lipid bilayer according to the electron microscopy study.

References

Karlsson, B., Hovmöller, S., Leonard, K.R. & Weiss, H. (1982). J. Mol. Biol., submitted for publication.

Leonard, K.R., Wingfield, P., Arad, T. & Weiss, H. (1981). J. Mol. Biol., 149, 259-274.

Intermicellar interactions in solutions of non-ionic detergents (M. Zulauf)

Aqueous micellar solutions of two non-ionic detergents, octyl tetraoxyethylene and octyl pentaoxyethylene, have been investigated as a function of temperature by photon correlation spectroscopy, viscosimetry, small-angle neutron scattering and neutron spin-echo spectroscopy. It was shown that the increase of the scattering intensities and the equivalent radii with temperature is a critical phenomenon extending over a wide temperature range, and is not due to micellar growth. Thus, the scattering properties of these systems do not reveal directly molecular weights and radii of the individual micelles, but rather their spatial arrangement.

These investigations were amplified by additional experimental and theoretical work. The physical parameters appropriate to describe the critical phenomenon of demixing of detergent micelles and water were determined in collaboration with M. Corti and V. Degiorgio (CISE, Milano). On the theoretical side, the pair correlation function of the micelles was calculated using a hard-sphere repulsive and a short-range attractive potential. The totality of the scattering data are consistent with predictions based on these calculations. Since the phase separation is entropy-driven, it is suggested that the attractive part of the potential is related to properties of hydration water bound to the head groups of the detergent.

Interactions of non-ionic detergents with porin proteins of E. coli

Interactions of three E.coli outer membrane proteins with non-ionic detergents of the octyl oligooxyethylene type and with octyl glucoside have been studied by equilibrium dialysis, thin-layer gel filtration, sedimentation equilibrium, sedimentation velocity, quasi-elastic light scattering and small-angle neutron scattering. Amounts of detergents bound to protein depend on temperature and total detergent concentration, and exceed the equivalent mass of single micelles for all amphiphiles tested. The following concept was developed: cooperative binding of detergents near the critical micelle concentration, proposed previously, is confirmed, but the amount appears to reflect the area of the hydrophobic protein surface rather than discrete binding sites. At higher detergent concentrations, pure detergent micelles interact among themselves and with the protein-detergent complexes to form loose clusters. This concept appears more realistic than that of micelle binding to protein, or that of protein insertion into pre-existing micelles.

To characterize these interactions at the structural level, deuterated and protonated matrix porin solubilized with the first type of detergent was studied by neutron small-angle and quasi-elastic light scattering in the temperature range 6 - 30°C. The results obtained are consistent with ultracentrifugal analyses, dielectric measurements, and estimates calculated from unit cell dimensions of 3-dimensional crystal forms, and from packing arrays in 2-dimensional crystal lattices.

Neutron scattering studies of glycoproteins

Three projects investigated several aspects of the neutron scattering properties of glycoproteins, in collaborations with the Kennedy Institute (London), the I.R.C.L. et Unite (Lille) and the Biochemistry Departments in Oxford and Sheffield Universities.

Physical properties of the hyaluronate binding region of proteoglycan from pig laryngeal cartilage (S.J. Perkins & A. Miller, EMBL, Grenoble, and T.E. Hardingham & H. Muir, London)

In brief, a survey of sugar matchpoints was made and compared with those of amino acids. These calculations were tested with neutron experiments on hyaluronate (and chondroitin sulphate) and on the hyaluronate binding region from cartilage. The latter is a globular glycoprotein with

sulphated carbohydrate residues. Its R_g (in conjunction with other data) showed that it is a globular molecule but is elongated. The full results were published in Perkins et al. (1981).

α_1 acid glycoprotein: a human plasma glycoprotein (S.J. Perkins in collaboration with G.Z. Li, ILL, & M.H. Loucheux-Lefebvre, Lille)

The glycoprotein with the highest carbohydrate content in human serum is α_1 acid glycoprotein (orosomucoid). This has a carbohydrate content of about 40%, and occurs in concentrations of 0.9 mg/ml in plasma. It is a highly stable and soluble glycoprotein. Small-angle scattering experiments on α_1 acid glycoprotein showed that it has a molecular weight of 37,700 and a matchpoint of 44.8% D_2O . The molecular weight, the matchpoint and a y of 0.704 ml/gm were accounted for in terms of the primary sequence and standard residue volumes for amino acids and carbohydrates.

The radius of gyration R_g of α_1 acid glycoprotein was found to be independent of concentration between 2-11 mg/ml, but undergoes a 20% expansion on going from a buffer containing 0.2M NaCl to one containing 1.0M NaCl. A contrast variation study of the expanded form showed that the R_g at infinite contrast is 24.9 Å and that the Stuhmann α^g is $30 \pm 10 \times 10^{-5}$. The latter is greater than that expected for globular proteins, and is accounted for by the surface disposition of the five glycan chains on a core of protein in α_1 acid glycoprotein.

The glycoproteins C1q, C1r and C1s of the first component C1 of component (S.J. Perkins in collaboration with R.A. Dwek & J. Boyd, Oxford & D.R. Burton, Sheffield)

The recognition of antigen by antibody is the basis of the body's defence. Following this recognition, various secondary immune responses are set in motion which lead to the elimination of the antigen-antibody complex. One of the most important of these is the triggering of the complement cascade. The initial event is the binding of the first component of complement C1 to the Fc region of IgG antibody. This is a critical event in immune defence. C1 (MW 800,000) is a Ca^{2+} -dependent complex of three glycoproteins C1r, C1s and C1q. The aim of this project is to describe the internal organization of this important complex, and to understand the events which lead to

conversion of C1r and C1s from inactive precursors to active proteases.

Contrast variation of C1q

The molecular weight calculated from the H_2O measurement was found to be 470,000, which is in excellent agreement with new unpublished estimates from recent composition and sequence studies which give 465,000 (K.R. Reid, Oxford, personal communication). The matchpoint was determined as 42% D_2O . In the Stuhrmann plot, a linear plot was obtained within the limits of error, but in remarkable distinction to other glycoproteins the slope has a very large negative value of -700×10^{-5} for the Stuhrmann alpha. The R_G at infinite contrast was found to be 124 Å.

Two samples of the collageneous tails of C1q were studied in 0% and 100% D_2O . The molecular weight from the H_2O measurement was found to be 230,000. The matchpoint was approximately 42% D_2O . The R_G in both contrasts was found to be the same at 107 Å. This experiment clearly assigns the origin of the negative Stuhrmann plot for C1q to the differences in scattering densities between the C1q heads and tails, as was predicted from the amino acid compositions. An experiment with C1q heads was performed. A molecular weight of about 35,000 was estimated, which is fully consistent with the known peptide sequence. The R_g was found to be 17 Å.

Contrast variation of C1r₂.C1s₂

These experiments using unactivated C1r₂.C1s₂ were performed in collaboration with Prof. M. Colomb's laboratory (CEN, Grenoble). The molecular weight in H_2O was found to be 370,000, in very good agreement with estimates from the known composition, giving 350,000. The matchpoint was found to be 43% D_2O . Linear Stuhrmann plots of positive slopes were obtained for R_G and R_0 , from which R_G is 126 Å and alpha is about 400×10^{-5} and the cross-sectional R_G is 14.8 Å and alpha is about 8×10^{-5} . These data are compatible with an extended rod.

The use of models in the understanding of the mechanism of oxygen binding by haemoglobin (F. Borras)

Models containing three, four and eight salt bridges have been explored to study the mechanism of oxygen binding by haemoglobin. Both the side chains forming a salt bridge, that is, the proton acceptor and the proton donor, are postulated to change pK on ligation of oxygen. Of these models, the one with eight salt bridges accounts for the degree of oxygenation and the Bohr effect at any pH and pO_2 value, and furthermore the predicted pK values for the Bohr groups correspond well with those measured experimentally. The model also fulfils the condition of linearity between fractional degree of oxygenation and fractional number of protons released.

It is postulated that there is a gradual change in structure on going from deoxy- to oxy-haemoglobin, owing to the rupture of the salt bridges. The path followed during this process will be both pH and pO_2 dependent. A formula describing the number of intact or broken salt bridges as a function of pH and pO_2 has been developed. It shows that the fractional number of broken salt bridges reaches a minimum value of 0.2 at around pH 6.3 in the absence of oxygen. However, if oxygen is added, this fractional number approaches 1.0 soon after the partial pressure of oxygen rises above 40 mm of Hg. This shows that although oxy-haemoglobin can be considered to contain no salt bridges, deoxy-haemoglobin is represented by several species which have different number of salt bridges, the proportions of which are pH dependent.

Electron microscopy (J.C. J  sior)

Work on the visualization of the molecular arrangement in collagen fibrils was discontinued at the beginning of 1981 because the approach that was used was found inappropriate to yield a satisfactory solution: this approach consisted mainly in finding by x-ray monitoring the best method of preservation to obtain ultra-thin sections of collagen fibres. Although some micrographs showed a structure (Hulmes & J  sior, 1981), this structure was not well enough preserved to fit the data obtained by x-ray diffraction of native fibrils. However, the search for the right method of preparation brought much useful information on the behavior of biological structures when treated chemically (fixed, dehydrated, stained and embedded) or mechanically (thin-sectioned), and all the experience so acquired has now been used to find answers to a simpler problem concerning another fibrillar protein: the visualization of the molecular arrangement in modified fibrinogen crystals. The

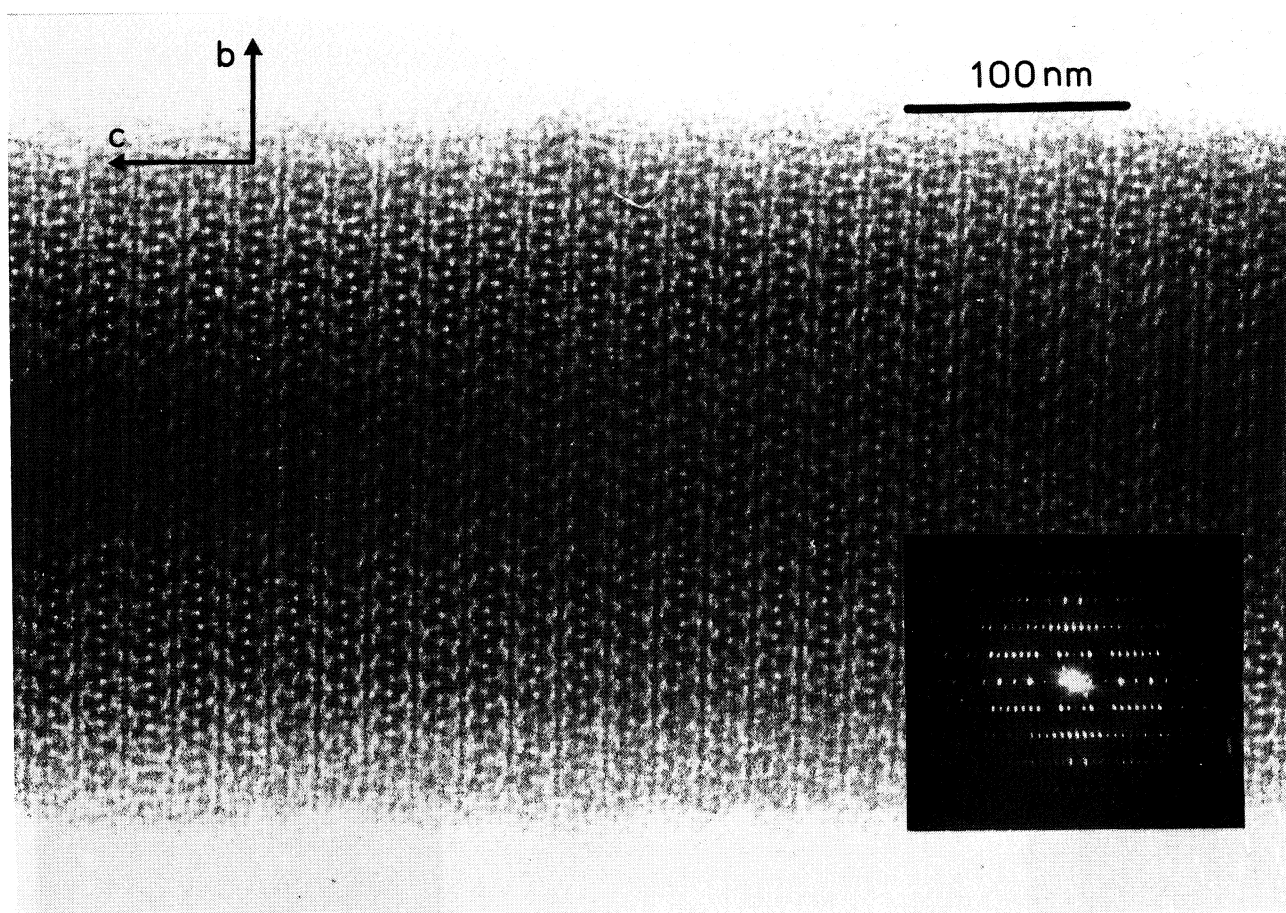


PLATE 74

Modified fibrinogen microcrystal negatively stained with 1% uranyl acetate. This highly ordered part of a crystal was not obtained from the crystal shown in Plate 75 because the latter was too thick for general clear imaging. In the corresponding optical diffraction pattern the true axial repeat is 43.5 nm and the true lateral repeat is 12.0 nm.

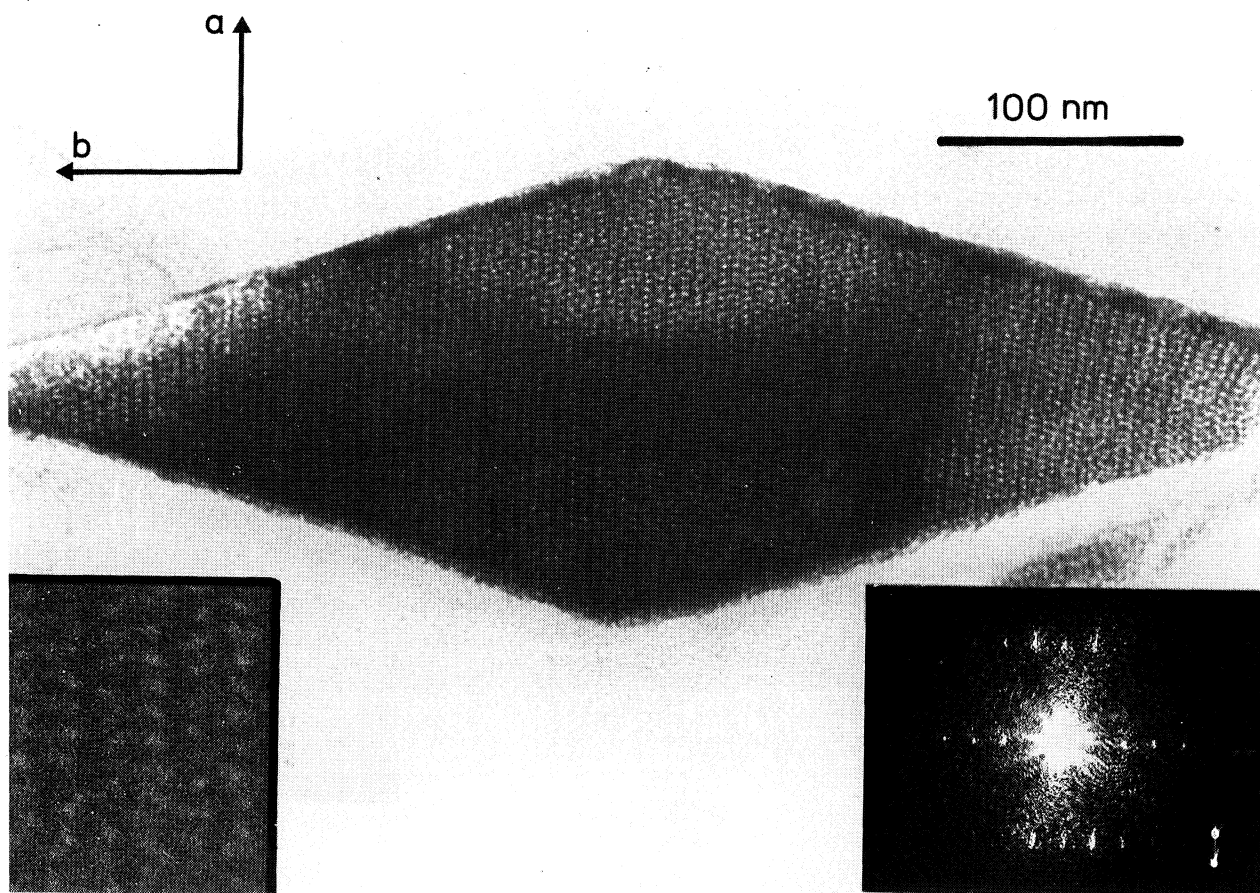


PLATE 75

Detailed cross-section through a modified fibrinogen microcrystal. The parallel rows correspond to the globular parts seen in Plate 74. Because of the dense packing the observation angle is quite important for a detailed projection. Inset is a 3.5x enlargement of part of this cross-section, showing a typical "herring bone" pattern. In the corresponding optical diffraction pattern the true periodicities along the a- and b-axes are 3.04 nm and 10.0 nm respectively. The resolution is better than 2.5 nm.

modified fibrinogen molecules (kindly supplied by L. Tranqui, Grenoble) form needle-like monocrystals (and not paracrystals as in the case of collagen) which are stable to observation in the electron microscope (Plate 74). They were studied by a method which differs completely from that used for collagen; it consists in cutting sections through a crystal deposited on a grid selected after preliminary observation in the electron microscope to determine its precise location on the grid, which has previously been marked with latex particles.

At the time of sectioning the relative position of the latex particles in the section will indicate the precise section plane through the object (its position along a selected object axis and the exact angle with this axis). This precision makes possible the direct sectioning of dispersed objects and eliminates the necessity of making oriented gels to obtain well-defined sections normal to the plane of the grid. The latex particles also provide a measure for the degree of compression occurring during the sectioning process, i.e. the deformation of the object in a direction normal to the knife edge. Although the method can be applied to any microcrystal, its application is most interesting for the study of sheet-like crystals (e.g. protein platelets) or fibril-like crystals (as in the present case with modified fibrinogen, Plate 75), the observation of the same crystal in two perpendicular projections being possible with both types. In the section, the preservation of the molecular arrangement extends to a resolution of 2.5 nm. This method could also be applied to the so-called two-dimensional crystals (e.g. of membrane proteins), or even to obtain precise cross-sections through other sections in order to obtain additional structural information. The length of the sectioned object may be as small as 1 micron thus making possible the study of vesicle-like objects. Finally the method could help to solve the problem of the missing conical zone in three-dimensional reconstruction studies by using the information contained in the cross-sections; it might also be the only possible approach to the study of the spatial conformation of crystals the spacings of which are smaller than 5 nm and where the use of tilted series is not possible. In the future the technique will be applied to other systems including collagen fibrils. The application of the additional structural information obtained from the sections to the problem of three-dimensional reconstruction will be made in collaboration with other groups.

Reference

Hulmes, D.J.S. & J  sior, J.-C. (1981). Proc. Nat. Acad. Sci., USA, 78, 3567-3571.

The use of inelastic neutron scattering to study protein dynamics (S. Cusack & B. Jacrot, EMBL, Grenoble, and J. Dianoux, ILL)

In recent years considerable theoretical and experimental progress has been made towards the understanding of the nature of conformational fluctuations in proteins and of their functional importance. Whether or not inelastic neutron scattering will be able to make a useful contribution to the study of protein dynamics remains to be demonstrated. One means of using this technique is to make measurements on proteins in D₂O buffer. The major contribution to the inelastic scattering is then incoherent scattering from the unexchanged protons, and the experiment should yield the proton-weighted vibrational spectrum of the protein. The availability of specifically-protonated, deuterated proteins would extend the potential of this kind of measurement.

We have used this approach to investigate the possibility of significant differences in the dynamic state of an enzyme with and without its substrate bound. As a model system we have used yeast hexokinase which catalyses the phosphorylation of glucose by ATP. In the absence of ATP glucose can be bound to the enzyme resulting in a marked conformational change of the protein. Previous attempts to compare the inelastic spectra of ligated and unligated hexokinase using the spectrometer IN5 have been inconclusive. Now using the new instrument IN6, with its significantly higher flux, we can claim to have the first reliable measurement of the inelastic spectrum of a protein obtained using neutrons.

Three samples were run (plus corresponding controls):

- 1) Hexokinase, unligated, at 15°C,
- 2) the same sample as in (1) but saturated with glucose (which had previously dissolved in D₂O buffer to minimize the addition of extra protons),

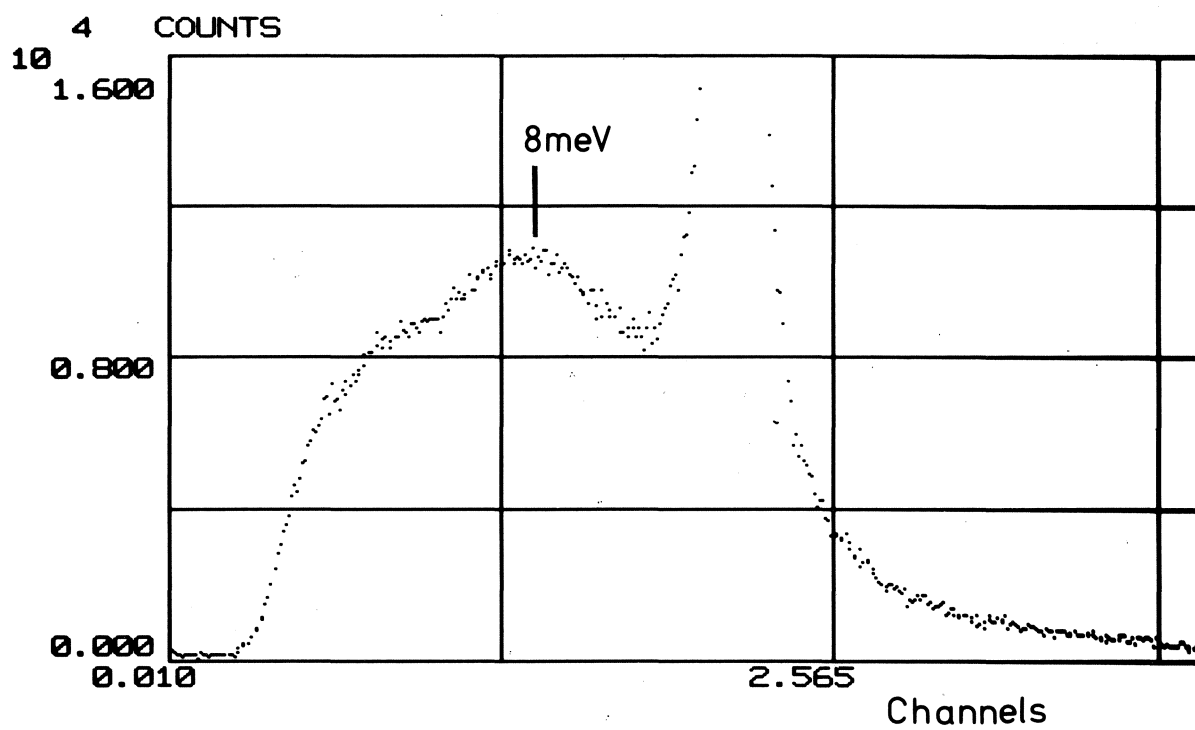


PLATE 76

Time-of-flight spectrum of unligated hexokinase.

- 3) A new sample of unligated hexokinase at 37°C, to assess temperature dependence in the inelastic spectrum.

The protein was at a concentration of about 40mg/ml in 100% D₂O Tris buffer at pH 8.5. About 0.8 ml of solution were used in a 1.5 mm thick quartz cell. IN6 was used with a wavelength of 4.1 Å and the detectors were grouped to give 24 time-of-flight spectra between scattering angles of $0.2 < q < 2.6 \text{ Å}^{-1}$. Spectra were accumulated for about 36 hours, giving very satisfactory statistics.

Plate 76 shows the corrected time-of-flight spectrum of unligated hexokinase at 15°C summed over all scattering angles. We found very little difference between the inelastic spectra of ligated and unligated hexokinase. Both show a maximum in the inelastic scattering at an energy transfer of about 8 meV (63 cm^{-1}). The spectrum of the protein at 37°C is significantly different, however. A full analysis of the data is in progress during which the quasi-elastic scattering and the variation of the inelastic scattering with scattering angle will be examined.

Publications during the year

Berthet, C., Devaux, C., Zulauf, M., Boulanger, P. & Jacrot, B. (1982). Molecular weight of adenovirus type 2 capsomers: A new characterization J. Mol. Biol., (in press).

Borras-Cuesta, F., Schoot, B. & Lindley, H. (1981). Evidence for periodicity in the amino acid sequence of myosin. Eur. J. Biochem., **115**, 475-478.

Cuilliel, M., Jacrot, B. & Zulauf, M. (1981). AT=1 capsid formed by protein of Brome Mosaic virus in the presence of trypsin. Virology, **110**, 63-72.

Cusack, S. (1982). Small-angle scattering from rod-like particles. In Neutron Scattering in Biology: ed. Worcester, D.; Academic Press, New York and London (in press).

Cusack, S. & Lees, S. (1982). Variation of longitudinal acoustics velocity by GigaHertz frequencies with water contents in rat tail tendon fibres. Biopolymers, (submitted for publication).

Giege, R., Dietrich, A., Jacrot, B., Zaccai, G., Borras, D., Thierry, J. C., Bacha, H., Remy, P., Renaud, J., Gangloff, D., Kern, D. & Ebel, J. P. (1981). Structural and kinetic studies on tRNA and aminoacyl-tRNA synthetase in the yeast valine system. Structural Aspects of Recognition and Assembly in Biological Macromolecules: ed. Balaban, M. et al.; Balaban ISS, Rehovot and Philadelphia, p.667-678.

Hulmes, D. J. S., J  sior, J.-C., Miller, A., Berthet-Colominas, C. & Wolff, C. (1981). Electron microscopy shows periodic structure in collagen fibrils cross-sections. Proc. Nat. Acad. Sci. USA, 78, 3566-3571.

Jacrot, B. (1982). X-rays and neutron small-angle scattering. In Proc. of NATO Summer School, Maratea: Plenum, New York, (in press).

Jacrot, B. & Zaccai, G. (1981). Determination of molecular weight by neutron scattering. Biopolymers, 20, 2413-2426.

J  sior, J.-C. (1981). Pr  servation des structures fibrillaires dans les coupes minces. Biol. Cell, 41, 7a.

Mellema, J. E., Andree, P. J., Krygsman, P. C. J., Kroon, C., Ruigrok, R. W. H., Cusack, S., Miller, A. & Zulauf, M. (1981). Structural investigations of influenza B virus. J. Mol. Biol., 151, 329-336.

Perkins, S. J. (1981). Estimation of deuteration levels in whole cells and cellular proteins by ¹H NMR spectroscopy and neutron scattering. Biochem. J., 199, 163-170.

Perkins, S. J., Miller, A., Hardingham, T. E. & Muir, H. (1981). Physical properties of the hyaluronate-binding region of proteoglycan from pig laryngeal cartilage: densitometric and small-angle neutron scattering studies of carbohydrates and carbohydrate-protein macromolecules. J. Mol. Biol., 150, 69-95.

W  thrich, K., Richarz, R., Perkins, S. J. & Tschesche, H. (1981). Protein-protein interactions in the complexes formed between BPTI and trypsin, anhydrotrypsin or trypsinogen: studies in solution by ¹³C NMR and ¹H NMR. In Structural Aspects of Recognition and Assembly in Biological Macromolecules: ed. Balaban, M. et al.; Balaban ISS, Rehovot and Philadelphia, p.21-34.

European Molecular Biology Laboratory
Postfach 10.2209
69 Heidelberg
Federal Republic of Germany

